AQUASOMES:

MULTILAYERED NANOPARTICULAR DRUG DELIVERY SYSTEMS

Onyinyechi Udo-Chijioke

Doctor of Philosophy

Aston University

December 2016

ASTON UNIVERSITY

Aquasomes: Multi-layered nano-particular drug delivery systems.

A thesis submitted by Onyinyechi Udo-Chijioke

for the degree of Doctor of Philosophy

2016

SUMMARY

Nanoparticulate delivery systems have been widely used in recent decades, available in a wide variety of structures, for targeted drug delivery. They provide controlled and prolonged release for drugs, peptides and biopharmaceuticals. Ceramic nanoparticles are one of the various nanocarriers, which have been employed in local targeted delivery, most commonly in the area of orthopaedic drug delivery to enhance treatment therapies.

This thesis therefore focused on the development of aquasomes, a ceramic nanoparticulate carrier system, for the delivery of proteins, growth factors and antibiotics for its potential application in bone regeneration in fracture healing. The suitability of non-aqueous silicone elastomer gels (NASEGs) as a topical/transdermal delivery system for proteins as well as protein-loaded aquasomes was also investigated.

Through process optimisation, a suitable lyophilisation method was developed and used for the preparation of bioactive aquasome formulations of growth factors, bone morphogenetic protein (BMP-2), vascular endothelial growth factor (VEGF-121), and antibiotic, gentamicin.

Physical characterisation of aquasomes using zeta potential and optimisation of preliminary aquasome formulations were optimised by utilising smaller nanocore sizes. In addition, scanning electron microscopy (SEM), confocal microscopy analysis and entrapment efficiency studies were performed to ascertain the drug loading efficiency of the different aquasome formulations. BMP-2 loading aquasomes exhibited an entrapment efficiency of 98.9% Protein loading on aquasomes yielded a higher negative zeta potential in comparison to blank nanocores. Confocal microscopy images elucidated the behaviour of nanocore particles showing agglomeration of nanocores and the presence of fluorescent drug adsorbed onto nanocores.

The bioactivity of the aquasome formulations were analysed via *in vitro* cell culture model assays and microbiological assays. BMP-2-loaded aquasomes were investigated for enhanced osteogenic proliferation and differentiation effects on osteoblast-like cells, MG63 cells. The enhanced osteogenic effect of HUVECs in co-culture with these cells was also examined. In addition, the committed differentiation of ATMSCs into osteoblasts induced by their exposure to BMP-2 -loaded aquasomes was also investigated. Results exhibited the enhanced osteogenic differentiation effect, analysed by alkaline phosphatase (ALP) secretion (a major biochemical marker of osteoblastic differentiation) from MG63 cells was dependent on the protein loading onto the aquasome formulation. However, differentiation of ATMSCs cultured in osteogenic medium was significantly higher than ATMSCs exposed to BMP-2 or VEGF-121 treatments.

Gentamicin-loaded aquasomes were investigated for their antimicrobial activity against *Staphylococcus aureus*, a major pathogen popularly implicated in cases of osteomyelitis. Results showed that gentamicin released from aquasomes exhibited excellent bactericidal activity against bacterial cultures without any reproduction of bacteria in 24 hours.

In conclusion, the aquasome formulations were able to offer controlled release of bioactive antimicrobials and growth factors over a prolonged duration. The amount of bio-actives released was dependent on the loading of the bio-actives in the fabrication process of aquasome formulations. However, minute (ng/μg) amounts of adsorbed growth factor/drug were observed in comparison to the loading (high ng/mg) within the duration of study.

It can be inferred these aquasomes can be employed in the sustained local and targeted delivery of antimicrobials and growth factors in orthopaedic treatments for enhanced fracture healing. However, the loading of bio-actives onto aquasome formulations may need to be optimised to increase the amount of bio-actives released to elicit more pronounced pharmacological effects.

Keywords: Ceramic nanoparticles, Aquasomes, BMP-2, VEGF 121, Gentamicin, Fracture healing.

To my Dad, who sacrificed pursuing his postgraduate academic career to take care of his family and has strived by all means to ensure his children are unlimited in their academic pursuits, living his academic aspirations through us.

ACKNOWLEDGEMENTS

As I fondly reflect on this journey, I pause to deeply express my profound gratitude to everyone that has made my academic sojourn a success through the years through their invaluable input and contributions. First and foremost, I will like to deeply appreciate GOD, my Heavenly Father and Lord of my life, who has provided, guided and made me who I am today. I sincerely appreciate YOU for the wisdom, strength, resilience, patience and direction you have given me all through this journey. Receive all the glory, in Jesus' name. Amen.

I would like to express my sincere gratitude to my supervisor, Dr Deborah Lowry, who has excellently supervised my through over the course of this research project. Her invaluable guidance, generous support and untiring patience, has made this project a reality. Her words of encouragement and enthusiasm kept me motivated all through this project. In addition to technical support, she believed in my abilities most especially when I was unsure of what direction I needed to go, which spurred me on during the course of this project. I am very grateful for your kindness, generosity, sacrifice and friendship.

I will also like to specially acknowledge Dr Lindsay Marshall and Ross Pallett, for teaching and directing me in my antimicrobial assays and for the bacterial strains used in this project, bringing my research ideas to life; Dr Amin Osatiashtiani of EBRI who taught and helped in the surface area analysis of my samples; Dr Eustace Johnson and Jonathan Sheard, for providing me with the osteosarcoma and mesenchymal cell lines used in this project and for their invaluable guidance in my cell culture studies. I will also like to thank Dr Andrew Ingham for taking the time to patiently give me expert training in freeze drying, Jiteen Ahmed for his invaluable technical assistance, Dr Sam Nyabam and Dr Wilson Oguejiofor for all their advice and assistance and Dr Raj Badhan for his supervisory advice during the writing of my thesis. Thank you all for your valuable input.

Furthermore, I wish to express my profound appreciation to all my colleagues at Aston University, particularly Fadi, Mandeep, Mohammed and Affiong for their friendship, encouragement and many random discussions that made working in the labs very interesting and offered assistance where they could. Also, I would like to acknowledge the School of Life and Health Sciences for providing me with the much needed support and equipment I have needed to produce and complete this thesis, also, Aston University for providing me with the much needed bursary to partly fund this PhD study.

Finally, I will like to express my deepest gratitude to my family for their emotional, spiritual, financial and professional support prior and all through my PhD studies. Your earnest support, care and sacrifice is of invaluable meaning to me and has always spurred me to keep on pushing forward and excelling in my academic pursuit. My heartfelt gratitude goes to my best friend-turned-fiancé whose support, encouragement and motivation has upheld me through this academic research process and made me believe in myself and my abilities when I doubted them. Thank you all for believing in me and for your unforgettable support throughout this journey. I am forever grateful.

TABLE OF CONTENTS

TABLE OF FIGURES

TABLE OF TABLES

ABBREVIATIONS

µg	microgram
ALP	Alkaline phosphatase
ANOVA	One-way analysis of variance
ATMSCs	Adipose Tissue Derived Mesenchymal Stem Cells
BAGs	Bioactive glasses
BMP-2	Bone Morphogenetic Protein -2
BSA	Bovine Serum Albumin
CFU	Colony forming unit
CO_2	Carbon dioxide
EDTA	Ethylenediamine-tetraacetic acid
ELISA	Enzyme-linked immunosorbent assay
FBS	Fetal bovine serum
HA	Hydroxyapatite
HUVECs	Human Umbilical Vascular Endothelial Cells
kDa	Kilodalton
MBC	Minimum Bactericidal Concentration
MG63	Bone Fibroblast Osteosarcoma cell line
MIC	Minimum Inhibitory Concentration
MTT	Thiazolyl Blue Tetrazolium Bromide
Mw	Molecular weight
NaOH	Sodium Hydroxide
NASEGS	Non-aqueous silicone elastomer gels
ng	nanogram
O D	Optical Density
PBS	Phosphate Buffer Saline
PLA	Poly (lactic acid)

PLGA	Poly (lactic co-glycolic acid)
PNPP	p-Nitrophenyl Phosphate
SAOS-2	Bone Osteosarcoma cell line
SEM	Scanning Electron Microscopy
SLNs	Solid lipid nanoparticles
TFA	Trifluoroacetic acid
UV/Vis	Ultra Violet/ Visible
VEGF	Vascular Endothelial Growth Factor

CHAPTER 1
INTRODUCTION

The control, manipulation and manufacture of structures and devices in the nanometre size range are referred to as nanotechnology. Such devices can change or mimic biological processes due to their small size, modified surfaces and multi-functionality (Singh and Lillard, 2009).

The prefix nano is derived from the Greek word “dwarf”. One nanometre (nm) is equal to one-billionth of a meter, that is, 10^{-9} m (Suri, Fenniri and Singh, 2007). The term “nanotechnology” was first used in 1974, when Norio Taniguchi, a scientist at the University of Tokyo, Japan, referred to materials in nanometres, in a scientific paper (Zhang and Webster, 2009). The size range that holds so much interest is typically from 100 nm down to the atomic level approximately 0.2 nm, because in this range materials can have different and enhanced properties compared with the same material at a larger size (Sahoo And Labhasetwar, 2003).

Nanotechnology drug delivery is a growing field experiencing an increasing acceptance in health care applications. Nanotechnology drug delivery is widely used in the health care industry in applications such as cancer treatments, neurology, cardiovascular disorders, and anti-infectives, amongst others. One important and active application area of nanotechnology drug delivery systems is to transport drugs to the final target site of therapeutic intervention within the body. The nanotechnology drug delivery market is witnessing rapid growth due to increase in research and development activities in nanotechnology to develop novel nano-medicine (BCC Research, 2016).

The global nanotechnology drug delivery market has been divided into different sectors based on technology and application. Based on technology, it has been segmented into liposomes, micelles, nanocrystals, nanoparticles, nanotubes, and others, (Figure 1.1). The nanoparticles segment dominated the global nanotechnology drug delivery market in 2014. This segment controlled the market as key nanoparticles such as inorganic nanoparticles, dendrimers, liposomes, and fullerenes are used in pharmaceutical drug delivery (Transparency Market Research, 2016).

Based on application, the market has been segmented into neurology, oncology, cardiovascular/physiology, anti-inflammatory/immunology, anti-infective, and others. Anti-infectives were the largest application segment of the nanotechnology drug delivery market due to rising prevalence of community-based and hospital-based infections.

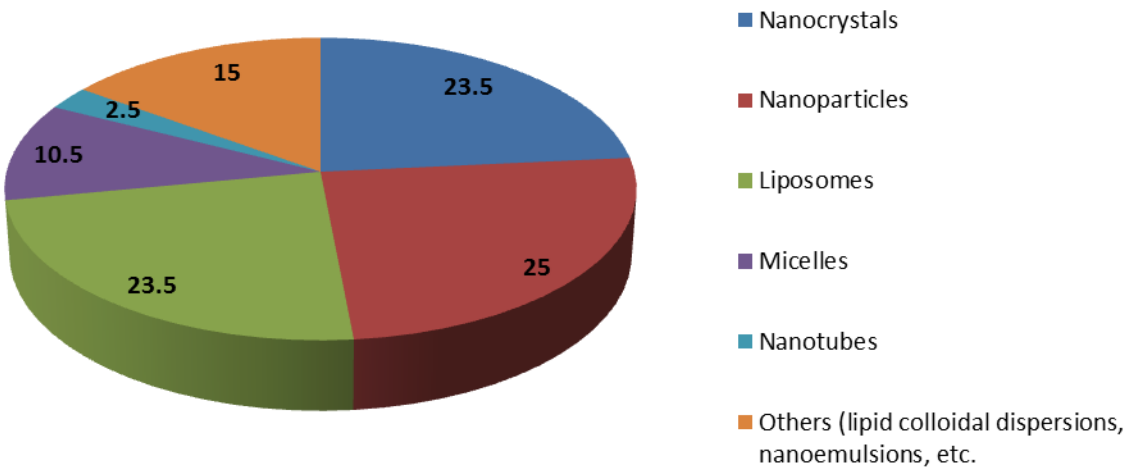

Figure 1.1 Global Nanotechnology drug delivery market by technology in 2014 (in %) (Adapted from: Transparency Market Research, 2016)

1.1 NANOPARTICULATE DELIVERY SYSTEMS

Nanoparticles used in biomedical research and drug delivery include inorganic nanoparticles, polymeric nanoparticles, solid lipid nanoparticles, liposomes, nanocrystal, nanotube, dendrimers and others (Faraji and Wipf, 2009).

The global market for nanoparticles in the life sciences was estimated at over $29.6 billion for 2014. This market is forecast to grow to more than $79.8 billion by 2019, to register a healthy compound annual growth rate (CAGR) of 22% (Figure 1.2), with its biggest increase from the area of drug delivery systems (BCC Research, 2014).

Nanocarriers have been predicted to account for 40% of a $136 billion nanotechnology-enabled drug delivery market by 2021, with a 60/40 split between nanocrystals and nanocarriers respectively, although developing new targeted delivery mechanisms may allow more value to be created for companies and entrepreneurs.

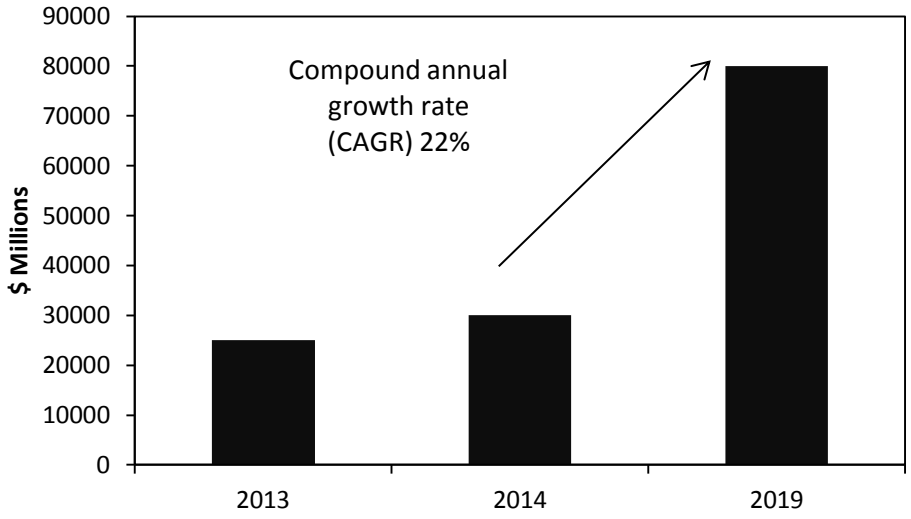

Figure 1.2 Global market for nanoparticles in Biotechnology and Pharmaceuticals. The graph also illustrates the compound annual growth rate (22%) (Reference: BCC Research (BIO113B), August 2014).

There has been increased interest in the development of biodegradable polymeric nanoparticles for drug delivery which can be attributed to their application in controlling the release of drugs, stabilizing labile molecules such as DNA, proteins and peptides from degradation and targeted drug delivery (Yang and Webster, 2009).

Nanoparticles are solid colloidal particles comprising macromolecular substances that vary in diameter from 1 to 100nm (IUPAC definition of Nano measurement) (Singh and Lillard, 2009). The drug or protein of interest is usually dissolved, adsorbed, entrapped, attached and/or encapsulated into or onto a nanomatrix. The nanoparticles are constructed and manipulated to possess and exhibit distinct properties and release characteristics best suited for the delivery of the drug or protein Lillard, 2009). A comparison of nanoparticulate carrier systems used in drug delivery is highlighted in Table 1.1 with schematic diagrams of these nanoparticles illustrated in Figure 1.3.

Table 1.1 Nanoparticulate carrier systems

(Utreja and Jain, 2001; Bianco, Kostarelos and Prato, 2005; Gillies and Fretchet, 2005; Xu et al, 2006; Faraji and Wipf, 2009; Malam et al, 2009; Umashankar et al, 2010; Huang et al, 2011; Jain et al, 2012; Akbarzadeh et al, 2013)

	Synthesis methods	**Polymer(s) used**	**Drug loading technology**	**Release mechanisms**
Polymer nanoparticles	Solvent evaporation, nanoprecipitation, salting out, dialysis	PLGA, PLA, Chitosan, Gelatin, PMMA, etc.	Incorporation into polymer matrix	Polymer degradation
Solid lipid nanoparticles	High shear homogenisation, ultrasound, high pressure homogenisation, solvent emulsification/evaporation	Triglycerides, partial glycerides, fatty acids, steroids, waxes	Solid lipid matrix: drug enriched core or drug-enriched shell	Lipid matrix degradation, diffusion by use of surfactants,
Micelles	Spontaneous self-assembly in water	Amphiphilic co-polymers or phospholipids, Pluronic®, Polyesters, Poly (L-amino acids), P.E.G.	Core can accommodate hydrophobic drugs and its shell hydrophilic drugs	pH-responsive release, thermo-responsive release, biodegradability of polymer, drug-dependent release
Liposomes	Mechanical dispersion methods: Sonication, freeze-thawed liposomes, lipid film hydration, micro-emulsification	Cholesterol and natural non-toxic phospho-lipids	Passively during or actively after liposome formation; hydrophilic drugs can be loaded in hydrophilic core and hydrophobic dugs in lipid bilayers	Enzymatic degradation and/or phagocytic attack, imitated by use of surfactants, pH-mediated release
Inorganic nanoparticles	Surface modification or functionalisation	Calcium phosphate, gold, carbon materials, silicon oxide, iron oxide, layered double hydroxides (LDHs)	Adsorption to functionalised/modified nanoparticle surface	Biological processes (endosomal release, phagocytosis, dissolution, desorption.
Dendrimers	Divergent or convergent synthesis methods	Polyamidoamine (PAMAM), Poly (propyleneimine), etc.	Chemical synthesis of polymer-drug or polymer-protein conjugates with dendrimer backbone forming highly branched macromolecules	pH-mediated response, enzyme-mediated response, induction of disulphide exchange reactions
Nanotubes	Chemically “rolling up” a graphene sheet to a form a single walled nanotubes (SWNT) or many layers to form concentric cylinders to form multi-walled nanotubes (MWNT)	Graphene	Functionalising external walls to increase water solubility and/or linking with different active molecules (peptides, proteins, nucleic acids, etc (Encapsulation, Internalisation)	Targeting via enhanced permeability and retention(EPR); pH- or temperature controlled release
Aquasomes	Lyophilisation and adsorption onto coated ceramic nanocores	Ceramic cores made of tin oxide, nano-crystalline calcium phosphates like brushite, nano-crystalline diamond.	Formation of inorganic cores, coating of cores with polyhydroxy oligomer and loading of the drug/protein of choice	Diffusion and desorption from oligomeric coating

Figure 1.3 Types of nanoparticles used in drug delivery (Adapted from Faraji and Wipf, 2009)

1.2 AQUASOMES

Aquasomes are nanoparticulate carrier systems, which constitute a most recent development in the areas of nanotechnology and genetic research for the targeted delivery of bioactive molecules such as peptides proteins, antigens, hormones, and genes to specific sites (Umashankar et al, 2010; Jain et al, 2012).

They are three-layered self-assembled structures, comprising a solid phase nanocrystalline core coated with an oligomeric film, which a biochemically active molecule (drug or biopharmaceutical) is adsorbed onto (Figure 1.4) (Girota and Bajaj, 2012). Its constituent carbohydrate film prevents destructive denaturing interaction between drug and solid carriers. They are also called as water bodies as their water like properties provides a platform for preserving the conformational integrity and biochemical stability of bio-actives (Girota and Bajaj, 2012). They maintain molecular confirmation and optimum pharmacological activity. The molecular conformation of proteins and drugs can be preserved by incorporating such biological molecules on aquasomes with natural stabilizers (natural sugar coating), which act as dehydroprotectants (Mesariya et al, 2011; Jain et al, 2012).

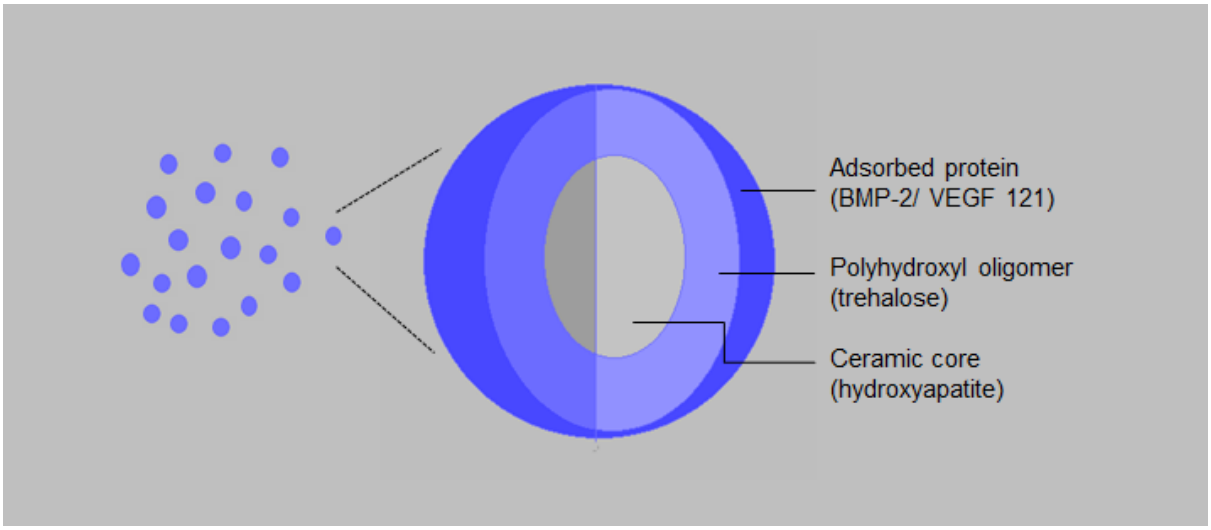

Figure 1.4 Schematic cross-section of the aquasome structure

1.2.1 Properties of aquasomes

The properties of aquasomes enable them to offer various added advantages in drug/protein/antigen delivery (Jain, Jain and Mahajan, 2014).

Aquasomes are large with active surfaces, which can be efficiently loaded with substantial amounts of drugs and biopharmaceuticals via ionic, entropic, non-covalent bonds, and van der waals forces. Due to their size and structural stability, aquasomes avoid clearance or degradation by the reticuloendothelial (RES) system (Jain et al, 2012).

As colloidal size particles, they are likely to be more concentrated in the liver and muscles and can be used for targeted drug delivery to these organs. The pharmacological or biological activity of proteins such as insulin and other antigens can be maintained without any difficulty in receptor recognition when adsorbed onto aquasome formulations because they do not experience any added surface modification (Mesariya et al, 2011). They preserve the conformational integrity and biochemical stability of bioactive molecules (Kossovsky et al, 1996)

The mechanism of action of aquasomes is controlled by their surface chemistry. They deliver adsorbed contents through a combination of specific targeting, molecular shielding and slow and sustained release processes (Mesariya et al, 2011; Jain et al, 2012).

1.2.2 Method of preparation and structure of aquasomes

The preparation of aquasomes is a three-step process which constitutes of the following processes:

Formation of an inorganic core: the fabrication of the inorganic core is dependent on the material selected. The common used materials are tin oxide core ceramic, nano-crystalline brushite (calcium phosphate dehydrate, self-assembled) and nano-crystalline diamond particles;

Coating of the core: Secondly, the inorganic core (usually ceramic) is coated with a carbohydrate (polyhydroxyl oligomer). The coating process is carried out by addition of carbohydrate into an aqueous dispersion of the cores under sonication. These are then subjected to lyophilisation to promote an irreversible adsorption of carbohydrate onto the ceramic surface. Here, the secondary drying process in freeze drying breaks the ionically bound water molecules causing the adsorption of the carbohydrate to the ceramic core. The unadsorbed carbohydrate was further removed by centrifugation.

Loading of the drug: the drug of choice is loaded to the coated particle by adsorption. A drug solution of known concentration is prepared in a suitable pH buffer and coated particles are dispersed into it. The dispersion is then lyophilized to create the aquasomes (Umashankar et al, 2010; Jain et al, 2012).

1.2.3 Characterisation of aquasomes

Aquasomes are characterised by their individual components: ceramic nanocore, polyhydroxyl coating and drug/protein adsorbed onto the ceramic nanocore. Different analytical methods are employed to detect the presence of and/or quantify the amount of the constituents (coating, drug/protein) per aquasome sample weighed. These analytical methods are highlighted in table 1.2.

Table 1.2 Characterisation of aquasomes

(Kim and Kim, 2002;, Rojas-Oviedo et al, 2007; Goyal et al, 2008; Pandey et al, 2011; Vengala et al, 2013; Nanjwade et al, 2013)

Ceramic core	Coated core	Drug/protein-loaded aquasomes
Size distribution analysis *Scanning electron microscopy (SEM), Transmission electron microscopy (TEM)*	***Concanavalin A-induced aggregation assay*** *Determines the amount of sugar coated over the core*	***Entrapment efficiency test*** *Analysing supernatant separated by high-speed centrifugation for unadsorbed drug/protein*
Structural analysis *FT-IR spectroscopy (potassium bromide sample disk method)*	***Anthrone assay*** *Determines the residual sugar remaining after coating*	***In vitro release studies*** *Using the partial replacement method at specified time intervals*
X-ray diffraction *Analysis of Crystalline or amorphous behaviour*	***DSC (differential scanning calorimetry)*** *Examine the effect of carbohydrate coating on ceramic core peaks*	***SDS-PAGE*** *Analysing the stability of proteins during the formulation of the aquasomes*

1.3 NANOPARTICULATE CARRIERS FOR THE TREATMENT OF FRACTURES

1.3.1 Anatomy of the bone

Bone at the tissue level undergoes continuous formation and resorption (Rodan, 1992; Hanley, 2012). Bone resorption refers to the process by which old bone tissue is broken down and minerals are released, resulting in a transfer of calcium from bone tissue to the blood. Resorption and formation is normally in balance (Hanley, 2012) and a negative balance between bone resorption and formation, frequently due to excessive resorption, is the basis of many bone diseases (Rodan, 1992).

1.3.1.1 Intracellular composition

Bone comprises four cellular components: osteoblasts, osteocytes, bone lining cells and osteoclasts (Figure 1.5) (Buckwalter et al, 1995)

1.3.1.1.1 Osteoblasts

Osteoblasts are derived from undifferentiated mesenchymal cells located in the marrow bone canals, endosteum and periosteum. Their differentiation and proliferation into osteoblasts occurs during intramembranous and endochondrial bone formation (replacement of cartilage by bone) (Downey and Siegel, 2006).

The major function of osteoblasts is the manufacture of organic matrix of bone (comprising proteins and polysaccharides) (Downey and Siegel, 2006)

Osteoblasts ultimately follow one of the following pathways:

- They may remain as active osteoblasts
- They may become surrounded by bone matrix and become osteocytes
- They become relatively inactive and form bone lining cells

1.3.1.1.2 Bone lining cells

Bone lining cells are thin and elongated cells that cover most bone surfaces in a major skeleton and are metabolically active. Evidence shows that in the presence of parathyroid hormone, these cells secrete enzymes that remove the osteoid covering of the bone matrix in preparing for bone resorption (Buckwalter et al, 1995). Evidence also indicates that bone lining cells regulate crystal growth in bone or function as a barrier between extracellular fluid and bone tissue (*Downey and Siegel, 2006*).

Figure 1.5. Images of bone cells

(a) Image of bone matrix deposition by an osteoblast;
(b) Bone resorption by an osteoclast;
(c) Osteocyte differentiation of osteoblastic cells grown on collagen substrates, and
(d) Osteocytes of mousse bone origin
(Reproduced with permission from: Guocheng Wang and Zufu Lu, University of Sydney; Wellcome images)

1.3.1.1.3 Osteocytes

Osteocytes make up to 90% of bone cells in a mature skeleton. Immature osteocytes resemble osteoblasts but mature as more bone matrix is laid down and moved further into bone tissue (their size also becomes relatively smaller as they lose more cytoplasm) (Ng et al, 1995).

They are located within lacunae (spaces) and have long cytoplasmic processes that project through canaliculi, (tunnel-like structures that extend radially throughout skeleton allowing for diffusion of nutrients in the mineralized bone matrix), and contact processes of adjacent cells. Such connecting processes are of paramount importance in cellular communication for the following reasons (Downey and Siegel, 2006):

- The important cellular network is thought to allow cell mediated exchanges of minerals between the fluids in the bone and the vascular supply.
- The cellular network is thought to sense mechanical deformation within bone that leads to resorption and thus formation of bone (Buckwalter et al, 1995).

1.3.1.1.3 Osteoclasts

Osteoclasts are the largest in size of all the bone cells. They are multinucleated cells responsible for bone resorption in both normal and pathological conditions (such as osteoporosis) (Downey and Siegel, 2006).

They have high mobility, moving along the surface of the bone from various sites. Their large surface area potentially allows extensive exchange between the intracellular and extracellular environment of the bone (Ng et al, 1997; Downey and Siegel, 2006).

1.3.1.2 Extracellular composition

The extracellular composition of bone makes up approximately 90% of its volume in comparison to the remaining 10% comprising cells and blood vessels. The extracellular matrix is composed of both organic and inorganic components.

The organic component consists predominantly of collagen (synthesized and secreted by osteoblasts and aggregated extracellularly). Type I collagen is dominant while types V, VI, VIII and XII is present in lesser amounts. Collagen fibrils are consistently assembled in an overlapping manner, retaining spaces between adjacent fibrils. Many intermolecular crosslinks are formed, producing a stable porous structure (Ng et al, 1997; Buckwalter et al, 1995; Downey and Siegel, 2006).

The inorganic component of bone is essential in providing the physiological functions related to storage of ions as well as a major portion of its tensile strength. It has been predicted that the minerals salts in bone comprises 99% calcium, 85% phosphorus and 40- 60% sodium and magnesium found in the human body. Vital physiological functions related to nerve

conduction and muscle contraction depend on the bone's inorganic composition appropriate extracellular homeostasis (Downey and Siegel, 2006).

1.3.2 Bone structure

The structure of bone is largely divided into **cortical** (compact) and **cancellous** (spongy) bone, with some structural similarities and differences. Cortical bone is dense and solid and surrounds the marrow space while trabecular bone is composed of a honeycomb- like bone interspersed in the bone marrow compartment (Clarke, 2008) (Table 1.3). Within these classifications, cortical and cancellous bone can be further classified into woven and lamellar bone.

Woven (primary) bone is formed where bone is quickly laid down such as in embryonic bone, fracture healing and pathological state such in hyperthyroidism. This is replaced with **lamellar (secondary)** bone which is created by remodelling of woven bone (Buckwalter et al, 1995, See Figure 1.6). The similarities and differences between woven and lamellar bone are highlighted in Table 1.3.

Figure 1.6 Structure of the bone.
a) External structure; b) Internal structure (Reference: Merriam-Webster Inc., 2013)

Table 1.3 Similarities and differences between cortical and cancellous bone and differences between woven bone and lamellar bone

(Ng et al, 1997; Downey and Siegel, 2006)

Similarities	
• Cortical and cancellous are made up of the same composition. • They are both made up of the same matrix structure	
Differences	
Cortical (compact) bone	***Cancellous (spongy) bone***
Cortical bone comprises the outer casing of long bones and vertebrae.	Cancellous bone is located in the interior of bone structure.
It accounts for 80% of mature skeleton and forms the shaft of long bones	Short bones (e.g. carpals), vertebrae, skull and pelvic bones have a greater percentage of cancellous bone
Cortical bone has a low surface-to-volume ratio	Cancellous bone possesses trabeculae which are characterized by a relatively high surface-to-volume ratio.
The shaft of long bones allows cortical bone to possess a higher resistance to tensional or bending forces. Its rigidity and density justify its shape and weight-bearing properties.	Cancellous bone provides greater resilience and shock absorption.
Cortical bone has a low metabolic rate. This is attributed partly to its reduced exposure to marrow cells and vascular supply as it is engrained within the bone matrix.	Cancellous bone has a relatively high bone metabolic rate and seems to respond rapidly to changes in mechanical loading and unloading. This is attributed partly to the better exposure of cancellous bone cells to the adjacent bone marrow cells and vascular supply.

	Woven bone	***Lamellar bone***
Structure	• Woven bone has a scattered, irregular appearance. • When histologically viewed, osteocytes in woven bone are more randomly scattered. • Collagen fibres are interlaced and randomly distributed by hydroxyapatite crystals deposited in a disorganized manner.	• Lamellar bone has a very orderly arrangement. • The osteocytes in lamellar bone are uniform in size and shape and are placed in line with other bone cells. • Hydroxyapatite crystals are deposited parallel to collagen fibres • Lamellar bone is composed of collagen fibres arranged in concentric sheets around blood vessels to form *harvesian systems.*

1.3.3 The process of bone remodelling

Bone remodelling is the constant process of ensuring the mechanical integrity of the skeleton is maintained. Bone is continually remodelled by the interaction by osteoclasts (which resorb existing bone) and osteoblasts (which form new bone, filling up the bone matrix resorbed by osteoclasts) (Hadjidakis and Androulakis 2006). Osteoclasts are anchored to the surface of the bone and create a micro acidic environment, which dissolves the bone's mineral content and subsequently releases enzymes, which remove the remaining collagenous matrix (Ng et al, 1997; Downey and Siegel, 2006; Amgen, 2012). After resorption, the osteoblasts move to the resorption space created by the osteoclasts, secrete, and deposit organic matter referred to as osteoid (which consists mainly of collagen). This mineral content of collagen (calcium and phosphate) crystallizes to form new bone matrix (Ng et al, 1997). Some osteoblasts become trapped in their secreted matrix and thus become osteocytes. Osteocytes form a network of interconnected cells occupying lacunae (pits) within the mineralised bone tissue. Other osteoblasts will either line the surface of the bone structure or undergo apoptosis. This process is referred to as bone remodelling.

Osteoblasts can form new bone matrix independently of concurrent osteoclast activity. This increase in bone mass maintains bone strength and promotes bone growth. (Hadjidakis and Androulakis 2006; Amgen, 2012). However, a variety of factors decrease osteoblast activity and promote osteoclast activity resulting in reduced bone mass. This is referred to as negative bone balance. Reduced bone density can be induced by drugs, disease state, hormones, growth factors or age.

1.3.4 Molecular signalling in response to mechanical stimuli (bone resorption)

Osteocytes direct bone remodelling in response to mechanical strain and other stimuli. This process is controlled by a system involving three key proteins: RANK (receptor- activator of nuclear factor kappa beta), its ligand RANKL (receptor-activator of nuclear factor kappa beta ligand) and a decoy receptor OPG (osteoprotegerin) (Wright et al, 2009). Orthotropic hormones to either increase or reduce the OPG/RANKL ratio (Figure 1.7) regulate the system.

Osteocytes and osteoblasts start the process of bone resorption by releasing RANKL, which bind to RANK on osteoclasts and its precursors, activating them. Osteoblasts also produce OPG, which suppresses bone turnover. OPG binds to RANKL, hindering its interaction with

RANK. Thus, the activation of bone remodelling is dependent on the balance between OPG and RANKL (Figure 1.8) (Hanley et al, 2012).

RANK is a member of the tumour necrosis factor receptor (TNFR) family. The expression of RANK is observed on a variety of cells including dendritic cells, osteoclast precursors and mature osteoclasts. RANK activation by the binding of RANKL initiates an internal signalling cascade via cytoplasmic adaptor proteins called TRAFs. RANK has three binding sites by TRAF 2, 5 and 6, with different binding affinities for each of them, which transmit the RANK stimulation signal and activate downstream pathways. This signalling cascade initiates the expression of genes leading to the differentiation of monocytes into osteoclasts and also the activation of mature osteoclasts (Wright et al, 2009).

RANKL is a tumour necrosis factor (TNF) - related cytokine expressed by different bone cells including osteoblasts and their immature precursors, T-lymphocytes, B-lymphocytes and megakaryocytes (Wright et al, 2009). The expression of RANKL is incited by various cytokines (IL-1, TNFα and IL-11) and calcitrophic hormones including prostaglandin E2 and 1,25-dihydroxyvitamin D_3 ($1,25D_3$). An amplified production of RANKL by osteoblastic cells leads to osteoclast differentiation and activation, resulting in bone resorption (Wright et al, 2009).

RANKL with the synergistic involvement of OPG, the decoy receptor, is understood to be the main mechanism in the control of bone turnover.

Figure 1.7 Schematic representation of RANK-RANKL relationship. This shows RANK-RANKL binding signaling pathways, indicating the inhibition of RANK-RANKL binding by OPG. (Adapted from Wright et al, 2009)

Figure 1.8 The interaction between RANK, RANKL and OPG
(Adapted from Hanley et al, 2012)

1.3.5 Growth factors in bone development and healing

The process of bone development is tightly regulated by both local and systemic factors (Downey and Siegel, 2006; Mundy et al, 2001). Hormones such as parathyroid and estrogen, Vitamin D_3 and calcitonin are systemic factors while local factors are cytokines, growth factors and prostaglandins (Mundy et al, 2001). This process involves a complex interaction of bone cells and cytokines working simultaneously with growth factors (Devescovi et al, 2008).

Growth factors are polypeptides that are locally acting modulators of cellular activities. Their effects may be autocrine, paracrine or endocrine. Their mechanism of action entails their binding to target cell receptors which induce an intracellular signal cascade that extends to the nucleus and determines the biological response. A single growth factor can also affect multiple cell types and elicit diverse functions (Lieberman et al, 2002; Devescovi et al, 2008).

the growth factors implicated in bone development include: bone morphogenetic proteins (BMPs), transforming growth factor- β (TGF-β), platelet-derived growth factor (PDGF), vascular endothelial growth factor (VEGF), fibroblast growth factor (FGF) and insulin-like growth factors (IGFs) (Linkhart, Mohan and Baylink, 1996; Ng et al, 1997; Mundy et al, 2001; Lieberman et al, 2002; Xiao et al, 2007; Devescovi et al, 2008). Their various osteogenic functions are highlighted in Table 1.4.

Table 1.4 Growth factors and their osteogenic functions

(Linkhart, Mohan and Baylink, 1996; Mundy et al, 2001; Devescovi et al, 2008)

Growth Factor	*Cell Source*	*Biologic effect*	*Action on bone*
BMPs	*Osteoprogenitor cells, osteoblasts, endothelial cells (BMP-2).*	*Chondro-osteogenesis (cartilage and bone formation), osteoinduction (BMP-2), ectopic bone formation.*	*Migration of osteo-progenitors, induction of bone cell proliferation, differentiation and matrix synthesis.*
TGF-β	*Platelet, osteoblast, BMSC, chondrocyte, endothelial cell, fibroblast, macrophage*	*Immunosuppression, angiogenesis, stimulation of cell growth, differentiation and extracellular matrix synthesis.*	*Recruitment of osteoblast and osteoclast pre-cursors, proliferation of un-differentiated mesenchymal osteoblast and chondrocyte differentiation, production of bone matrix.*
PDGF	*Platelet, osteoblast, BMSC, chondrocyte, endothelial cell, fibroblast, macrophage*	*Proliferation of connective tissue cells, macrophage and smooth muscle cell chemotaxis, angiogenesis*	*Migration, proliferation and differentiation of osteoprogenitors.*
VEGF	*Platelet, osteoblast*	*Angiogenesis*	*Conversion of cartilage into bone, osteoblast differentiation and differentiation.*
FGF	*Macrophage, monocyte, BMSC, chondrocyte, osteoblast, endothelial cells.*	*Angiogenesis, proliferation of fibroblast and smooth muscle cells of vessels*	*Chondrocyte maturation (FGF-1), Differentiation and proliferation of osteoblasts, induction of apoptosis of mature osteocytes, inhibition of apoptosis of immature osteoblasts.*
IGF	*Osteoblasts, chondrocyte, hepatocyte, endothelial cell*	*Regulation of growth hormone effects; mediating effects of mechanical stress on bone formation*	*Stimulates bone cell mitogenesis (IGF-1), proliferation and differentiation of osteoblasts, bone matrix synthesis and bone resorption (stimulates osteoclasts).*

1.3.6 TGF-β, IGFs and BMPs

TGF-β is a powerful stimulator of endochondral and intramembranous bone formation. It is ctivated by 1, 25- dihydroxy Vitamin D, parathyroid, sex steroids and BMP-2 (Linkhart, Mohan and Baylink, 1996). It is present in bone matrix in concentrations of 0.1mg/kg dry weight. Continued exposure to TGF-β inhibits bone cell differentiation and the formation of mineralised nodules (Mundy et al, 2001). TGF-β needs to be exposed to bone cells for transient periods to enable its stimulatory effects to be exerted on bone cells (Linkhart, Mohan and Baylink, 1996). This proposes that TGF-β may have vital chemotactic functions in normal bone remodelling, attracting osteoblast precursors to sites of active bone resorption (Solheim, 1998).

BMPs are growth factors that have the unique ability of eliciting ectopic cartilage and bone formation, a process which is similar to endrochondral bone formation (Mundy et al, 2001; Xiao, Xiang and Shao, 2007). They enhance differentiated function in cultural osteoblasts and are vital for embryonic osteogenesis. BMP-3 (osteogenin) has been known to inhibit osteoclastic bone resorption and is chemotactic for monocytes (Mundy et al, 2001).

IGFs I and II are the most abundant growth factors in bone matrix acting as paracrine or autocrine regulators of bone formation (Ng et al, 1997). IGFs stimulate the proliferation and differentiation of osteoblast progenitors, osteoclast progenitors and marrow stromal cells (Ng et al, 1997). The secretion of IGFs is amplified by parathyroid, parathyroid receptor protein, 1,25-dihydroxyvitamin D, prostaglandin E_2 and inhibited by cortisol (Linkhart, Mohan and Baylink, 1996). They are known for stimulating bone cell mitogenesis as well as collagen synthesis in bone organ culture (Mundy et al, 2001).

1.3.7 The role of osteogenesis in fracture healing

Angiogenesis can be defined as the formation of new blood vessels from pre-existing ones (Carano and Filvaroff, 2003). In fracture healing, vascularisation is observed before bone formation (Deckers et al, 2002). Vascularisation in bone tissue allows oxygen, nutrients and other growth factors be transported to bone and surrounding tissues for normal bone metabolism (Kanczler and Oreffo, 2008). There are a number of systemic and local factors that are active during fracture healing that have direct and/or indirect angiogenic functions (Geris et al, 2008). They include members of the fibroblast growth factor (FGF), transforming

growth factor (TGF), bone morphogenetic protein (BMP) and vascular endothelial growth factor (VEGF) families (Carano and Filvaroff, 2003; Geris et al, 2008).

The synergistic nature of osteogenesis and angiogenesis in bone regenerated is well established, evidenced by several studies indicating the roles of various osteogenic and angiogenic cytokines and growth factors involved in the various processes (Patel et al, 2008). Angiogenesis usually precedes osteogenesis for the establishment of vascularisation via the expression of angiogenic growth factors while osteogenic growth factors are constantly expressed during bone formation and remodelling (Kempen et al, 2009).

In fracture healing, there are four stages in which there is a complex interaction involving specific cell types, growth factors and extracellular matrix (Carano and Filvaroff, 2003; Schindeler et al, 2008). Each stage is classified by a definite set of cellular and molecular events which are not clearly demarcated from each other but overlap considerably between the different stages during fracture repair (Dimitriou et al, 2005; Schindeler et al, 2008). These four stages include inflammation, soft callus (fibrocartilage) formation, hard callus formation and bone re-modelling (Schindeler et al, 2008; Geris et al, 2008).

1.3.8 Stages of fracture healing

1.3.8.1 Inflammation

A bone fracture is usually accompanied with disruption of local tissue integrity, cortical bone and periosteum tears, discontinuity of normal vascular function as well as a distortion of the marrow architecture. The fracture site becomes hypoxic, osteocytes and surrounding tissues become deprived of their nutrition (Geris et al, 2008). This leads to the activation of non-specific wound healing pathways, that is, an inflammatory response (Schindeler et al, 2008; Kanczler and Oreffo, 2008).

The bleeding at the fracture site is contained by the surrounding tissue and develops into a hematoma (Dimitriou et al, 2005; Kanczler and Oreffo, 2008). This inflammatory response brings inflammatory cells, leukocytes and macrophages. Consequently, an invasion of the fracture region by fibroblasts, mesenchymal stem cells and endothelial cells also occurs (Geris et al, 2008). Granulocytes, lymphocytes and monocytes penetrate hematoma through the fractured fragments and combat any present infection, and consequently secrete cytokines and growth factors and cause clotting to progress into a fibrinous thrombus. With time, capillaries grow into the clot and are eventually reorganised to form granulation tissue.

This stage is regulated by and involves the secretion of a range of cytokines and growth factors which include TGF-β, PDGF, FGF-2, VEGF, M-CSF, IL-1, IL-6 and BMPs (Schindeler et al, 2008).

1.3.8.2 Soft callus (fibrocartilage) formation- endochondral ossification

The initially formed granulation tissue is gradually replaced by fibrous tissue, forming a soft callus. Mesenchymal stem cells (MSCs) directly differentiate towards osteoblasts, (regulated by present growth factors and perceived mechanical stimuli). This is usually observed near the cortex, away from the fracture site, producing woven bone matrix, forming a hard callus (intramembranous ossification) (Carano and Filvaroff, 2005; Geris et al, 2008).

Many fractures may also heal by the process of endochondral ossification (Schindeler et al, 2008). Endochondral ossification is characterised by a recruitment, proliferation and differentiation of undifferentiated mesenchymal cells into cartilage which becomes calcified forming a bony callus (Dimitriou et al, 2005). The semi-rigid soft (cartilaginous) callus provides a template for the bony callus that will later supersede it (Schindeler et al, 2008).

Mesenchymal progenitors differentiate into chondrocytes which synthesize cartilaginous matrix until previously deposited granulation tissue is replaced by cartilage. When cartilage production is deficient, fibroblasts replace the region with fibrous tissue (Dimitriou et al, 2005).

Fibroblast and chondrocyte proliferation/differentiation are stimulated by the coordinated expression of growth factors including TGF-β2 and –β3, PDGF, FGF-1 and IGF. Also, BMP-2, -4, -5 and -6) aid in the promotion of cell proliferation and chondrogenesis (Schindeler et al, 2008). The effects of these factors enable chondrocytes to produce significant amounts of extracellular matrix proteins, particularly collagen II (*ibid.*).

Chondrocytes mature into hypertrophic chondrocytes, biochemically preparing the cartilage matrix to undergo calcification (Geris et al, 2008).

1.3.8.3 Hard callus formation

The hard callus formation stage is also referred to as primary bone formation, which signifies the most active part of osteogenesis. Here, there is a high level of osteoblast activity and the formation of mineralised bone matrix. The soft cartilaginous callous is gradually removed by osteocytes, secreted by hypertrophic chondrocytes, and becomes mineralised with calcium hydroxyapatite, deposited by osteoblasts, which are oxygenated and subjected to the

appropriate mechanical stimuli, to form a hard callus of woven bone with simultaneous revascularisation (Dimitriou et al, 2005; Patel et al, 2008, Geris et al, 2008).

Soft callus remodelling involves the gradual removal of the fibrocartilage and replacement with woven bone. It was previously suggested that osteoclasts play a vital role in soft callus remodelling but recent evidence illustrates that they are mostly redundant in this process. Remodelling of the soft callus is described as a non-specific catabolic process which can involve the activity of different cell types (Dimitriou et al, 2005; Schindeler et al, 2008). Matrix metalloproteinases can be identified as a fundamental class of collagenases and gelatinases responsible for the breakdown of extracellular matrix (Dimitriou et al, 2005; Schindeler et al, 2008).

This new bone or hard callus is usually irregular and under-remodelled (Figure 1.9). Mature osteoblasts which differentiate from osteoprogenitors in the presence of osteogenic factors produce a combination of proteinaceous and mineralised extracellular matrix tissue which forms the irregular and unmodified hard callus (Dimitriou et al, 2005; Patel et al, 2008; Kanczler et al, 2010).

Osteogenic factors critical to this stage of bone healing include members of the BMP family which have the unique ability to induce *de novo* bone formation (Schindeler et al, 2008; Patel et al, 2008; Kanczler et al, 2010). The osteoprogenitor cells capable of promoting bone formation during repair include mesenchymal cells from the bone marrow. Osteoprogenitors may also be derived from other sources such as the surrounding vasculature and local tissues (Dimitriou et al, 2005; Schindeler et al, 2008).

Angiogenesis is very vital to the formation of the hard callus, with an increase in oxygen consumption at the local fracture site which is necessary for osteoblast differentiation (Schindeler et al, 2008, Kanczler et al, 2010). Newly generated blood supply to the callus is crucial for sufficient supply of nutrients, macromolecule transportation, cell invasion and maintenance of the appropriate metabolic microenvironment (Kempen et al, 2008; Kanczler et al, 2010).

Figure 1.9 The process of fracture healing. (a) Hematoma formation; (b) Soft callus formation; c) Hard callus formation; d) Bone modelling (Carano and Filvaroff, 2003).

1.3.9 Angiogenesis factors involved in bone repair

1.3.9.1 Vascular endothelial growth factor (VEGF)

VEGF is the major angiogenic factor involved in normal angiogenesis, appropriate callus architecture and mineralisation in fracture repair (Carano and Filvaroff, 2003). VEGF production is the major coupling mechanism between angiogenesis and osteogenesis during fracture repair (Geris et al, 2008).

VEGF expressed is detected on chondroblasts, chondrocytes, osteoprogenitor cells and osteoblasts (Kanczler and Oreffo, 2008; Geris et al, 2008). VEGF expression is induced by most osteoinductive growth factors as well as prostaglandins.

Additionally, VEGF has been observed to play a vital role in cartilage maturation and resorption. VEGF produced by hypertrophic chondrocytes instigates the endochondral ossification cascade by recruiting and differentiating osteoclastic cells that resorb cartilage and attracts osteoblasts (Geris et al, 2008). Exogenously administered VEGF, in the absence of osteoprogenitors or a scaffold, boosted bone formation in an *in vivo* model of mouse femur fractures (Carano and Filvaroff, 2003).

1. 3.9.2 Fibroblast growth factors (FGFs)

FGFs are potent angiogenic factors which are expressed by monocytes, macrophages, mesenchymal cells, osteoblasts and chondrocytes and exert their paracrine and autocrine effects on mesenchymal and epithelial cells, osteoblasts and chondrocytes (Montero et al,

2000; Dimitriou et al, 2005). FGF-2 has the capability to accelerate fracture when exogenously administered during the early healing stage of a fracture (Kanczler and Oreffo, 2008).

FGF- 2 has been shown to be an important modulator of cartilage and bone cell function (Montero et al, 2000). α-FGF majorly stimulates chondrocyte proliferation and β-FGF stimulates chondrocyte maturation and bone resorption (Dimitriou et al, 2005). Although its mechanism of action has not been properly elucidated, it has the ability to instigate angiogenesis, the proliferation and differentiation of osteoblasts to aid in the repair of bone fractures (Paccica et al, 2003; Carano and Filvaroff, 2003; Kanczler and Oreffo, 2008).

According to Paccica and colleagues (2003), the presence of β-FGF increased blood flow and vessel formation in the zone of distraction osteogenesis. An increase in the expression of VEGF and β-FGF were observed in distraction osteogenesis. Distraction osteogenesis is a unique and effective way to treat limb length inequality resulting from congenital and posttraumatic skeletal defects. Bone is surgically broken into two and segments separated gradually, allowing new bone to form in the distraction gap. B-FGF was found to localise at the leading edge of the distraction gap, where budding osteogenesis was emerging.

1.3.9.3 Matrix metalloproteinases (MMPs)

Matrix metalloproteinases (MMPs) are a family of extracellular endopeptidases that selectively degrade components of the extracellular matrix which allows the invasion of new blood vessels into the avascular hypertrophic cartilage (Schnaper et al, 1996; Schindeler et al, 2008). They generally require zinc in their catalytic site for activity. They are synthesised as inactive zymogens which are proteolytically cleaved to become active, in the extracellular matrix (Rundhaug, 2003).

MMPs are well associated with angiogenesis. They are produced by an array of cell types which include epithelial cells, fibroblasts and inflammatory cells. They contribute to angiogenesis not just by the degrading extracellular matrix (ECM), allowing endothelial cells to detach and migrate into new tissue, but also by releasing angiogenic factors (bFGF, TGF-β and VEGF) bound to the extracellular matrix (Schnaper, et al, 1996; Stetler-Stevenson, 1999; Rundhaug, 2003).

MMPs are also necessary for tube formation (Rundhaug, 2005). Treatment of endothelial cells with exogenous MMP-2 induced a dose-dependent morphologic change of tube formation, associated with angiogenesis. Conversely, the effect reaches a plateau and any further addition of MMP-2 reversed tube formation. These effects were observed to be MMP-2 activity as they were inhibited by TIMP-2 (tissue inihibitors of metalloproteinase-2) (Schnaper et al, 1996; Stetler-Stevenson, 1999). Angiogenic factors can induce the expression of MMPs in endothelial cells and stromal cells but MMPs can improve the bioactivity of these angiogenic factors (Rundhaug, 2005)

1.3.10 Osteoporosis

Osteoporosis is the absence of equilibrium between formation and resorption in the bone microenvironment that constitutes a disease state such as in osteoporosis or primary hyperthyroidism.

Osteoporosis is a systemic disease condition of micro-architectural loss of bone characterised by a reduced mineral density (BMD) and weakened bone structure which increases bone fragility and decreases bone resistance to low-energy trauma (Downey and Siegel, 2007; Hanley et al, 2012). Causes of osteoporosis include the following: poor bone acquisition during youth and acceleration bone loss during aging; a combination of hormone deficiency, poor nutrition, decreased physical activity and various pharmacological agents (Downey and Siegel, 2007).

The major cause of osteoporosis is the decrease in the female sex hormone, estrogen, which is referred to as post-menopausal osteoporosis. An increase in bone resorption is related to a rise in the number of osteoclasts, which is connected to a decrease in estrogen production. The increase in osteoclasts is caused by an increase in the cytokines that regulate the production of osteoclasts (Downey and Siegel, 2006).

1.3.10.1 Delivery and carrier systems for the treatment of osteoporosis

Different literature has been published on the localized delivery of growth factors (also recombinant growth factors) using bone implants with materials such as hydroxyapatite, biodegradable polymers and titanium (Linkhart, Mohan and Baylink, 1996; Devescovi et al, 2001).

There are various possible problems related with the use of peptide growth factors in the therapy of osteoporosis. One of the observable issues is that of delivery. With peptides having short half-lives, their parenteral delivery causes a severe limitation with osteoporotic patients (Mundy et al, 2001). This is because most bone factors have non-osteogenic functions and thus will have adverse side effects when administered systematically. Such effects include hypoglycaemia (for IGF-1) or fibrosis due to mesenchymal cell proliferation (TGFβ) (Mundy et al, 2001). This is the rationale behind the local administration of growth factors to bone.

According to Schliepaeke (2010), an ideal carrier system or in paraphrase, a polymer suitable for the delivery of bone growth factors would provide sufficient mechanical strength to withstand soft tissue pressure in addition to connecting penetrability and degradability for unhindered bone ingrowth and eventual replacement by regenerated bone on the other. Most carriers for the delivery of growth factors have such growth factors adsorbed to their surface by soaking. This type of loading process generates a burst release of growth factors in most cases (Schliepaeke, 2010).

The biofunctionalization of carriers is reliant upon the characteristics of the carrier material/ polymer with respect to degradability. For non-biodegradable materials, loading of the growth factors onto the surface will be suitable. Conversely, in the case of biodegradable materials, it is more suitable and desirable for the growth factors to be incorporated into the polymer matrix for gradual release over time with regard to degradation (Schliepaeke, 2010).

Polymers with low melting points will be most suitable for the controlled release of bone growth factors as high melting points will denature the proteins or impair the functionality of the proteins. Therefore, a biodegradable polymer will be the material of choice in this study.

Based on its unique function of stimulating ectopic bone formation, bone morphogenetic protein (BMP, bone growth factor) has been complexed and adsorbed on various materials mentioned previously in various literatures. Its ability to stimulate bone formation by inducing the proliferation of osteoblasts, as well as indirectly stimulate angiogenesis (formation of blood vessels) has been exploited in the research areas of orthopaedics (bone tissue engineering, bone fracture healing, bone implantation) (Sigurdsson et al, 1997; Liu, Engest and Kuffer, 2007; Fei et al, 2008) and dentistry (osteointegration of dental implants) (Sasche and Wagner, 2005). However, the incorporation of bone growth factors into the polymer matrix has not been explored. In this present study, the adsorption of bone growth factors adsorbed onto a polymeric coating is to be exploited in the present study.

1.4 TOPICAL AND TRANSDERMAL DRUG DELIVERY

1.4.1 Topical Delivery

Topical delivery is the delivery of drugs with the skin as the target organ (in comparison to transdermal delivery, which aims at the delivery of drugs to the systemic circulation). To understand topical delivery, the structure of the skin should be elucidated.

The skin's structure is sub-divided into three main layers as illustrated in Figure 1.10 (Desai and Lee, 2007).

- **Epidermis:** This is the uppermost layer of the skin, consisting of cells such as Langerhans cells, melanocytes and the stratum corneum as its outermost part. The stratum corneum comprises dead flattened cells, (made of a tough, fibrous protein *keratin*), embedded in a lipid bilayer, which serves principally as a waterproof barrier. These cells are continuously replaced with newer cells that move upward.
- **Dermis:** This is a thick layer of connective tissue which comprises hair follicles, nerve endings, sweat glands and blood vessels. Drug molecules that successfully diffuse through the epidermis are distributed systemically due to the rich supply of blood vessels here.
- **Subcutaneous (Fat) layer:** This layer aids in body temperature regulation. Certain drugs accumulate here, decreasing plasma concentration of drugs.

Figure 1.10 Structure of the skin. (Adapted from Ahava, 2012)

1.4.2 Transdermal Delivery

The transdermal route of drug delivery is a viable route of administration in comparison to the oral route, through which several drugs are administered into the systemic circulation.

In a transdermal drug delivery system (TDDS), the drug is stored in the either in a reservoir or impregnated into the fabric of the patch. A drug concentration gradient is developed when a TDDS is applied to the skin and the drug starts to move down the gradient. A second drug reservoir is established in the stratum corneum. As the drug moves further into the skin, it is absorbed into the local capillary vasculature and is then transported into the systemic circulation (Margetts and Sawyer, 2007).

There are two designs of transdermal patch currently available: the reservoir, or membrane-controlled system, and the matrix system. A reservoir patch holds the drug in a gel or solution and delivery is determined by a rate-controlling membrane between the drug reservoir and the skin (Margetts and Sawyer, 2007; Praunitz and Langer, 2008).

The rationale behind transdermal delivery (advantages) and limitations is highlighted in Table 1.5 and 1.6 respectively.

Table 1.5 Advantages and limitations of transdermal drug delivery

(Delgarro-Charro and Guy, 2001; Desai and Lee, 2007; Ranade and Hollinger, 2004; Prausnitz and Langer, 2008)

Advantages of transdermal delivery
Avoids first pass metabolism *It is a significant option for delivering drugs that undergo extensive first pass hepatic metabolism and with poor oral bioavailability.*
Constant plasma concentration *Drug administration creates a steady drug serum concentration during the dosing interval. In some cases, this is related to rarer systemic side effects of drugs.*
Advancement over traditional hypodermic injections *It offers an advantage over hypodermic injections which are painful, create hazardous medical waste and can pose a risk of disease transmission by needle re-use, in the case of developing countries.*
Reduces dosage frequency *It is a very useful route of delivery for drugs with short half-lives and reduces dosage frequency.*
Permits self-administration *Drug administration via a transdermal patch is user-friendly, convenient and permits self-administration. It allows for improved patient compliance and acceptability of drug therapy.*
Alternative to oral route *It is a vital alternative route of administration for patients with difficulty in tolerating oral delivery of drugs or are susceptible to gastrointestinal irritation; it is also suitable for nauseous or unconscious patients.*
Easy cessation of therapy *Drug therapy can be withdrawn immediately*

Table 1.6 Limitations of transdermal delivery

(Delgarro-Charro and Guy, 2001; Desai and Lee, 2007; Ranade and Hollinger, 2004; Prausnitz and Langer, 2008)

Limitations of transdermal delivery
Constricted criteria
Drugs suitable for transdermal delivery need to meet certain physicochemical criteria. Drugs that have large molecular weights or hydrophilic character are poor candidates. Lipophilic drugs are better candidates for transdermal delivery.
Tailored to potent drugs
Transdermal drug are only suitable for relatively potent drugs especially those that have effective plasma concentrations in the nanomolar/ml range.
Incidence of skin irritation
Skin irritation and sensitisation can be a problem with transdermal delivery. A skin reaction can occur if a drug, vehicle, adhesive or permeation enhancers are irritating to the skin. Rotation of the application site can minimize side effects

As seen above, the limitations of traditional transdermal delivery (via patches) is primarily associated with the barrier function of the skin, offering protection from chemicals and invasive pathogens, which limits the amount and the type of drug delivered via the skin to the systemic circulation (Desai and Lee, 2007, Delgaro-Charro and Guy, 2001). Some physicochemical factors generally affect topical and transdermal delivery. They are shown in Table 1.7.

It is noteworthy to mention that the second and third generations of transdermal technology have overcome a number of these limitations. The second-generation transdermal systems focus on the use of conventional chemical enhancers (liposomes, dendrimers, and in some cases, prodrugs) to enhance skin permeation, iontophoresis and non-cavitational ultrasound, which provide a driving force for drugs across the stratum corneum. The third-generation transdermal systems cause a stronger disruption of the stratum corneum, while still protecting deeper tissues. Such methods include novel chemical enhancers, electroporation, cavitational ultrasound and more recently microneedles, among others. These have demonstrated delivery of macromolecules and vaccines.

Transdermal delivery (and topical delivery) is highlighted in this paper because of the potential use of non-aqueous silicone elastomer gels in these areas. As explained in later sections, gels are well-known conventional dosage forms in these areas of drug delivery. These non-aqueous silicone elastomer gels offer an added advantage: they are suitable

vehicles for hydrophobic drugs (Sene *et al*, 2002), as hydrophobicity is a criterion for effective topical delivery into the dermis and transdermal delivery into the systemic circulation (Delgaro-Charro and Guy, 2001).

Table 1.7 Physicochemical properties affecting transdermal delivery

(Desai and Lee, 2007; Barry, 2002)

Physicochemical properties affecting transdermal delivery
Molecular size
The permeation of a drug through the skin is as a result of passive diffusion through the stratum corneum and this varies largely from drug to drug.
Skin hydration
This increases the rate of drug penetration through the skin.
Drug concentration
Drug concentration in the formulation and the surface area to which dosage form is applied directly affect the rate of drug transport through the skin.
Diffusion co-efficient (D)
The diffusion co-efficient (D) in a topical vehicle is dependent on the properties of the drug and the diffusion medium and the interaction between them.
Partition co-efficient (K)
the partition co-efficient is important when establishing the flux of a drug through the stratum corneum when it presents itself as the major diffusional barrier, of which it differs from drug to drug, vehicle to vehicle.

Transdermal systems became popular for the delivery of viable drugs such as NSAIDs (fentanyl), Scopolamine, its use in hormonal replacement therapy (Estradiol, Nitro-dur, etc), smoking cessation (nicotine patches), among other implications (Delgaro-Charro and Guy, 2001). These non-aqueous silicone elastomer gels can also be employed as delivery systems for protein or peptide delivery (such as delivery of vaccines). Although proteins are generally hydrophilic and do not meet the physicochemical criteria of drug candidates for transdermal delivery, these gels can be employed in new delivery technologies to enhance transdermal delivery.

The delivery of cancer drugs to the skin, via these silicone elastomer gels, can be inferred. Although the delivery of drugs for cancer prophylaxis is presently available (Moses, Brem

and Langer, 2003), cancer drug candidates can be delivered to the skin locally in close proximity to diseased cells, for treatment of pre-malignant skin conditions such as actinic keratosis and non-melanoma skin cancers such as squamous skin cell cancer or basal skin cell cancer, with existing cancer drugs such as 5-fluorouracil, imiquimod, 5-aminolevulinic acid (ALA) (using photodynamic therapy) and diclofenac sodium. This mode of therapy can minimise side effects while enhancing drug efficacy (McGillis and Fein, 2004).

1.4.3 Gels as Drug Delivery Systems

Gels are defined as semi-solid systems made of small amounts of solid distributed in copious amounts of liquid vehicle, assuming solid-like properties. They form a three-dimensional polymeric matrix, which are made of physically, or chemically linked polymer chains (das Neves and Bahia, 2006).

The use of polymeric gels as pharmaceutical dosage forms is extremely popular. Gels are widely used in oral, topical, transdermal as well as in vaginal drug delivery (das Neves et al, 2009). These gels are generally manufactured using hydrophilic polymers which include: poly (acrylates), chitosan, cellulose derivatives (such as hydroxyethyl cellulose, hydroxypropyl cellulose, sodium carboxy-methyl-cellulose), hyaluronic acid and its derivatives, pectin, starch, poly (ethylene glycol), sodium alginate, etc. (Valenta and Aulner, 2004). These gels are also incorporated into other dosage forms (such as gelling/thickening agents in syrups and cosmetics) (Allen, Popovich and Ansel, 2011).

Silicone as a polymer has played a vital role in drug delivery, biomedical applications as well as in cosmetics since its introduction in the 1950's (Sene *et al*, 2002, Colas, Siang and Ulman, 2006). The varying applications of silicone range from its use in the manufacture of catheters, cardiac pacemakers, stents and shunts; its use as drug excipients, actives in topical formulations, as drug delivery systems such as pressure sensitive adhesives and antifoams; to its use in cosmetics such topical creams, personal care products and sexual lubricants (Colas, Siang and Ulman, 2006).

The use of non-aqueous silicone elastomer gels was recently reported for use as a vaginal delivery system for maraviroc, a HIV-1 entry inhibitor (Forbes et al, 2011). Based on the usefulness and variability of the applications of silicone in transdermal, topical and vaginal drug delivery in the past, the rationale behind drug delivery via these routes will be discussed.

1.4.4 Pharmaceutical Characterisation of Gels

1.4.4.1 Rheological and textural characterisation of gels

Rheology is defined as the study of the deformation and flow of matter (Al-Achi, 2013). Viscosity (η) can be described as the resistance of a fluid to flow or movement. Viscosity is usually illustrated as a hypothetical cube made up of thin layers. When a force (shearing force) is applied to the top layer, the layers will move at a decreasing velocity and the bottom layer will be motionless. The force applied to the top of the cube is defined as the shear stress (σ) and is expressed in Newtons per m^2. A velocity gradient, or the shear rate (Y), will exist and is equated to the differential change in velocity divided to the height of the hypothetical cube, expressed in m s^{-1}. Viscosity is defined as the ratio of shear stress to shear rate (Al-Achi, 2013).

1.4.4.2 Newtonian and non-Newtonian fluids

The concept of viscosity was initially quantified by Newton who assumed that the rate of flow (Y) was directly proportional to the applied stress (σ). In simple fluids which obey this relationship in which the shear stress divided by the shear rate remains equal independent of the shear rate, are referred to as Newtonian fluids. Examples include water and glycerol.

Conversely, many common liquids are rather complex fluids and do not follow this relationship and are referred to as non- Newtonian. Such fluids are defined as those fluids in which the relationship between shear stress and shear rate is not a constant. Variation in shear rate is not directly related to the shear stress. Examples include emulsions, suspensions and gels.

1.4.4.3 Non- Newtonian fluid behaviours

1.4.4.3.1 Plastic (or Bingham) flow

Plastic or Bingham flow refers to when a material does not flow until a certain value of shear stress is exceeded of which at lower stresses the substance behaves as a solid (elastic) material. As shown in figure 1.11, such behaviour is illustrated when the rheogram does not pass through the origin but intersects with the shear stress axis at a point referred to as the yield value, σy. Plastic materials are often referred to as Bingham bodies (who performed original studies with these materials). Plastic flow is exhibited by concentrated suspensions, particularly if the continuous phase is of high viscosity or if the particles are flocculated.

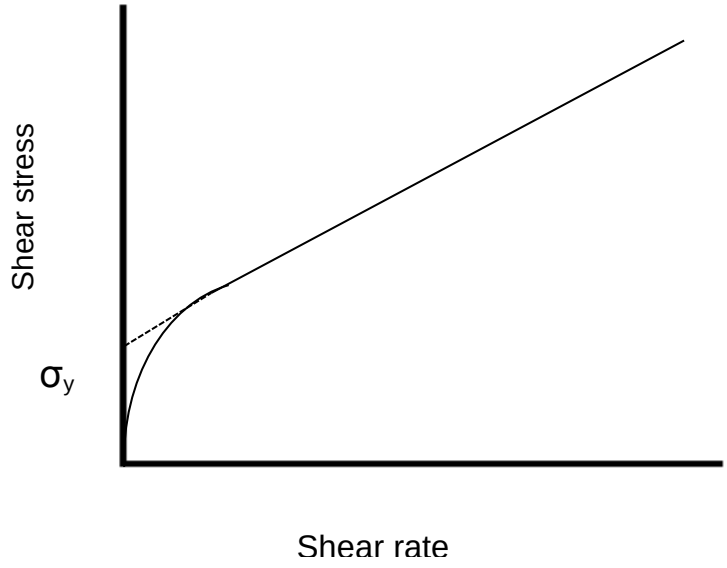

Figure 1.11 Rheogram illustrating plastic behaviour of materials

1.4.4.3.2 Pseudoplastic flow

Pseudoplastic fluids demonstrate a decreasing viscosity with an increasing shear rate. This is also referred to as shear thinning (Al-Achi, 2013). Such fluids have no singular characteristic value of viscosity. Such viscosity is referred to as apparent viscosity and is only relevant when related to the shear rate with which it was measured. A range of apparent viscosities is required to characterise a pseudoplastic fluid, by means of a flow curve (Figure 1.12)

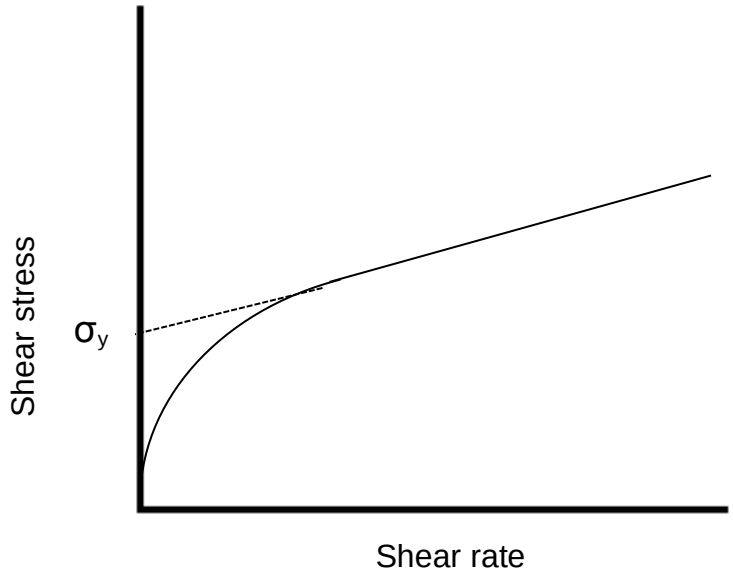

Figure 1.12 Rheogram illustrating pseudoplastic behaviour of materials (shear thinning).

In the absence of an adequate quantitative elucidation of pseudoplastic flow, the most extensively used is the Power Law, given as:

$$\sigma^n = \eta' \dot{\gamma}$$

Where η' is a viscosity co-efficient and the exponent *n* an index of pseudoplasticity.

Materials that exhibit pseudoplastic behaviour include naturally and chemically modified hydrocolloids such as methylcellulose and tragacanth, synthetic polymers such as polyvinylpyrrolidone and polyacrylic acid, paints, emulsions and various other dispersions.

1.4.4.3.3 Dilatant flow

A dilatant fluid is characterised by an increasing viscosity caused by an increase in shear rate (the opposite behaviour of pseudoplasticity). As such a material increases in volume during shearing, they exhibit shear thickening (Figure 1.13).

Although this behaviour is less common than pseudoplasticity, it may be exhibited by fluids containing high levels of small deflocculated particles such as clay slurries, corn starch in water, sand/water mixtures, etc.

In conditions of zero or no shear, the particles are closely packed and the interparticulate spaces are at a minimum, sufficient for the vehicle to fill. At low shear rates, the fluid adequately lubricates the relative movement of the particles. As the shear rate is increased, the uniform distribution of the particles is disrupted and clumps are formed, resulting in creation of larger voids wherein the fluid drains into, increasing the resistance to flow and a rise in viscosity. This effect is progressive with an increase in shear rate. However, the effect is reversible and the removal of shear rate restores the fluid nature.

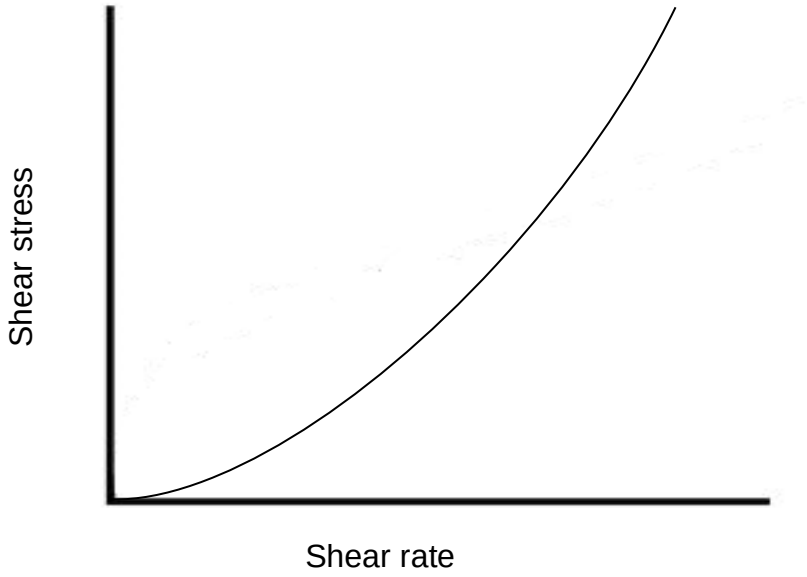

Figure 1.13 Rheogram illustrating dilatant behaviour of materials (shear thickening)

1.4.4.2 Rheological Testing of Gels

Rheological testing provides information about the structure of materials and the effect that time or an applied force has on such a material (das Neves et al, 2009).

The constituents of a gel can strongly influence its rheological properties. These rheological properties partly govern important features such as spreadability and retention characteristics at the application site (vital in mucosal delivery) which culminate to the final clinical outcome of the drug incorporated into the gels (Jones, Woolfson and Brown, 1997). The rheological and mechanical properties of gels are generally characterised using oscillatory rheology and texture profile analysis (TPA) respectively (das Neves and Bahia, 2006).

1.4.4.2.1 Oscillatory rheometry and texture profile analysis

Oscillatory rheometry allows for complete characterisation of both elastic and viscous components of the gels studied (das Neves and Bahia, 2006). As gels (particularly hydrophilic gels) exhibit non-Newtonian flow behaviour, a single measurement of viscosity at a defined shear rate is insufficient in the characterisation of a gel sample. Thus, a 'multipoint' measurement able to decompose the rheological behaviour of the gel into viscous and elastic components is usually employed (das Neves and Bahia, 2006).

Texture profile analysis (TPA) provides vital information on the mechanical parameters of the gels such as hardness (force required to attain a given deformation), adhesiveness (the work necessary to overcome the attractive forces between the surface of the sample and the surface of the probe) and compressibility (the force per unit time required to deform the product the first compression cycle of the probe) (Jones, Woolfson and Djokic, 1996; Jones, Woolfson and Brown, 1997). As topical administration of gels will be subjected to shearing forces like those encountered under physiological conditions, the effect of such oscillatory stresses, on the structural properties of the gels are also quantified with these methods (Woolfson and Brown, 1997).

To characterise the rheological properties of a gel using oscillatory rheometry, controlled stress rheometers are employed. Dynamic stress tests are performed to expose the gel sample to a range of shear forces similar to physiological shear rates within a time limit to analyse the effect of such forces on the gel sample. Cone and plate geometry (in comparison with plate-plate geometry, using steel plates) are often used. TPA involves the use of a solid analytical probe which is depressed twice into a sample to a defined depth and at a specific rate, permitting a delayed period between successive compressions (das Neves et al, 2009; Jones, Woolfson and Brown, 1997).

1.4.4.3 In vitro permeation studies (diffusion testing) of hydrophilic and non-aqueous silicone elastomer gels

As previously established, transdermal (and topical) drug delivery are advantageous as alternative routes of drug administration having the primary attribute of avoiding first pass metabolism of drugs by the liver as well as decreasing side effects. to further characterise topical (or transdermal) dosage forms, permeation studies need to be performed to ascertain the biocompatibility of the dosage form as well as establish the permeation characteristics of drugs at the site of administration (Ng et al, 2010; Levintova, Plakogiannis and Bellantone, 2011). The most popular and basic *in vitro* permeation experiments are performed using Franz cell type experiments *(*Ng et al, 2010).

In vitro diffusion is the passive diffusion of a permeant (drug) from a vehicle to the donor, through a synthetic or biological membrane into a receptor fluid. The permeant is the molecular species or compound moving through or into the membrane. Permeation is the movement of the permeant through the membrane encompassing partitioning and diffusion through the membrane. Flux is the amount of permeant that crosses the membrane per unit area into the circulating system per unit time. For an *in vitro* permeation system, this is expressed in unit mass per unit area per unit time. Diffusivity is a property of the permeant and it is a measure of its penetrability through a specific membrane expressed in units of area per unit time. The permeability co-efficient describes the rate of permeant penetration per unit concentration expressed in distance per unit time. The permeability barrier is a lipid barrier dependent on the amounts, types and organisation of lipids present in a tissue.

Generally, there are a few important considerations that are considered before *in vitro* permeation is investigated which are highlighted below:

1.4.4.3.1 Franz cell set-up

Static cell (vertical or side-bi-side): With static cell set-ups, the receptor chamber has a fixed volume (containing a stirred receptor fluid), `whose compartment is water jacketed to control temperature, as well as a sampling port. The flux (rate of permeation across the membrane) is determined by the permeability of the compound and the permeation of the tissue. The flux in turn determines the concentration of the permeant in the receptor chamber.

Continuous flow cell: Continuous flow cell also has a fixed volume receptor, water jacketed to control temperature. However, Franz type cells are stirred, have continuous flow which causes turbulence in the receptor and simulates stirring. This set-up mimics *in vivo* (equates blood flow), evaluates compound uptake into membranes, finite or infinite dose permeation and steady state flux of compounds. The flux also determines the permeation of the compound and permeability of the tissue. The flux thus determines the concentration of permeant in the receptor chamber and also the rate of clearance (flow rate).

1.4.4.3.2 Membrane type

Human tissue *ex vivo*, small animals (like rats, mice or rabbits), large animals (such as dogs, pigs, etc.), polymeric membranes (usually an appropriate inert synthetic membrane such as polysulfone, cellulose acetate/nitrate mixed ester, silicone, etc.) or human skin equivalents (tissue engineered three-dimensional skin constructs) are the types of membranes usually employed for Franz cell experiments dependent on various methodologies (Permegear, 2012). Though synthetic membranes will not offer an adequate representation of lipid perturbation effects undergone by biological samples, diffusion behaviour can be inferred. They are also preferred as the most cost effective, easily sourced and structurally simpler alternative to skin (Ng et al, 2010).

1.4.4.3.3 Donor formulation

As aforementioned, gels, creams, suspensions, powders or adhesive patches have been identified as transdermal and/or topical and/or vaginal dosage forms. A variation of the formulation, drug concentration and the addition of permeation enhancers give information about the characteristics of the permeant.

The concentration (of drug or permeant) in the vehicle will depend on the study aims. An infinite dose, in which the drug will not be depleted from the vehicle during the experiment, will be used to understand the permeation behaviour in the absence of enhancers. Such an experiment is similar to Franz cell *in vitro* permeation validation, which analyses the amount of drug that can permeate through the membrane for a specific duration (Ng et al, 2010). Consequently, a finite dose will mimic the actual amount of drug/permeant in marketable dosage forms. It could be used to determine the amount of active ingredient (drug or permeant) needed in the dosage form to demonstrate an effective drug response.

1.4.4.3.4 Receptor media

The most important consideration of the choice of receptor media is its *in vivo* application. The selection of receptor media is also dependent on the nature of the drug/permeant and type of diffusion cell used. The solubility of the drug/permeant is also an important factor because the compound needs to be at its desired form in the donor compartment to prevent any slow rate of diffusion which will cause solubility to be another rate-limiting step of its diffusion. Aqueous receptors are used for hydrophilic to moderately hydrophobic permeants while more hydrophobic permeants will require an addition of polar solvents or surfactants to the receptor media.

1.4.4.3.5 Sampling time

Sampling time intervals, frequency and volume are dependent on the research question. Possible experimental rationale includes: determining the total amount if drug/permeant that diffuses through or is retained in the membrane after a long interval, the amount of drug that crosses the membrane at shorter sampling intervals or the flux of drug diffused per time interval.

These factors when considered enable the researcher to correctly answer the research question to be investigated and thus, the in vitro permeation studies adequately represent the in vivo application for the topical/transdermal dosage form being examined for drug delivery.

1.5 NANOPARTICULATE CARRIERS FOR THE TREATMENT OF BONE INFECTIONS

1.5.1 Osteomyelitis

The term “osteomyelitis” comprises a broad group of infectious diseases characterized by infection of the bone and/or bone marrow (Roy et al, 2012). It is usually simultaneous with bone destruction and caused by a pathogenic micro-organism (Prieto-Perez et al, 2014).

Osteomyelitis is a progressive infection that results in inflammatory destruction, necrosis, and new bone formation, which can progress to a chronic and persistent stage. This disease is classified based on etiology, pathogenesis, and degree of bone involvement, as well as age and the immune condition of the patient. It can involve different structures such as the bone marrow, cortex, periosteum, and parts of the surrounding soft tissues, or remain localized (Jorge, Chueire and Baptista, 2009). Given this heterogeneity, the following methods of classification have been proposed.

1.5.2 Classification systems for osteomyelitis

1.5.2.1 Waldvogel classification

One of the most important classifications of osteomyelitis relevant in clinical studies is the Waldvogel classification of osteomyelitis (Lima et al., 2014; Table 1.8). Osteomyelitis is divided according to physiopathology and duration of infection. Based on the physiopathology, infections are classified into: haematogenous osteomyelitis; osteomyelitis secondary to a contiguous focus of infection; and osteomyelitis associated with peripheral vascular insufficiency. Based on the evolution of disease, infections are classified into acute and chronic osteomyelitis (Low and Waldvogel, 2004).

Table 1.8 Waldvogel classification of osteomyelitis *(Adapted from Lima et al., 2014)*

1.5.2.2 Cierny and Mader classification

In Cierny and Mader classification, osteomyelitis is divided according to bone anatomy and physiological factors of the host. Here, four anatomical stages are described, according to specific bone involvement and three types of hosts, based on patient's clinical conditions (Lima et al., 2014). This classification system is most useful in defining treatment strategies and takes into account only infections in the long bones of the body (Lew and Waldvogel, 2004).

1.5.3 Pathogenesis of Osteomyelitis

In vivo animal studies of bone infection have demonstrated that the bone is normally resistant to infection. Therefore, osteomyelitis occurs only when there is a large inoculum of pathogens, trauma leading to bone damage or the presence of foreign material (Eid and Berbari, 2012). The pathogenic mechanism of osteomyelitis is influenced by a number of factors which begins with the spread of the organism. Bacterial infection may reach the bone

by haematogenous seeding, direct inoculation and airborne contamination, which can occur as a result of fractures or as a post-surgical complication (Gogia et al, 2009). Fungal osteomyelitis usually results from a spreading fungal infection in the body rather than direct inoculation of the bone. Once osteomyelitis reaches a chronic state, it can progress to affect surrounding muscles, tendons, and skin (Eid and Berbari, 2012).

Bacteria enter the bone haematogenously through the Haversian system, the structural unit of the bone (osteon) (See Figure 1.14). They adhere to the bone and trigger an acute inflammatory response. Bacteria have various different mechanisms to facilitate cell-cell and cell-implant adhesion (Gogia et al., 2009). Certain major causes of infection, such as *Staphylococcus aureus,* adhere to bone by expressing receptors (adhesins) for components of bone matrix (fibronectin, laminin, collagen, and bone sialoglycoprotein); the expression of the collagen-binding adhesion permits the attachment of the pathogen to cartilage (Lew and Waldvogel, 2004; Popat et al., 2007 Sanchez et al., 2013; Arciola et al., 2015).

Figure 1.14 Cross section of the bone structure. The diagram illustrates the singular units of bone structure (osteons) as well as the spatial arrangement of compact and spongy bone types (Reproduced from National Cancer Institute, 2016).

During an acute infection, various inflammatory factors and leukocytes are attracted to the inflamed area, to generate toxic oxygen radicals and secrete enzymes in an attempt to kill the bacteria. Pus resulting from the inflammatory response spreads into vascular channels, raising intraosseous pressure and impairing blood flow. Vascular channels become compressed and obliterated resulting in ischaemia and contributing to bone necrosis. Bone segments void of viable blood flow become separated to form *sequestra* (Figure 1.15) and may continue to harbour bacteria. Antibiotics and inflammatory cells cannot reach this avascular area leading to failure in treatment. Outside the sequestrum, there is reactive hyperaemia associated with increased osteoclastic activity. This activity in turn causes bone loss and localised osteoporosis. Meanwhile, bone apposition occurs with new bone forming around the sequestrum.

Figure 1.15 Steps in the progression of chronic osteomyelitis

I: From sequestrum, an area of devascularised dead bone, progression of intramedullary infection towards an intra-capsular location can lead to septic arthritis; progression of infection towards a sub-periosteal location can lead to periosteal elevation. II: New bone formation as a result of massive periosteal elevation. III: Extension of sequestrum and necrotic material through cortical bone creates a fistula and ultimately breaks through the skin *(Adapted from Lew and Waldvogel, 2004).*

1.5.4 Causal organisms

Among pathogenic microorganisms, *Staphylococcus aureus* is by far the most commonly involved in osteomyelitis in humans, followed by *Enterobacteriaceae* and *Pseudomonas* species (Lew and Waldvogel, 2004; Gogia et al., 2009). A summary of diverse etiology of osteomyelitis is summarised in table 1.9. *S. aureus* elaborates a range of extracellular and cell-associated factors contributing to its virulence. First are factors promoting attachment to extracellular matrix proteins, called bacterial adhesins. The ability of *S. aureus* to adhere is

considered crucial for the early colonisation of host tissues, implanted biomaterials, or both. *S. aureus* expresses several adhesins on its surface, each specifically interacting with one host protein component, such as fibrinogen, fibronectin, collagen, vitronectin, laminin, thrombospondin, bone sialoprotein, elastin, or von Willebrand factor. The second set of factors promotes evasion from host defences (protein A, some toxins, capsular polysaccharides). The third set promote invasion or tissue penetration by specifically attacking host cells (exotoxins) or degrading components of extracellular matrix (various hydrolases). Finally, the ability of *S. aureus* to invade mammalian cells may explain its capacity to colonise tissues and to persist after bacteraemia. *S. aureus* can promote its endocytic uptake by epithelial or endothelial cells. *S. aureus* that has been internalised by cultured osteoblasts can survive within the cells. Intracellular survival could explain the persistence of bone infections (Jorge et al, 2009; Gogia et al., 2009; Gomes, Pereira and Bettencourt, 2013).

S. aureus and *S. epidermidis* can also form biofilms, which are difficult to treat with antimicrobial agents. A biofilm is a microbial community characterised by cells that attach to substratum or interface to each other, embedded in a matrix of extracellular polymeric substance, and showing an altered phenotype in terms of growth, gene expression, and protein production. Biofilms can act as a diffusion barrier to slow down the penetration of antimicrobial agents and nutrients. The inherent resistance of biofilms to antimicrobial factors seems to be mediated by several factors including low metabolic rates, adaptive stress responses, and downregulated rates of cell division of the deeply embedded microbes (Sanchez et al, 2013; Campoccia et al, 2010).

Table 1.9 Etiology of osteomyelitis

(*Lew and Waldvogel, 2004; Jorge et al, 2009; Calhoun, Manring and Shirtliff, 2009)*

Age	***Etiology***
Newborn babies	*S. aureus, Enterobacter spp., Streptococcus (Group A and B)*
Children	*S. aureus, Enterobacter spp., Streptococcus (Group B), Haemophilus influenza*
Susceptibility factors	***Etiology***
Injectable drug users	*S. aureus, P. aeruginosa, Serratia marcescens, Candida spp.*
Immunocompromised	*S. aureus, Bartonella hensalae, Aspergillus spp., Mycobacterium avium complex, Candida albicans*
Urinary infection	*P. aeruginosa, Enterococcus spp.*
Spinal column surgery	*S. aureus, coagulase-negatuve staphylococci, aerobic gram-negative bacilli*
Orthopaedic fixation devices	*S. aureus, coagulase-negatuve staphylococci, Propionibacterium spp.*
Hospitalisation (nosocomial source)	*Enterobacteriaceae, P. auroginosa, Candida spp.*
Diabetes mellitus, vascular insufficiency, contaminated open fracture	*Enterococcus spp., Gram-negative bacilli, anaerobes*

1.5.5 Local antibiotic therapy for osteomyelitis

The local use of antibiotics as a prophylaxis treatment for bone infections was incorporated in general medical practice in the 1970s. Buchholz and Engelbrecht first reported that bone cement mixed with antibiotics was effective in the prophylaxis and treatment of infection in total hip replacement using polymethylmethacrylate (PMMA) beads (El-Husseiny et al., 2011; Gogia et al., 2009). *In situ* transplantation of a local antibiotic delivery system worked to eliminate bacteria growth alongside reducing dead space in the bone defect (Nair et al., 2011). In 1979, Klemm fabricated gentamicin-impregnated beads and used them to occupy dead space after debridement of infected bone (Klemm, 1979).

The major advantage local antibiotic therapy offers over systemic therapy is lower serum antibiotic concentrations thus reducing toxicity-related side effects (Joosten et al., 2005; Nandi et al., 2009). Based on the commonly implicated causative microbes involved in osteomyelitis, the most widely accepted antimicrobial agents in local delivery systems are amino glycosides and to a lesser extent various β-lactam agents and quinolones. Importantly, a combination therapy of antibiotics proves useful in the reduction of the toxicity of individual agents, to prevent the development of antimicrobial resistance and to treat mixed infections involved in osteomyelitis and also demonstrate a synergistic effect (Nandi et al., 2009, Gogia et al, 2009). Antibiotic agents used in local bone delivery systems such as tobramycin, clindamycin, vancomycin, gentamicin, amongst others, are selected based on certain criteria (table 1.10).

Release of the antibiotic in such systems depends on the rate of dissolution of drug in its matrix allowing its penetration through the pores of the carrier. The amount of release in highly soluble β-lactam agents depends on the surface area of the carrier and on the initial concentration of the drug in the prepared systems. For relatively insoluble agents like quinolones; the rate of drug release depends on the porosity of the matrix and on the dissolution of the drug in the matrix (Allababidi and Shah, 1998).

Drug delivery systems (DDSs) developed for local delivery of antibiotics can be classified into non-biodegradable (or non-resorbable) and biodegradable (or resorbable) delivery systems.

Table 1.10 Criteria for determining antibiotic agents used in local bone delivery systems (*Kanellakopoulou and Giamarellos-Bourboulis, 2000, Nandi et al., 2009; Gogia et al., 2009, Campoccia et al., 2010)*

Criteria for use of antibiotics in local bone delivery
Activity against the most common bacterial pathogens involved in chronic osteomyelitis
Local release at concentrations exceeding several times (usually 10 times) the minimum inhibitory concentration (MIC) for the involved pathogen
Inability to trigger any adverse effects
Not enter the systemic circulation
Stability at body temperature
Favourable water solubility (B.C.S. Class I)

1.5.5.1 Non-biodegradable delivery systems

The most widely used non-biodegradable delivery systems for local antibiotic delivery are polymethylmethacrylate (PMMA) beads. The major drawback associated with non-biodegradable systems is the need to remove the system from the application upon completion of antibiotic release, due to non-biodegradability (Kanellakopoulou and Giamarellos-Bourboulis, 2000), thermal damage to the antibiotic and poor elution properties. Also, resistant bacteria may appear on the carrier-surface during the later stages of low level antibiotic release (Azi et al., 2010).

Commercially available polymethylmethacrylate (PMMA) cements consist of a powdered polymer mixed with a liquid monomer to form a solid structure. Currently, there are five antibiotic-laden PMMA bone cement products that are approved by the U.S. Food and Drug Administration (FDA). These five products include Simplex P, which contains 1 g tobramycin (Stryker Howmedica Osteonics, Mahwah, NJ); Palacos G, which contains 0.85 g gentamicin (Zimmer, Warsaw, IN); SmartSet GHV and SmartSet MHV, which contain 1 g gentamicin (Depuy Orthopaedics, Inc., Warsaw, IN), and the Prostalac prosthesis (DePuy Orthopaedics, Inc.). Premixed antibiotic PMMA beads are available and widely used in Europe under the name Septopal (Biomet Merck, Dordrecht, the Netherlands) and

popularized by Klemm (1979) but are not currently approved in the United States (Wu and Grainger, 2006; Gogia et al., 2009; Azi et al., 2010).

Non-commercial preparations of beads prepared by surgeons themselves are also in use. Physician-made beads are individually manufactured by the surgeon using commercially available PMMA polymer mixed with a powdered antibiotic or can be created with the assistance of an individually made bead mould. However, these types of beads have the disadvantage of a lack of thorough mixing of the antibiotic into the material and a lack of uniform size of bead, resulting in lower antibiotic availability (Nelson et al., 1997; Kanellakopoulou and Giamarellos- Bourboulis, 2000; Wu and Grainger., 2006).

the requirements of antibiotics incorporated into non-biodegradable delivery systems is their thermostability at high temperatures (up to 100°C, where polymerisation occurs) and hydrophilicity (Azi et al., 2010). Aminoglycosides, such as gentamicin and vancomycin, are heat stable and are therefore extensively used in these preparations (Nandi et al., 2009). The most extensively studied antibiotic is gentamicin, an excellent additive to PMMA, which is attributed to its broad spectrum of action and good thermostability (Gogia et al., 2009; Azi et al., 2010).

Drug elution characteristics from PMMA vary from one antibiotic to another. Leakage of antibiotic from minute cracks in the cement has been established as the mechanism of elution. Certain antibiotics such as polymyxin B sulfate, tetracycline and Chloramphenicol do not elute from PMMA due to their insufficient thermostability. It has been evidently observed that *in vitro* elution of both aminoglycosides and quinolones are at very high concentrations, but the peak of release occurs on the first day (Nandi et al, 2009).

1.5.5.2 Biodegradable delivery systems

The general criteria for selecting a polymer for use as a biomaterial are to match the mechanical properties and the time of degradation to the need of the application. The ideal polymer to be used for orthopaedic applications will exhibit the characteristics described in table 1.11

.

Table 1.11 Criteria for selecting biomaterials for orthopaedic applications

Criteria for biomaterial use in orthopaedic applications
Inability to induce an inflammatory/toxic response incommensurate to its beneficial effect.
Easily metabolised into its final degradation product, in the body during or after fulfilling its purpose in the body, leaving no toxic trace
Easily processed into its final product form
Adequate shelf life
Easily sterilisable before application

Since the advent of the use of PMMA beads introduced by Buchholz and Engelbrecht in 1970, an alternative osteomyelitis treatment has been investigated, more specifically a treatment which will make a follow-up surgery to remove PMMA beads after antibiotic release unnecessary (Campoccia et al., 2010). In addition, the use of PMMA in local antibiotic treatment has added disadvantages of development of antibiotic resistance due to prolonged release of sub-therapeutic levels of antibiotic, systemic toxicity to absorbed monomer in some cases and lack of participation in the bone healing process (Gogia et al., 2009;). These limitations of PMMA bone cement led to an investigation for other alternatives as vehicle antibiotic delivery systems. The major focus for this area of research has been on biodegradable materials (Kanellakopoulou and Giamar, 2000).

The use of biodegradable delivery systems in orthopaedic treatments also offers other advantages. An implant prepared from biodegradable polymer can be engineered to degrade at a rate that will slowly transfer load to the healing bone, thus eliminating the dead space and, eventually, to guide its repair (Middleton and Tipton, 2000; Nandi et al, 2009). The majority of these biodegradable materials are biocompatible and non-toxic, breaking down into degradation products, which are normal metabolites of the body's metabolism, making clearance from the body easier without any toxic build-up (Gunatillake and Adhikari, 2003).

Biodegradable delivery systems have been categorised into two major groups based on their material composition: natural-based and synthetic biodegradable delivery systems (Rezwan et al., 2006; El-Husseiny et al., 2011). Natural based materials are further classified based on their origin and can be either polysaccharides (starch, alginate, chitin/chitosan, hyaluronic acid derivatives) or proteins (soy, collagen, fibrin gels, silk). Synthetic biodegradable polymers comprise polyesters (such as poly (lactic acid) (PLA)

and poly (glycolic acid) (PGA), as well as poly(lactic-co-glycolide) (PLGA) copolymers), poly(e-caprolactone) (PCL), polypropylene fumarate (PPF) and poly-hydroxyalkanoates (PHB, PHBV, P4HB, PHBHHx, PHO)); polyanhydrides; bioactive glasses (BAGs) and calcium phosphates and other ceramics (Middleton and Tipton, 2000; Rezwan et al., 2006; Puppi et al, 2010; El-Husseiny et al, 2011).

1.5.5.3 Hydroxyapatite

Drug delivery systems (DDSs) exhibiting the properties of biocompatible bioceramics are highly desirable and are thus shaped as powders, blocks, cements, scaffolds, porous devices and coatings for this purpose (Mizushima et al, 2006; Zhou and Lee, 2011; Arcos and Vallet-Regis, 2013). One major example commonly used for this property is synthetic hydroxyapatite (HA). Hydroxyapatite is the inorganic component of the bone structure. Synthetic hydroxyapatite is chemically and structurally similar to the mineral phase of bone demonstrating remarkable osteogenic and osteoconductive properties (Itokazu et al, 1998).

Because of its chemical and structural similarities to the inorganic phase of human bone, hydroxyapatite (HA) shows excellent biocompatibility (Arcos and Regis, 2013). Many research studies have been focused on the use of hydroxyapatite as antibiotic carriers for treating bone infection, since their chemical composition is very similar to the bone mineral phase (Baro et al, 2002).

Induction of bone growth into HA blocks is very unfavourable because of its slow degradation rate and that it is slowly replaced by host bone after implantation (Mizushima et al, 2006). Porous HA bodies and granules are quite popular in the clinical setting to guide and allow new host bone in-growth through the pores (Zhou and Lee, 2011).

Synthesized HA is very brittle and therefore cannot be used for load bearing applications. Hence, implant materials composed of hard and soft phases (composite materials) are used for total bone replacement (Zhou and Lee, 2011). HA and other polymers are fabricated into composite materials to synergise the osteoinductive and osteogenic properties with the improved mechanical properties as well as good biocompatibility. Such polymers include poly-methyl methacrylate, poly (3-hydroxybutyrate-co-3-hydroxyvaleate), polyacrylic acid, poly (lactic acid-co-glycolic acid) polymers (PLGA) and carbon nano-tubes (CNTs), among others (Schnieders et al, 2006; Zhou and Lee, 2011).

Antibiotic impregnated hydroxyapatite has also been used to treat patients with chronic osteomyelitis after removing necrotic tissue. The ceramic material was gradually

incorporated into the host bone and uneventful healing was observed within three months with no recurrence of infection (Nandi et al, 2009).

Gentamicin loaded hydroxyapatite cement has been investigated using *in vitro* and *in vivo* studies for its effectiveness against post traumatic chronic osteomyelitis. In HA-gentamicin-treated animals, no growth was detectable after 7 days of culture. No histopathological evidence of infection was observed in the HA/gentamicin-treated group while different stages of chronic osteomyelitis were observed in other groups (Joosten et al, 2004).

Micro porous HA was analysed for antibacterial activation using three different antibiotics including gentamicin, in comparison to dense HA. Bacteria inhibition tests against different pathogenic bacteria were performed for testing the antibiotic adsorption and the microbiological effectiveness after loading with different antibiotics. Results demonstrated that the adsorbed amount on the micro-porous HA was largely higher than that on dense HA and an increase in the duration of antibiotic release was observed (Chai et al, 2007).

1.6 AIMS AND OBJECTIVES

Current literature has extensively investigated the use of ceramic nanoparticles, in particular, calcium phosphates, as nanoparticulate delivery systems for local delivery to the bone in form of coated transplants, scaffolds, composites or sponges as well as cements and blocks. However, there has been no research to harness the controlled release advantage of aquasomes, which can be likened to coated (or modified) ceramic nanoparticles for sustained delivery of bone growth factors or antibiotics to aid in bone regeneration. The aim of the present research is to investigate the potential of aquasomes as drug delivery systems to aid in fracture healing, treat bone infections and achieve the topical/ transdermal sustained delivery of proteins, antibiotics and growth factors.

Objectives

A summary of the objectives in this thesis are:

1. To investigate the amount of protein that can be adsorbed unto the nanoparticulate biodegradable polymers (aquasomes) using BSA as a model protein; and the amount of protein (BSA) that can be released over a specified period.
2. To investigate the effect of nanocore sizes (20nm, 40nm and 60nm compared with large HA nanoparticles and coating time on the calculated surface areas available for drug/protein adsorption.
3. To investigate the release of BSA from loaded aquasomes for topical/transdermal drug delivery using non-aqueous silicone elastomer gels (NASEGS) and aqueous semi-solid polymeric gels. (HPMC and HEC)
4. To characterize the rheological and textural parameters of NASEGS, HPMC and HEC gels and its correlation to protein (BSA) release
5. To analyse the feasibility of *in vitro* permeation of BSA from loaded aquasomes using Franz cell equipment.
6. To determine the amount of BSA that can be released from aquasomes (in comparison to drug/protein alone) without having a toxic effect on human cells, using human dermal fibroblasts (HDFa) as a model via MTT toxicology assay.
7. To investigate the efficacy of antibiotic (gentamicin) released from aquasomes by challenging its bactericidal activity against low and high inoculums of *S. aureus*.

8. To investigate the osteogenic, differentiation and angiogenic effects of growth factor loaded aquasomes (BMP-2 and VEGF 121) when exogenously added to osteoprogenitor cells (MG63), mesenchymal cells (ATMSCs) and endothelial cells (HUVECs) respectively while using SAOS-2 cells (osteosarcoma cell line) as an osteoblastic cell model.

CHAPTER 2
MANUFACTURE AND OPTIMISATION OF AQUASOMES

2.1 INTRODUCTION

2.1.1 Nanoparticles

Nanoparticles are an important area of research in the field of drug delivery because they can deliver a wide range of drugs to varying areas of the body for sustained periods of time (Hans and Lowman, 2002).

Generally, nanoparticles can also be used to provide targeted (cellular/tissue) delivery of drugs, to improve oral bioavailability, to sustain drug/gene effect in target tissue, to solubilize drugs for intravascular delivery, and to improve the stability of therapeutic agents against enzymatic degradation (nucleases and proteases), especially of protein, peptide, and nucleic acids drugs (Panyam and Labhasetwar, 2002).

Nanoparticles used in biomedical/research and drug delivery include inorganic nanoparticles, polymeric nanoparticles, solid lipid nanoparticles, liposomes, nanocrystals, nanotubes, dendrimers, etc. (Faraji and Wipf, 2009).

Biodegradable polymers have been widely explored for the fabrication of drug delivery systems. There has been increased interest in the development of biodegradable polymeric nanoparticles for drug delivery which can be attributed to their application in controlling the release of drugs, stabilizing labile molecules such as DNA, proteins and peptides from degradation and targeted drug delivery (Hans and Lowman, 2002; Faraji and Wipf, 2009; Singh and Lillard, 2009).

2.1.2 Vital characteristics for drug delivery via nanoparticles

2.1.2.1 Particle size

The *in vivo* distribution, biological fate, toxicity and targeting ability of nanoparticles are mainly determined by their particle size and size distribution. They also influence drug loading, drug release and stability of nanoparticles (Singh and Lillard, 2009; Baratt, 2000; Baratt, 2003).

In comparison to microparticles, nanoparticles have a comparative high cell uptake and wider cellular and intracellular targets owing to their small size and mobility. Smaller particles also have a larger surface area-to-volume ratio therefore most of the drug associated with small particles would be at or near the particle surface, leading to faster drug release (Baratt, 2000; des Rieux et al, 2006).

2.1.2.2 Surface properties of nanoparticles

The surface charges of nanoparticles influence their opsonization, which in turn influences their clearance half-life in the blood circulation. Zeta potential analysis is used to characterise the surface charge of particles. It measures the electrical potential of particles which is influenced by the composition of that particle and its dispersion medium. Zeta potential can be used as a marker of particle stability. Nanoparticles with a zeta potential of ±30mV are stable in suspension. Such stability is vital in preventing aggregation. Surface modification of nanoparticles to decrease hydrophobicity increases its stability (Patil et al, 2007; des Rieux et al, 2006).

Nanoparticles can be recognised by the host immune system when administered and cleared by phagocytosis in the circulation. The hydrophobicity of a nanoparticle affects the binding of opsonins (blood components) to its surface. Non-modified nanoparticles are rapidly opsonized and cleared from the blood circulation (Patil et al, 2007).

To increase the probability of successful drug targeting, opsonization must be reduced to prolong the circulation of nanoparticles *in vivo*. This can be accomplished by coating nanoparticles with hydrophilic polymers/surfactants or fabricating nanoparticles with hydrophilic properties (Singh and Lillard, 2009).

2.1.2.3 Drug loading and release

The drug loading capacity of a successful nano-carrier delivery system must be high enough for the effective delivery of the therapeutic agent to its targeted site. Appropriate absorption/adsorption is achieved by incubating the nano-carrier with a concentrated drug solution. Drug loading, entrapment and adsorption efficiency is dependent on the matrix composition, molecular weight of drug, drug-polymer interactions and the presence of end functional groups (Singh and Lillard, 2009).

The rate of drug release is dependent upon drug solubility, desorption of the adsorbed drug, drug diffusion through nanoparticle matrix and nanoparticle erosion and/or degradation processes. This demonstrates that solubility, diffusion and degradation govern drug release from nanoparticles. Larger particles have a slower burst release effect than smaller nanoparticles. Also, the amount of drug loading is directly proportional to the amount and rate of drug release (Hans and Lowman, 2002).

The method of incorporation greatly affects the release profile of the absorbed/adsorbed drug. If the drug is incorporated during nanoparticle formulation, the system will exhibit a small burst effect and sustained release characteristic. If the nanoparticle is coated with a

polymer, the release of the drug is then determined by desorption or diffusion of the drug from the polymeric membrane (Singh and Lillard, 2009).

2.1.3 Nanoparticulate delivery systems

Nanoparticles are solid colloidal particles comprising macromolecular substances that vary in size from 10 to 1000nm (however, particles greater than 200nm are not usually pursued in nano-medicine, i.e., the width of micro-capillaries) (Singh and Lillard, 2009).

The characteristic properties of nanoscale materials (such as physical, chemical, mechanical, electrical, magnetic and optical properties) can be utilized to strengthen the performance of drug delivery systems. More precisely, the nanometre size of a drug carrier provides numerous advantages for drug delivery purposes, which include larger surface area, increased dispersability, and optimizable mechanical properties, amongst others (Yang and Webster, 2009).

In addition to size benefits, nanoparticles also have various properties that can be tailored for specific applications owning to their exceptional bulk or surface properties (Rieux et al, 2006; Yang and Webster, 2009). The drug or protein of interest is usually dissolved, adsorbed, entrapped, attached and/or encapsulated into or onto a nano-matrix. The nanoparticles are constructed and manipulated to possess and exhibit distinct properties and release characteristics best suited for the delivery of the drug or protein (Barratt, 2000; Singh and Lillard, 2009).

2.1.4 Inorganic nanoparticles

Ceramics can be described as solid compounds that are formed by the application of heat, and sometimes heat and pressure, comprising at least one metal and a non-metallic elemental solid or a non-metal, a combination of at least two non-metallic elemental solids, or a combination of at least two non-metallic elemental solids and a non-metal (Habraken, Wolke and Jansen, 2007).

Ceramic nanoparticles are generally composed of silica, alumina, calcium phosphates, zirconia and titanium dioxides. They can also be composed of metals, metal oxides and metal sulphides. These nanostructures can be engineered to vary in surface composition, size, shape and porosity to evade the reticuloendothelial system (RES) and act as an

encasement to protect a drug or protein from denaturation or degradation (Faraji and Wipf, 2009).

Calcium phosphates (CaPs) are a major class of inorganic nanoparticles which are popular as biomaterials attributing to their biocompatibility and chemical similarity to human bone (Ginebra et al, 2006). There are different types of CaPs available which differ in calcium/phosphate ratio as well as physical properties (Kalita et al, 2007; see table 2.1 below). These include hydroxyapatite (HA), beta-tricalcium phosphate (β-TCP), biphasic calcium phosphate (BCP), amorphous calcium phosphate (ACP), carbonated apatite (CA) or calcium deficient HA (CDHA) (Verron et al, 2010).

Table 2.1 Physical properties of various phases of calcium phosphates (*Kalita et al, 2007)*

Phases	***Chemical formulae***	***Ca/P ratio***	***Density (g/cm^3)***
Hydroxyapatite (HA)	$Ca_{10}(PO_4)_6(OH)_2$	*10/6*	*3.16*
α-Tricalcium phosphate (α-TCP)	$Ca_3(PO_4)_2$	*3/2*	*2.86*
β-Tricalcium phosphate (β-TCP)	$Ca_3(PO_4)_2$	*3/2*	*3.07*
Tetracalcium phosphate (TTCP)	$Ca_4P_2O_9$	*2/1*	*3.05*

2.1.5 Aquasomes

Aquasomes were originally fabricated by Nir Kossovsky in 1996 (Kossovsky et al, 1996), to control molecular polymorphisms of bio-actives to retain their biological activity. Since then, an increasing body of literature has demonstrated the potential of aquasomes as nanocarriers systems for hydrophobic drugs, oxygen, antigen, proteins and peptides (Table 2.2).

Often referred to as ‘water bodies’, due to their water-like properties, aquasomes additionally provides a platform for preserving the conformational integrity and biochemical stability of bio-actives (Girota and Bajaj, 2012).

They are three-layered self-assembled structures, comprising a solid phase nano-crystalline core coated with an oligomeric film which a biochemically active molecule (drug or

biopharmaceutical) is adsorbed onto as illustrated in Figure 1.4 (Khopade et al, 2002). The preparation of aquasomes is a three-step process which constitutes of the following processes: formation of an inorganic nanocore (usually ceramic), coating of the nanocore with a polyhydroxyl oligomer (usually a sugar) and the loading of the drug/protein of interest. The systematic process is highlighted in Table 2.3.

2.1.5.1 Rationale behind the development of aquasomes

Aquasome formulations protect bio-actives via its oligomeric coating. Its' constituent carbohydrate film prevents destructive denaturing interaction between drug and solid carriers (Kossovsky et al, 1996). Aquasomes maintain molecular confirmation and optimum pharmacological activity. The molecular conformation of proteins and drugs can be preserved by incorporating such biological molecules on aquasomes with natural stabilizers (the natural sugar coating), which act as dehydroprotectants (Mesariya et al, 2011; Jain et al, 2012).

Table 2.2 Application of aquasomes in drug delivery in the literature

Applications researched	*References*
Insulin delivery	*Cherian et al (2000)*
Oral delivery of acid labile enzyme	*Rawat et al (2008)*
as an oxygen carrier	*Khopade et al (2002)*
In antigen delivery	*Kossovky et al (1995)*
In drug delivery; *as a nano-carrier for hydrophobic drugs*	*Umashankar et al, (2010);* *Sutar and Mokale (2012)*
In gene delivery	*Jain et al (2012)*
In vaccine delivery	*Goyal et al, 2008*

2.1.5.2 Properties of aquasomes

Aquasomes have functionalized active surfaces which can be efficiently loaded with substantial amounts of drugs and biopharmaceuticals via ionic, entropic, non-covalent bonds, and van der waals forces (Kossovsky et al, 1995; Goyal et al, 2008). Due to their size (<1μm,

based on the size or nanocore used), and structural stability, aquasomes avoid clearance or degradation by the reticuloendothelial (RES) system (Jain et al, 2012).

As colloidal size range particles, they are likely to be more concentrated in the liver and muscles (Yadav et al, 2011). Also, because contents are adsorbed on their surface, in the case of antigen delivery, issues associated with receptor recognition are avoided and pharmacological action is attained quickly (Kossovsky et al, 1995).

The mechanism of action of aquasomes is controlled by their surface chemistry. They deliver adsorbed contents through a combination of specific targeting, molecular shielding and slow and sustained release processes (Mesariya et al, 2011; Jain et al, 2012).

Table 2.3 Method of preparation and structure of aquasomes
(*Rojas-Oviedo et al, 2007, Nanjwade et al, 2013)*

Formation of inorganic core
Dependent on the material selected
Materials used: ceramic, nano-crystalline brushite and nano-crystalline diamond particles
Coating of core
Ceramic core is coated with a polyhydroxyl oligomer (mostly sugars)
The coating process is carried out by addition of carbohydrate into an aqueous dispersion of the cores under sonication.
Resulting suspension is subjected to lyophilisation to promote an irreversible adsorption of carbohydrate onto the ceramic surface.
The unadsorbed carbohydrate is removed by centrifugation.
Drug/protein loading
The drug/protein of choice is loaded to the coated particle by adsorption.
Drug/protein solution of known concentration is prepared and coated particles are dispersed into it.
the dispersion is then lyophilized to create the aquasomes

2.1.6 Aims and Objectives

In this study, the primary focus was to optimise the present aquasome formulation fabricated by the research group as reported in Lowry and Abdulrazzaq (2012), by analysing the effect of nanocore size and an increase in coating time (with oligomeric coating) on the drug/protein loading during aquasome manufacture. The following objectives formed the foundation for the research questions that required investigation.

1. Comparison between solid hydroxyapatite cores with particle size of 950±160nm previously used in aquasomes and nano-hydroxyapatite with smaller defined diameters (20nm, 40nm, 60nm).
2. Comparison of surface on naked solid hydroxyapatite cores (950±160nm) vs. nano-hydroxyapatite with defined diameters (20nm, 40nm, 60nm) which represent a range of small nanoparticle sizes for nanoparticulate drug delivery.
3. Investigation of the effect of increase in coating time on increased surface area available for drug/protein adsorption.
4. Elucidation of surface characteristics of the aquasomes and demonstration of the adsorption drug/protein onto the nanocores, using BMP-2 loaded aquasomes and fluorescent labelled aquasomes (metronidazole, in this case), by imaging techniques.
5. Optimisation of analytical methods employed in protein quantification and individual aquasome constituents while in formulation.

2.2 MATERIALS AND METHODS

2.2.1 Materials

Nano-sized hydroxyapatite powders (20nm, 40nm, 60nm) were purchased from MKNano Corporation (Ontario, Canada). Solid hydroxyapatite cores (with particle size marketed as <200nm) were purchased from Sigma Aldrich (Poole, UK), D (+)-Trehalose dehydrate was purchased from Acros organics (Belgium). Metronidazole, Phosphate Buffer Saline (PBS, tablets), trifluoroacetic acid (TFA) and methanol were also purchased from Sigma Aldrich (Poole, UK). Lyophilised rhBMP-2 was purchased from eBioscience (Hatfield, UK). BMP-2 ELISA kit was purchased from Peprotech Ltd. (UK). All reagents and materials were of analytical grade.

2.2.2 Methods

2.2.2.1 Selection and coating of ceramic nanocores

Hydroxyapatite cores, with particle size claimed as <200nm from Sigma Aldrich (Poole, UK) was used in fabricating previous aquasome formulations in the research group (AQUA1). However, the mean particle size of the HA nanocores were measured to be 950 ± 160 nm. To analyse the effect of nanocore size and coating times on drug/protein loading, different HA nano-powders and varying coating times were chosen and compared. 20nm, 40nm and 60nm nano-hydroxyapatite powders from MKNano Corporation (Canada) were chosen for this study. Very small nanoparticles within the range of 1–20 nm have long circulatory residence times with slow extravasation from the vasculature. Nanoparticles that are between 30 and 100 nm in diameter are small enough to avoid reticuloendothelial and phagocytic clearance, in contrast to larger nanoparticles, which are efficiently cleared. These properties play a role in passive and active targeting which in turn determine the efficacy of drug delivery using nanoparticles of such sizes (Faraji and Wipf, 2009).

To coat the nano-hydroxyapatite cores with an oligomeric film, 100mg of each of the nano-hydroxyapatite sizes was mixed (100rpm) with a 0.1M trehalose solution for 1.5h, 2.5h and 3h at 4°C. Previous research by the group explored the coating times of 1h and 2.5h with the unoptimised solid HA cores. Hence, this led to the investigation of a shorter (1.5h) and longer (3h) coating times with the HA nanocores (20nm, 40nm and 60nm) for any significant difference in zeta potential.

The dispersion was subsequently centrifuged (1500rpm, 10mins) and supernatant was discarded. Cores were washed in PBS buffer or distilled water to remove unadsorbed trehalose. Trehalose-adsorbed cores were then freeze-dried to promote the irreversible adsorption of trehalose onto the hydroxyapatite cores. The naked nano-hydroxyapatite cores and the freeze-dried trehalose-coated nanocores were then analysed for their surface area using a porosimeter. The process of fabrication of aquasomes is illustrated in Figure 2.1.

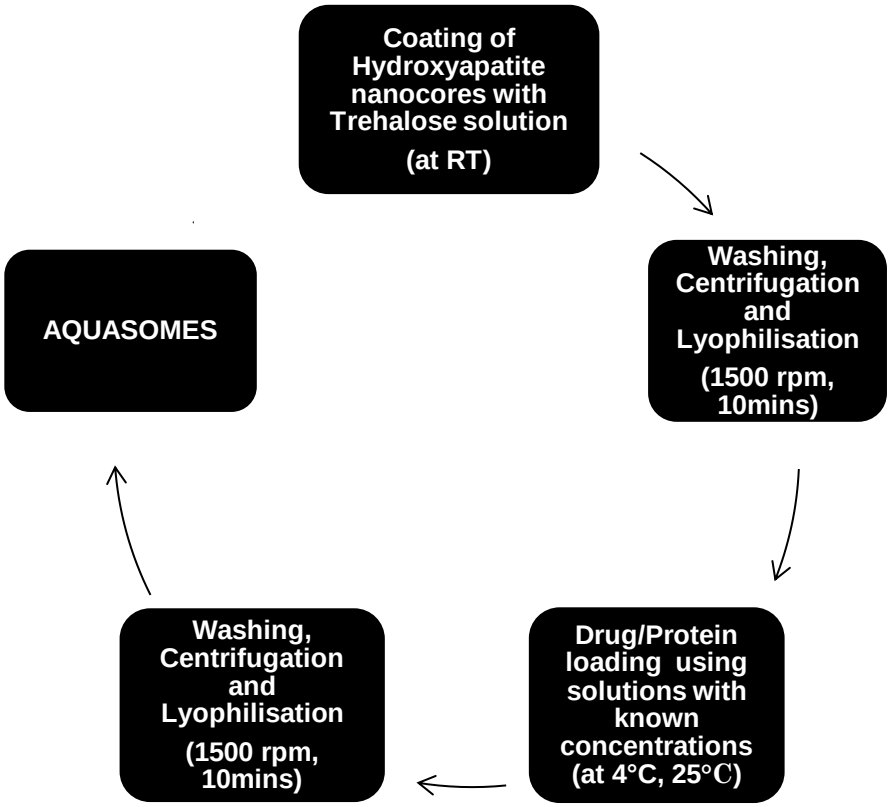

Figure 2.1 A cycle illustrating the fabrication process of aquasomes

The freezing protocol used is as follows: Thermal treatment at -45°C for 60mins maintaining the vacuum pressure at less than 350mbar. The primary drying step involved was in two phases: -40°C for 10.5hours and further drying at 20°C for 4hours while the vacuum pressure was kept at 50µbar (Tang and Pikal, 2004). Freezing (thermal treatment) temperature was chosen with respect to the collapse temperature (T_c) of trehalose (-34°C). This temperature chosen was required to be well below this temperature to avoid product collapse. Protein/drug solution with a known concentration (50ng/ml BMP solution for BMP-loaded aquasomes and 2mg/ml metronidazole solution for metronidazole-loaded aquasomes) was added to trehalose-coated cores. Drug/protein solution concentrations were chosen based

on therapeutic and antimicrobial effects observed in literature. The aqueous dispersions were mixed for a further 3.5 hours at 4°C, centrifuged (1000rpm, 10mins) and washed with PBS to remove unadsorbed drug/protein molecules in solution. They were then freeze-dried to yield drug/protein loaded aquasomes.

2.2.2.2 Zeta potential analysis

Naked hydroxyapatite nanocores, trehalose-coated hydroxyapatite cores and BMP-loaded aquasomes were characterised through zeta potential analysis measuring the positive charge emitted by the carbohydrate (trehalose) coating in comparison to naked hydroxyapatite particles. A small quantity of naked hydroxyapatite cores and coated cores was mixed with distilled water and placed into the probe for zeta analysis using the NanoBrook 90Plus Zeta Particle Size Analyzer (Brookhaven Instruments Corp., NY). The mean and standard error of the results were compared.

2.2.2.3 Surface area analysis

To optimise the aquasome formulation, smaller nanocore sizes (20nm, 40nm and 60nm) were chosen and coated with trehalose for difference durations. The surface areas were compared to analyse the effect of nanocore size and coating time on the surface area available for drug/protein adsorption. These optimised aquasome formulations were also compared with an earlier aquasome formulation (AQUA1) with larger nanocore sizes. Surface area analysis was performed by nitrogen (N_2) physisorption on a Quantasorb Nova 1000 instrument at 77 K, after outgassing approximately 100-200 mg of sample (HA nanopowders) which was accurately weighed into the sample tube, at 120 °C for at least 2 h. Subsequently, the data was processed using NOVAWin software version 2.1. Surface areas were calculated using the Brunauer–Emmet–Teller (BET).

Sample preparation:

Outgassing: Before the specific surface area of the sample can be determined, it is necessary to remove gases and vapours that may have become physically adsorbed onto the surface after manufacture and during treatment, handling and storage. If outgassing is not achieved, the specific surface area may be reduced or may be variable because an intermediate area of the surface is covered with molecules of the previously adsorbed gases or vapours. The outgassing conditions are critical for obtaining the required precision and accuracy of specific surface area measurements on pharmaceuticals because of the sensitivity of the surface of the materials.

Conditions: The outgassing conditions must be demonstrated to yield reproducible BET plots, a constant weight of test powder, and no detectable physical or chemical changes in the test powder. The outgassing conditions defined by the temperature, pressure and time should be chosen so that the original surface of the solid is reproduced as closely as possible. Outgassing of many substances is often achieved by applying a vacuum, by purging the sample in a flowing stream of a non-reactive, dry gas, or by applying a desorption-adsorption cycling method. In either case, elevated temperatures are sometimes applied to increase the rate at which the contaminants leave the surface. Caution should be exercised when outgassing powder samples using elevated temperatures to avoid affecting the nature of the surface and the integrity of the sample.

If heating is used, the recommended temperature and time of outgassing are as low as possible to achieve reproducible measurement of specific surface area in an acceptable time. For outgassing sensitive samples, other outgassing methods such as the desorption-adsorption cycling method may be employed.

2.2.2.4 Scanning Electron Microscopy (SEM)

To understand the morphology of the nanocores and loaded aquasomes and the mechanism in which the drug is adsorbed, the surface morphologies were evaluated with a scanning electron microscope.

Approximately 1mg samples of aquasome formulation (BMP-2, metronidazole) were lightly sprinkled on the carbon surfaces of universal specimen stubs taped with double-sided adhesive strip. Samples were then double coated with a thin layer of gold under low vacuum for about 3 minutes in the presence of Argon gas using a sputter coater, Polaron SC500 (Polaron Equipment Ltd, Watford, UK) at 20 mA. The particle surface morphology was captured using a Cambridge Stereo Scan (S90) Electron Microscope to produce micrographs including acceleration voltage and magnification.

2.2.2.5 Confocal imaging

Metronidazole, a fluorescence-emitting drug, was used to fabricate aquasomes to illustrate how the drug is adsorbed onto the nanocores. 1mg of the formulation was put on microscope coverslips, a drop of oil was placed on a microscope slide and the coverslip placed on the drop, such that the aquasomes were in contact with the mounting medium (oil). The prepared sample was viewed using a Leica TCSSP5 II confocal microscope (Wetzlar, Germany) with

an oil objective at 63X magnification (HCX PLAPO 63X/1.4-0.6 oil CS). The wavelength used was 488nm, for green fluorescence with resolution and speed of 1024X1024/100Hz; 10Hz.

Metronidazole-loaded aquasomes were analysed in the confocal imaging assay solely for the fluorescent emitting properties of metronidazole, which enables appropriate labelling of the aquasomes.

2.2.2.6 Optimisation of analytical protocols: ELSD vs. ELISA

To optimise the analytical methods used in quantifying protein and/or oligomeric sugar, the option of a more efficient and rapid assay was explored. The analysis of the individual aquasome constituents while still being adsorbed onto the ceramic nanocores was been investigated. Current practice analyses each constituent (in this case, oligomeric coating, trehalose; protein, BMP-2) using separate analyses, in which indirect methods at best are used to quantify the adsorbed oligomeric coating and drug/protein.

In this study, the ELISA technique was compared to the ELSD (Evaporating Light Scattering Detector) liquid Chromatography technique. Schematic diagrams illustrating the various steps involved in both analytical processes are shown in Figures 2.2 and 2.3.

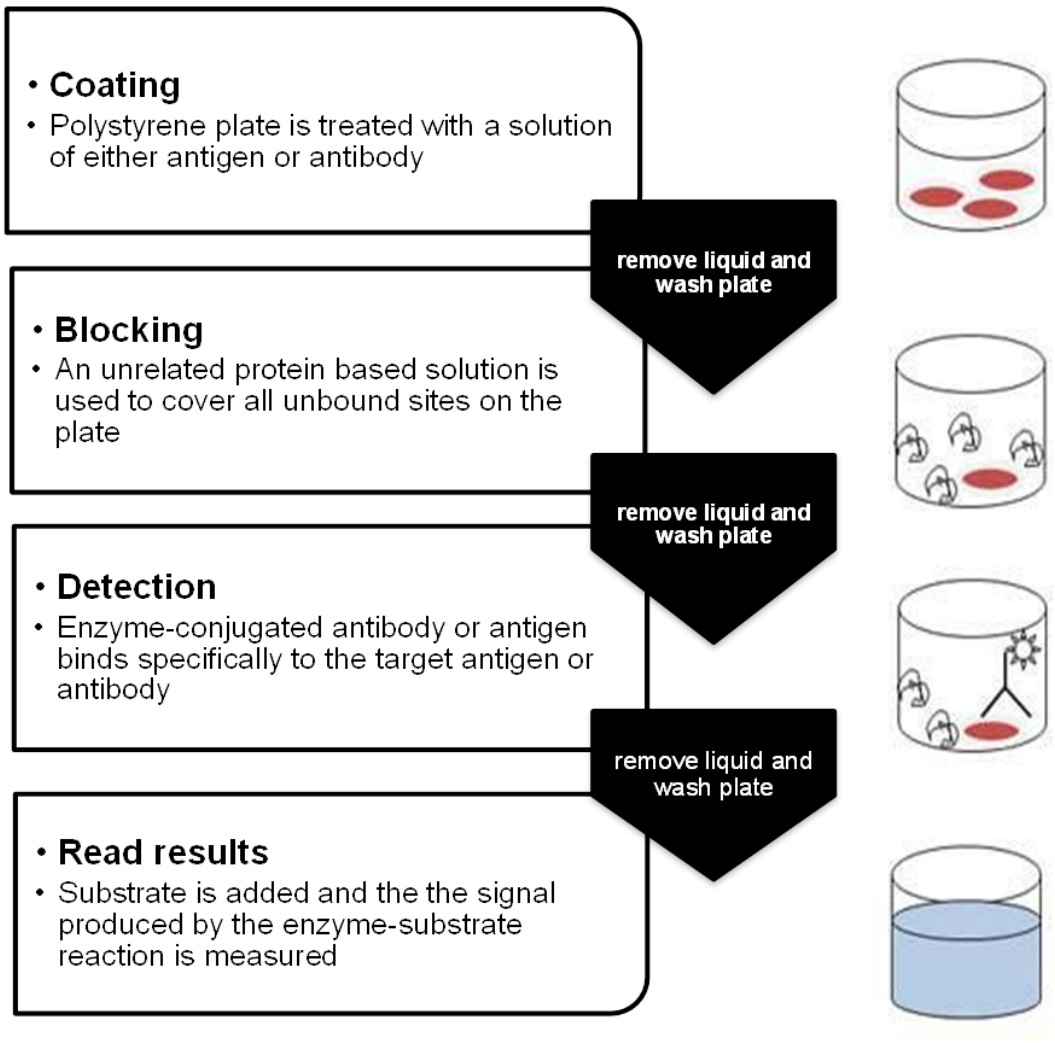

Figure 2.2 ELISA overview flowchart and schematic diagram. This figure is a representative diagram illustrating the general steps involved in an ELISA assay showing the coating of the plate, blocking of unbound sites, and detection of antigen with intermittent washing between these steps.

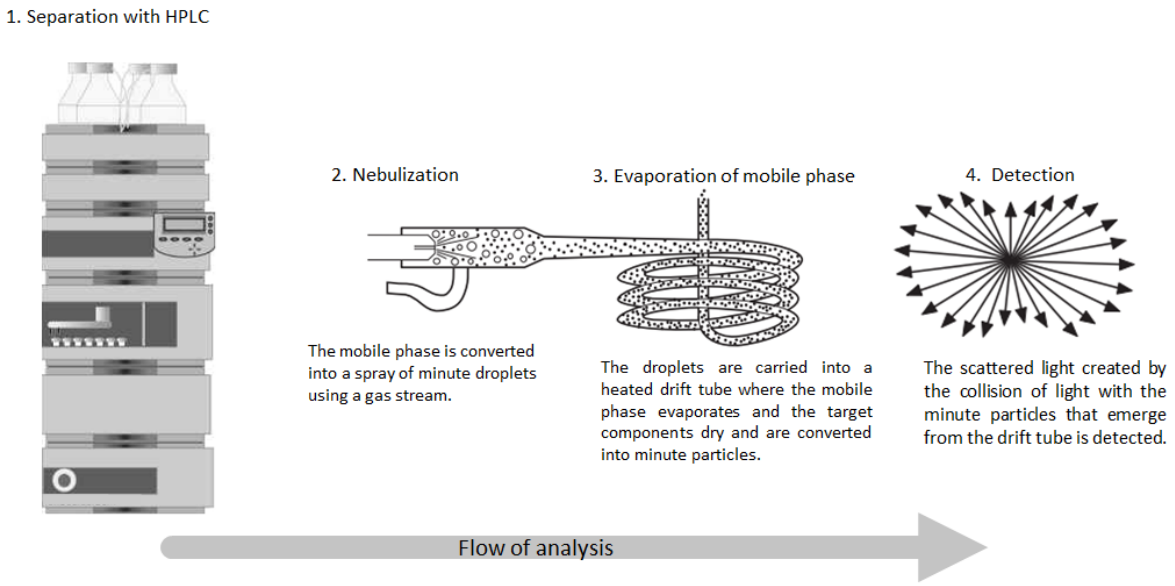

Figure 2.3 Schematic diagrams illustrating the flow of analysis using evaporating light scattering detection (ELSD). The steps involved in ELSD analysis include nebulization, evaporation of mobile phase and detection of analyte (Waters, 2016, Young and Dolan, 2003).

The systematic process of detection using the ELSD is discussed below highlighting the steps of nebulization, evaporation of mobile phase and optical detection.

Nebulization:

A nebulizer combines a gas flow of an inert gas (such as nitrogen) with the column effluent to produce an aerosol of uniformly sized droplets. A concentric flow nebulizer allows the carrier gas flow to be controlled. A high gas flow produces small droplets requiring less heat to evaporate the solvent while a low gas flow produces large droplets, requiring more heat to evaporate the solvent.

Mobile-phase evaporation or desolvation:

Evaporation occurs as a function of time, temperature and pressure of the carrier gas. Therefore, the use of HPLC mobile phases that easily and rapidly evaporate and desolvate is of importance. Solvents with fairly low boiling points and low viscosities such as the common HPLC mobile phases like water, acetonitrile, methanol, ethanol and TFA are generally used. This is because viscous and high-boiling solvents might fail to completely separate from analyte molecules or species before the detection step. This incomplete separation then adds to the background noise and decreases the analyte signal response, resulting in low

sensitivity (slope of the calibration plot) and high limits of detection (LOD). The evaporated HPLC solvents are condensed and captured in the recommended solvent trap and exhaust routing.

Optical detection:

Light striking the dried particles that exit the drift tube are scattered and the photons are detected by a photodiode or photomultiplier tube at a fixed angle from the incident light. The intensity of scattered light is proportional to the mass of solute passing through the detection chamber.

The size (diameter) of the analyte particles determines how the light is scattered. The detector measured the intensity of the scattered light at 60° relative to the excitation beam to minimise polarisation effects and stray light. Particles of different sized exhibit different sizes exhibit different angular distributions of the scattered light, and particles whose sizes and shapes vary have different light-scattering cross sections. In general, larger particles scatter more light yielding more intense signals and peak responses.

A photomultiplier tube (PMT) converts the scattered light signal to a voltage that can be recorded and analysed. The stronger the scatterings, the more intense the final signal on the ELS detection chromatogram. The scattered light is a rough measure of the mass of material represented by a chromatographic peak. To some degree, this “mass” response can be compound-independent. However, many factors can also affect the mass response, particularly the density of the analyte in a small dried particle. It is also important to note that the output of an ELS detector has no direct relation to the molecular weight of an analyte (Agilent Technologies, 2012: Waters Corporation, 2006)

In vitro release studies were performed using phosphate buffer saline (PBS, pH 7.4) as release media, simulating body fluid. BMP-loaded aquasomes were placed in 10ml capacity vials and filled with 10ml of PBS and placed in an orbital shaking incubator (100rpm, 37°C). Using the partial replacement method, 500µl samples were taken and replaced with the same volume of fresh pre-warmed release media at hourly time intervals for the duration of 8h. Samples were analysed using an ELISA assay. BMP-2 standards were prepared with 0.05% Tween-20 and 0.1% BSA (50µl Tween-20 and 100mg BSA) in PBS as diluent and a calibration curve was used to determine corresponding BMP concentrations in supernatant solutions.

BMP ELISA was conducted as described by the manufacturers protocol, 100µl of capture antibody was added to each ELISA plate well (n=3), sealed and left to incubate overnight. Capture antibody was aspirated from the wells and each plate was washed 4 times using 300µl of wash buffer per well. Plates were blotted onto paper towels to remove all the liquid and 300µl of block buffer was added to each well. Plates were incubated for at least 2 hours. Plates were further aspirated, washed 4 times and blotted onto paper towels.

100µl of the samples from each time point of the *in vitro* release study were added to the wells (n=3). The plates were sealed and incubated for 2 hours. Plates were again aspirated, washed 4 times and blotted on paper towels. 100µl of Avidin peroxidase was added to each well. Plates were incubated for 30mins at room temperature (25°C).

SigmaFast™ OPD was used as a substrate. One OPD tablet (*o*-Phenylenediamine dihydrochloride) and one urea hydrogen peroxide tablet were dissolved in 20ml of distilled water. Care was taken to wrap the solution in foil as it is light-sensitive. 100µl of SigmaFast OPD solution was added to each well and monitored for colour development. Absorbance readings were monitored at 5minute intervals for 50mins. Optical density was then read at 405nm.

The ELSD HPLC method was developed to detect the amount of BMP present in samples and compared with the standard BMP ELISA on accuracy and sensitivity. A calibration of BMP standards ranging from 0.25 to 30ng/ml was run through the ELSD and results were compared with the calibration using the BMP development ELISA.

BMP standards were analysed by reverse phase high performance liquid chromatography (HPLC) (YL instrument, Anyang, Korea) using a SEDEX 90LT ELSD detector (Sedex Sedere, Alfortville, France) in isocratic mode. The mobile phase consisted of a 0.5 ml/min flow rate, 50:50 percentage ratio of 0.1% trifluoroacetic acid (TFA) in water and methanol. A Luna C18 column (5micron, 150x 40mm *id*, Phenomenex, Ireland) and an optical gain of 2 were used. An injection volume of 30µl was used and BMP had a retention time of 3.2min.

2.2.2.7 Statistical analysis

The differences in surface areas between the varying HA nanoparticle sizes and coating times were tested for statistical significance using the one-way ANOVA on GraphPad Instat statistical software.

2.3 RESULTS AND DISCUSSION

The emphasis of this study was to optimise the present aquasome formulation fabricated by the research group by investigating the effect of nanocore size and an increase in coating time (with oligomeric coating) on the drug/protein loading during aquasome manufacture. Another objective was the optimisation of analytical methods employed in protein quantification and individual aquasome constituents while in formulation, in comparison to present quantification techniques which separately analyse individual components of aquasomes.

2.3.1 Zeta potential analysis

The zeta potential of the naked hydroxyapatite cores and the trehalose-coated cores were analysed to measure the surface charge of the carbohydrate coating on the nanocores (Table 2.4). The successful coating of nanocores by the adsorption of trehalose to hydroxyapatite with different coating times was determined by change in carrier charge in comparison to blank hydroxyapatite nanocores. BMP-loaded aquasomes were also analysed and compared for a change in carrier charge in comparison to coated nanocores. The zeta potential of HA nanocores in distilled water decreased slightly for the coated 40nm HA while the zeta potential of 20nm and 60nm nanocores increased and then decreased slightly increased, with no particular trend as coating time.

A study by Rouahi and colleagues (2006) showed that the zeta potential of different HA nano-powders exhibit different zeta potential values, which is dependent on the surrounding medium.

the zeta potential values of a HA powder formulation (HAD) in distilled water decreased from 0 −20 mV in comparison to another formulation (HAL) which stayed around 0 mV during all the immersion time. In non-complete culture medium, the zeta potential decreased to −5 to −7 mV for the two powders while in complete culture medium, the zeta potentials were also similar for the two powders and stayed around −15 mV. This value of zeta potential corresponding likely to the surface charge of adsorbed proteins. From these results, it can be hypothesized that a large amount of proteins was adsorbed on HAL powder since the zeta potential decreased from 0 to −15 mV after immersion in complete culture medium. This was confirmed by the quantification of proteins desorbed from the powders since more proteins were desorbed from HAL than from HAD.

Similar results were observed in a study by Gbureck, Probst and Thull (2002). The zeta potential of calcium phosphate powders such as di-calcium phosphate anhydride (DPCA), tetra-calcium phosphate (TTCP) and hydroxyapatite were measured in various

organic/aqueous media with different pH values. Higher negative zeta potential values were observed: -15 to -18mV and -35 to -45mV in water and 0.05mol/L sodium phosphate solution respectively.
This illustrates the fact that the experimental conditions can largely influence the zeta potential. The zeta potential values were lower when the powders in the different media were permanently shaken at room temperature than when it was intermittently shaken at 4°C. This is a well-known phenomenon.

Moreover, for salt-type minerals such as calcite and apatite, the preferential hydrolysis of the surface species and preferential dissolution of ions, which is often accompanied by a reaction with the solution constituents and possible uptake of the solid, have been proposed to be the major controlling mechanism of zeta potential.

In another study by Doostmohammadi and colleagues (2012), a negative zeta potential was discovered to facilitate bone cell activity. Results from this study showed that at pH 7.4 (found in many situations *in vivo*), the zeta potential of the bovine bone-derived HA was −9.25 mV in physiological saline. The particles had a negative zeta potential above pH 6 in physiological saline. This negative zeta potential for bone-derived HA could be an advantageous property particularly if the material is implanted in bone containing viable cells. Calcium phosphates, such as HA, with negative zeta potential promote apatite nucleation, bone regeneration, as well as osseointegration (Zhou et al, 2015). With regards to the present research, these findings are advantageous as BMP-2 loaded aquasomes were fabricated for culturing with osteoblast like cells to stimulate osteogenic proliferation and differentiation.

Table 2.4 Zeta potential analysis of various sizes of hydroxyapatite cores coated with trehalose for 1.5, 2.5 and 3 hours

Nanocore sample	Zeta potential (mV)
BMP-loaded aquasomes	
Using 60nm nanocores	*-0.3233±0.54*
Coated nanocores (with different coating times)	
20nm	
1.5h	*-1.1866±0.23*
2.5h	*-1.465±0.29*
3h	*-1.1033±0.12*
40nm	
1.5h	*-1.0133±0.03*
2.5h	*-1.4633±0.14*
3h	*-1.6033±0.14*
60nm	
1.5h	*-1.61±0.25*
2.5h	*-.1.575±0.27*
3h	*-1.51±0.24*
Uncoated nanocores	
20nm	*-1.085±0.06*
40nm	*-0.71±0.05*
60nm	*-0.8633±0.06*

2.3.2 Comparison between the surface areas of hydroxyapatite nanoparticles and nano-hydroxyapatite powders (20nm, 40nm and 60nm)

Surface areas were calculated using the Brunauer–Emmet–Teller (BET). The BET instrument determined the specific surface area (m^2/g) of HA nanoparticles/ nano-hydroxyapatite powder samples. The sample is initially degassed to remove any gas or vapours which may have adsorbed onto the surface of the samples from the ambient air, enhancing adsorption of nitrogen gas (adsorbate). If samples are not degassed, the surface area results can be low and non-reproducible because the surface area has already been adsorbed by other gas molecules/vapours. The sample is then dried with nitrogen purging or in a vacuum applying elevated temperatures. The volume of gas adsorbed to the surface of the particles is measured at the boiling point of nitrogen (-196°C). The amount of adsorbed gas is correlated to the total surface area of the particles including pores in the surface. The surface area is calculated using BET method over the range of P/P_0 = 0.02 - 0.2 where a linear relationship was maintained. Traditionally, nitrogen is used as adsorbate gas because it is chemically inert and the experimental temperature to perform a complete adsorption/desorption isotherm measurement is that of the liquid Nitrogen (77K).

BET is an extended version of the Langmuir model. Langmuir assumed that energy of absorption for the first monolayer is generally considerably larger than that of the second and higher layers, thus forming multilayer is only possible at much higher pressures than the pressure required for formation of the first monolayer (Roquerol, Roquerol and Singh, 1999). According to the BET model, the molecules in the first layer were assumed to act as sites for the second-layer molecules, and so on to infinite layers. It is also assumed that the adsorption behaviour of all layers above the first monolayer is the same. Moreover, assuming that the multilayer has an infinite thickness at $p/p_0 = 1$, Brunauer, Emmet and Teller were able to derive their famous BET equation, which is usually expressed in the following linear form (Brunauer, Emmet and Teller, 1938):

$$\frac{p}{n(p^0-p)} = \frac{1}{n_m C} + \frac{C-1}{n_m C} \times \frac{p}{p^0} \qquad \text{Equation 2.1}$$

Where n is the total adsorbed number of molecules, n_m is the monolayer capacity and C is an empirical constant that is assumed to be exponentially related to the net heat of adsorption (energy of adsorption by the first monolayer minus the energy of adsorption by the subsequent layers) as the following simplified equation:

$$C \approx EXP\left(\frac{E_1-E_L}{RT}\right) \qquad \text{Equation 2.2}$$

Using the BET method over the range P/P_0 = 0.03–0.18, where a linear relationship was maintained, surface areas were calculated based on the following equation 2.3:

$$a_{BET} = n_m L\sigma \qquad \text{Equation 2.3}$$

Where BET surface area is related to n through the effective molecular cross-sectional area, σ, which is equal to 0.162 nm^2 for N_2 at 77 K and L, is Avogadro's number (Table 2.5).

Table 2.5 Definition of Symbols used in the calculated BET surface areas

Symbol	Definition
P	partial vapour pressure of adsorbate gas in equilibrium with the surface at 77.4 K (b.p. of liquid nitrogen), in pascals,
P_o	saturated pressure of adsorbate gas, in pascals,
V_a	volume of gas adsorbed at standard temperature and pressure (STP) [273.15 K and atmospheric pressure (1.013×10^5 Pa)], in millilitres,
V_m	volume of gas adsorbed at STP to produce an apparent monolayer on the sample surface, in millilitres,
C	Dimensionless constant that is related to the enthalpy of adsorption of the adsorbate gas on the powder sample.

Appendix I, II, III and IV are adsorption/desorption isotherms for un-optimised HA, 20nm, 40nm and 60nm nano-hydroxyapatite powders. Adsorption occurs when a gas is brought into contact with a solid, part of it is taken up and remains on the outside attached to the surface. In physical adsorption (physisorption), there is a weak Van der Waals attraction between the adsorbate and the solid surface. An adsorption isotherm is obtained by measuring the amount of gas adsorbed across a wide range of relative pressures at a constant temperature (typically liquid N_2, 77K). Conversely, desorption isotherms are achieved by measuring gas removed as pressure is reduced.

Appendix I, II, III and IV illustrate the characteristics of type II adsorption isotherms, which describe adsorption on macro-porous adsorbents, (in this case, hydroxyapatite), with strong adsorbate-adsorbent interaction or affinity. The hydroxyapatite nanoparticles used in this study were in the form of loose powders and thus had interparticulate pores between the particles. Such isotherms also indicate indefinite multi-layer adsorption after completion of the first monolayer and are found in adsorbents with a wide distribution of pore sizes. Near to the first point of inflexion, a monolayer is completed, successfully followed by adsorption which continues to occur in consecutive layers.

Un-optimised hydroxyapatite nanocores (AQUA1) which has a large nanoparticle size distribution with a size range between 925-1100nm had a surface area of 22.742 m^2g^{-1}. Nano-hydroxyapatite powders with particle sizes 20nm, 40nm and 60nm had surface areas of 54.42, 58.18 and 65.37 m^2g^{-1} respectively illustrating a directly proportional relationship between smaller nanoparticle size and larger surface area. These calculated BET surface areas are summarised in table 2.6 showing a trend of decreased surface area with an increase in HA core size

Table 2.6 Table showing the calculated BET surface areas of the hydroxyapatite nanocore samples

Sample	Calculated BET surface areas (m^2g^{-1})
20nm nanopowder	65.377
40nm nanopowder	58.188
60nm nanopowder	54.423
Unoptimised HA particles (950±160nm)	22.742

In a study by Dasgupta, Bandyopadhyay and Bose (2009), a system was developed to manufacture different phases of CaPs. Calcium to phosphate ratios was kept at 1:5:1 to synthesize tri-calcium phosphate. After subsequent steps, the resultant powder was heated to at least 600°C to be calcined to obtain a high purity nano-crystalline powder. The different temperatures yielded different crystalline phases of CaPs. Nano-CaPs calcined at 600°C showed the highest average BET surface area not only because of their smaller particle size (48-69nm), but also because of their higher particle aspect ratio. The BET specific average surface area for the powders calcined at 600°C and 800°C were 73 and 57 m^2g^1, respectively, the difference being statistically significant. The results of this study relate to the results in this chapter agreeing with theory that the smaller the size of nanoparticles (20nm, 40nm and 60nm), the larger the surface-to-volume ratio which is available for drug/protein adsorption in the fabrication of aquasomes.

In the study by Dasgupta, Bandyopadhyay and Bose (2009), BSA was used as a model protein. The adsorptive property of BSA was investigated by the change in BET surface area of CaP nanoparticles. Results from the study showed that the adsorbed amount of BSA increased with increasing surface area of the nano-CaPs immersed in the BSA solutions. The higher the surface area, the higher the surface charge density of the nano-CaPs, results in a higher degree of electrostatic interaction between the BSA and the nano-CaPs. These

results clearly demonstrate that surface area affects drug/protein loading and thus a smaller hydroxyapatite nanoparticle size translates to a larger surface area, which increases drug/protein loading capacity in aquasome formulation.

2.3.3 The effect of coating on calculated BET surface areas

Appendix V, VI and VII (a, b and c), show the adsorption/desorption isotherms for trehalose coated nano-hydroxyapatite powders. The majority of these plots illustrate the characteristics of type III adsorption isotherms, which describe multilayer adsorption on macro-porous adsorbents, (in this case, hydroxyapatite), with weak adsorbate-adsorbent interaction or affinity. It can be deduced that the coating of the nano-HA powders with trehalose led to the weak Van der waals forces between the adsorbate (N_2 gas) and the adsorbent (nano-HA cores), thus resulting in type III adsorption/desorption isotherms.

Comparing the surface areas of the individual nano-sizes (20nm, 40nm, 60nm) with the different coating times (1.5h, 2.5 h and 3h); no consistent trend was observed in the calculated surface areas (Table 2.7). The difference in the calculated surface areas in 20nm samples coated with trehalose for the different durations (1.5h, 2.5 h and 3h) were 60.176, 56.242 and 58.689m^2g^{-1} respectively (Appendix V), which do not show direct proportionality between coating and surface area. This was also observed for 40nm nano-HA which had the calculated surface areas of 54.889, 52.184 and 53.558m^2g^{-1} respectively (Appendix VI). In contrast, with the 60nm nano-HA, there seemed to be a direct proportionality between coating time and surface areas with the calculated surface areas as 47.767, 48.145 and 50.439m^2g^{-1} respectively (Appendix VII). The differences in the calculated surface areas between the individual three nano-HA sizes with different coating times were found to be statistically significant ($p<0.01$). However, the differences between the surface areas for each nano-HA size (20nm, 40nm and 60nm) with the different coating times were found to be statistically insignificant ($p<0.01$). These results evidently show that an increase in the duration of trehalose coating does not give a significantly different calculated BET surface area but the decrease in particle size and a uniform size distribution gives a definitely significant difference in the calculated surface areas.

Table 2.7 **Calculated BET surface areas of the different nano-hydroxyapatite samples after coating**

	BET surface area ($m^2 g^{-1}$)		
	1.5h	2.5h	3h
20nm	60.176	56.242	58.689
40nm	54.889	52.184	53.558
60nm	47.767	48.145	50.439

Drug release is also affected by particle size. Smaller particles have a larger surface area-to-volume ratio and thus, most of the drug associated with small particles would be at or near the particle surface, leading to faster drug release. In contrast, larger particles have large cores, which allow more drug/protein to be encapsulated per particle and give slower release (Redhead et al., 2001). However, in the case of aquasomes, the oligomeric coating, trehalose, offers a controlled release property owing to its gel formation when hydrated.

A successful nano-delivery system should have a high drug-loading capacity, thereby reducing the quantity of matrix materials for administration. Generally, this is achieved by incubating the nano-carrier with a concentrated drug solution. If the nanoparticle is coated by polymer, the release is then controlled by diffusion of the drug from the polymeric membrane. Membrane coating acts as a drug release barrier; therefore, drug solubility and diffusion in or across the polymer membrane becomes a determining factor in drug release (Singh and Lillard, 2009). Aquasomes are a good example of this kind of nano-carrier system. Drug loading is achieved by incubating hydroxyapatite nanocores with a concentrated drug/protein solution. The coating of the hydroxyapatite nanocores with an oligomeric film determines the diffusion and consequently the release of the drug from the nanocarriers system.

In the current study, trehalose was used as a polyhydroxyl oligomer coating. The effect of coating time on surface area available for drug/protein loading was investigated. This is graphically represented in Appendix IX. In comparison to the uncoated HA nanocore samples, the BET calculated surface area of the coated nanocores were slightly lower. However, this can be attributed to the BET experimental method in which the sites for N_2 adsorption on HA nanocores have been coated with trehalose resulting in a reduced calculated surface area value. The calculated BET surface area for 20nm, 40nm and 60nm after 1.5h, 2.5h and 3 h of coating were 60.776, 56.242 and 58.689m^2g^{-1}; 54.889, 52.184 and 53.558 m^2g^{-1}; 47.767, 48.145 and 50.439m^2g^{-1}. Comparing the surface area of the nano-HA

powders with the different coating times, there was no constant trend found. The difference in the surface area with the different coating times (for each nano-HA size) were statistically insignificant ($p<0.05$). This is in agreement with previous research data by the research group (Abdulrazzaq and Lowry, 2012) in which the coating time showed no significant difference and therefore, the loading step can be carried out in 2.5 h, compared with longer processes

Trehalose is a non-reducing homo-disaccharide in which two glucose units are linked together in a α-1,1-glycosidic linkage (α-D-glucopyranosyl-α-D-glucopyranoside). Because of the inherent properties of trehalose, specifically prevention of starch retro-gradation and stabilization of proteins and lipids, it has proved quite useful in a number of industries including food processing, cosmetics and pharmaceutics (Jain and Roy, 2008). It has been shown to possess high thermostability and a wide pH-stability range. Trehalose solutions with a pH of 3.5- 10 were heated at 100°C for 24hr and no degradation of trehalose was observed (Higashiyama, 2002).

The characteristics of trehalose responsible for its bio-protective role are attributed to its solid state and solution properties. One of the most important reasons why trehalose is such an important bio-protectant is due to the existence of a number of polymorphs, both in the crystalline as well as amorphous states. These include two crystalline forms, trehalose dihydrate (T_h) and trehalose anhydrous (T_α and T_β); and one amorphous form. Careful dehydration of the dihydrate under defined conditions leads to the formation of the anhydrous crystal (T_β), and further dehydration of the dihydrate by heating at temperatures below 85°C, result in another anhydrous form (T_α). This transformation is reversible, and the anhydrous form can be hydrated back to the dihydrate form without any loss of integrity of the crystalline structure. The anhydrous crystalline form Tα is thought to absorb moisture, undergoing a reversible transition to the crystalline dihydrate form. This reversibility, without alteration of the three-dimensional structure of the disaccharide, is important in its protective action (Jain and Roy, 2008).

The unusual protectant capabilities of trehalose could also be partly due to its ability to bind water. This observation is related to the number of intramolecular hydrogen bonds found in trehalose. Because trehalose forms only one intramolecular hydrogen bond, there are more sites available to hydrogen bond with water, resulting in a higher hydration number (Ekdawi-Sever, Conrad and de Pablo, 2000).

In this instance, where trehalose is the polyhydroxyl oligomer, which is the hydrogen bonding substrate for the drug/protein of choice in the aquasome formulation, the rate of diffusion of the drug/protein from the formulation is dependent on the diffusivity co-efficient of trehalose

in water, hence offering the sustained drug/protein release property of the aquasome delivery system (Ohtake and Wang, 2010).

It has been proposed that with an increase in density, the free volume decreases, which consecutively causes a decrease in diffusivity and thus an increase in viscosity. The faster diffusion co-efficient for sucrose (polyhydroxyl oligomer, used in earlier aquasome formulations; Han et al, 2007) can be attributed to its smaller hydration number in comparison with trehalose, as the hydrated sucrose is smaller in size compared with trehalose, it can diffuse more readily. The hydration number is defined as the average number of water molecules that are hydrogen bonded to the sugar molecule. These properties of trehalose highlighted above have demonstrated its ability to stimulate sustained release. Thus, its function in the presently fabricated loaded aquasome formulations is of specific importance.

2.3.4 Understanding the morphology of aquasomes: Scanning Electron Microscopy (SEM) and confocal imaging

To understand the morphology of loaded aquasomes, SEM images of BMP-2 and metronidazole loaded aquasomes and confocal images of metronidazole- loaded aquasomes were studied. This was investigated to elucidate the interactions of the drug/protein with the ceramic nanocores and also to establish the formation of aquasomes. Figure 2.4 (a) and (c), illustrates the morphology of the aquasome surface with agglomeration of individual aquasomes of BMP-loaded and metronidazole-loaded aquasomes respectively. Figure 2.4 (b) and (d) show the individual sizes of the aquasomes, highlighting the wide range of nanocore sizes used with the un-optimised aquasome formulations.

The SEM images of the BMP-loaded and metronidazole-loaded aquasomes showed that the individual nanoparticle sizes ranged from 70-150nm illustrating that the delivery system is within the nanoscale range. However, a lower population of larger sized nanocores with sizes up to 346nm exhibited a greater range of size distribution. Using the AQUA1 formulation, the confocal images illustrated that the BMP/metronidazole is adsorbed onto individual nanoparticles as well as agglomerates of nanocores. Smaller particles have a higher possibility of agglomeration during storage, transport, and dispersion (Singh and Lillard, 2009). This large range of size distribution attributed to the need for optimisation with smaller nanocores with a lower size distribution, which may offer more advantages associated for nanoparticulate delivery systems.

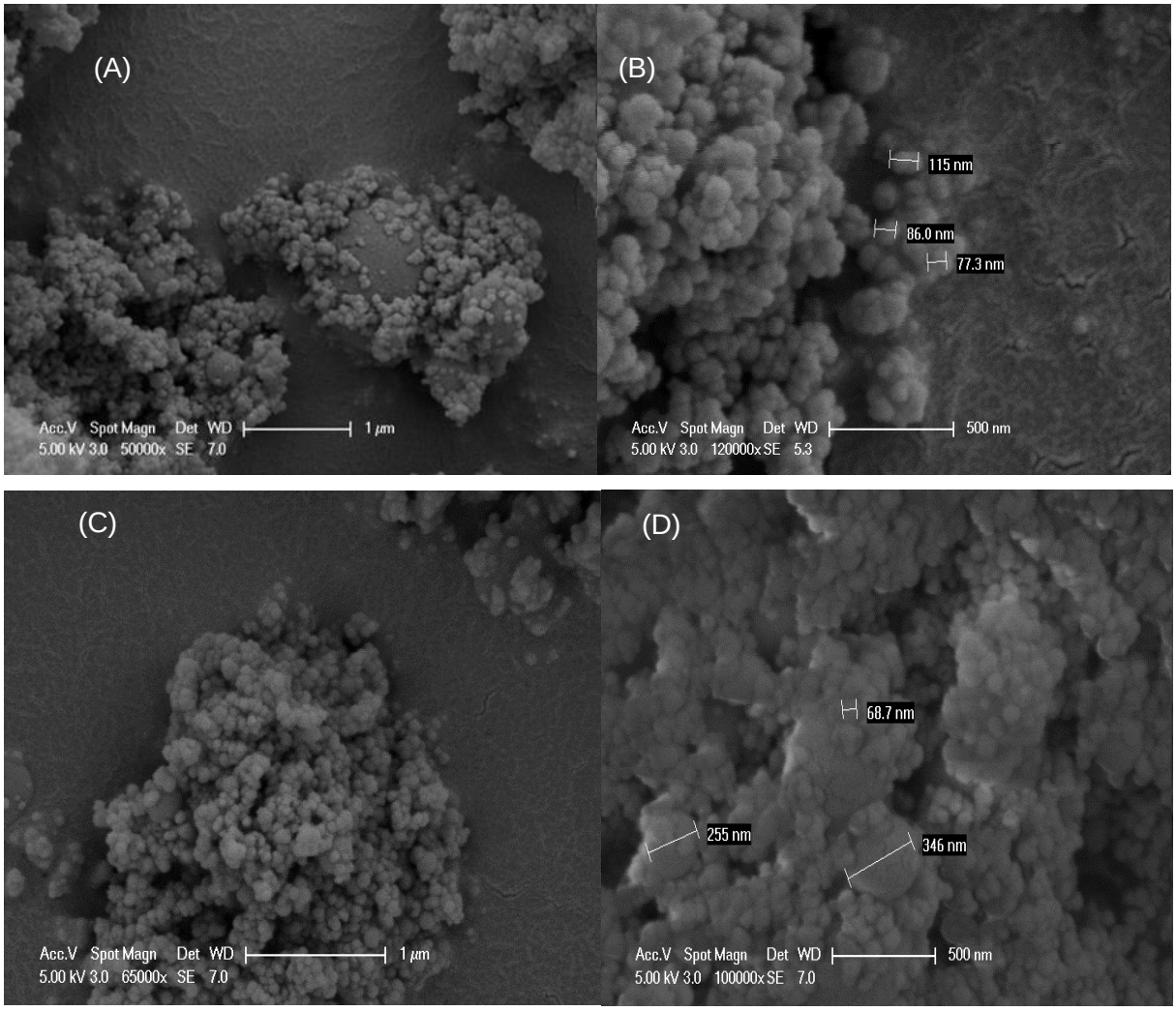

Figure 2.4 SEM images of BMP-loaded and metronidazole-loaded aquasomes.
(A) And (C) show SEM images of BMP-loaded and metronidazole-loaded aquasomes with (B) and (D) highlighting the sizes of the aquasomes (unoptimised). Images reveal the range of varying sizes in the hydroxyapatite nanocores used in the formulation (unoptimised).

Figure 2.5 (a) and (b) show the confocal images of the fluorescent emitting drug, metronidazole, loaded onto aquasomes. These images illustrate the presence of drug in the formulation as well as the fashion in which the drug is adsorbed (around agglomerated nanocores).

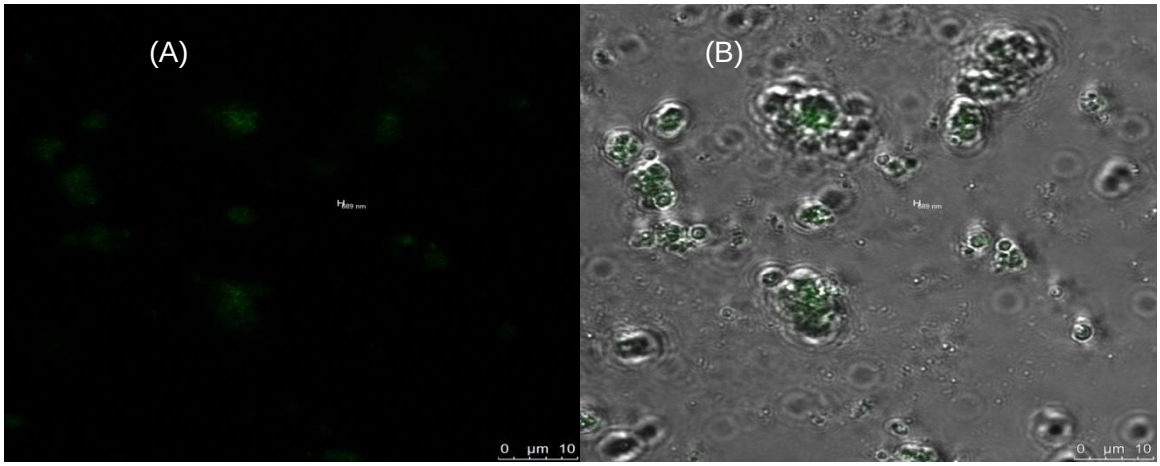

Figure 2.5 Confocal images of metronidazole-loaded aquasomes.
(A) and (B) show aquasome formulations with the fluorescence-emitting drug (on black and grey backgrounds) illustrating the presence of metronidazole in the formulation as well as the fashion in which the drug is adsorbed (around clumps of nanocores).

2.3.5 The effect of nanoparticle size on calculated surface areas in aquasome formulations

The nanoparticle size of the aquasomes, as a drug/protein carrier, plays an important role in its delivery function. The advantages include (Rieux et al, 2006; Singh and Lillard, 2009; Yang and Webster, 2009):

i) improved transport across cell membranes, hence, reducing clearance from the body and providing a more targeted drug delivery;
ii) larger surface area- to-volume ratios and subsequently more surface reactivity, thus, increasing drug loading ability, providing controlled dissolution rates and drug bioavailability;
iii) increased dispersibility for homogeneous drug loading and release of drug molecules;
iv) optimizable mechanical properties (such as matching the strength and ductility of natural bone), therefore, serving as a strong immediate matrix backbone;
v) size similarity to natural tissue components (e.g., HA crystals in natural bone are 50 × 25 nm, thus, enabling better tissue acceptance by bio-mimicking tissue architecture.

In this study, the nanoparticle size, size distribution and coating of the nano-hydroxyapatite was the primary focus, in the optimisation of aquasome formulations for higher drug loading and efficacy in delivery. Particle size and size distribution are the most important characteristics of nanoparticles. They can influence drug loading, drug release and stability of the nanoparticles (Panyam and Labhasetwar, 2002). The size of the particles plays an

important role if surface adsorption is the method of choice for antigen/allergen loading on the delivery systems (Pandey et al, 2011). The sub-micron size of nanoparticles most importantly offers a number of distinct advantages over microparticles *in vivo.* Generally, nanoparticles have relatively higher intracellular uptake in comparison to microparticles. A study by Desai and colleagues (1997) demonstrated that 100 nm size nanoparticles showed a 2.5-fold uptake compared to 1μm and a 6-fold higher uptake compared to 10 μm microparticles in Caco-2 cell line (Desai et al, 1997).

Recent research in aquasome formulations have shown that formulations with smaller nanocore sizes have the advantage of higher protein/drug/antigen loading. Pandey and colleagues (2011) produced ultrafine aquasomes with high allergen loading. The aquasome formulations characterised showed sizes of the hydroxyapatite nanocore, blank aquasomes and OVA-loaded aquasomes as 39±11, 43±14 and 47±19 respectively. Rojas-Oviedo and colleagues (2007) created varying formulations of indomethacin loaded aquasomes with calcium carbonate nanocores and lactose coating, with particle Goyal and colleagues (2008) reported the fabrication of aquasomes loaded with antigen for an immunogenic response with average hydroxyapatite nanocore size of 150nm, coated hydroxyapatite cores (with cellobiose and trehalose)with an average size of 247.26nm and 264.14nm respectively, and BSA-loaded aquasomes with average nanocore sizes of 286.56nm and 291.24nm respectively. These results demonstrate that aquasome formulations must have nanocores within the nano-meter range. However, smaller nanocore sizes ensure higher drug/antigen/protein loading.

From the results in this study, the correlation between particle size, size distribution and the surface area available for “loading” of the coating oligomer is evidently shown. The un-optimised hydroxyapatite nanocores had larger nanocore sizes generally described as >60<200nm, with a very wide size distribution. Consequently, the calculated surface area was 22.742m^2g^{-1}, a lower surface area than the nano-hydroxyapatite powders. The HA nanopowders had a very narrow size distribution and finer nanoparticle sizes which was directly linked to the surface areas available for coating. The calculated surface areas for the nanohydroxyapatite powders (20nm, 40nm and 60nm) were 65.377, 58.188 and 54.423m^2g^{-1} respectively, which showed a 3-fold increase in comparison to the un-optimised HA nanocores.

2.3.6 Comparison of ELSD and ELISA techniques for protein quantification

To optimise the analysis of protein quantification and/or oligomeric sugar used in this study, the option of a more efficient and rapid assay was explored. The analysis of the individual aquasome constituents while still being adsorbed onto the ceramic nanocores was investigated. Current practice analyzes each constituent (in this case, oligomeric coating, trehalose; protein, BMP-2) using separate analyses, in which indirect methods at best are used to quantify the adsorbed oligomeric coating and drug/protein.

The enzyme-linked immunosorbent assay (ELISA) is a common laboratory technique, which is used to measure the concentration of an analyte (usually antibodies or antigens) in solution. The basic ELISA, or enzyme immunoassay (EIA), is distinguished from other antibody-based assays because separation of specific and non-specific interactions occurs via serial binding to a solid surface, usually a polystyrene multiwell plate, and because quantitative results can be achieved.

ELISAs are very sensitive and accurate. Nonetheless, they are multi-step assays, which can be time consuming (Figure 2.2). However, when automated, they can be simple and easy to perform. ELISAs can be quite complex, including various intervening steps and the ability to measure protein concentrations in heterogeneous samples such as blood. The most complex and varying step in the overall process is detection, where multiple layers of antibodies can be used to amplify the signal.

In comparison, the Evaporating Light Scattering Detector (ELSD) is capable of analysing all substances that have an evaporation temperature lower than that of the mobile phase, and can attain roughly the same level of detection sensitivity for any compound. For this reason, they are well suited to the detection of components such as sugars, fats, surfactants, synthetic macromolecules, and steroids, as these components have low light absorbance, making them difficult to detect with UV detectors. The ELSD-HPLC technique can also analyse samples that require neither UV nor fluorescent activity.

The detection of BMP-2 standard samples using the ELSD was used in comparison to the standard BMP ELISA. Analysing the calibration plots of both methods, the R^2 value of the ELSD was closer to 1 (0.9949) showing higher linearity in comparison to the ELISA. The process of ELSD analysis is illustrated in Figure 2.3. These steps include nebulisation, evaporation of the mobile phase and detection of the analyte(s) of interest and are elucidated in Section 2.2.2.6 (Young and Dolan, 2003).

The results from the ELSD study demonstrated that the ELSD was more sensitive than the standard BMP ELISA. Another advantage of the ELSD method over the standard ELISA method is the high speed of analysis of samples as samples generally have shorter retention times making it faster to analyse a large batch of samples in comparison to the labour-intensive process of ELISAs. Compared with spectroscopic detectors, ELSDs produce more uniform detection sensitivity for most analytes, regardless of their physical and chemical properties. This makes it possible to analyse proteins like BMP-2 amongst in minute concentrations such as nanograms as well as picograms.

Results from the calibration of BMP standards ranging from 0.125 to 30ng/ml using an ELSD exhibited a R^2 value of 0.9949 (Appendix VIII) in comparison to the BMP ELISA R^2 value of 0.9543 (Appendix X). Results from the calibration of trehalose standards ranging from 0.19 10 12mM are illustrated in Appendix IX. The high sensitivity of ELSD and ease-of-use make the ELSD method more viable for use in comparison with the labour-intensive process of ELISAs.

Comparing the ELSD and ELISA methods of detection, ELISAs generally demonstrate high but limited specificity to proteins, antibodies and other antigens. However, the ELSD is more universal and can analyse any substance less volatile than the HPLC mobile phase. In contrast, the ELSD method is not a spectroscopic detector which means a linear relationship between absorbance and the concentration of species detected may not always be the case (Beer-Lambert's law). Nonetheless, when considering ease and speed of detection as well as sensitivity, the HPLC- ELSD method presents an alternative faster choice in protein detection. In addition, due to the number of processes involved in ELISA analysis, various errors may occur leading to lower values compared to the ELSD technique which requires a single step of manufacturing of samples to be analysed and running them with the ELSD-HPLC.

2.4 CONCLUSION

The unoptimised HA nanocores (AQUA1) which showed a large and a non-uniform size distribution was compared with the hydroxyapatite nanocores with defined diameters (20nm, 40nm, 60nm) which showed a more uniform size distribution. This size distribution of nanoparticles had an effect on morphology of the aquasomes with aggregates of nanocores clumped together around large HA nanocore particles in some cases as seen with the SEM imaging.

The particle sizes and size distribution of the HA nanocores most importantly affect their surface area-to-volume ratio. The nano-HA powders had larger surface areas, which allowed more adsorption of drug/protein molecules in the fabrication of aquasomes.

The effect of coating time on trehalose coating of nano-HA and subsequently the surface area available for drug/protein adsorption was investigated. An increase in coating time from 1.5h to 3h showed no significant difference in the calculated surface areas. Thus, a shorter coating time of 1.5h can be adopted in aquasome fabrication which will both be more energy efficient and time saving in the overall aquasome manufacture process. In comparison, smaller nanocore size increases the surface area available for drug/protein adsorption as a significant difference was observed between the surface areas of the nanocore sizes after the different durations of trehalose coating.

In conclusion, the particle size to be chosen requires consideration based on the research question to be answered as well as *in vivo* correlation, taking into account the mode of delivery (local, systemic) and the nanoparticle pharmacokinetics (nanoparticle clearance). The final dosage form (cements, tablets, powders) in which the aquasomes will be formulated into will also determine the particle size to be chosen. Smaller nanoparticle sizes have been associated with clumping/aggregation and therefore subject to end use of aquasome formulations, particle size will influence the aesthetics of the final formulation and will need to be chosen to favour both functionality and appearance of the final formulation.

The ELSD (Evaporating Light Scattering Detector) linked with the HPLC has shown a high sensitivity in the detection of proteins, comparable to the ELISA technique. Its short sample analysis time offers high throughput in analysis of samples which is a preferred feature compared to the ELISA technique which requires a longer multi-step process which can be time consuming.

The ELSD technique can be adopted in the detection of proteins usually administered in the nano-gram range fabricated into aquasome formulations. However, for the purpose of the

present study, the concurrent detection of trehalose and BMP-2 require further method development to separate both moieties to analyse both aquasome components with one analytical technique.

CHAPTER 3

THE USE OF NON-AQUEOUS SILICONE ELASTOMER GELS (NASEGS) AS TOPICAL/TRANSDERMAL DELIVERY SYSTEMS FOR AQUASOMES

3.1 INTRODUCTION

3.1.1 Topical and transdermal delivery

Topical delivery is the delivery of drugs with the skin as the target organ, in comparison to transdermal delivery, which aims at the delivery of drugs to the systemic circulation. The transdermal route of drug delivery is another viable route of administration in comparison to the oral route, through which a number of drugs are administered into the systemic circulation. The rationale behind transdermal delivery (advantages) and limitations are detailed in Table 1.4.

the limitations of traditional -transdermal delivery (via patches) is primarily associated with the barrier function of the skin, offering protection from chemicals and invasive pathogens, which limits the amount and the type of drug delivered via the skin to the systemic circulation (Desai and Lee, 2007, Delgaro-Charro and Guy, 2001).

3.1.2 Gels as drug delivery systems

A gel is defined as a soft, solid or solid-like material which consists of at least two components, one of which is a liquid present in abundance. Its elastic and resilient characteristics should be observable by the human eye and, as a consequence, on a time scale of seconds, a gel should not flow under the influence of its own weight (Hägerström, 2003).

Gels are widely recognized as valuable dosage forms in drug delivery via the skin. These polymeric systems present several advantages, namely their safety, versatility, easiness of use, low price and acceptability.

Hydrophilic gels are common dosage forms in oral, vaginal, rectal, topical, transdermal and nasal delivery. Cellulose polymers (hydroxyethyl cellulose (HEC), hydroxypropyl methylcellulose (HPMC)) and natural based polymers such as sodium alginate, pectin and gelatine are used in the manufacture of gels as well as incorporated into other dosage forms (such as gelling/thickening agents in syrups and cosmetics) (Allen, Popovich and Ansel, 2011).

Silicone as a polymer has played a vital role in drug delivery, biomedical applications as well as in cosmetics since its introduction in the 1950's (Sene *et al*, 2002, Colas, Siang and Ulman, 2006). Non-aqueous silicone elastomer gels (NASEGS) are widely and safely used as personal lubricants for vaginal and rectal application. Recently, the use of NASEGs was reported for use as a vaginal delivery system for maraviroc, a HIV-1 entry inhibitor (Forbes et al, 2011). Also, these NASEGs were modified into hydrophilically-modified SEGs, (h-SEGs),

for sustained release of the model ARV microbicide compounds maraviroc and emtricitabine (Forbes et al, 2014).

These non-aqueous silicone elastomer gels offer an added advantage: they are suitable vehicles for hydrophobic drugs (Sene *et al*, 2002), as a drug's partition coefficient between an oil and water phase.

Transdermal delivery (and topical delivery) is highlighted in this study because of the potential use of these non-aqueous silicone elastomer gels (NASEGS) in these research areas. NASEGS are currently being investigated for various delivery routes including the transdermal route. In the current research, these gels are being investigated for the delivery of protein or peptides (such as delivery of vaccines). Although proteins are generally hydrophilic and do not meet the physicochemical criteria of drug candidates for transdermal delivery, these gels can be employed in new delivery technologies to enhance transdermal delivery.

3.1.3 Gels as dosage form for aquasome delivery

In the past, nanoparticles and microparticles have been widely studied for oral and parenteral drug delivery. They have also been identified as being useful in transdermal/topical delivery (Alves et al, 2007). Their large surface area makes them important in cosmetic and pharmaceutical applications. Owing to their characteristic sustained drug release, nanoparticulate carrier systems have an added advantage for effective topical drug delivery *(*Alves et al, 2007*).*

Aqueous gels are widely used as topical/transdermal dosage forms owing to their ease and relatively low cost of manufacture. However, they are associated with messiness and leakage from application site (particularly in vaginal delivery). Therefore, a suitable alternative gel dosage form with properties including better retention at the application site to achieve the desired therapeutic effect was needed. NASEGS are hydrophobic gels and have exhibited these properties (Forbes et al, 2011).

Aquasomes are ceramic-based nano-sized carriers that consist of hydroxyapatite (HA), oligosaccharide (trehalose, cellobiose), and the target drug/protein/antigen. Outer surface of aquasomes on which antigens are non-covalently linked consists of polyhydroxyl oligomers or sugar molecules such as cellobiose, trehalose, maltose, sorbitol, and lactose, which create a quasi-aqueous film that prevents the denaturation or degradation of the protein. Carbohydrate film on ceramic particle retains the drugs spatial properties (Kim and Kim, 2002; Umashankar et al, 2010; Khopade et al, 2002).

In the present experiment, aquasomes containing HA coated with trehalose and protein were prepared. Aquasomes were prepared by coating of HA with trehalose and subsequently by coating of bovine serum albumin (BSA) as a model protein.

Gels were chosen as a suitable dosage form for the topical and transdermal delivery of BSA-loaded aquasomes and were pharmaceutically characterized for suitability in topical/transdermal delivery. Rheological, textural and *in vitro* permeation studies give valuable information on the performance of gel dosage forms *in vitro* by analysing the retention at the application site, “perceived feel” of the gel and the ability of the dosage form to permeate the rate-limiting stratum corneum (Jones, Woolfson and Djovic, 1996)

In this study, the *in vitro* release profiles of BSA; rheological and textural parameters of aqueous gels (HEC and HPMC) were compared with those of ST- elastomer gels. As a model protein for transdermal/topical delivery, BSA-loaded aquasomes were fabricated and further analysed using *in vitro* release and permeation experiments.

3.1.4 Aims and Objectives

The aim of the present research is to investigate the potential of nanoparticulate biodegradable polymers incorporated into aqueous and non-aqueous gels as drug delivery systems for the topical/ transdermal sustained delivery of proteins.

Objectives

1. To investigate the release of BSA from BSA-loaded nanoparticles (aquasomes).
2. To investigate the release of BSA from the BSA loaded aquasomes incorporated into NASEGS and aqueous semi-solid polymeric gels.
3. To characterize the rheological and textural parameters of NASEGS and aqueous semi-solid polymeric gels and its correlation to drug release.
4. To analyse the feasibility of *in vitro* permeation of BSA from BSA-loaded aquasomes using Franz cell equipment and comparing release profiles of hydrophilic and hydrophobic drugs/proteins.
5. To determine the amount of BSA that can be released from aquasomes (in comparison to BSA alone) that can stimulate a biological response without having a toxic effect (via MTT assay), using human dermal fibroblasts as an *in vitro* cell culture model.

3.2 MATERIALS AND METHODOLOGY

3.2.1 Materials

Bovine Serum Albumin (BSA, granules) and hydroxyapatite (<200nm, particles) were purchased from Sigma Aldrich (Poole, UK). D-(+)-Trehalose dihydrate powder was purchased from Acros organics (Belgium). Phosphate Buffer Saline (PBS, tablets) were purchased from Thermos Scientific (UK). Trifluoracetic acid (TFA) and methanol were purchased from Fisher Scientific (UK). ST- Elastomer 10 and Cyclomethicone were gifted by Dow Corning (USA). Hydroxypropyl methylcellulose (HPMC) and hydroxyethyl cellulose (HEC) were purchased from BD Pharmaceuticals (UK). All reagents and materials were of analytical grade.

3.2.2 Methodology

3.2.2.1 Preparation of Aquasomes

BSA-loaded aquasomes were manufactured with 1mg/ml BSA solutions in distilled water using the same protocol as outlined in Chapter 2 (Section 2.2.2.1).

3.2.2.2 Characterisation of Aquasomes

3.2.2.2.1 Characterisation of the coated cores

Trehalose-coated hydroxyapatite cores were characterised via zeta potential analysis measuring the positive charge emitted by the carbohydrate (trehalose) coating in comparison to naked hydroxyapatite particles. A small quantity of naked hydroxyapatite cores and coated cores was mixed with distilled water and placed into the probe for zeta analysis using the NanoBrook 90Plus Zeta Particle Size Analyzer (Brookhaven Instruments Corp., NY). The mean and standard deviation of the results were compared.

3.2.2.2.2 Characterisation of BSA-loaded aquasomes

The method detailed in section 3.2.2.2.1 was repeated for the BSA-loaded aquasomes. The mean and standard deviation of the results were recorded and compared to those of the naked hydroxyapatite cores and BSA solutions.

3.2.2.2.3 Aquasome in vitro release studies

In vitro release studies were performed using phosphate buffered saline (PBS, pH 7.4) as release media. PBS was chosen to simulate physiological body fluid and is commonly used in *in vitro* topical studies (Salgado et al, 2010, Salerno et al, 2010). The samples were placed in 10ml of PBS and placed in a shaking water bath (100rpm, 37°C). Using the partial replacement method, 1ml samples were taken at hourly time intervals for the duration of 8h, and immediately replaced with 1ml fresh warmed PBS. Samples were analysed using high performance liquid chromatography (HPLC) with ultraviolet and fluorescence detection described in section 3.2.2.3.

3.2.2.3 Analysis of BSA using High Performance Liquid Chromatography (HPLC)

In vitro release samples of bovine serum albumin (BSA)-loaded aquasomes were analysed using an Agilent 1200 series run in gradient mode. Phase A was 0.1% trifluoroacetic acid (TFA) in water and phase B was acetonitrile. A gradient method was performed with the percentage ratio of phase A to Phase B at 95:5 from 0-18mins, 35:85 from 18-25mins and 95:5 from 25mins untils 30 mins. The total run time was 30 mins. A Jupiter C5 column (5 micron, 250 x 4.60mm *id*, Phenomenex, Ireland) was used; detection wavelength 220nm was employed for UV detection and fluorescent readings were at 296nm (excitation) and 380nm (emission). An injection volume of 10μL was used and BSA had a retention time of 25min.

3.2.2.4 Comparison of *In Vitro* Release of BSA from Aqueous Semi-Solid Polymeric Gels and Non-Aqueous Silicone Elastomer Gels (NASEGS)

BSA release from BSA-loaded aquasomes incorporated into non-aqueous silicone elastomer gels (NASEGS) and aqueous semi-solid polymeric gels were compared with the release profiles of incorporating the BSA alone in the gels.

3.2.2.4.1 Preparation of BSA/Gel Formulations

3.2.2.4.1.1 Aqueous gels

Hydroxypropyl methyl cellulose (HPMC) and hydroxyethyl cellulose (HEC) gels were prepared (5% w/v) by mixing the required weights of polymer with distilled water using a Polytron mixer overnight (800-1200 rpm; 25°C). HPMC and HEC gels were chosen for this study because they constitute two of the most commonly used aqueous gelling agents in topical formulations. After mixing, samples were kept sealed in individual containers and stored at 4°C until needed.

3.2.2.4.1.2 Silicone gels

NASEGS were prepared by hand-mixing the required weights of ST-Elastomer 10 and cyclomethicone, which acts as a cross-linker (90/10 %w/w, 80/20 %w/w, 70/30 %w/w, 60/40 %w/w) and stored in individual containers at room temperature (25°C).

3.2.2.4.1.3 Protein and protein loaded aquasome incorporation

BSA was incorporated into the gels by mixing. Based on the theoretical and practical estimation that BSA loaded onto aquasomes is between 6±1 mg per 100 mg of aquasome formulation, BSA was weighed and incorporated into gels per 1g of gel (Table 3.1).

Table 3.1 The amount of BSA incorporated in silicone and aqueous gels

BSA loading (%)	Weight (mg/g) gel *
100	7
75	5.25
50	3.5
25	1.7

**(n=3)*

3.2.2.4.2 In vitro release studies of BSA from gels

1g of each gel formulation was placed into individual jars containing 20ml of PBS and placed in a shaking water bath (100rpm, 37°C). Using the partial replacement method, 1ml samples were taken and replaced with an equal volume of fresh pre-warmed PBS at hourly time intervals for the duration of 8h. Samples were analysed using the HPLC methods described in section 3.2.2.4. All formulations were carried out in triplicate.

3.2.2.5 *In Vitro* Permeability Studies of Gels

The *in vitro* permeation studies of incorporated BSA using the Franz cell set up was performed to establish the amount of BSA which can permeate through 0.4μm polycarbonate membrane released from the silicone gel formulations.

3.2.2.5.1 Preparation of samples

Samples were prepared using the methods highlighted in section 3.2.2.4.1. However, aquasomes were not incorporated into silicone gels.

3.2.2.5.2 Franz cell experiments

The Franz cell set-up is the most commonly used experiment that studies drug permeation *in vitro.* Permeation studies need to be performed to ascertain the tissue permeation characteristics of the dosage form as well as establish the permeation characteristics of drugs at the site of administration (Figure 3.1). The heated water pump was switched on and left to equilibrate the Franz cell setup at 37◦C for 15 min. Membranes (polycarbonate, 0.4 µm pore size, 10 µm thickness) were pre-soaked for 24h in phosphate buffer saline at 25°C. Membranes were mounted on the Franz cell setup (n=3) and 0.8-1g of BSA/incorporated gel was spread onto the membranes. All Franz cell openings including the donor-receptor interface were occluded with Parafilm to prevent evaporation.

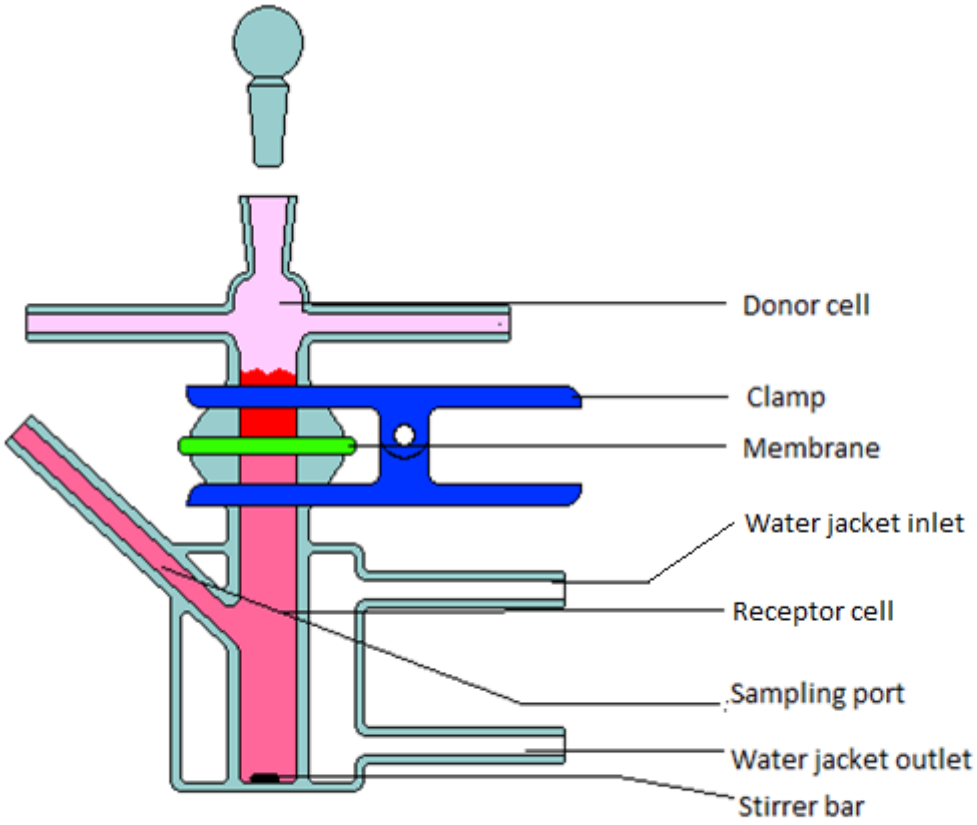

Figure 3.1 Static Franz cell set-up
(Reproduced with permission from Permegear, 2012)

The receptor compartment (PBS, 23ml) was stirred at 300rpm using a magnetic stirrer. Samples volumes (1-2 ml) were taken at hourly intervals for the duration of 8 hours for HPLC analysis (section 3.2.2.3) and replaced with equal volumes of fresh preheated medium via the sampling port. Air bubbles developing under the membrane were removed via the side arm by carefully tilting the Franz cell.

The permeation study was validated by using saturated BSA solutions in place of the sample gels. After a temperature equilibration period of 15mins, 0.1ml to 1ml of saturated solutions was introduced to the donor compartment (n=3). After the duration of 8h and 24h, an aliquot from each receptor compartment was taken and assayed using the HPLC apparatus (section 3.2.2.3) and receptor drug concentrations were calculated.

3.2.2.6 Rheological Characterisation and *In Vitro* Permeation Studies of Gels

3.2.2.6.1 Viscometric and Oscillatory Analyses

Viscometric and oscillatory analyses were carried out with a Bohlin Rheometer fitted with 20mm (parallel plate) and 40mm (cone and plate) diameter plates. The gel samples (2g approx.) were transferred to the base plate of the rheometer, followed by lowering of the plate to produce a gap depth of between 0 to 104µm. Excess gel was removed before initiating the test. The viscoelastic region which is defined as the region where stress is directly proportional to strain and G' remains constant, was determined by range of strain measurements from 0.05 to 0.15 for the NASEGS and 0.025 to 0.05 for the aqueous semisolid polymeric gels. The viscosity, elastic and complex moduli were determined at the strain of 0.05 and at a frequency range of 2-50Hz. All measurements including shear sweep and stress sweep were performed at body temperature (37±0.1 °C) for a period of 60s with a shear rate ranging from 0.01/s to 100/s. All measurements were done in triplicates. Calculations of the viscosity (storage moduli, G') and elastic (loss moduli, G") were performed using a computer programme supplied by TA instruments (Leatherhead, UK).

3.2.2.6.2 Texture profile analysis

Texture profile analysis measurements were taken with a Brookfield CT3 Texture analyser with a TA-10 probe using a fixed base table. The hardness, adhesiveness and cohesiveness were analysed with a delay time of 15s between each compression. Gel samples were

stacked up in glass cylindrical vials up to a fixed height of 10cm for each gel formulation. All tests were done repeatedly and consistent results were recorded.

3.2.2.7 *In vitro* cell toxicology assay (Thiazolyl Blue Tetrazolium Bromide (MTT) assay)

To investigate whether the concentrations of BSA adsorbed onto the aquasomes were toxic to human cells, using human dermal fibroblasts (HDFa) as a model, a thiazolyl blue tetrazolium bromide (MTT) assay was performed to measure cell death after exposure of cells to different concentrations of BSA for 24 h, representing short term exposure to aquasomes (acute toxicity).

Human dermal fibroblasts (HDFa) were cultured in basal medium (Medium 106, Gibco®) supplemented with antibiotic supplement (Amphotericin B/Gentamycin) at 37°C in humidified air with 5% CO_2, without serum Cells are cultured at 37°C in humidified air with 5% CO_2. Cells were trypsinised using a dilute trypsin solution (made with 15-20% of 0.25% Trypsin EDTA solution diluted with HBSS), centrifuged (1000rpm) and re-suspended in fresh media. Cells were counted and recorded for concentration per ml. Cell suspension was diluted with serum-free media to 75,000 to 100,000 cells per ml. 100µl of cells (7,500- 10,000 cells per ml) was added into each well and incubated overnight (37°C, 5% CO_2).

On day 2, after allowing cells to attach to the bottom of the wells, serum-free media was carefully removed. Cells were treated with 7, 5.6, 3.5 and 1.7mg/ml BSA-spiked serum-free medium (n=4), leaving a final volume of 100µl per well. After 24h, 20µl of 5 mg/ml MTT was aseptically added to each well. MTT reagent was also added to a set of wells without cells, acting as blank.

Plates were incubated for 3.5 h at 37°C in an incubator. Wells were aspirated and 150µl of dimethyl sulphoxide (DMSO) was added per well. Well plates were covered with tinfoil and cells were agitated using an orbital shaker for 20mins. The absorbance readings of wells were then measured at 590nm with a photometric scan between 540nm to 590nm to assay absorbance values at different wavelengths (Multiskan Spectrum- UV/Vis Microplate Spectrophotometer).

The cell viability was calculated using the formula below:

$$\text{Cell viability (\%)} = \frac{[\text{O.D. OF TREATED WELL- O.D. OF BLANK}]}{[\text{O.D. OF UNTREATED WELL - O.D. OF BLANK}]} \times 100\%$$

3.2.2.8 Statistical Analysis of Results

Statistical analysis was performed using GraphPad Prism software package. Data was analysed using a one-way ANOVA with Tukey's multiple comparisons post-hoc test.

3.3 RESULTS AND DISCUSSION

Non-aqueous silicone elastomer gels (NASEGS) and aqueous gels (HEC and HPMC) were used as delivery systems to study the release of protein (alone) and protein from protein-loaded aquasomes. In this study, BSA was used as a model large, electronegative protein to investigate the various release profiles. Texture profile analysis and rheological characterisation were also employed to further characterise and analyse the mechanical performance of the gel formulations as required for pharmaceutical use. *In vitro* permeation and toxicity assays were also implemented to explore the release of BSA to mimic in vivo conditions and to examine amounts of BSA released from the aquasome formulations.

3.1 Evidence of Drug Loading

The successful adsorption of BSA onto aquasome nano-carriers was evidenced by zeta potential analysis and *in vitro* release.

3.4.1.1 Zeta potential analysis

The zeta potential of the naked hydroxyapatite cores and the trehalose-coated cores were compared to establish the presence of the carbohydrate coating on the nanocores (Table 3.3). The successful coating of nanocores by the adsorption of trehalose to hydroxyapatite and subsequent loading of BSA onto coated hydroxyapatite nanocores was determined by change in carrier charge in comparison to blank hydroxyapatite nanocores.

The measurement of the electrostatic potential at the electrical double layer surrounding a nanoparticle in solution is referred to as the zeta potential. Nanoparticles with a zeta potential between −10 and +10 mV are considered approximately neutral, while nanoparticles with zeta potentials of greater than +30 mV or less than −30 mV are considered strongly cationic and strongly anionic, respectively (Clogston and Patri, 2011). The significance of zeta potential is that it can be related to the stability of particle dispersions like aerosols, emulsions and suspensions. Zeta potential is a property involving not only the particles but also their environment, e.g., pH, ionic strength, and even the type of ions in the suspension (Xu, 2008). The zeta potential indicates the degree of repulsion between adjacent, similarly charged particles and between adsorbents and their adsorbed ions/substances. Molecules and particles that are small enough have a high zeta potential (negative or positive) that confers stability, i.e. the particles will resist aggregation. When the potential is low, attraction exceeds repulsion and the particles tend to aggregate (Doostmohammadi et al, 2012). pH and concentration of solute in a solution are factors that can affect zeta potential.

From the results in table 3.2, the adsorption of BSA onto BSA-loaded aquasomes show a more electronegative charge (-29.49 ±1.49 mV), in comparison to the blank hydroxyapatite cores (-9.92 ±2.00mV). Similar studies by Pandey and colleagues (2011) showed that OVA-loaded aquasomes yielded the negative zeta potential of −11.34±1.4mV. Goyal and colleagues (2008) who also fabricated BSA-loaded aquasomes (with trehalose coating) showed that the BSA-loaded aquasomes yielded the negative zeta potential of 25.32 ± 1.26 mV.

Theoretically, the skin carries a negative surface charge due to the phospahtidyl-choline and carbohydrates found in mammalian cells and contain negatively charged groups (Honary and Zahir, 2013). Successful transdermal delivery has been limited to drug moieties with the right combination of molecular weight, lipophilicity and charge (Uchechi, Ogbonna and Attama, 2014). However, according to the *ex vivo* work of Morykwas, Thornton and Bartlett (1987), the surface charge of human skin is +23.0mV. This charge permits the adherence and thus transdermal delivery of negative charged proteins such as BSA. Research shows that BSA strongly adsorbs onto skin but cannot permeate through the stratum corneum unless aided by permeation enhancers or via new transdermal drug delivery technologies shuch as iontophoresis, sonophoresis, microneedles, etc. (Petchsangsai et al, 2012; Hans and Das, 2013).

Table 3.2 Comparison between zeta potential values of protein and protein-loaded aquasomes

	Zeta potential (mV)*
Hydroxyapatite (HA) cores	-9.92 ± 2.00
Trehalose-coated HA cores	-1.15 ± 0.02
BSA	-21.67 ± 4.99
BSA- loaded aquasomes	-29.49 ± 1.49

(*n=3)

3.4.1.2 In vitro cumulative release studies of BSA - loaded aquasomes

A release study of BSA- loaded aquasomes was performed for the duration of 8 hours, with samples taken at hourly time points. The *in vitro* cumulative release plot is presented in figure 3.2 with the percentage amount of BSA released presented in figure 3.3. The amount

of BSA released ranged from 11.19μg to 15.38μg (1.6 to 3.57%). BSA release from aquasomes showed an initial burst release between the 1st and 3rd hour release showing amount of BSA release from 11.19 μg to 14.65 μg. After duration of 3 hours, the amount of BSA released from aquasomes began to plateau showing similar amounts of BSA released ranging from 14.65 μg to 15.38 μg. Percentage release of BSA from loaded aquasomes highlight the sustained release characteristic of BSA-loaded aquasomes demonstrating that more than 90% of BSA is still remaining in the aquasome formulation. This suggests the application of BSA-loaded aquasomes for sustained prolonged release of proteins.

The hydration of the oligomeric coating, trehalose, determines the release of BSA from the aquasomes. The hydration of trehalose forms a gel which offers a controlled release property in the aquasome formulation, which consequently leads to the desorption of BSA upon further hydration of the trehalose gel from the surrounding release medium.

Similar findings were observed by Goyal and colleagues (2008) which also investigated the in vitro cumulative release of BSA from trehalose coated aquasome formulations. The study showed that BSA desorbed from nano-carriers follow a typical biphasic pattern. An initial faster release rate was observed within hours followed by slow release rate in second phase. The possible region might be surface desorption of BSA followed by sustained release of antigen from aquasomes matrix. In comparison to cellobiose-coated aquasomes, it was noted that cellobiose coated aquasomes released BSA faster than trehalose coated aquasomes and plain HA ceramic core, this may be attributed to the zeta potential differences and adsorption patterns of BSA antigen onto the surface of HA nanocores, which restricts its movement from matrix to external aqueous phase.

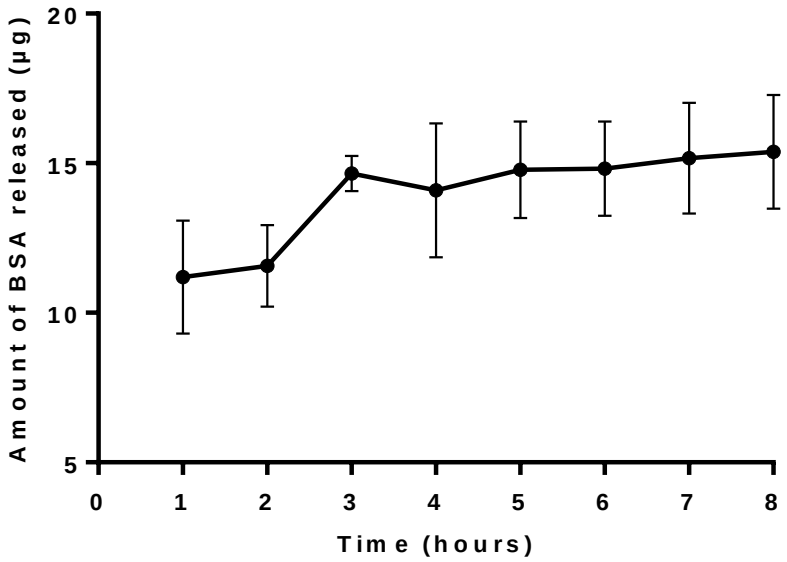

Figure 3.2 In vitro cumulative release of BSA from BSA- loaded aquasomes over a period of 8h. This graph represents the cumulative amount of BSA released at each time point when an in vitro release study of BSA from loaded aquasomes was carried out in PBS (pH 7.4) for the duration of 8 hours. Results show biphasic release of BSA from aquasomes showing initial burst release in the first 2 hours which plateaued afterwards during the 8 hour study period (n=3).

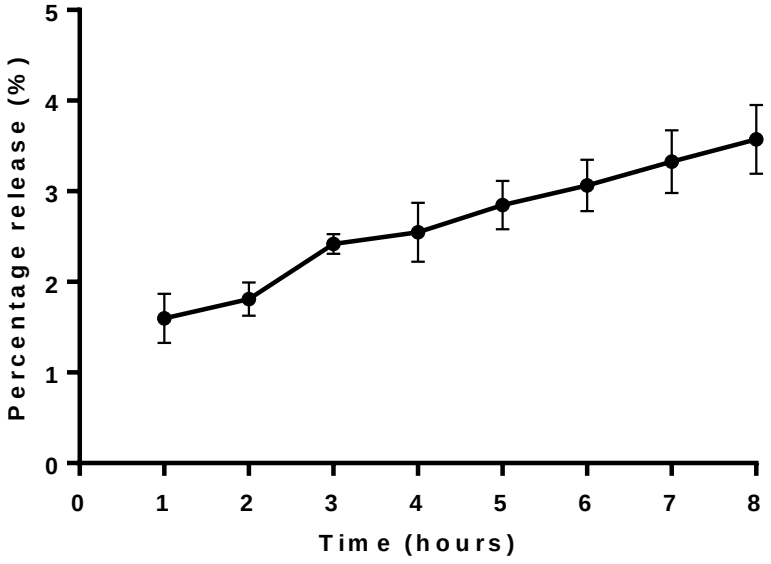

Figure 3.3 In vitro percentage release of BSA from BSA- loaded aquasomes. This graph represents the percentage cumulative amount of BSA released at each time point when an in vitro release study of BSA from loaded aquasomes was carried out in PBS (pH 7.4) for the duration of 8h. Results show that percentage release ranged from 1.59% to 3.57% demonstrating the sustained release characteristic of BSA- loaded aquasomes (n=3).

3.4.2 Texture Profile Analysis (TPA) and Rheological Characterisation of Gels

In the development of topical dosage forms, several desirable attributes contribute to the ultimate patient acceptability and clinical efficacy of the product. These include optimal mechanical properties (e.g. ease of removal of product from the container, good spreadability on the substrate, e.g. skin, mucous membranes), good bio-adhesion (to ensure retention at the site of application), acceptable viscosity, drug release and drug absorption (Jones et al., 1996a, Jones et al, 2001). A useful method by which the mechanical properties of gels are determined is by texture profile analysis. Additionally, the rheological performance of the gels is analysed to quantify the general rheological characteristics of gels and evaluate the contribution of viscosity to textural characteristics (Jones et al., 1997).

The mechanical and rheological characterisation of the various gels were performed to establish the relationship between drug release and the rheological characteristics of gels and also the textural characteristics in relation of product performance and suitability.

3.4.2.1 Texture profile analysis (TPA)

Mechanical characterisation of gels to measure hardness, adhesiveness and cohesiveness (Table 3.5) of both NASEGS and aqueous semi-solid polymeric gels were performed to establish the relationship between gel structure and drug release. TPA measurements yielded observed differences in user perceived “feel” of the gels (Table 3.5). Results showed that hardness (g) increased with an increased ratio in ST-Elastomer for silicone gels and hardness (g) was higher for aqueous semi-solid polymeric gels. The formulations with the varying percentage weight ratios of ST-Elastomer and cyclomethicone (NASEGS): 60/40, 70/30, 80/20 and 90/10 had corresponding hardness values of 8.33±2.88g, 15.00±5.00g, 18.33±2.86g and 65.00±8.66g respectively. The hardness of the silicone elastomer gels was dependent on the elastomer/cyclomethicone ratios. This correlates with the research performed by Forbes et al, (2011). The increase in polymeric concentrations of HEC, HPMC and HPMC II in the gel formulations also had a direct correlation to the increase of texture profile analysis (TPA) and rheological parameters of the gels. The corresponding hardness values of these aqueous gels were 6.67, 11 and 70g respectively. This also relates with similar research performed by Jones et al, (1997a). The TPA analysis demonstrated that hardness of the ST-elastomer gels was exponentially higher than that of the aqueous gels.

The varying formulations of the NASEGS exhibited similar release profiles with formulations 70/30 ST and 80/20 ST having the best optimal sustained release profiles and desired mechanical properties (in this study, evidenced by suitable viscoelasticity and hardness, consistent with a true gel; Table 3.5). The 90/10 ST formulation lacked the desired

spreadability characteristic with gels while the 60/40 ST formulation was very runny, similar to the aqueous gels (Figure 3.4). This was evidenced by the TPA results obtained. The mechanical properties of 80/20 ST illustrated better gel spreadability. This desirable hardness is required in the development of topical gel formulations which will influence patient compliance and subsequently clinical efficacy. Spreadability of gels, creams, ointments and lotions is the net result of a combination of rheological contributions, which include viscosity and structural rigidity (hardness) (Table 3.3). Good spreadability affects adherence to the skin which ensures that a topical medication is properly administered to the skin thus enhancing clinical efficacy.

Table 3.3 TPA parameters used to characterise gels in this study

Texture profile analysis parameters
Hardness (strength)
The force required in attaining a given deformation.
Adhesiveness
A quantity that simulates the work required in overcoming the attractive forces between the surface of the sample and the surface of the probe with which the sample comes into contact.
Cohesiveness
The strength of internal bonds or forces holding the structure of the polymeric system together.

Texture profile analysis (TPA) of gels analyses the textural properties of gels such as 'perceived' feel of a product and the retention of the product at the application site, which provides invaluable knowledge about the predictive performance of the gel under various conditions (Section 3.4.2) (Jones et al, 1996; Jones et al, 1997). As seen in Table 3.4, the hardness increased with an increase in ratio of ST-Elastomer. This result infers that hardness increases with polymeric concentration (Jones, Woolfson and Djovic, 1996). The cohesiveness showed a decrease with an increase in ST-Elastomer component, with the 60/40 formulation with cohesiveness of 0. However, from the results, adhesiveness had no correlation with an increase in the ST-Elastomer component.

Table 3.4 Texture profile analysis measurements

Gel formulation	*Hardness (g)*	*Adhesiveness (J)*	*Cohesiveness*
	ST-elastomer formulation (w/w %)		
60/40	8.33 ± 2.88	0	0
70/30	15.00 ± 5.00	0.0006 ± 0.0001	1.41 ± 0.2464
80/20	18.33 ± 2.86	0.0003 ± 0.0003	0.98 ± 0.4206
90/10	65.00 ± 8.66	0.0036 ± 0.0008	0.97 ± 0.0461
	Aqueous gel composition (5 w/v %)		
HEC	6.67	0.0001 ± 0	0
HPMC 1	11	0.0003 ± 0.0004	0.0003
HPMC 2	7	0.0016 ± 0.0002	0.0016

*(n=3)**

3.4.2.2 Oscillatory Measurements

Products designed for topical administration will be subjected to shearing forces, e.g. chewing, breathing, swallowing, talking, flexing processes of skin, that are oscillatory in nature. Therefore, it is important to examine the effects of such oscillatory forces on the product rheology, and hence, on their clinical performance (Jones et al., 1996a; Jones et al., 1996b).

To accurately evaluate the relationship between molecular structure and viscoelastic behaviour measurements are conducted in regions where the viscoelastic properties observed are independent of imposed stress or strain levels. That is, experiments must be conducted in the linear viscoelastic region. The linear viscoelastic region (LVR) was determined between the strains of 0.01 to 0.15. Oscillatory sweep tests were performed between 0.002 to 50 Hz within the LVR (strain of 0.05- 0.15) for all silicone gel samples. Aqueous gels were analysed with a lesser magnitude (0.025- 0.05) of strain as higher magnitudes yielded incorrect rheograms. Rheograms were plotted as viscosity and elastic moduli against frequency.

For the silicone elastomer gels, the viscosity and elasticity moduli are clear and distinct in the rheograms within the frequency range measured (Fig. 3.4 A to H), while viscosity and elasticity moduli have cross-over points with the aqueous gels, exhibiting loss of gel structure (Fig. 3.6 and 3.7). For the silicone elastomer gel formulation examined (80/20 formulation), the storage modulus (elastic modulus) and loss modulus (viscosity modulus) increased as a function of increasing oscillatory frequency (0-10Hz). Similar results were observed with the 90/10 with higher values, which maintained its gel structure up to 25 Hz; and 70/30 formulation with lower values, which maintained its gel structure up to 6.25 Hz, in comparison to the 80/20 formulation. In the range of strain values used, the storage modulus was higher than the loss modulus, indicating a more elastic character. These results showed that the gels possessed viscoelastic properties. However, for the aqueous gels and the 60/40 silicone elastomer gel formulation, the viscosity modulus was higher than the elastic modulus which crossed over at a higher frequency in which the integrity of gel structure was lost (60/40 at 1 Hz, 5% HEC at 20 Hz, 5% HPMC (60S) at 12 Hz and 5% HPMC (90000S) at 2.14Hz). The aqueous gels and the 60/40 silicone elastomer gel exhibited more of a viscous property at lower frequencies.

The rheological characterization of the ST-elastomer gels and aqueous semi-solid polymeric gels were compared to further examine the correlation between rheological behaviour and drug release profiles. The apparent viscosity (σ) profiles of the gels tested illustrated non-Newtonian, pseudoplastic behavior, commonly attributed to polymeric gel systems (das Neves et al, 2009). This behavior is seen to be important for good spreadability of topical/transdermal dosage forms. From figures 3.4 a) to f), it is illustrated that the linear viscoelasticity region was identified with the viscosity modulus (G') and elasticity modulus (G") clearly defined without any destruction of the microstructure of the gel shown in the cross-over of the G' and G" plots, within the strain range 0f 0.01 to 0.1Pa. However, the cross-over point was reached when exposed to the strain of 0.15Pa at 3.5Hz (figure 3.4g). The viscosity modulus (G'), as the name implies, represents the characteristic viscosity of the gel while the elasticity of the gel characterizes the elastic property of the gel. The measurements in the figures highlighted above, when maintained after shear forces are applied, infer that the structural integrity of the gel is intact. When there is a cross-over of the G' and G" plots, this implies that there is destruction of the microstructure of the gel.

For the aqueous semi-solid polymeric gels (HEC and HPMC I), cross-over points were reached at frequencies > 10Hz with the exception of HPMC II (90000S) whose cross over point was at 5Hz, illustrating destruction of the gel (Figures 3.5 to 3.7). Higher values of G' in ST- Elastomer gels elucidate the more solid-like and more rigid micro-structure of the gels in comparison to the aqueous semi-solid polymeric gels. The higher values of the storage

modulus (or elasticity modulus G') in comparison to the loss modulus (or viscosity modulus G") for the gels tested in the frequency range considered also indicate that the gel systems are predominantly elastic (das Neves et al, 2009). Due to slippage (lack of grip during rheological testing) at frequencies higher than 25Hz, the G' and G" plots of the silicone gels grew wider apart. This is illustrated in figures 3.5- 3.7.

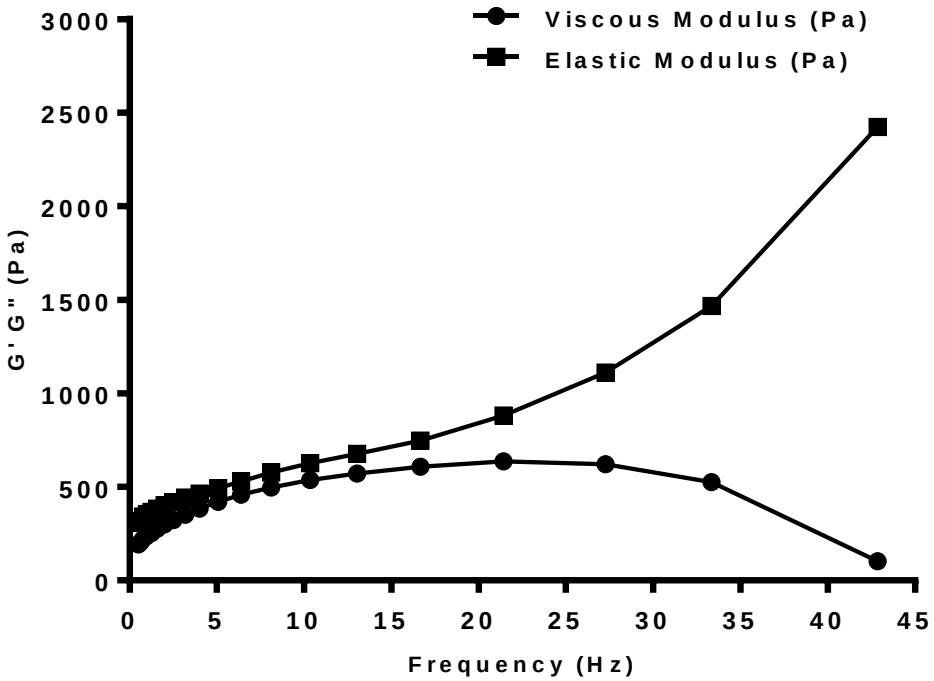

Figure 3.4 A Rheogram showing the viscosity and elasticity moduli of 80/20 ST-elastomer gel formulation at various strain measurements used in analysing the mechanical spectrum (LVR). (0.01 Strain)

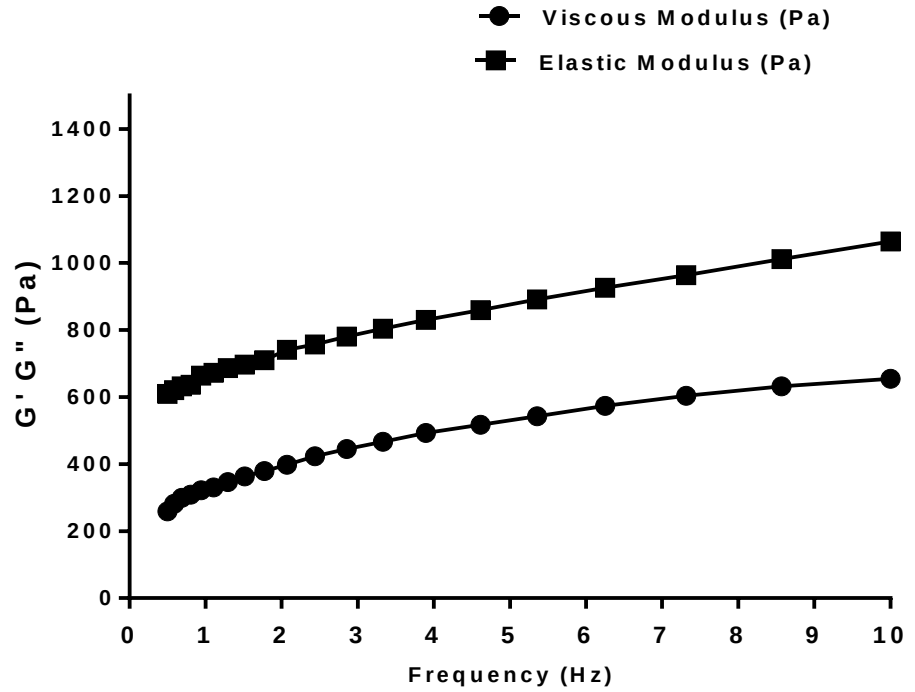

Figure 3.4 B Rheogram showing the viscosity and elasticity moduli of 80/20 ST-elastomer gel formulation at various strain measurements used in analysing the mechanical spectrum (LVR). 0.015 Strain

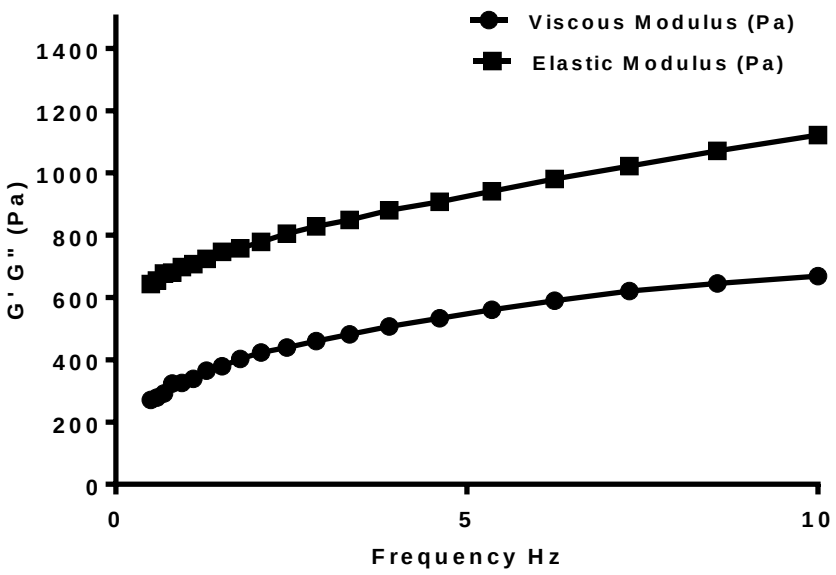

Figure 3.4 C. Rheogram showing the viscosity and elasticity moduli of 80/20 ST-elastomer gel formulation at various strain measurements used in analyzing the mechanical spectrum (LVR).0.02 strain

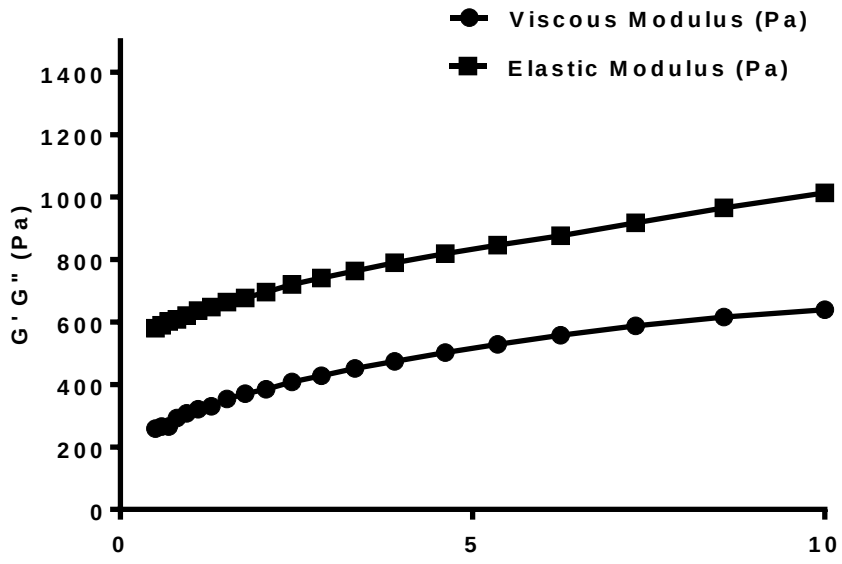

Figure 3.4 D Rheogram showing the viscosity and elasticity moduli of 80/20 ST-elastomer gel formulation at various strain measurements used in analysing the mechanical spectrum (LVR). (0.025 strain)

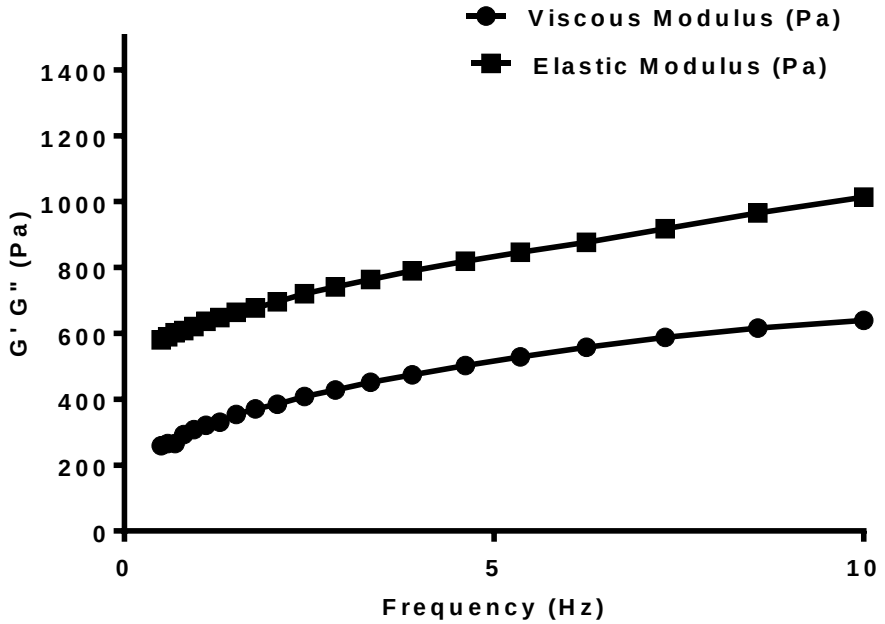

Figure 3.4 E. Rheogram showing the viscosity and elasticity moduli of 80/20 ST-elastomer gel formulation at various strain measurements used in analysing the mechanical spectrum (LVR). 0.03 Strain

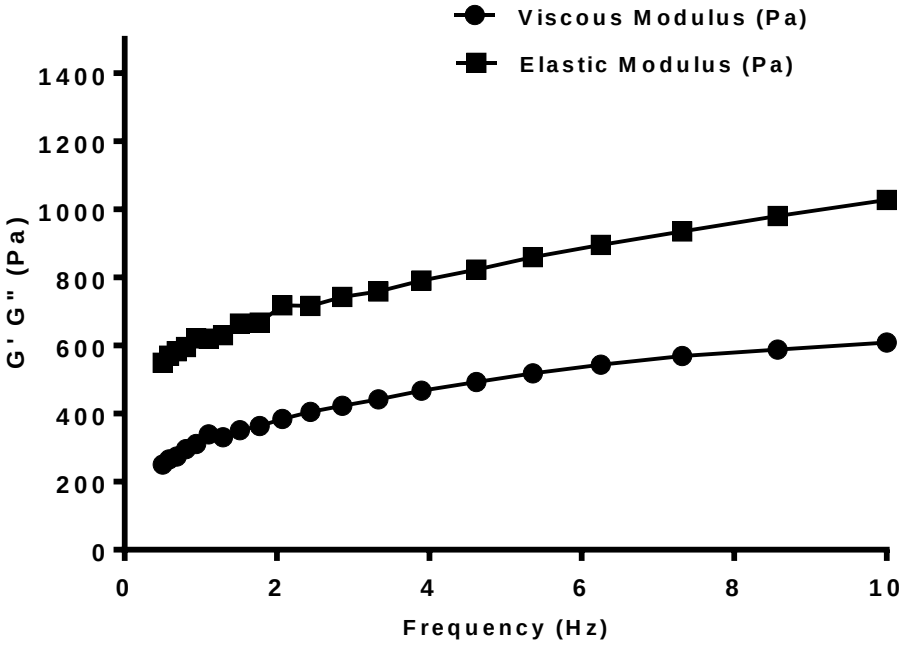

Figure 3.4 F Rheogram showing the viscosity and elasticity moduli of 80/20 ST-elastomer gel formulation at various strain measurements used in analysing the mechanical spectrum (LVR). (0.1 Strain)

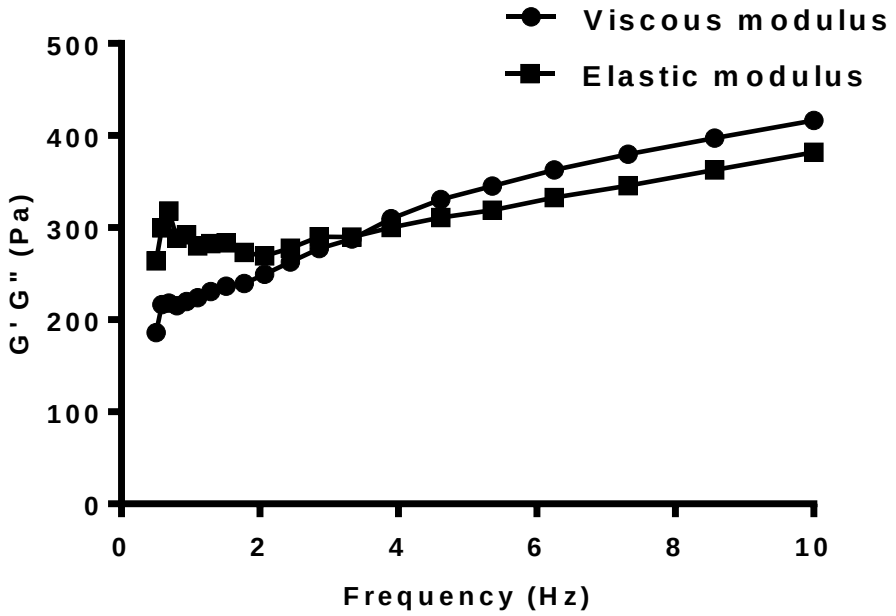

Figure 3.4 G. Rheogram showing the viscosity and elasticity moduli of 80/20 ST-elastomer gel formulation at various strain measurements used in analyzing the mechanical spectrum (LVR). (0.15 strain)

Rheological characterisation of gels provides information on the properties of gels and semi-solids that may be related to product performance such as drug release and product stability. From the correlation of the results of the *in vitro* release study with the various formulations of ST-gels (90/10%, 80/20%, 70/30% and 60/40%) and their rheological and textural characterisation, it can be deduced that protein release profiles are affected by the rheological parameters of the gels. The weak structure of the 60/40% formulation, evidenced by its low hardness value and complete destruction of gel structure (at the frequency of 10Hz) best describes the immediate release of BSA from the gels. the 90/10% formulation exhibited the next highest *in vitro* release profile, despite having the highest value for hardness, viscosity modulus (G') and elasticity modulus (G"). Reasons for this result are unclear. However, in comparison to the 80/20% and 70/30% formulations which had similar but statistically different ($p<0.0001$) *in vitro* release profiles, hardness, viscosity modulus (G') and elasticity modulus (G") results, it is observed that they had small amounts of drug released over 8 hours. The highest percentage release of 90/10%, 80/20%, 70/30% and 60/40% were 11.2%, 5.7%, 5.5% and 13.9%. This illustrates the sustained release

characteristic of the 80/20% and 70/30% gels which can be applied as modified gel dosage forms for the sustained delivery of proteins.

An increase in hardness, viscosity and elasticity moduli with an increase in polymer concentration is observed as normal and can be explained by macromolecular entanglement phenomena. Higher concentrations of polymer increase entanglement density (the number of intermolecular contacts per unit volume) and thus viscoelastic properties have a resultant increase (Talukdar et al, 1996).

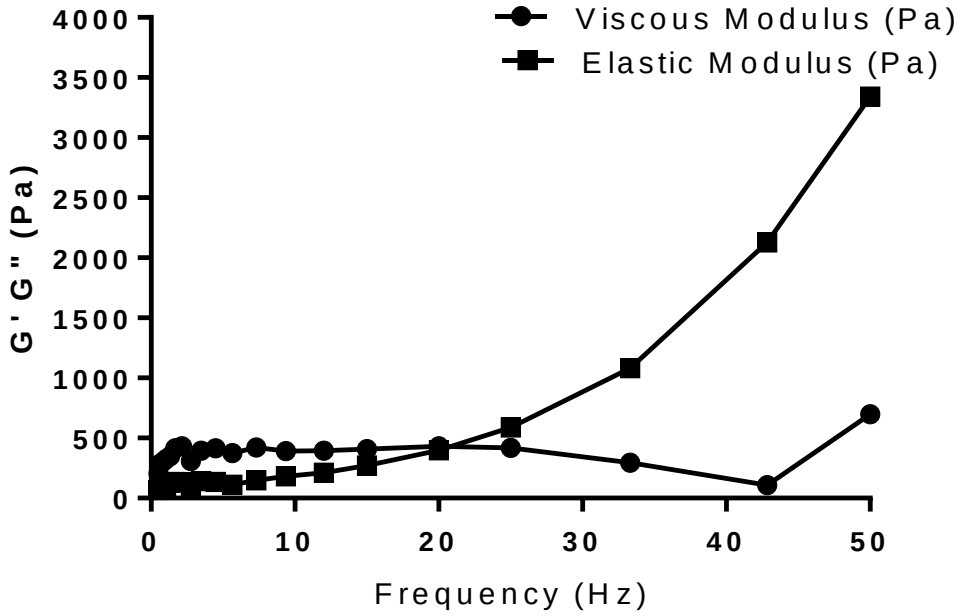

Figure 3.5 Rheogram showing viscosity (G') and elastic (G") moduli of 5 % w/v HEC gels

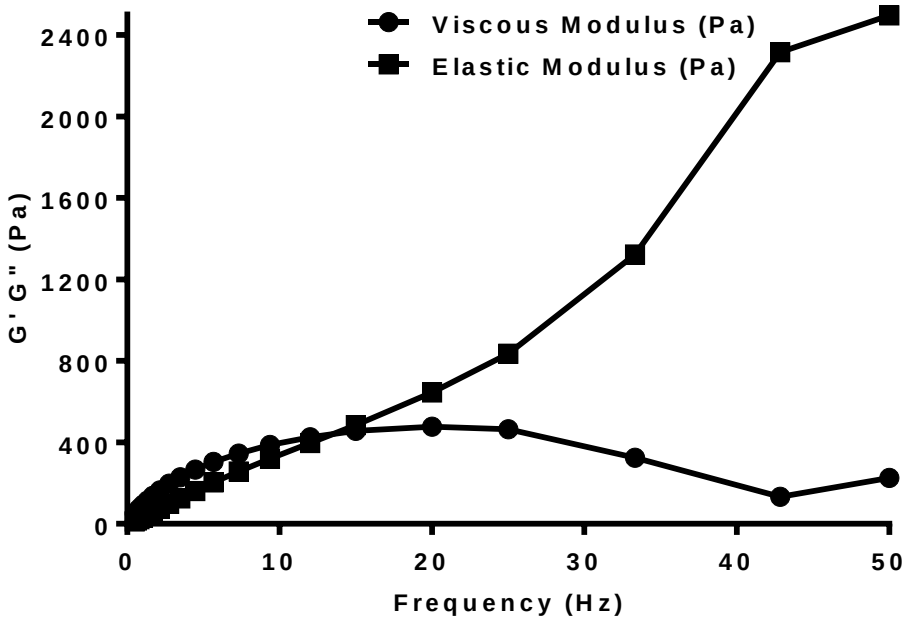

Figure 3.6 Rheogram showing viscosity (G') and elastic (G") moduli of 5 % w/v HPMC (60S) gels

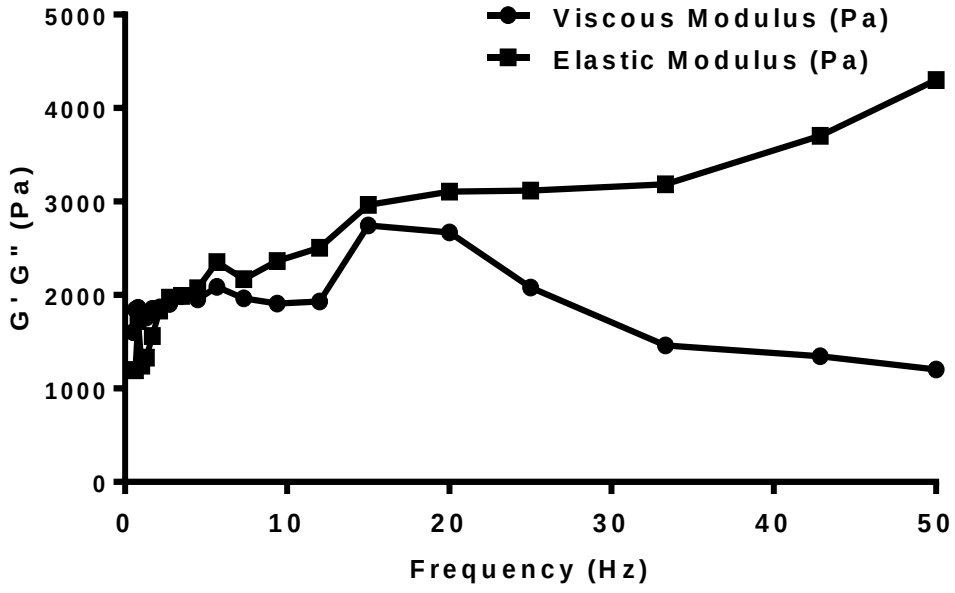

Figure 3.7 Rheogram showing viscosity (G') and elastic (G") moduli of 5 % w/v HPMC (90000S) gels

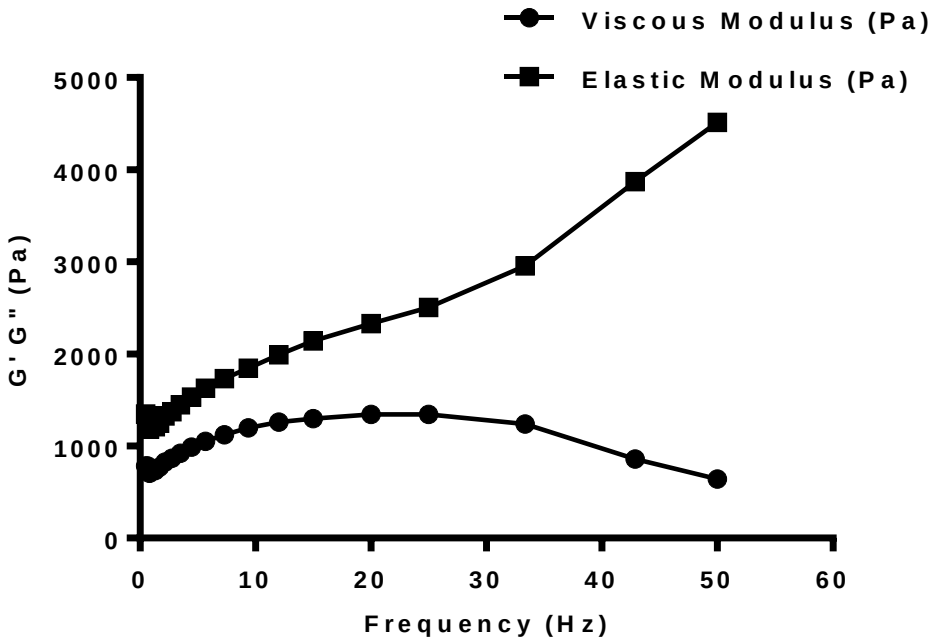

Figure 3.8 Rheogram showing viscosity (G') and elastic (G") moduli of 90/10 ST elastomer gels.

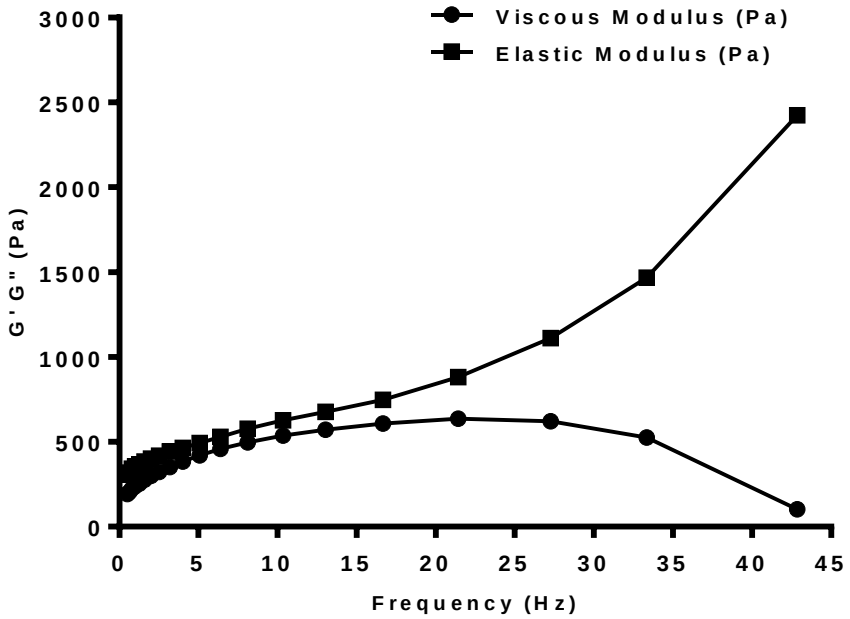

Figure 3.9 Rheogram showing viscosity (G') and elastic (G") moduli of 80/20 ST elastomer gels

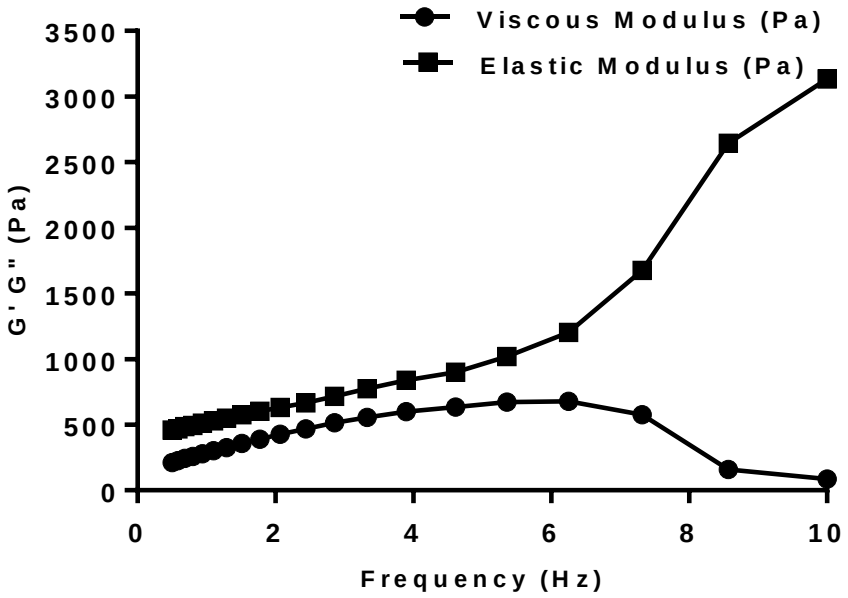

Figure 3.10 Rheogram showing viscosity (G') and elastic (G") moduli of 70/30 ST elastomer gels.

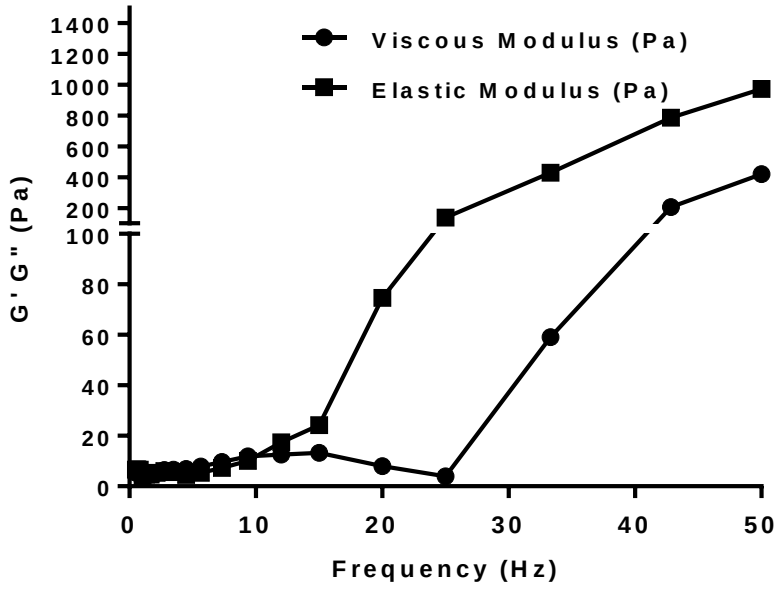

Figure 3.11 Rheograms showing viscosity (G') and elastic (G") moduli of 60/40 ST elastomer gels.

3.4.3 Comparison of BSA Release Profiles from of Non-Aqueous Silicone Elastomer Gels (NASEGS)

3.4.3.1 Comparison of BSA release profiles from various compositions of non-aqueous silicone elastomer gels (NASEGS)

Non-aqueous silicone elastomer gels (NASEGS) were employed to investigate the topical/transdermal delivery of free protein (BSA) and BSA-loaded aquasomes, where BSA was used as a model protein**.** The NASEGS have two components, ST elastomer and cyclomethicone. Their proportions can be varied to produce gels of different viscosities. Four different formulations of ST-elastomer gels were manufactured to compare BSA release from the silicone gel. The formulations varied the composition ratio of ST-Elastomer to cyclomethicone (90/10, 80/20, 70/30 and 60/40). The resulting formulations were loaded with 7mg of BSA per 1g of gel formulation, based on the entrapment efficiency of aquasomes per 100mg of HA (for each aquasome formulation). The *in vitro* release of BSA from the different formulations of NASEGS is presented in figure 3.12.

Figure 3.12 shows the BSA release profiles from silicone gel formulations had similar trends, with no significant difference ($p > 0.05$) in the release profiles. The results demonstrated that the silicone gel formulations have similar release profiles, which were dependent on percentage BSA loading. The release of BSA from the different formulations of the NASEGS varied based on the different formulations used. The 60/40 %w/w formulation had the highest amount of drug released (0.98mg) followed by 90/10 %w/w (0.78mg), 80/20%w/w, (0.40mg) and 70/30 %w/w (0.38mg). The 80/20% and 70/30% formulation showed little difference in *in vitro* release profiles, and the difference was found to be insignificant (adjusted p value= 0.9954). The difference between the BSA release profiles of "90/10 %w/w vs. 60/40 %w/w" formulations were also found to be insignificant (adjusted p value= 0.2306). These results highlights the fact that the BSA rate of release from the formulations compared was similar irrespective of the formulation as there was no statistical difference between the BSA release profiles compared. Nonetheless, the choice for the most suitable formulation will depend on the other characteristics (rheological and textural properties, as elucidated in the previous sections).

The percentage release of BSA from the various NASEG formulations differed based on the composition of polymer in the gel structure. 90/10% and 60/40% formulations had the highest percentage of BSA release with their highest points of release as 13% in the first hour and 13. 15% at the 5^{th} hour time point respectively. Other time points revealed the percentage BSA release from these formulations ranging from 11.11 to 13.1% and 8.8 to 13.1% at each

time point respectively. 80/20% and 70/30% NASEG formulation had the lowest percentage release as 5.25% and 5.12% at the 2nd hour time point respectively. Other time points revealed the percentage release of BSA from these formulations ranging from 4.5% to 5.2% and 3.5 to 5.1% at each time point, respectively. These results show that the 70/30% and 80/20% NASEG formulations yield a lower percentage release which translates to sustained and prolonged release of BSA.

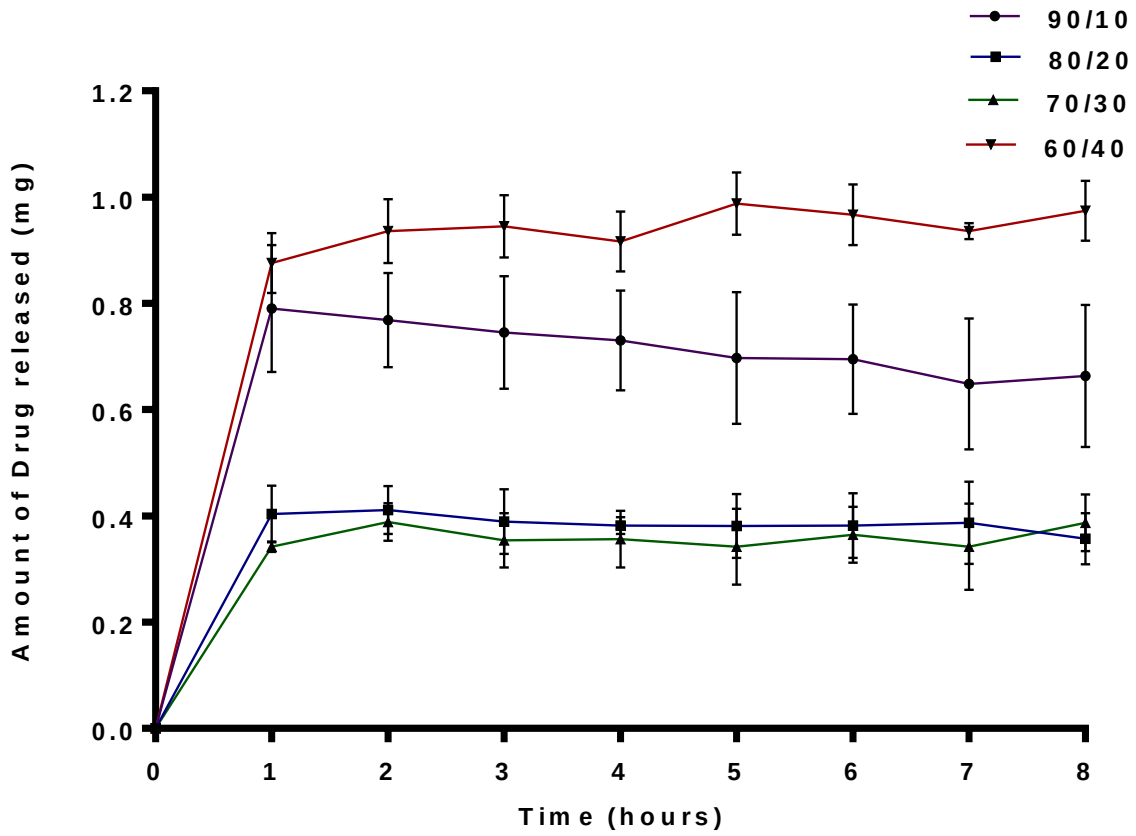

Figure 3.12 In vitro release of BSA from different formulations of NASEGS. This graph presents the in vitro release of BSA incorporated into silicone gels composed of various ratios of ST elastomer and cyclomethicone. 90/10, 80/20, 70/30, and 60/40% w/w represents the ratio of ST to cyclomethicone in the gel formulation and each gel is loaded with 7mg of BSA per 1g of gel formulation (n=3).

3.4.3.2 Comparison of various BSA release profiles from 80/20 composition of non-aqueous silicone elastomer gels (NASEGS)

The amount of drug released at each time point for the samples of each 80/20 silicone gel formulation containing different BSA loadings per 1g of gel (7mg, 5.6mg, 3.5mg and 1.7mg) were investigated. The optimised non-aqueous silicone elastomer gel 80/20 %w/w was chosen based on its favourable textural and rheological characteristics similar to a true gel, maintaining its semi-solid structural integrity, which is characteristic of a true gel. The phenomenological definition proposed by Almdal et al (1993), states that a gel is a soft, solid or solid-like material, which consists of at least two components, one of which is a liquid present in abundance. The elastic and resilient character should be observable by the human eye and, consequently, on a time scale of seconds, a gel should not flow under the influence of its own weight. From previous research performed in the group, the BSA loadings were chosen in comparison to the total amount of BSA that can be adsorbed per 100mg of aquasome formulation, analysed by an entrapment efficiency experiment (7mg- 100%, 5.6mg- 75%, 3.5mg- 50% and 1.7mg- 25%) (results not shown).

The entrapment efficiency experiment determines the amount of drug/protein adsorbed or "entrapped" onto the nano-carrier formulation per *x* mg of formulation. This is determined by calculating the difference between the amounts of drug/protein left in supernatant vs. the amount of drug/protein initially incorporated into the drug/protein solution during the fabrication of the nano-carrier formulation. This can also be achieved by dissolving the nano-carrier formulation in an appropriate solvent that will break chemical bonds between the drug/protein and polyhydroxyl coating (trehalose) without degrading drug/protein (such as 0.05N NaOH). The amount of drug/protein is detected in resulting supernatant solutions using appropriate analytical methods such as ultra violet spectroscopy (Chai et al, 2007).

In comparison, the differences in BSA release profiles of "90/10 vs. 80/20 %w/w", "90/10 %w/w vs. 70/30 %w/w", "80/20 %w/w vs. 60/40 %w/w" and "70/30 %w/w vs. 60/40 %w/w" were found to be significant (adjusted p values= 0.0357, 0.0204, 0.0002 and 0.0001 respectively). This confirms that the release of BSA from the different formulations of the NASEGS varied significantly based on the different formulations used. This trend highlights the fact that the properties of the formulations compared influenced the BSA rate of release.

The BSA release profile from the 80/20 %w/w formulation (Figure 3.13) showed sustained release demonstrating the controlled release property of the silicone elastomer gels.

The release of various loadings of BSA (7mg, 5.6mg, 3.5mg and 1,7mg) from NASEGS over an 8h period is presented in figures 3.14 respectively. The release profiles from the silicone formulations were dependent on drug loading. Figure 3.14 illustrates that the increased BSA loading in the silicone gels enhanced the rate of release of BSA from the gel's insoluble matrix. The differences between the BSA release profiles of "100ST vs. 75ST" and "100ST vs. 50ST" were found to be statistically insignificant (adjusted p values= 0.3901 and 0.0686 respectively). This was also observed when the BSA release profiles of "75ST vs. 50ST" and "50ST vs. 25ST" as the differences were found to be insignificant (adjusted p values= 0.7724 and 0.1899 respectively). In comparison, the differences in the BSA release profiles between "100ST vs. 25ST" and "75ST vs. 25ST" were found to be statistically significant (adjusted p values= 0.0003 and 0.0245 respectively).

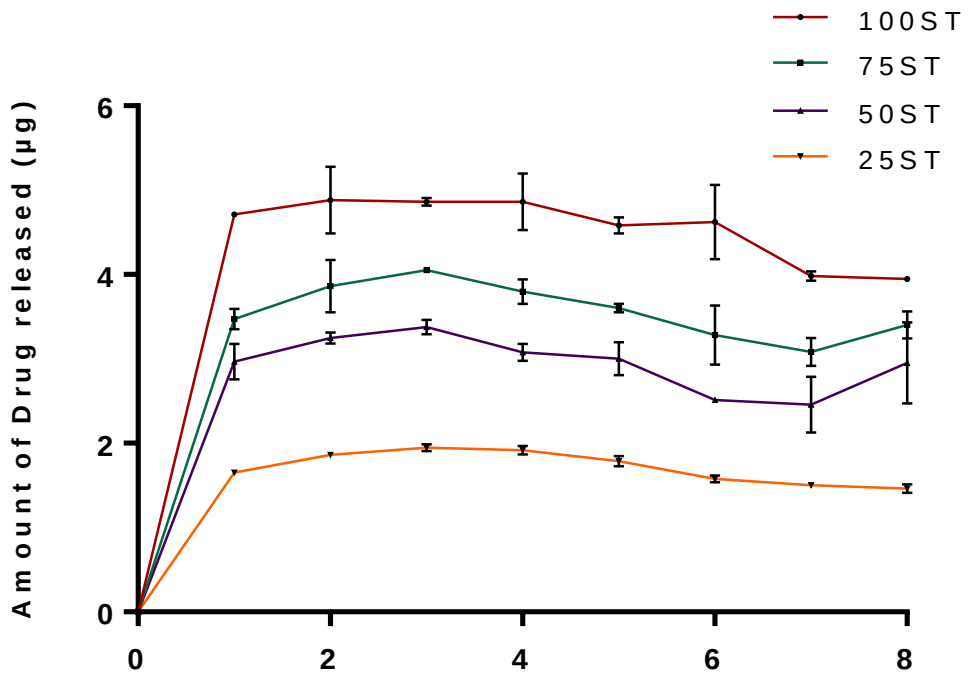

Figure 3.13 In vitro release profile of BSA from non- aqueous silicone elastomer gels. This graph represents the amount of drug released at each time point for the samples of each silicone gel formulation made with different BSA loadings. 100ST represents 7mg; 75 ST, 5.6mg; 50 ST, 3.5mg and 25 ST 1.7mg of BSA incorporated into per 1g of the 80/20 %w/w formulation of the non-aqueous silicone elastomer gels (n=3).

According to Patel et al (2011), drug release rate from insoluble polymer matrices is controlled by the pore size and number of pores, and tortuosity of the matrix. The release mechanism will also depend greatly on how the drug is dispersed within the system (dissolved, molecularly dissolved, or dispersed).

From the statistical inferences, the difference in the BSA loadings between 100ST vs. 75ST", "100ST vs. 50ST", "75ST vs. 50ST" and "50ST vs. 25ST" were insignificant and thus do not affect the rate of BSA release from the silicone gels. This can be attributed to the dispersion of the small amounts of BSA, which is a water-soluble protein within the insoluble silicone matrix. As illustrated in Figure 3.14, the drug release mechanism from silicone matrix differs depending on the physiochemical properties of the drugs (Kajihara et al, 2003). Lipophilic/hydrophobic drugs or proteins diffuse through the silicone matrix, demonstrating more solubility in silicone. However, water-soluble drugs/proteins rely on the hydration of the pores within the matrix for release. The differences in the BSA loadings between "100ST vs. 25ST" and "75ST vs. 25ST" were found to be statistically significant which illustrate that a significant increase in BSA loading. The increase in BSA loading will increase the number of pores within the matrix which when dissolved into the surrounding release medium, will affect the hydration of the polymer matrix and thus increase the rate of BSA release from the silicone gels.

BSA release from the gels show constant release but does not follow zero-order kinetics; drug release decreases with time due to the increasing distance drug molecules have to travel to reach the surface of the gel. However, pore-forming agents can be added to decrease tortuosity and facilitate drug release. It may be explained that the decrease in the tortuosity of the silicone gel's insoluble matrix increased the rate of BSA release owing to BSA's high solubility in release media. The addition of BSA (soluble protein, pore-forming agent) increased the rate of hydration of the pores/ channels in the gel matrix thus increasing the rate of BSA release to the surrounding release medium (Kajihara et al, 2003).

A. Water soluble drug

B. Lipophilic drug

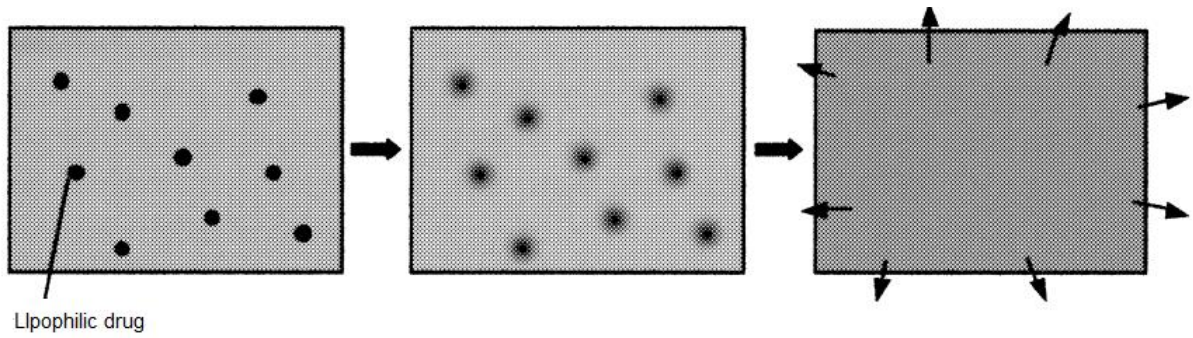

Figure 3.14 Release mechanisms of drugs with different physiochemical properties from a silicone carrier such as NASEG. A water-soluble protein like BSA incorporated into the insoluble NASEG creates channels when hydrated allowing the subsequent release of BSA from the gels. Insoluble or weakly soluble drugs diffuse through the NASEGs and thus released from the gels.

3.4.4 Comparison of BSA Release Profiles from Aqueous Gels

The release of BSA from the aqueous gels, HPMC and HEC, also had similar release profiles, starting with a burst with a near plateau release trend and a very gradual decline in amount of BSA released at the tail end of the 8h study. In comparison to release from the NASEGS, the amount of BSA released was very high (see Figures 3.16, 3.17 and 3.18). The high BSA release and gradual decline in drug release shows that the HPMC and HEC gels were rapidly hydrated, leading to a high rate BSA dissolution, depleting the amount of BSA remaining within the gels.

Figure 3.16 presents the amount of drug released at each time point for the aqueous gel formulation, HEC, with various BSA loadings (7mg, 5.6mg, 3.5mg and 1.7mg) and the 5 %w/v formulation of the HEC gels. The 5%w/v formulation was chosen because of similarities to a semi-solid gel structure. The HEC gel formulations have similar release

profiles, dependent on drug loading. The differences between the BSA release profiles of “25HEC vs. 50HEC”, “50HEC vs. 75HEC” and “75HEC vs.100HEC” were found to be statistically insignificant (adjusted p values= 0.2277, 0.3159 and 0.3694 respectively). In comparison, the differences between the BSA release profiles of “25HEC vs. 75HEC”, “25HEC vs. 100HEC” and “50HEC vs.100HEC” were found to be statistically significant (adjusted p values= 0.0043, <0.0001 and 0.0095 respectively). This trend can be attributed to the rate of BSA release from the HEC aqueous gel. Since the gels exhibits an immediate release property to the incorporated drug/protein, attributed to the erosion and diffusion mechanisms occurring concurrently, the rate of BSA release is faster and is irrespective of BSA loading for similar drug loadings because the gel structure is hydrated very quickly and does not depend solely on the diffusion of BSA (water soluble protein) to hydrate the gel structure for BSA to be released.

Figure 3.17 presents the amount of drug released at each time point for the aqueous gel formulation, HPMC, with various BSA loadings (7mg, 5.6mg, 3.5mg and 1.7mg) and the 5 %w/v formulation of the HPMC gels. As for the HEC gels the 5%w/v formulation was chosen because of similarities to a semi-solid gel structure. The HPMC gel formulations have similar release profiles, dependent on drug loading. The differences between the BSA release profiles of “25HPMC vs. 50HPMC”, “50HPMC vs. 75HPMC” and “75HPMC vs.100HPMC” were found to be statistically insignificant (adjusted p values= 0.0732, 0.3986 and 0.6697 respectively). In comparison, the differences between the BSA release profiles of “25HEC vs. 75HEC”, “25HEC vs. 100HEC” and “50HEC vs.100HEC” were found to be statistically significant (adjusted p values= 0.0013, <0.0001 and 0.0481 respectively).

The same trend observed with HEC gels was also observed with BSA release from HPMC gels. This trend can be attributed to the rate of BSA release from the HPMC aqueous gel and thus follows the same mechanism of release.

The HPMC and HEC aqueous gels exhibit the characteristics of a viscous hydrophilic matrix system (Figure 3.15). In the presence of water, they form matrix systems in which the increased viscosity occurs as a result of simple entanglement of adjacent polymer chains but without proper crosslinking. They form dynamic structures in which the chains are able to move relative to one another and the drug diffuses through the interstitial continuum (Aulton, 2007).

The mechanism of drug release from a viscous hydrophilic matrix complex is centred on diffusion of the drug through, and erosion of, the outer hydrated polymer on the surface of

the matrix (Figure 3.15 a) (Jain, 2008). In this instance, where BSA (a soluble protein) is incorporated into HPMC/HEC (a viscous hydrophilic matrix system), gradual erosion of the HPMC/HEC gel by the surrounding release medium and the diffusion of the BSA through the hydrated gel matrix occurs as more water permeates into the core of the matrix. This is illustrated in Figure 3.15 c (Patel et al, 2011).

As the outer layer becomes fully hydrated, the polymer chains become completely relaxed and can no longer maintain the integrity of the gel layer, leading to disentanglement and erosion from the surface of the matrix. Water continues to penetrate through the gel, until it has been completely eroded (Tiwari and Rajabi-Siahboomi, 2008; Jain, 2008; Patel et al, 2011).

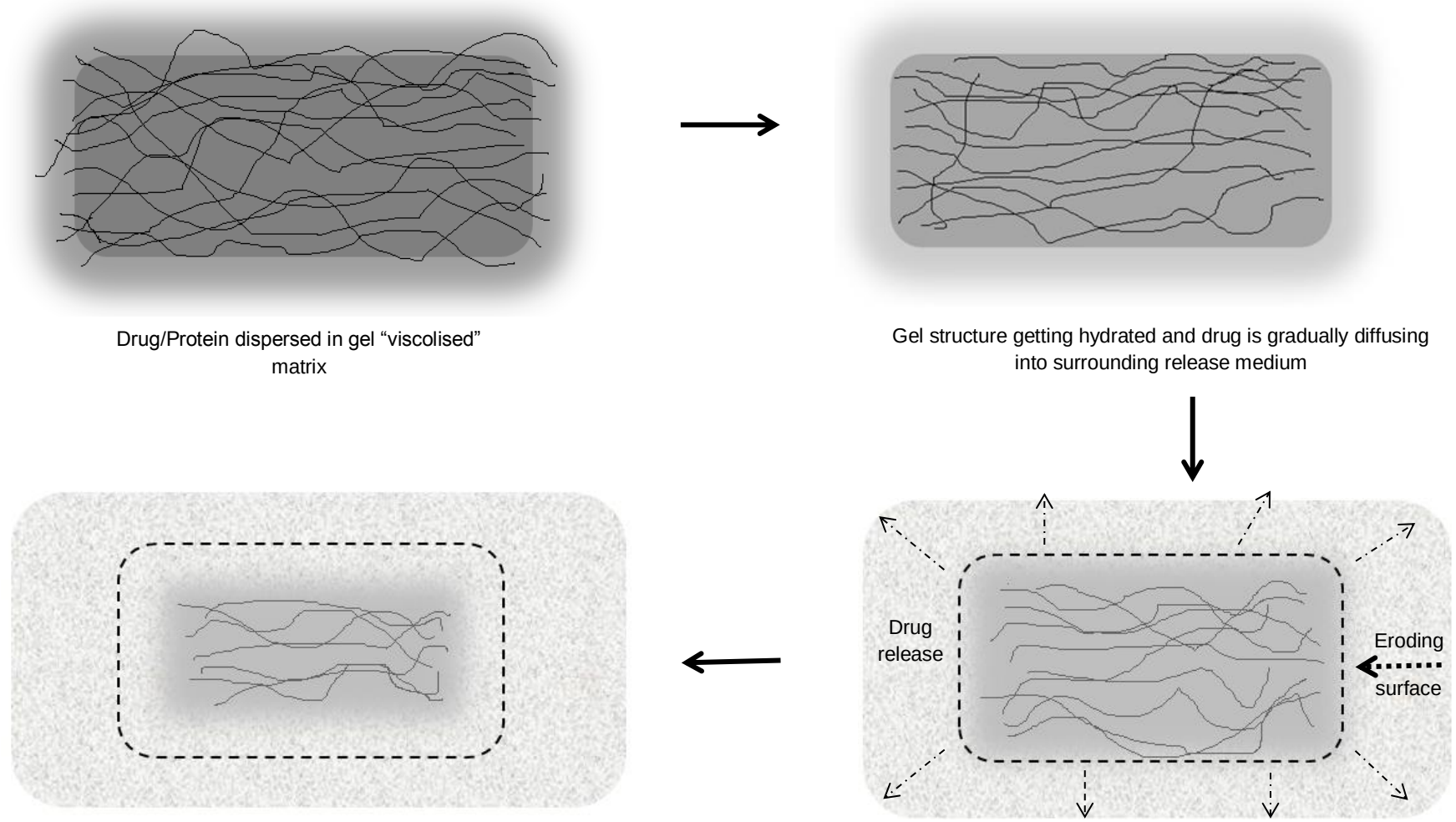

Figure 3.15 Schematic diagram illustrating BSA release from hydrophilic gels. a) viscolised hydrophilic matrix showing an entanglement of polymer chains without any proper crosslinking; b) true gel matrix which form a polymeric structure in the presence of crosslinks, and c) drug release from a viscolised hydrophilic matrix gel such as HEC or HPMC used in the present study.

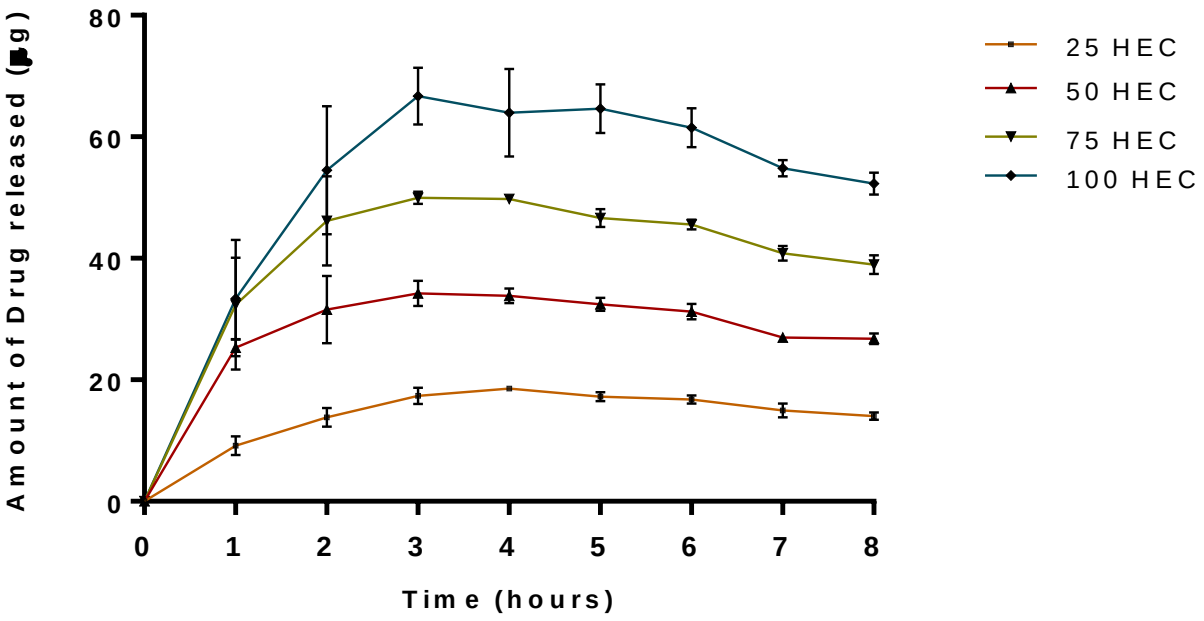

Figure 3.16 ***In vitro*** **release of BSA from hydroxyethyl cellulose (HEC, aqueous) gels.** This graph presents the amount of drug released at each time point for the aqueous gel formulation, HEC, with various BSA loadings. 100HEC represents 7mg; 75 HEC, 5.6mg; 50 HEC, 3.5mg and 25 HEC 1.7mg of BSA incorporated into per 1g of the 5 %w/v HEC gel formulation (n=3).

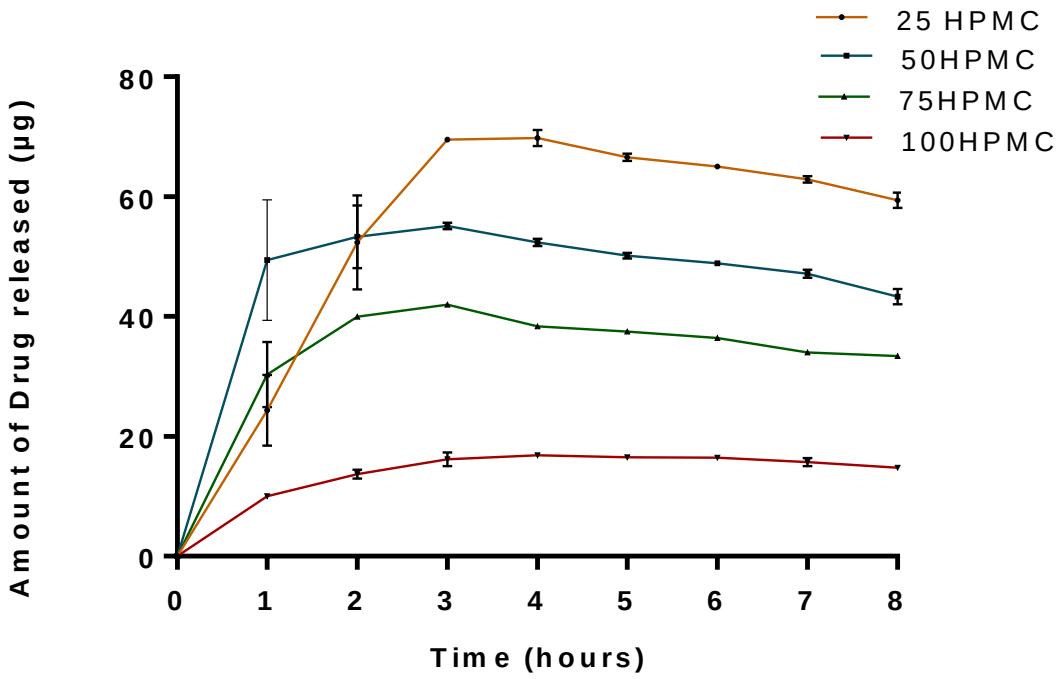

Figure 3.17 In vitro release of BSA from hydroxylpropyl methyl cellulose (HPMC, aqueous) gels. This graph presents the amount of drug released at each time point for the aqueous gel formulation, HPMC, with various BSA loadings. 100HPMC represents 7mg; 75 HPMC, 5.6mg; 50 HPMC, 3.5mg; and 25HPMC, 1.7mg of BSA incorporated into per 1g of the 5 %w/v HPMC gel formulation (n=3).

3.4.5 Comparison of BSA Release from BSA-Loaded Aquasomes and Non-Aqueous Silicone Elastomer Gels (NASEGS) Loaded With BSA

To examine the possible application of aquasomes in topical/transdermal delivery, preliminary studies were performed in comparison to the drug/protein alone to establish these claims. A suitable dosage form for the topical/transdermal delivery of aquasomes was required to enable protein/drug delivery to the skin. NASEGS and aqueous gels were compared in this study to examine the appropriate aquasome formulation for sustained topical/transdermal delivery. Aquasomes were incorporated into NASEGS to formulate a dosage form suitable for topical/transdermal delivery. The release profiles, rheological and mechanical characterization of these gels were then compared with the commonly used aqueous semi-solid polymeric gels (made with HEC and HPMC) using BSA, the model protein.

The release of BSA from the aquasomes incorporated into the NASEGS manufactured with different BSA loadings (7mg, 5.6mg, 3.5mg and 1.7mg, with the drug adsorbed onto the aquasome coating), was investigated. The 80/20 %w/w silicone gel formulation was chosen based on rheological and textural properties (Section 3.4.5). Figure 3.19 presents a comparison of the release profiles of BSA from various loadings of BSA-loaded aquasomes incorporated in the NASEGS. The release of BSA was dependent on the diffusion of the release medium through interstitial pores which hydrates the aquasome formulation within the insoluble matrix. The trehalose coating is hydrated and forms a gel, which controls the release of the BSA adsorbed and as a result, offers the sustained release of BSA. Results show that BSA release from NASEGS was similar and the amount of BSA released was within a narrow range, regardless of the BSA loading on aquasomes incorporated into the NASEGS.

The release of BSA from NASEGS was compared to that released from BSA-loaded aquasomes incorporated into the non- aqueous silicone elastomer gels (80/20 %w/w) (figure 3.20). BSA directly incorporated into the silicone gels had a much higher amount of drug released (5.28μg as its highest amount at the 2nd hour time point, 0.075%) than from the BSA-loaded aquasomes while the amount of BSA released from the aquasome-silicone gel formulations was less than 1μg (0.014% of incorporated amount of BSA). The different release profiles can be employed for different drug delivery applications depending on the desired drug release characteristic (sustained or immediate release). However, the release of BSA from the BSA-loaded aquasomes incorporated into the silicone gels was governed by two factors: sustained release of BSA from the trehalose gel formed when in contact with the release medium and also the diffusion of the BSA through the pores of the gel. This causes BSA to have an extended release from the silicone gels. This extended release property is useful for proteins or drugs that require small amounts of drug to be released over a longer period. *Root t* release kinetics, with a readily soluble drug/protein like BSA from the silicone gels, can be applied in the release of drug/protein which require sustained release but in higher amounts. Here, BSA represents a protein, a readily water soluble protein/drug and a pore forming agent, which is dispersed in an insoluble matrix. In higher quantities, it readily allows pores to be water filled, initiating release of BSA. As a pore-forming agent, it can be incorporated with another protein or a protein-loaded aquasome formulation which requires its release to be in higher amounts compared to the amount released (ng) with aquasomes alone distributed within the silicone gels (Kajihara et al, 2000; Kajihara et al, 2003).

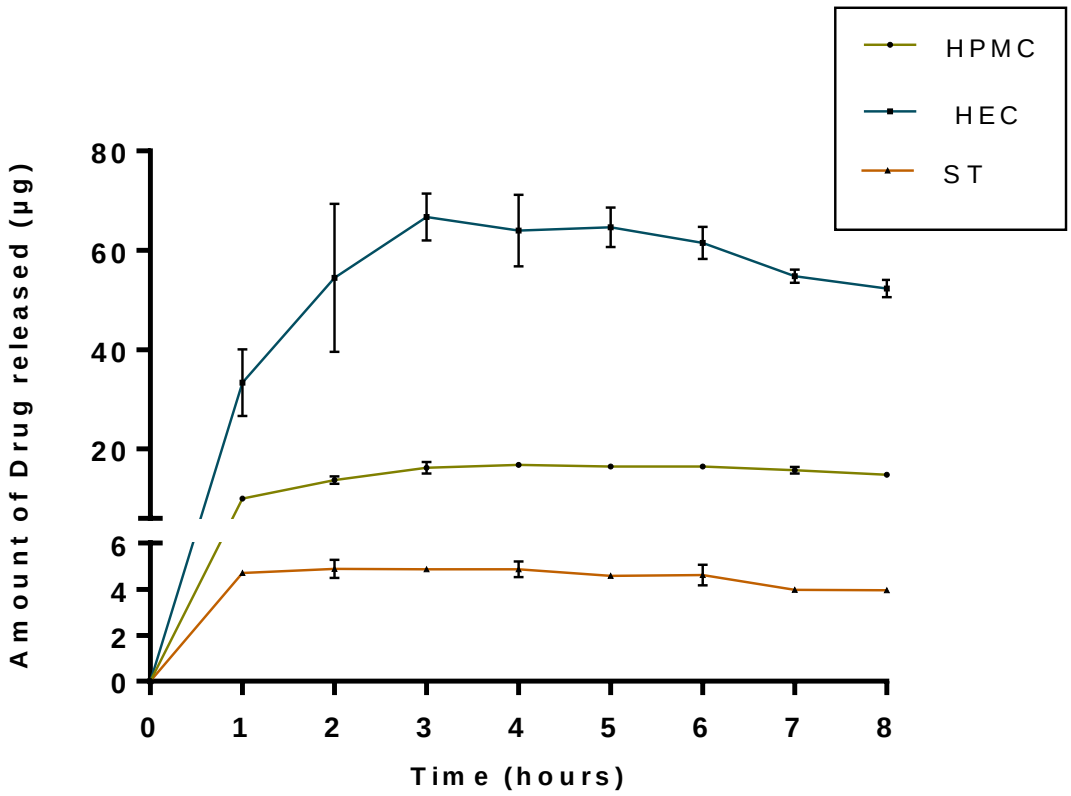

Figure 3.18 Comparison of the in vitro release profiles of BSA from aqueous gels (HPMC and HEC gels) and silicone elastomer gels. This graph compares the amount of BSA released at each time point for the aqueous gel formulations, HEC and HPMC, and the silicone gels with the same loading: 7mg of BSA per 1g of gel formulation (n=3).

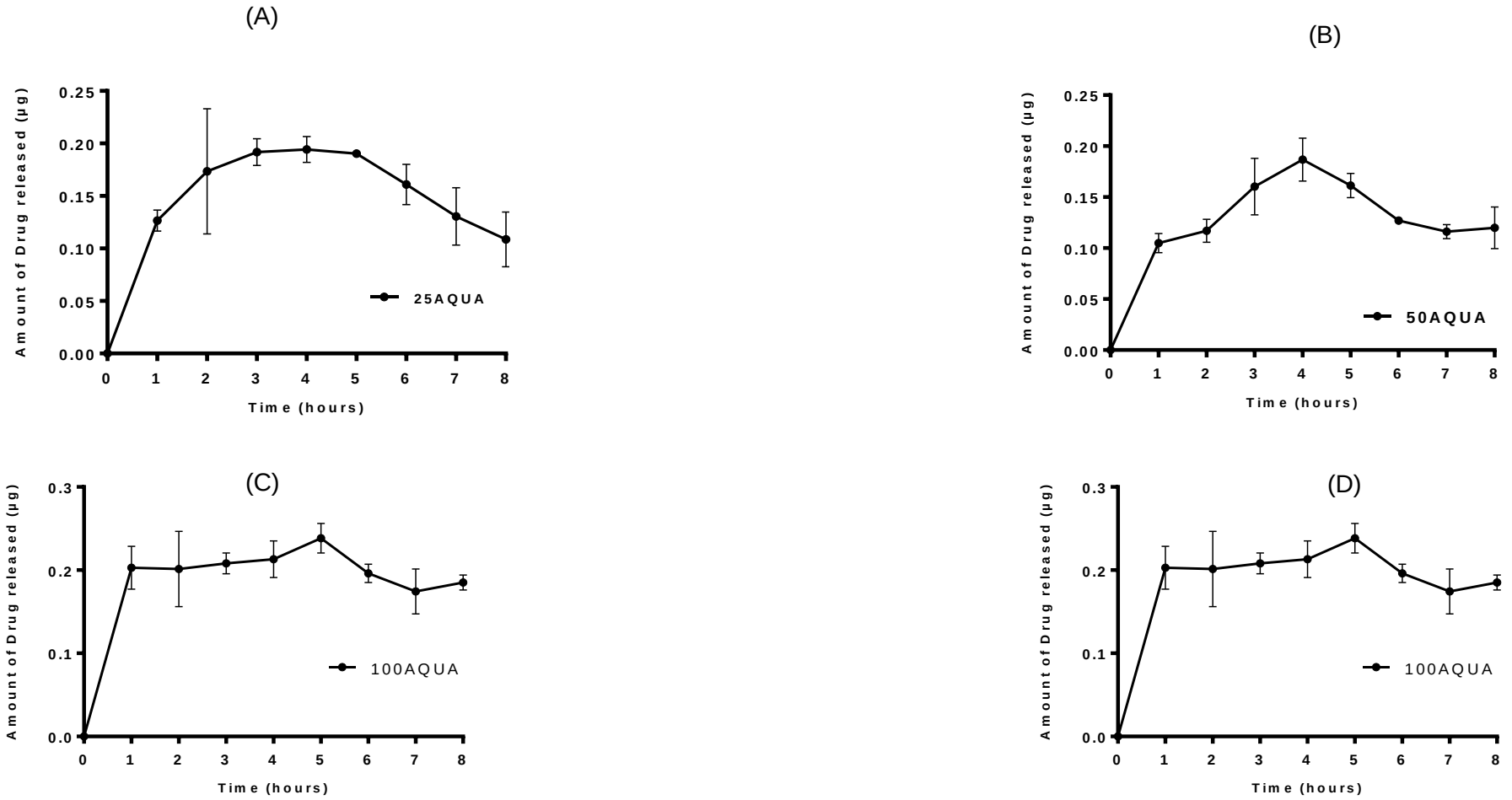

Figure 3.19 ***In vitro*** **release profile of BSA from BSA-loaded aquasomes incorporated in NASEGs.** This graph compares the amount of drug released at each time point for the BSA-loaded aquasomes incorporated into the silicone gels (80/20% gel formulation). Entrapment efficiency experiment estimates that 7mg of BSA is adsorbed per 100mg of aquasome formulation. 100AQUA, 75AQUA, 50AQUA and 25AQUA represent 100mg, 75mg, 50mg and 25mg aquasome formulation (n=3).

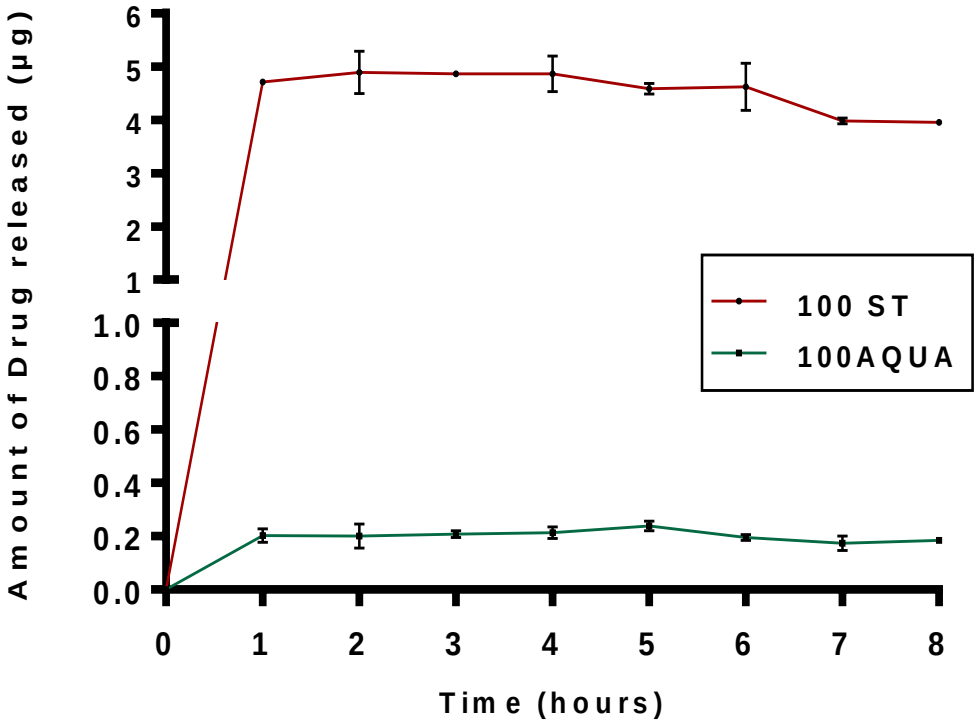

Figure 3.20 Comparison of the in vitro release profile of BSA from BSA-loaded aquasomes and BSA directly incorporated in non-aqueous silicone elastomer gels (NASEGS). 7mg/g of BSA was incorporated in NASEGS (ST) illustrating the total amount of BSA incorporated per 100mg of aquasome formulation (n=3).

Drug release from insoluble matrices can follow one of four matrix system release mechanisms as detailed in Table 3.8 (Nokhodchi et al, 2012).

Table 3.8 Drug release mechanisms from insoluble matrices

Drug release mechanisms from insoluble matrices
● Drug molecularly dissolved in the matrix and drug diffusion occurs by a solution-diffusion mechanism ● Drug dispersed in the matrix and then, after dissolution of the drug, diffusion occurs via a solution- diffusion mechanism ● Drug dissolved in the matrix and diffusion occurs through water pores in the matrix ● Drug dispersed in the matrix and then, after dissolution, diffusion occurs through water-filled pores.

The amount of drug released from insoluble simple monolithic dispersion systems do not follow zero order kinetics but follow root square kinetics i.e. the amount of drug released is normally proportional to the square root of the time of exposure to the surrounding release medium. The amount of drug released decreases with time of exposure to the release medium. This occurs because the drug is released initially from the surface region where there is a short diffusion pathway. As the duration of dissolution progresses, the area of drug exposed to the release medium decreases. A constantly increasing depletion zone is formed within the matrix as the drug dissolves and so the diffusion pathway increases in length (Patel et al, 2011).

It can be concluded that the rate of drug release is controlled by the rate of diffusion of the surrounding release medium into the gel matrix (Verma et al, 2013). This explains the release profiles of BSA from the NAEGs and thus elucidates the shape of the release profile curves. The release profile has a shape of a parabola as a function of time. The drug release profiles of BSA from the aqueous semi-solid polymeric gels formulated with HPMC and HEC are similar to generic tablets. In the presence of the aqueous release medium, the polymer chains simply disentangle and are diluted because they lack proper crosslinking, release the drug into the surrounding medium (Gupta, Vermani and Garg, 2002). A distinction should be noted between aqueous gels and hydrogels. Hydrogels are cross-linked

hydrophilic polymers which swell in the presence of an aqueous environment, while maintaining their 3D structure (Aulton, 2007; Gupta, Vermani and Garg, 2002).

The amount of drug release is dependent on the drug concentration in the dosage form. Therefore, the rate of drug release is defined as the concentration change divided by corresponding time change.

3.4.6 *In Vitro* Permeation Studies

To examine the performance of the gels on the skin and its ability to effectively deliver proteins/drug through the stratum corneum, *in vitro* permeation studies are employed. The use of *in vitro* static diffusion cells to assess skin permeability has evolved into a major research methodology, elucidating the relationships between skin, drug and formulation. Such testing is highly useful not only for the design and development of formulations but also for toxicity screening and quality-control purposes (Ng et al, 2010[a]).

Franz-type diffusion studies usually involve the use of synthetic membranes to model real skin. Although the artificial membranes will not model the lipid perturbation effects undergone by biological samples, inferences regarding partitioning and diffusion phenomena can be made. Synthetic membranes may be preferred to skin tissue as they are more easily resourced, less expensive and structurally simpler (Ng et al. 2010[b]).

In this study, Franz cell experiments were performed using 0.4µm pore size polycarbonate membranes to mimic the stratum corneum (10µm thickness) and silicone elastomer gels incorporated with 7mg/g of gel (figure 3.21). This dosage concentration was chosen based on the loading efficiency of aquasomes for BSA estimated at 7mg of BSA adsorbed per 100mg of aquasome formulation, analysed by an entrapment efficiency experiment. Preliminary tests for the investigation of the *in vitro* permeation of BSA-loaded aquasomes in ST-Elastomer gels were performed by incorporating free BSA into the gels. as elucidated by Ng et al (2010), the thickness of the membrane used can be a rate-limiting factor in diffusion, in comparison to the polycarbonate membrane (thickness of 10µm), acted as a rate limiting factor in BSA diffusion.

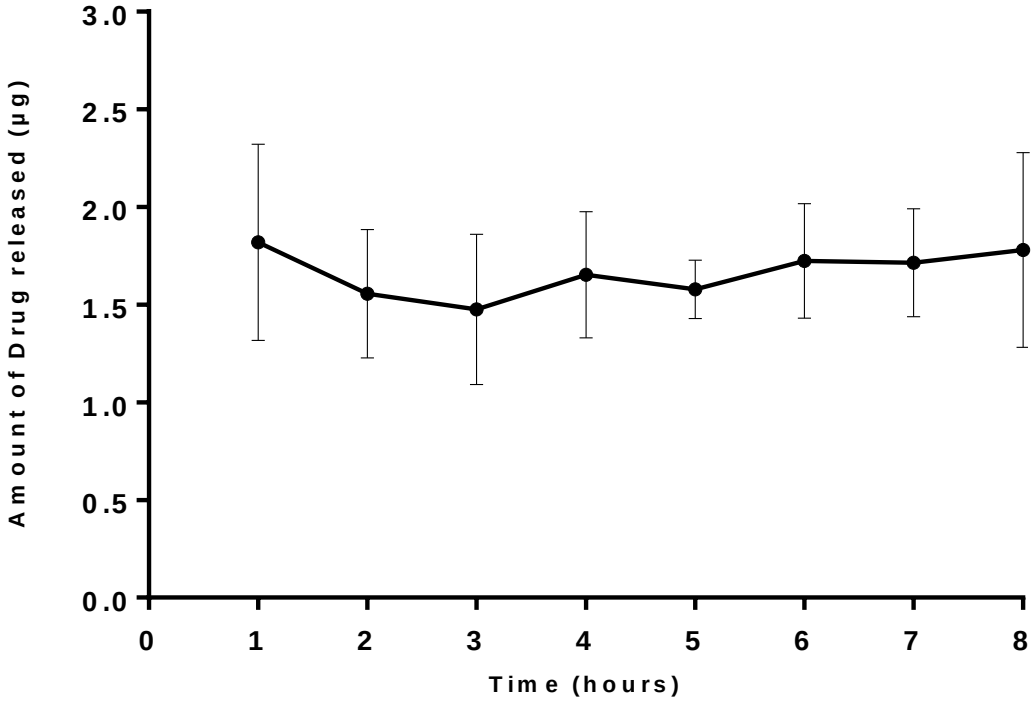

Figure 3.21 Cumulative amount of BSA permeated through 0.4µm polycarbonate membranes. *In vitro* permeation study was carried out using 7mg BSA per g of NASEG for duration of 8h. PBS (pH 7.4) was used as the receptor media (n=3).

The physicochemical properties of the drug may have also acted as a rate limiting factor as BSA (hydrophilic protein, M.W: > 66,000Da) exhibited a low cumulative drug release profile (Fig. 3.21). Literature illustrates that release of proteins from silicone elastomers offer a sustained and prolonged release profile (Kajihara et al, 2000).

In this study, BSA was used as a model protein to investigate the delivery of proteins from NASEGS. From the *in vitro* permeation results using 0.4µm polycarbonate membrane as the rate limiting factor, the permeation of BSA from NASEGS through the membrane showed a sustained amount of 1.5 – 2.0µg BSA at every time point for the duration of 8 hours. These minute amounts of BSA released from NASEGS and permeated through the membrane indicate that release of BSA from loaded aquasomes incorporated into NASEGS will yield less than optimal results of BSA release. However, these amounts of BSA released can be applied in the delivery of potent proteins which elicit a pharmacological response with small amounts. According to Kajikara and colleagues (2000), the sustained and prolonged delivery of potent proteins such as cytokines and growth factors, required at low concentrations to exert a biological effect, can be successfully achieved with mixing such proteins with albumin for desired release characteristics. This is because protein drugs cannot diffuse through

silicone and the addition of hydrophilic proteins in higher amounts will cause the formation of pore channels through the silicone matrix when exposed to the release medium and thus will enhance the release of the protein drug of interest (see Figure 3.21, Kajikara et al, 2003).

It has previously been investigated in numerous studies that ST-elastomer gels have a more favourable affinity to hydrophobic [lipophilic] drugs compared to hydrophilic drugs (proteins like BSA), owing to their hydrophobic structure (Mashak and Rahimi, 2009; Forbes et al, 2013). The hydrophobic nature of silicone elastomers is somewhat lipophilic and can be swollen by lipids or other nonpolar agents (Curtis and Colas, 2005). Lipophilic drugs are able to diffuse through the silicone matrix and thus have favourable release and permeability profiles. Hydrophobic drugs have a constant release rate from hydrophobic polymers (Kajikara *et al*, 2001).

The underlying theory, which describes the transport of drug across a barrier membrane in Franz diffusion cell, is the Fick's Law of passive diffusion,

$$J = K.\frac{Cv}{h}$$

Where *J* is flux, Cv is permeant concentration in vehicle, h is membrane thickness and K is the partition constant of the permeant between the membrane and vehicle (Ng et al, 2010; Moser et al, 2001).
In vitro permeation investigations have employed the use of synthetic membranes made from different materials, having different pore sizes and membrane thicknesses (Ng et al, 2010). This is usually carried out to compare the rate of flux of a drug through different membranes, mimicking the various thicknesses and pore sizes throughout the skin. Commonly used membranes are made from silicone, cellulose and polysulfone.

The successful permeation of a drug in a topical formulation through skin and concurrent exertion of a biological effect is dependent on two factors: the drug's diffusion out of the vehicle to the skin's surface and consecutive permeation through the stratum corneum. These steps are dependent on the physicochemical properties of the drug, vehicle and barrier, as highlighted in Table 1.5 (Kriwet and Muller-Goymann, 1995).

Nanoparticulate carriers present some advantages for topical/transdermal applications as their display sustained drug release profiles important to expose the skin to the drug for prolonged durations. Alves et al (2007) carried out a study to investigate the in vitro penetration of a drug model, nimesulide, from hydrophilic gels containing nanocarriers,

nanospheres, nanocapsules and nanoemulsions were used in this study. Nimesulide is a NSAID (non-steroidal anti-inflammatory drug) under the class of COX-2 inhibitors.

Nimesulide exhibits low solubility in water (0.001mg/ml). *In vitro* penetration was analysed using the Franz cell technique, using full thickness human skin as membrane. The influence of nanocarriers on drug release was compared with free drug in aqueous gel. Nimesulide formulations were prepared by nanoprecipitation and interfacial deposition and incorporated into Carbopol 940® gels.

Nimesulide was detected in the stratum corneum for the gel containing nimesulide-loaded nanocapsules and nimesulide-loaded nanospheres but not for the gel containing nimesulide-loaded nano-emulsion. The presence of nimesulide was significantly higher for the gel containing nimesulide-loaded nanocapsules in comparison to drug-loaded nanospheres and nanoemulsions. The drug was detected in the receptor compartment of the Franz cell apparatus for none of the formulations which illustrates from previous studies that particulate drug carriers (micro- and nano- particles) improve drug residence in the skin without increasing transdermal transport (Alvarez-Roman et al, 2004 in Alves et al, 2007).

Interestingly, results from this study showed that none of free drug incorporated into the vehicle (Carbopol 940®) i.e. without nanocarriers diffused into the skin surface. It is argued here that the modified distribution of nimesulide when delivered via nanoparticles is as a result of alterations in thermodynamic activity which causes an increase in drug diffusion through the vehicle. (Alves et al, 2007).

3.4.7 *In Vitro* Toxicity Assay (MTT Assay)

A thiazolyl blue tetrazolium bromide (MTT) assay was performed to measure cell death after exposure of cells to BSA at different concentrations for 24 h, representing short term exposure to aquasomes (acute toxicity). The amount of BSA that can be released from aquasomes (in comparison to BSA alone) and stimulate a biological response without having a toxic effect, was examined. Human dermal fibroblasts (HDFa) were used as a model dermal cell line and exposed to similar BSA concentrations as would be released from BSA-loaded aquasomes. Figure 3.22 illustrates the cell viabilities of HDFa cells, after exposure to 7.0, 5.6, 3.5 and 1.7mg/ml of BSA dispersed in serum-free culture medium.

Measurement of cell viability and proliferation forms the basis for numerous *in vitro* assays of a cell population's response to external factors. The reduction of tetrazolium salts is known as a reliable way to examine cell proliferation. The yellow tetrazolium MTT (3-(4, 5-dimethylthiazolyl-2)-2, 5-diphenyltetrazolium bromide) is reduced by metabolically active cells, in part by the action of dehydrogenase enzymes, to generate reducing equivalents

such as NADH and NADPH. The resulting intracellular purple formazan can be solubilized and quantified by spectrophotometric means. An increase in the absorbance values with concentration illustrates a corresponding increase in the formation of MTT formazan. The MTT cell proliferation assay measures the cell proliferation rate and contrarily, when metabolic events lead to apoptosis or necrosis, the reduction in cell viability.

The percentage cell viabilities of HDFa cells exposed to varying concentrations of BSA-spiked media were plotted in a bar graph to illustrate the cell viabilities in correspondence to the different BSA concentrations. Figure 3.22 illustrates that the BSA concentrations used in the fabrication of BSA-loaded aquasomes were not toxic to HDFa cells. On the contrary, BSA enhanced the growth of HDFa cells over the duration of 24h. Exposure of the HDFa cells to 7.0mg/ml BSA-spiked media yielded 130.34% viability, 5.6mg/ml yielded 119.98%, 3.5 mg/ml yielded 112.71% and 1.7mg/ml 105.25% viabilities. These differences in cell viabilities were found to be statistically significant ($p<0.0001$).

BSA was used as a model protein in this study and has been established in general cell culture protocols to ensure optimal cell growth and proliferation. It is commonly used to enhance the growth of various immortalised and primary cell lines, mimicking the protein-rich cell milieu *in vivo*. Further investigations in cell culture were not pursued as BSA is a well-established serum protein for optimising cell growth in *in vitro* studies.

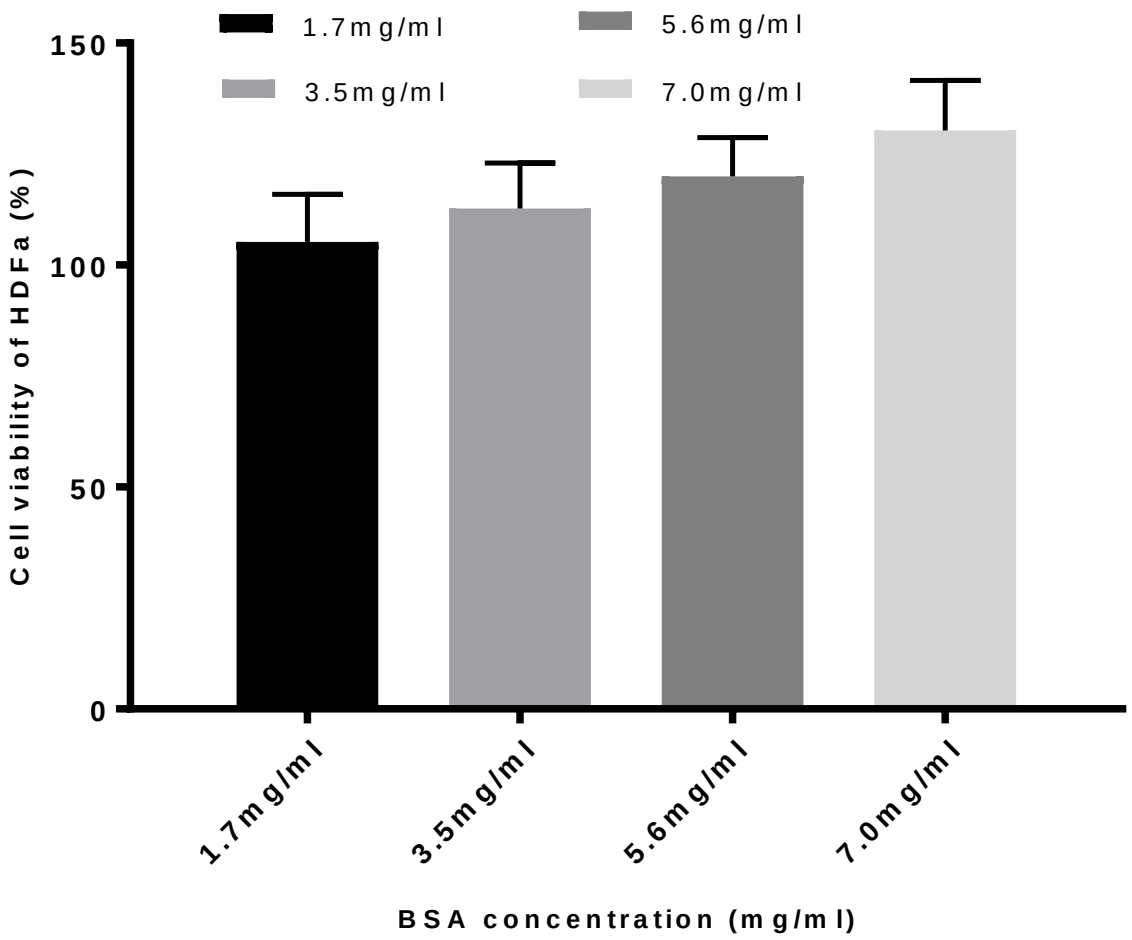

Figure 3.22 Cell viability of HDFa cells. MTT assay of HDFa cells exposed to varying concentrations of BSA (7. 5.6, 3.5 and 1.7mg/ml) after 24 hours. Results show that BSA had no toxic effect on the cells but rather increased the viability of the cells over the period of 24 hours (n=24).

3.5 CONCLUSIONS

The present study focused on the use of non-aqueous silicone elastomer gels (NASEGS) as a suitable topical/transdermal delivery for aquasome delivery. NASEGS were employed to investigate the topical/transdermal delivery of free protein (BSA) and BSA-loaded aquasomes, where BSA was used as a model protein. Aqueous gels, made of HPMC and HEC, are common drug dosage forms and were used in this study to compare the drug release, rheological and textural parameters of NASEGS. As a model protein for transdermal/topical delivery, BSA-loaded aquasomes were fabricated and further analysed using *in vitro* release and permeation experiments.

BSA release from aquasomes exhibited biphasic release behaviour with an initial burst release which plateaus after 2 hours. The percentage release of BSA from loaded aquasomes showed a range of 1.6 to 3.57% indicating the potential of BSA-loaded aquasomes for sustained and prolonged release of proteins.

BSA release profiles from the various NASEG formulations demonstrated that amounts of BSA released are dependent on BSA loading into NASEGS. The release profile of BSA from NASEG formulations showed constant release of BSA for every time point during the 8-hour study. BSA release from aqueous gels showed a higher amount of release illustrating the higher rate of hydration of the aqueous gel matrix thus resulting in high amounts of BSA released. NASEG compositions (90/10%, 80/20%, 70/30% and 60/40%) also influenced BSA release, rheological and textural parameters that determine the suitability of a NASEG formulation fit for topical delivery. Based on the results from the in vitro release, study, rheological and textural parameters, 80/20% formulation showed favourable results as the NASEG formulation with optimum characteristics as a pharmaceutical topical gel.

Incorporation of BSA-loaded aquasomes into NASEGS yielded minute amounts of BSA release (less than 1µg, 0.014%) which can be applied to the release of potent antigens, proteins and peptides which require small amounts to exert their pharmacological effect. Incorporation of hydrophilic proteins in higher loadings with such potent peptides and antigens can enhance the release of such peptides/antigens by increasing the ingress of water into the hydrophobic gel matrix of NASEGS. BSA released from loaded aquasomes was also found to be released in smaller quantities in comparison to BSA directly incorporated in NASEGS.

BSA was also investigated for acute toxicity in human cells, using HDFa cells as a cell culture model. BSA was found to enhance proliferation of cells within 24 hours. This is

generally expected as BSA is used in cell culture medium to enhance cell growth and viability.

In conclusion, BSA-loaded aquasomes show potential as protein carrier delivery systems which can be applied in various areas of protein where small amounts of protein release are required. NASEGS have demonstrated suitability as a dosage from for the delivery of protein-loaded aquasome formulations for topical delivery.

CHAPTER 4

GENTAMICIN-LOADED AQUASOMES AS POTENTIAL ANTIBIOTIC DELIVERY SYSTEMS FOR THE TREATMENT OF BONE INFECTIONS

4.1 INTRODUCTION

One of the major and prevailing complications in orthopaedic surgical procedures and fracture treatments are pathogenic infections which may lead to rejection from host, disunions or ultimate bone destruction (El-Husseiny et al., 2011). Such infections cause inflammations of the bone tissue (osteomyelitis) (Lew and Waldvogel, 2004). Osteomyelitis is a disease in transition, with ongoing changes in predisposing factors, causative organisms and treatment. It is a disease which is heterogeneous in its pathophysiology, clinical presentation and management (Gomes, Pereira and Bettencourt, 2013, Lima et al., 2014).

This infection may be restricted to one portion of the bone or can involve several regions including the marrow, cortex, periosteum and the surrounding soft tissue (Soriano and Evora, 2000; Lew and Waldvogel, 2004).

4.1.1 Progression and Etiology of Osteomyelitis

Bacteria enter the bone haematogenously through the Haversian system, the structural unit of the bone (osteon). They adhere to the bone and trigger an acute inflammatory response. Bacteria have various different mechanisms to facilitate cell-cell and cell-implant adhesion (Gogia et al., 2009). Certain major causes of infection, such as *Staphylococcus aureus, (S. aureus)* adhere to bone by expressing receptors (adhesins) for components of bone matrix (fibronectin, laminin, collagen, and bone sialoglycoprotein); the expression of the collagen-binding adhesion permits the attachment of the pathogen to cartilage (Lew and Waldvogel, 2004; Popat et al., 2007 Sanchez et al., 2013; Arciola et al., 2015).

Among pathogenic microorganisms, *S. aureus* is by far the most commonly involved in osteomyelitis in humans, followed by *Enterobacteriaceae* and *Pseudomonas* species (Lew and Waldvogel, 2004; Gogia et al., 2009). The ability of *S. aureus* to adhere is thought to be crucial for the early colonisation of host tissues, implanted biomaterials, or both. *S. aureus* expresses several adhesins on its surface, each specifically interacting with one host protein component, such as fibrinogen, fibronectin, collagen, vitronectin, laminin, thrombospondin, bone sialoprotein, elastin, or von Willebrand factor. *S. aureus* and *S. epidermidis* can also form biofilms (a microbial community characterised by cells that attach to substratum or interface to each other) which are difficult to treat with antimicrobial agents.

4.1.2 Local antibiotic therapy for osteomyelitis

The major advantage local antibiotic therapy offers over systemic therapy is lower serum antibiotic concentrations thus reducing toxicity-related side-effects (Joosten et al., 2005; Nandi et al., 2009). Based on the commonly implicated causative microbes involved in osteomyelitis, the most widely accepted antimicrobial agents in local delivery systems are amino glycosides and to a lesser extent various β-lactam agents and quinolones. Importantly, a combination therapy of antibiotics proves useful in the reduction of the toxicity of individual agents, to prevent the development of antimicrobial resistance and to treat mixed infections involved in osteomyelitis and also demonstrate a synergistic effect (Nandi et al., 2009, Gogia et al, 2009).

Release of the antibiotic in such systems depends on the rate of dissolution of drug in its matrix allowing its penetration through the pores of the carrier. The amount of release in highly soluble β-lactam agents depends on the surface area of the carrier and on the initial concentration of the drug in the prepared systems. For relatively insoluble agents like quinolones, the rate of drug release depends on the porosity of the matrix and on the dissolution of the drug in the matrix (Allababidi and Shah, 1998).

4.1.3 Hydroxyapatite as a biomaterial for antibiotic local delivery

Drug delivery systems (DDSs) exhibiting the properties of biocompatible bioceramics are highly desirable and are thus shaped as powders, blocks, cements, scaffolds, porous devices and coatings for this purpose (Mizushima et al, 2006; Zhou and Lee, 2011; Arcos and Vallet-Regis, 2013). One major example commonly used for this property is synthetic hydroxyapatite (HA). HA is the inorganic component of the bone structure. Synthetic HA is chemically and structurally similar to the mineral phase of bone demonstrating remarkable osteogenic and osteoconductive properties (Itokazu et al, 1998).

Because of its chemical and structural similarities to the inorganic phase of human bone, HA (HA) shows excellent biocompatibility (Arcos and Regis, 2013). Many research studies have been focused on the use of ceramic materials HA as antibiotic carriers for treating bone infection, since their chemical composition is very similar to the bone mineral phase (Baro et al, 2002).

Antibiotic impregnated HA has also been used to treat patients with chronic osteomyelitis after removing necrotic tissue. The ceramic material was gradually incorporated into the host bone and uneventful healing was observed within three months with no recurrence of infection (Nandi et al, 2009).

Gentamicin loaded HA cement has been investigated using *in vitro* and *in vivo* studies for its effectiveness against post traumatic chronic osteomyelitis. In HAC/gentamicin-treated animals, no growth was detectable after 7 days of culture. No histopathological evidence of infection was observed in the HAC/ gentamicin-treated group while different stages of chronic osteomyelitis were observed in other groups (Joosten et al, 2004).

Micro porous HA was analysed for antibacterial activation using three different antibiotics including gentamicin, in comparison to dense HA. Bacteria inhibition tests against different pathogenic bacteria were performed for testing the antibiotic adsorption and the microbiological effectiveness after loading with different antibiotics. Results demonstrated that adsorbed amount on the micro-porous HA was largely higher than that on dense HA and an increase in the duration of antibiotic release was observed (Chai et al, 2007).

4.1.4 Aims and objectives

The overarching aim for this chapter is focused on investigating the efficacy of the aquasome delivery system in exerting sustainable bactericidal activity against an osteomyelitis relevant pathogen (*Staphylococcus aureus*). The following objectives were set to achieve this aim.

1. To successfully fabricate gentamicin-loaded aquasomes which exhibit antibacterial activity against a known pathogen by the release of gentamicin

2. To fabricate gentamicin-loaded aquasomes with sustained release and bactericidal activity and to determine the amount of gentamicin released at each time point that yields antibacterial activity.

3. To examine the efficacy of gentamicin-loaded aquasomes in exerting a bactericidal effect against *Staphylococcus aureus,* (which is implicated in nearly all cases of osteomyelitis), in comparison with negative controls.

4.2 MATERIALS AND METHODS

4.2.1 Materials

Nano-sized hydroxyapatite powders (60nm) were purchased from MKNano Corporation (Ontario, Canada). D (+)-Trehalose dehydrate was purchased from Acros organics (Belgium). Dulbecco's Phosphate Buffer Saline (PBS, tablets were purchased from Sigma Aldrich (Poole, UK). Gentamicin sulphate was purchased from Bio-West (UK). LB Agar (Miller Luria-Bertani agar), LB Broth (Miller Luria-Bertani broth) were purchased from Fisher Scientific (UK) and McFarland Reagent. Lab strain of *Staphylococcus aureus* were gifted by Dr Lindsay Marshall. All reagents and materials were of analytical grade.

4.2.2 Methodology

4.2.2.1 Preparation of Gentamicin-Loaded Aquasomes

(a) Coating phase

100mg of nano-sized hydroxyapatite (HA) powder was weighed and placed in 10ml capacity freeze dryer vials. 0.1M trehalose solution was prepared with distilled water and 10ml of trehalose solution was added to each vial containing HA powder. The resulting suspension was mixed for 2.5 h.

(b) Freeze drying and secondary drying phases

HA-trehalose suspension was further centrifuged at 1000rpm for 5mins. Supernatant was discarded, leaving the coated HA nanocores. Coated HA nanocores were washed with 2.5ml phosphate buffer saline (PBS) solution and centrifuged again at 100rpm for 5mins.

Coated HA nanocores were manually freeze-dried by manually freezing the HA slurries at -20°C to speed up freezing of samples while manually reducing the shelf temperature of the freeze dryer to -32°C, a temperature slightly higher than the T_g of trehalose, -34°C. Coated HA nanocore slurries are then transferred to the cooled freeze dryer shelves and the condenser and vacuum pump (500μBar) are turned on to start the freeze-drying process. This freeze-drying step lasted for the duration of 12-16 h. Subsequently, shelf temperatures were sincreased to 30°C to evaporate any residual non-sublimed moisture content. This drying step lasted for the duration of 4 h.

(c) Drug loading phase

2mg/ml gentamicin sulphate solutions were prepared with distilled water and 10ml of 2mg/ml gentamicin solution was added to each vial containing freeze dried coated HA nanocores. The resulting suspension was coated and further freeze dried as explained in the coating phase (a) and freeze-drying and secondary drying phases (b) above.

4.2.2.2 In Vitro Release Study of Gentamicin Loaded Aquasomes

In vitro release studies were performed using phosphate buffered saline (PBS, pH 7.4) as release media. Gentamicin-loaded aquasomes were placed into 10ml capacity vials and filled with 10ml of PBS and placed in an orbital shaking incubator (100rpm, 37°C). Using the partial replacement method, 1ml samples were taken and replaced with fresh pre-warmed release media (PBS) of the same volume at hourly time intervals for the duration of 8h. Samples were analysed using UV spectrophotometry at the maximum detection wavelength (λ_{max}) of gentamicin, 257nm. Gentamicin standards were prepared with PBS as diluent and a calibration curve was used to determine corresponding gentamicin concentrations in supernatant solutions according to Beer-Lambert's law.

4.2.2.3 Bacterial zone inhibition assay (Control Assay)

To determine the activity of the components of gentamicin-loaded aquasomes, hydroxyapatite (HA) nanocores, coated nanocores and gentamicin were individually tested against lawns of *Staphylococcus aureus* for antibiotic activity.

Lab *Staphylococcus aureus* was incubated in LB (Miller Luria-Bertani) broth overnight. Lawns of *S. aureus* were prepared using LB agar as a substrate. 20mls of LB agar was pipetted into single vent petri dishes close to a Bunsen burner flame to maintain aseptic conditions, and left to cool to room temperature. Lawns of S. aureus were prepared on the agar surface by streaking bacterial suspension in a perpendicular motion, using sterile cotton swabs. Glass Pasteur pipettes were used to puncture holes into the agar, sufficient to contain 50µl of control solutions/ suspensions (HA and coated HA, 2mg/ml suspensions; gentamicin, 0.5, 1.0, 2.0, 3.0 and 4.0mg/ml standard solutions). Control solutions/suspensions were pipetted into the holes and incubated for 24 h in an incubator (37°C, 5% CO_2).

Diameters of the zones of bactericidal activity were measured in mm and graphically represented to compare antibiotic activity of aquasome components as well as the varying concentrations of gentamicin standards.

4.2.2.4 Antimicrobial activity assay of Gentamicin-loaded aquasomes

To determine the antimicrobial activity of gentamicin loaded aquasomes, varying microbial loads of *S. aureus* were exposed to gentamicin loaded aquasomes (n=3). Multiple colonies of *S. aureus* were harvested from a lawn with a sterile inoculating loop, dispersed in sterile PBS and thoroughly mixed to maintain a homogenous bacterial suspension. The turbidity of the bacterial suspension was: (A) compared with 0.5 McFarland standard solutions and; (B) measured at O.D of 1 at 625nm.

S. aureus stock solution, (a), was further diluted in a 1:100 dilution with sterile PBS. 10ml of 1:100 diluted *S. aureus* suspensions were pipetted into bijou vials containing 100mg gentamicin loaded aquasomes with extra free volume for bacterial aeration. Control group constituted 1:100 *S. aureus solutions* without aquasomes.

S. aureus stock solution, (b), was further diluted in a 1:100 dilution with sterile PBS. 50ml of the 1:100 diluted *S. aureus* suspension was pipetted into 250ml conical flasks containing 500mg gentamicin loaded aquasomes (100mg per 10ml) with extra free volume for bacterial aeration. Control group constituted 1:100 diluted *S. aureus solutions* without aquasomes.

Samples (100µl) were taken hourly from *S. aureus* stock solution, (b) {with O.D. =1}, for 8 h and after 24 h without replacement as sample total volume had a negligent effect on the antimicrobial activity of gentamicin on *S. aureus*. Samples (100µl) were taken hourly from *S. aureus* stock solution, (a), {with O.D. = 0.5}, for 8 h and after 24 h with an individual experimental setup for each time point.

Samples were further diluted from a range of 10^{-1} to 10^{-6}. 20µl of serially diluted samples were aliquoted and plated on LB agar plates in triplicates, with corresponding control culture dilutions and incubated for 24h for bacterial growth. After 24 h, any colonies present were counted and the colony forming units (CFU) were calculated with the formula below:

CFU/ml **=** Average colony count **x** 50 **x** Dilution used

To illustrate the antimicrobial activity of gentamicin against *S. aureus,* the results were graphically represented plotting the log CFU against the hourly time points.

4.2.2.5 In vitro cell toxicology assay (Thiazolyl Blue Tetrazolium Bromide (MTT) assay)

to investigate whether the certain concentrations of gentamicin adsorbed onto the aquasomes were toxic to cell lines used in this study (SAOS-2, MG-63, HUVECs), a thiazolyl blue tetrazolium bromide (MTT) assay was performed to measure cell death after exposure of cells to different concentrations of gentamicin for 24 h, representing short term exposure to aquasomes (acute toxicity).

MG63 and SAOS-2 cells were grown in DMEM/F-12 supplemented with 10 % FBS, 1 % L-glutamine, 1 % NEAA, 1% penicillin/streptomycin. Human Umbilical Vein Endothelial Cells (HUVECs, Gibco, UK) were cultured in Medium 200 (M200, Gibco, UK) supplemented with the LSGS kit (Gibco, UK) which is constituted of the following concentrations per 500ml M200: fetal bovine serum, 2% v/v; hydrocortisone, 1 μg/ml; human epidermal growth factor, 10 ng/ml; basic fibroblast growth factor, 3 ng/ml; and heparin, 10 μg/ml. Cells are cultured at 37°C in humidified air with 5% CO_2. Cells were trypsinised using a dilute trypsin solution (made with 15-20% of 0.25% Trypsin EDTA solution diluted with HBSS), centrifuged (1000rpm) and re-suspended in fresh media. Cells were counted and recorded for concentration per ml. Cell suspension was diluted with complete media to 75,000 to 100,000 cells per ml. 100µl of cells (7,500- 10,000 cells per ml) was added into each well and incubated overnight (37°C, 5% CO_2).

On day 2, after allowing cells to attach to the bottom of the wells, serum-free media was carefully removed. Cells were treated with 10, 20, 30, 40 and 50ng/ml BMP-2/VEGF121-spiked serum-free media (n=3), leaving a final volume of 100µl per well. After 24h, 20µl of 5 mg/ml MTT was aseptically added to each well. MTT reagent was also added to a set of wells without cells, acting as blank.

Plates were incubated for 3.5 h at 37°C in an incubator. Wells were aspirated and 150µl of dimethyl sulphoxide (DMSO) was added per well. Well plates were covered with tinfoil and cells were agitated using an orbital shaker for 20mins. The absorbance readings of wells were then measured at 590nm with a photometric scan between 540-590nm to assay absorbance values at different wavelengths (Multiskan Spectrum- UV/Vis Microplate Spectrophotometer).

The cell viability was calculated using the formula below:

$$\text{Cell viability (\%)} = \frac{[\text{O.D OF TREATED WELL- OD OF BLANK}]}{[\text{OD OF UNTREATED WELL -OD OF BLANK}]} \times 100\%$$

4.2.2.6 Statistical analysis of results

Statistical analysis was performed using GraphPad Prism software package. Data was analysed using a two-tailed paired t-test (significance level, $p<0.05$).

4.3 RESULTS AND DISCUSSION

Gentamicin is a commonly used antibiotic to prevent bacterial infection around bone implants. It is an aminoglycoside antibiotic, with wide spectrum of activity against bacteria, particularly gram-negative bacteria. It works by binding the 30S subunit of the bacterial ribosome, interrupting protein synthesis. When given orally, gentamicin is not effective (a characteristic common to all aminoglycosides) (Lambert, 2004; Popat et al., 2007). This is because it is absorbed from the small intestine, and then travels through the portal vein to the liver, where it is inactivated. Therefore, it can only be given intravenously, intramuscularly or topically. Delivery via these routes is often not effective because the drug cannot readily reach the infection site in bone tissue, particularly in necrotic or avascular tissue left after surgery. This limitation cannot be overcome with increased systemic doses because of organ toxicity associated with antibiotics at higher concentrations. Thus, local antibiotic therapy has become an accepted and common adjunct to systemic antibiotics to prevent infection. This not only offers the advantages of a high local antibiotic concentration without any systemic toxicity but also an effective way of delivering antibiotics right at the site of implantation (Popat et al., 2007). The use of gentamicin in local antibiotic delivery systems is regarded as a gold standard of treatment and its prolific use has been recorded in various literature, with gentamicin-PMMA beads (non-biodegradable) and collagen-gentamicin sponge as commercially produced antibiotic delivery systems (Kanellakopoulou and Giamarellos-Bourboulis, 2000; Nandi et al., 2009).

The bactericidal activity of gentamicin-loaded aquasomes against *S. aureus* was determined for possible implementation in the treatment of local bone infections. *S. aureus* is the major causative organism in bone infections and thus the aim of this research was to represent a bone disease state and establish the efficacy of gentamicin-loaded aquasomes as an antibiotic eluting delivery system.

Infection is defined as a homeostatic imbalance between the host tissue and the presence of microorganisms at a concentration that exceeds 10^5 organisms per gram of tissue (Zilberman and Elsner, 2008). The incidence of bone infections is high in immunocompromised patients and is a prevalent problem in orthopaedic surgeries (Lew and Waldvogel, 2004). The success of bone implantation surgeries depends not only on the bone–implant integration, but also on the presence of a sterile environment around the implant, which will prevent bacterial infection. If not prevented, bacterial infection can result in serious and life threatening conditions such as osteomyelitis (Popat et al., 2007). Osteomyelitis is a debilitating disease, characterized by the inflammatory destruction of bone and surrounding

tissues. Disease is most commonly preceded by hematogenous spread of microorganisms to the bone from either a contiguous infection or directly following trauma. *S. aureus* is the microorganism most commonly associated with hematogenous and post-traumatic osteomyelitis, accounting for more than half of all the cases (Lew and Waldvogel, 2004),

4.3.1 Bacterial zone inhibition assay (Control Assay)

Figure 4.1 illustrates the non-bactericidal activity of trehalose-coated and uncoated nano-HA cores against lawns of *S. aureus* used in this study. These served as negative controls. These demonstrated, on a smaller scale, the vulnerability of bone substitutes and bone graft materials such as blocks and granules made of HA, β-tricalcium phosphate, or calcium sulphate to microbial colonisation leading to bone infections and thus bone implantation failure (Teller et al., 2006).

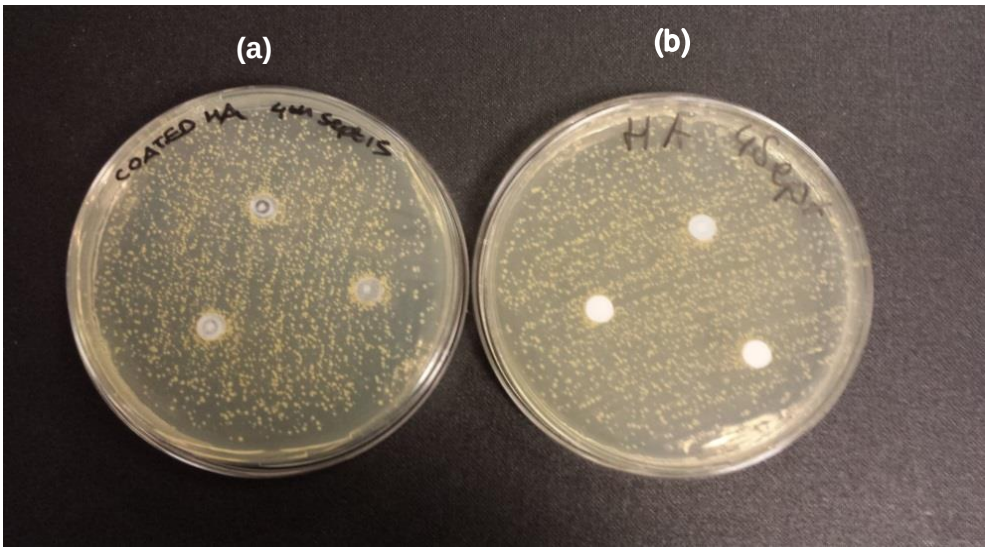

Figure 4.1 Images from antimicrobial assay, showing negative controls of coated and uncoated hydroxyapatite (HA). Image above shows the controls of (a) coated and (b) uncoated HA. Lawns of S. aureus were incubated with naked HA nanocores and trehalose-coated HA nanocores in triplicates and showed no zone of inhibition, illustrating the non-bactericidal/bacteriostatic activity of HA nanocores (coated or uncoated) (n=3).

Biofilms are surface attached communities consisting of mono- or polymicrobial species that are surrounded by a self-produced extracellular polymeric matrix. Generally, biofilms represent a protected mode of growth enabling the organisms to persist within

immunocompetent hosts, and are regarded as a significant pathogenic event in the development of a number of chronic human infections, including osteomyelitis (Sanchez et al., 2013). A bacterial biofilm can progressively form on the implant surface, recruiting inflammatory cells and evoking inflammation, compromising the osseointegration process or even determining bone resorption, leading to mobilization, functional impairment and failure of the treatment (Campoccia et al., 2010). Slower penetration of antibiotics in the extracellular matrix of biofilms and the expression and exchange of biofilm-specific resistance genes further diminish the effectiveness of antibiotics against bone infections (Barth et al., 2011). *S. aureus* can form biofilms *in vitro*, furthermore staphylococcal biofilms are a significant factor contributing to non-union indicating that staphylococcal biofilms play a critical, yet not fully understood role in the development of chronic osteomyelitis and related infectious complications (Palmer and Sewecke, 2011; Sanchez et al., 2013).

Figure 4.2 illustrates the bactericidal activity of gentamicin standards (0.5, 1.0, 2.0, 3.0 and 4.0 mg/ml). Zones of inhibition were measured and results showed that gentamicin concentration was directly proportional to the diameter of the zone of inhibition in mm (n=3) as shown in table 4.2 below. Figure 4.3 shows a graphical representation of the zones of inhibition of *S. aureus* growth when samples of gentamicin standards were incubated with lawns of S. aureus (n=3), illustrating the bactericidal activity of the gentamicin standards. The differences in diameter were found to be statistically significant ($p<0.05$).

Table 4.2 Zone of inhibition (diameters) for gentamicin standards

Gentamicin concentration (mg/ml)	***Diameter of zone of inhibition (mm)****
0.5	28.83±0.28
1	31.5±0.5
2	32.83±0.28
3	34±0
4	34.5±0.86

**Results were found to be significant when p< 0.05, n=3*

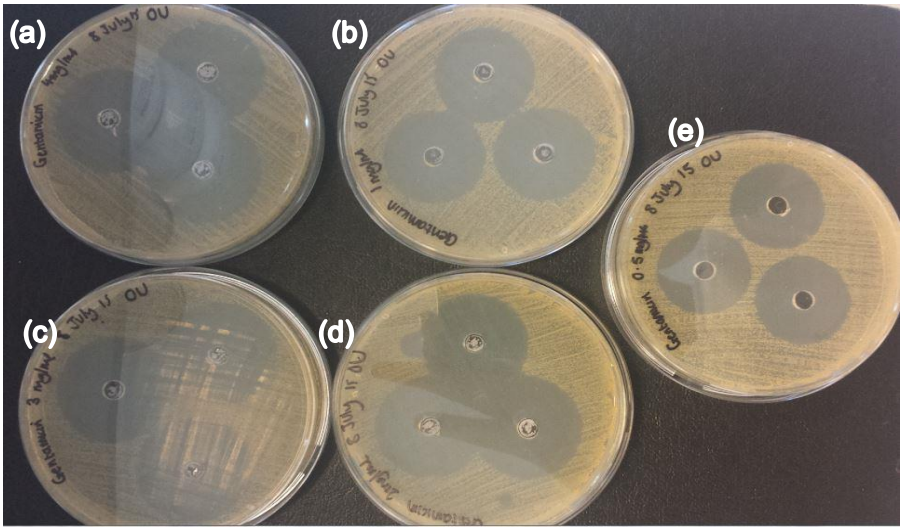

Figure 4.2 Images from antimicrobial assay, illustrating the bactericidal activity of gentamicin standards. Image above shows gentamicin positive controls. Lawns of S. aureus were incubated with varying concentrations of gentamicin (0.5 (e), 1.0 (b), 2.0 (d), 3.0 (c) and 4.0 (a) mg/ml) in triplicates and showed corresponding increasing diameters of zones of inhibition, illustrating the bactericidal activity of gentamicin standards (n=3).

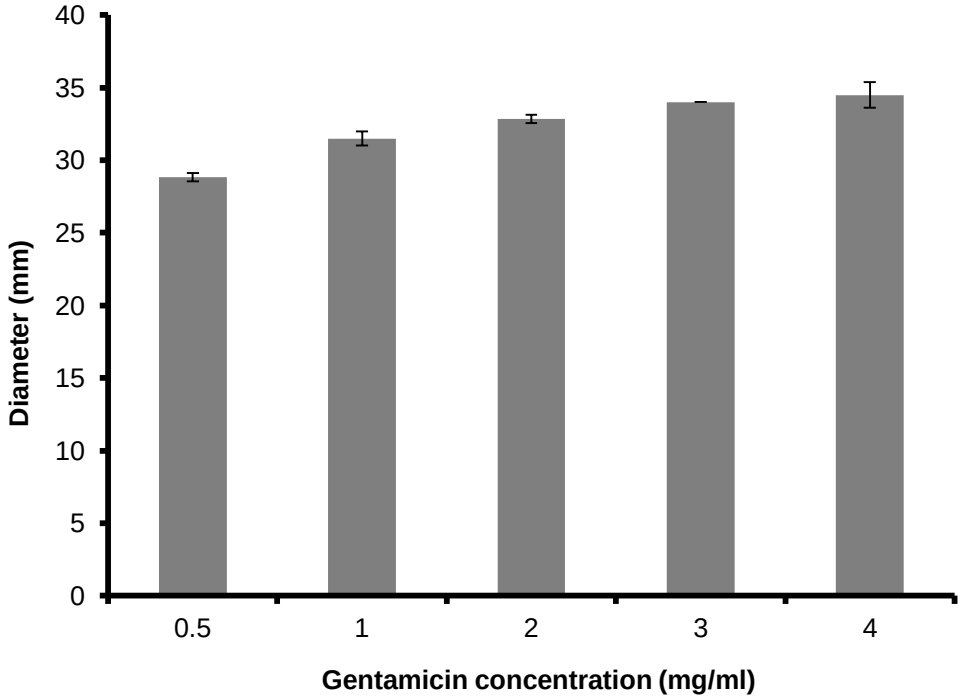

Figure 4.3 A graphical representation of zones of inhibition illustrating the bactericidal activity of gentamicin standards. Lawns of *S. aureus* were incubated with varying concentrations of gentamicin (*0.5 (e), 1.0 (b), 2.0 (d), 3.0 (c)* and *4.0 (a)* mg/ml) in triplicates and showed corresponding increasing diameters of zones of inhibition, illustrating the bactericidal activity of gentamicin standards (n=3).

4.3.2 *In Vitro* Release Study of Gentamicin Loaded Aquasomes

A release study of gentamicin- loaded aquasomes, fabricated with 2mg/ml gentamicin sulphate solutions, was performed for the duration of 8 h with samples taken at hourly time points. The *in vitro* cumulative release plots (figure 4.4A) show that the amount of gentamicin released from the aquasomes was consistently between 1.0 to 1.4mg/ml at every time point. Percentage release (figure 4.4B) shows a range of 5.05 to 6.42% for each time point. The release of gentamicin after 8 h demonstrates sustained release of gentamicin from the aquasomes. The release of gentamicin from aquasome formulations ranged from 1.011 to 1.28mg at each time hourly point. In an antibiotic study by Akins and Rybak (2000), the *in vitro* activities of different antibiotics against *S. aureus* including gentamicin, was investigated. The minimum inhibitory concentrations (MICs) and minimum bactericidal concentrations (MBCs) of gentamicin for three strains of *S. aureus* in an *in vitro* infection model were calculated to be 128/128, 0.5/1.0 and 0.25/0.5 μg/ml. These findings demonstrate that gentamicin released from loaded aquasomes is about 10 times higher than the highest MIC of *S. aureus.*

(A)

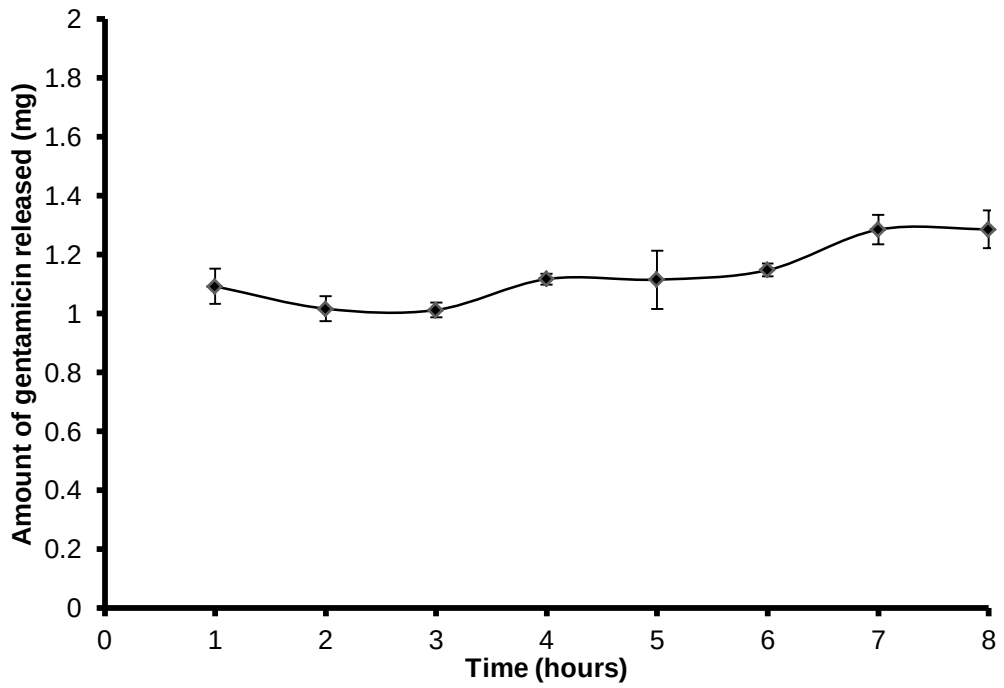

(B)

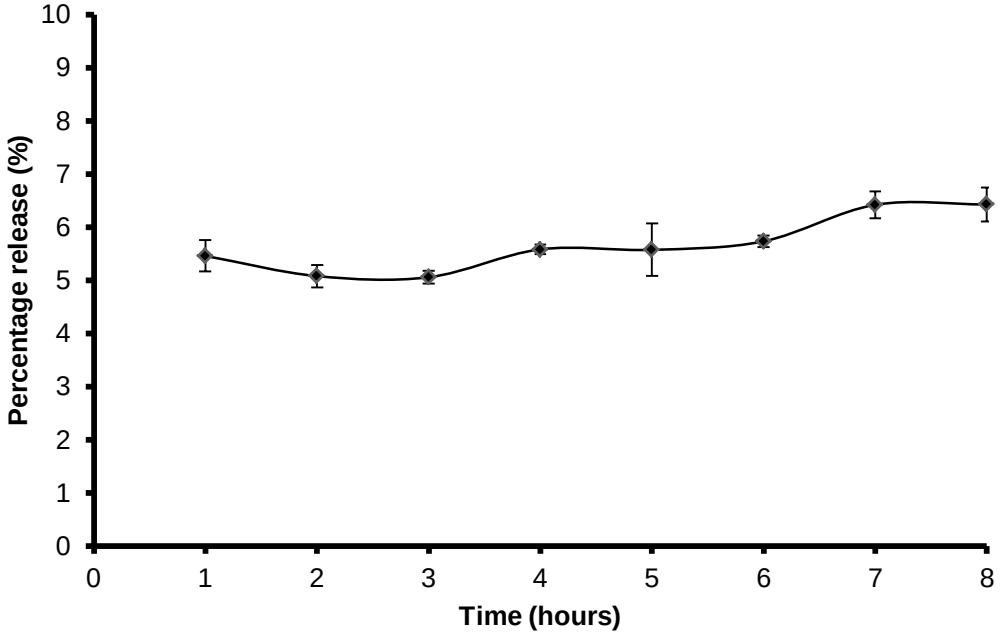

Figure 4.4 ***In vitro*** **release of gentamicin from gentamicin-loaded aquasomes.** Fig. 4.4 A shows the cumulative release of gentamicin from aquasomes (fabricated with 2mg/ml gentamicin solutions) for the duration of 8h; Fig 4.4B illustrates the percentage release of gentamicin from the aquasome formulation. Percentage release results show 5.05 to 6.42% gentamicin release after 8h (n=3).

4.3.3 Antimicrobial activity assay of Gentamicin-loaded aquasomes

Figure 4.5 pictorially represents the results from the antimicrobial assay illustrating the progressive bactericidal activity of gentamicin released from gentamicin-loaded aquasomes [images 1 (a) to 3(a) and 4(b) to 6(b)] against *S. aureus* (0.5 McFarland standard turbidity concentrations) over the duration of an 8h release study in comparison with the negative controls (1 (b) to 3(b) and 4(a) to 6(a)) (S. aureus in sterile PBS).

The ceramic nanocore used in this study was hydroxyapatite (HA). Calcium phosphates (CaPs) such as HA and β- tricalcium phosphate have attracted significant interest in simultaneous use as bone substitutes and drug delivery vehicles. CaPs are more biocompatible than many other ceramic and inorganic nanoparticles. Degradation products of CaPs are Ca^{2+} and PO_4^{3-}, which are already natural occurring metabolites in the body and are also found in relatively high concentrations (1–5 mM) in the bloodstream. This natural occurrence of CaP is one of the primary advantages over other synthetic drug delivery systems (DDSs), which might trigger an immunogenic response (Bose and Tarafder, 2012).

HA has been exhaustively researched in the literature for its excellent bioactivity, biocompatibility and osteoconductivity. Its inherent properties make it an excellent biomaterial for use in orthopaedic medicine. Based on its properties, it does not require removal after implantation in comparison to PMMA beads, because of its resorbable property. Hence, numerous studies have been published illustrating HA as an excellent antibiotic carrier material in orthopaedic medicine.

The surface modification of HA has been shown to offer an added sustained release property of adsorbed antibiotics in comparison to HA (in its various forms: blocks, cements, powders) soaked in antibiotic solutions. These surface modifications include increased porosity, reduction of individual particle sizes or coating with another material which offers a prolonged release effect (Chai et al, 2007; Arcos and Vallet-Regi, 2013).

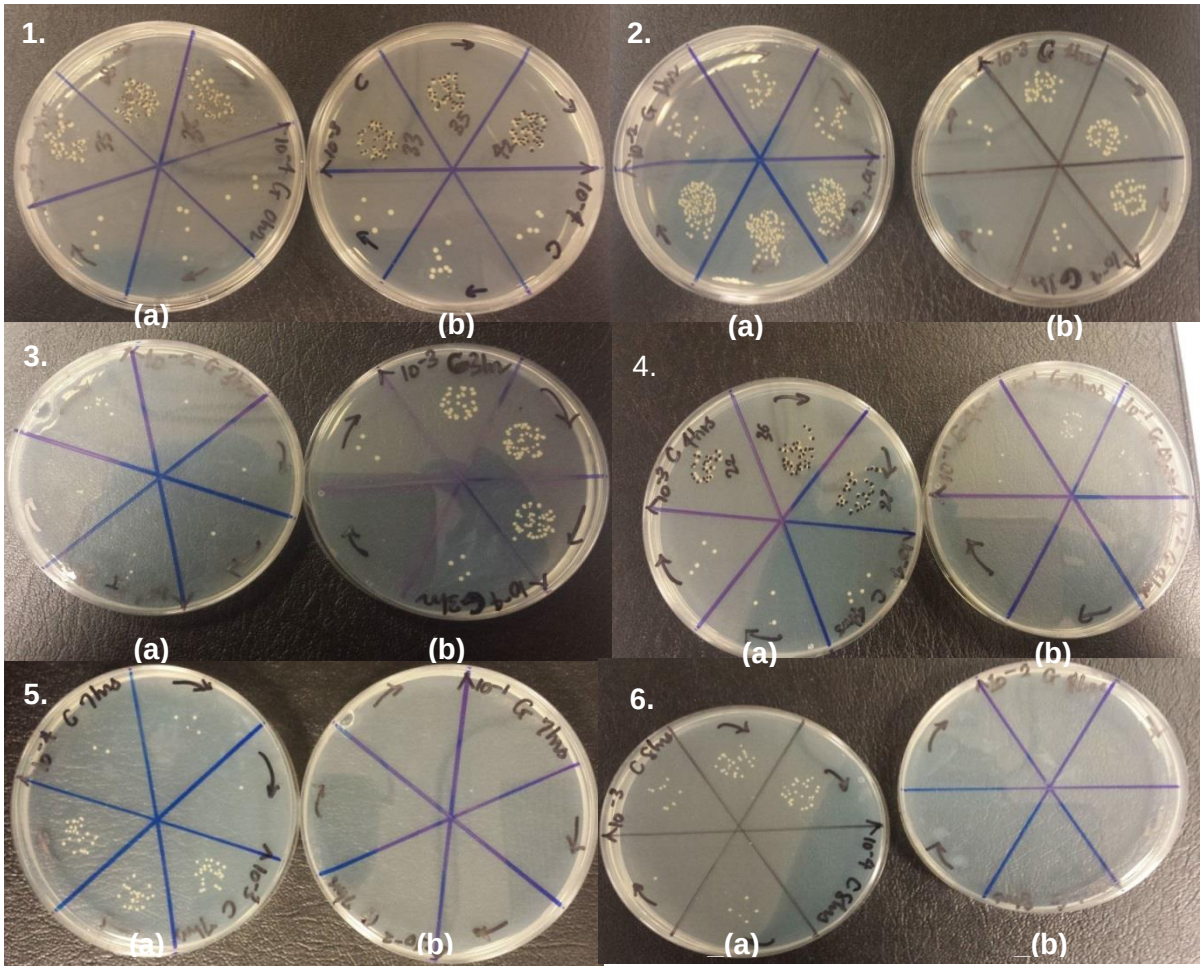

Figure 4.5 Images from antimicrobial assay (S. aureus stock solution, A, optical density O.D. =0.5). These images illustrate the bactericidal activity of gentamicin-loaded aquasomes. Images show results at the various time points, with the test (G) and control (C) plates: 1. 0hr (a) test (G) plate, (b) control (C) plate; 2. 1hr (a) test (G) plate, (b) control (C) plate; 3. 3hrs (a) test (G) plate, (b) control (C) plate; 4. 4hrs (a) control (C) plate, (b) test (G) plate; 5. 7hrs (a) control (C) plate, (b) test (G) plate; 6. 8hrs (a) control (C) plate, (b) test (G) plate. Serially diluted sample aliquots were plated on agar plates in triplicates from test and control groups and incubated for 24h. Test results show that gentamicin loaded aquasomes demonstrated bactericidal activity up to 24h.

Chai et al (2007) investigated antibiotic adsorption on microporous and dense HA and the microbiological effectiveness after loading with different antibiotics. The impregnation time, antibiotic impregnating concentration, impregnation condition and other factors, which might influence the antibiotic loading effect, were studied by exposure to different releasing solvents and different pathogenic bacteria (most prevalent in bone infections): Staphylococcus aureus, Staphylococcus epidermidis and Escherichia coli. The results showed that, for all three types of antibiotics (vancomycin, ciprofloxacin and gentamicin), adsorbed amounts on the micro-porous HA were hugely higher than that on dense HA. The micro-porosity of test HA had also significantly prolonged the release time of antibiotics even under mimic physiological conditions. The human plasma used in this study is regarded, as a mimic physiological solution for *in vitro* antibiotic (ATB) releasing study, so the results can be representative of results in *in vivo* conditions. The results clearly demonstrated that the porous structure of test HA material induced a sustained antibiotic delivery effect (increasing the release time from 24 h observed with dense HA to 72 h).

β- Tricalcium phosphate (TCP) is also used in bone regenerative medicine. The solubility of β-TCP is much higher than HA, and thus β-TCP is termed a bio-resorbable ceramic. It exhibits excellent biocompatibility, absorbability and osteoconductivity. The cements based on β-TCP have been widely used in bone tissue engineering. Wu et al (2013) developed a bactericidal gentamicin-doped β-tricalcium phosphate (β-TCP) scaffold reinforced with a gelatin/genipin hydrogel (G-β-TCP). Gelatin hydrogel has been used to achieve a sustained release of gentamicin. Gelatin reacts with genipin to form a hydrogel, which formed a drug-eluting layer along the inner walls of the pore structure the results showed that the gentamicin-doped G-β-TCP had a much longer drug releasing period, while the gentamicin was completely released from pure TCP cements (β-TCP) within one day. Around 17% of the drug was released from G-β-TCP on the first day, followed by a zero-order release profile in which 2–4μg of drug released daily. A standard strain of *S. aureus* (ATCC25923) was selected to evaluate the antibacterial activity and therapeutic effect of this scaffold. G-β-TCP significantly inhibited growth of S. aureus both *in vitro* and *in vivo*. In a rat osteomyelitis model, osteomyelitis was totally cured after implantation of G-β-TCP for three weeks (Wu et al, 2013).

In comparison to the two research studies highlighted above, the present study also demonstrates the efficacy of the gentamicin loaded aquasomes to exert bactericidal effects against pathogenic bacteria prevalent in bone infections: *S. aureus*. Figure 4.6 and 4.7 graphically illustrate the bactericidal activity of gentamicin aquasomes against low inoculum (O.D=0.5) and high inoculum (O.D=1) of *S. aureus.* The micro porous HA investigated by Chai et al (2007) acted as an ATB delivery system with pores as cavities for the ATBs to be

loaded into. This led to a more sustained release of ATB over 72 h in comparison to the dense HA. A similar result was observed with the β-TCP scaffold used by Wu and colleagues (2013), in which the gelatin hydrogel was used to achieve a sustained release of gentamicin which led a longer release period in comparison to gentamicin loaded onto pure β-TCP cements which was released within one day. The self-assembled structure of gentamicin-loaded aquasomes has an incorporated trehalose coating which acts as the release mechanism for gentamicin. Its hydration forms a gel which acts as a controlled release barrier for gentamicin release into the surrounding milieu.

Trehalose was used in the current study as a sustained release coating based on its solution properties. The strong and prominent hydrogen bonds network of trehalose impacts on its solution properties, such as diffusivity and viscosity. In comparison to sucrose, trehalose demonstrated a lower water diffusion co-efficient and higher viscosity, although the density was similar (Ekdawi-Sever et al, 2001). According to the Noyes-Whitney equation, the rate of dissolution of a drug particle is inversely proportional to the viscosity of the dissolution medium. This generally applies to both *in vivo* and *in vitro* situations whereby the medium into which the drug is dissolving exhibits Newtonian behaviour.

Another research study exhibited the same trend of results where the release profiles of a gentamicin carrier system (composed of calcium phosphates, poly (DL-lactide) (PLA) and gentamicin) was investigated (Baro et al, 2002). One of the formulations developed (F-D) was composed of 80% phosphates (25% HA and 75% tricalcium phosphate, TCP), 20% PLA (MW, 30 kDa) and 3.5% gentamicin sulphate (GS) and was coated with PLA (MW, 200 kDa). To explain the *in vitro* release mechanism of this implant, an uncoated implant (F-X), with identical matrix composition, was prepared. Results showed that the PLA coating delayed the gentamicin release, indicating that part of the antibiotic released from the matrix diffuses through the polymer coating film. This agrees with the present study where gentamicin is released through the hydration of the trehalose polymer matrix (Figure 4.4A). The selected formulation was also tested in the femur of rabbits and showed a faster release rate *in vivo* than *in vitro*. This is due to a greater degree of PLA degradation, changes in the phosphate blend, and bone tissue invading the implant. Gentamicin concentration in the areas of the bone closest to the implant was higher than the minimum inhibitory concentration (MIC) against *S. aureus*.

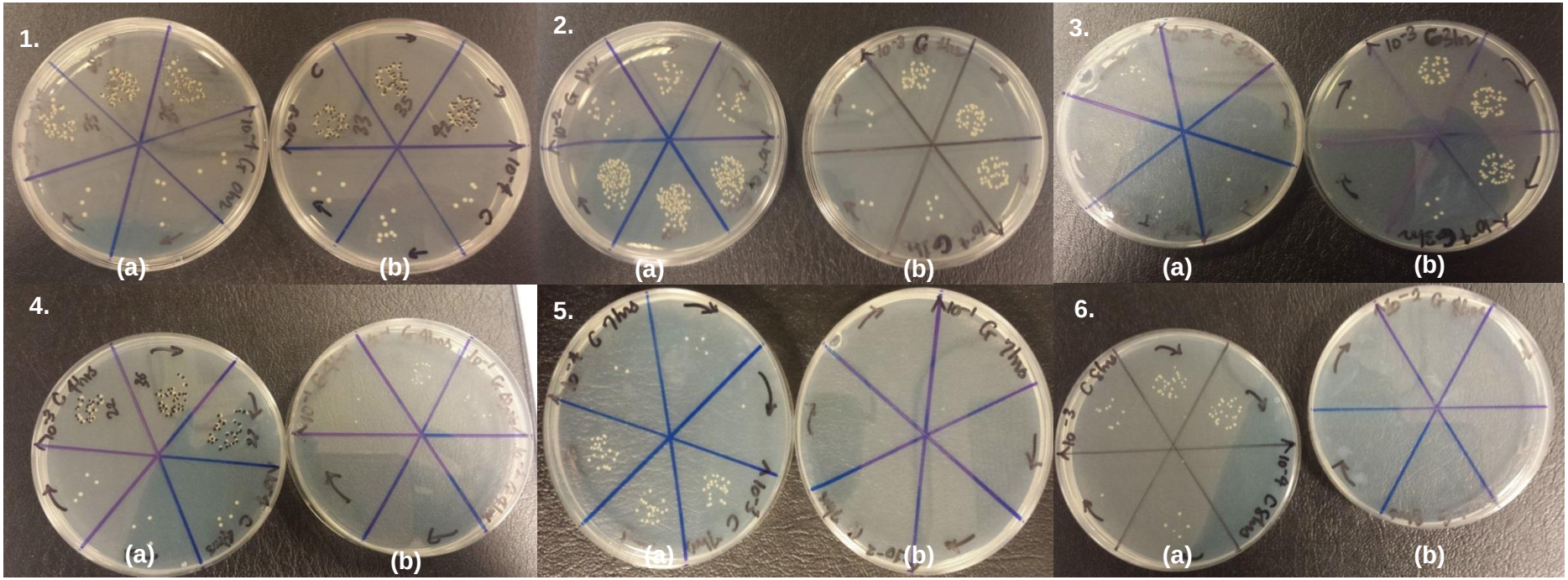

Figure 4.6 Images from antimicrobial assay (S. aureus stock solution, (B), optical density O.D. =1). These images illustrate the bactericidal activity of gentamicin-loaded aquasomes. Images show results at the various time points, with the test (G) and control (C) plates: 1. 0hr (a) test (G) plate, (b) control (C) plate; 2. 1hr (a) test (G) plate, (b) control (C) plate; 3. 3hrs (a) test (G) plate, (b) control (C) plate; 4. 4hrs (a) control (C) plate, (b) test (G) plate; 5. 7hrs (a) control (C) plate, (b) test (G) plate; 6. 8hrs (a) control (C) plate, (b) test (G) plate. Serially diluted sample aliquots (10^{-1} to 10^{-10}) were plated on agar plates in triplicates (20µl per replicate) from test and control groups and incubated for 24 h. Colonies were counted and CFU/ml was calculated. Test results show that gentamicin loaded aquasomes demonstrated bactericidal activity up to 24 h.

Figure 4.6 pictorially represents the results from the antimicrobial assay illustrating the progressive bactericidal activity of gentamicin released from gentamicin-loaded aquasomes [images 1 (a) to 3(a) and 4(b) to 6(b)] against *S. aureus* [with the turbidity concentration measured with the optical density (O.D.) = 1] over the duration of an 8h release study in comparison with the negative controls [1 (b) to 3(b) and 4(a) to 6(a)] (*S. aureus* in sterile PBS). Bactericidal activity was observed after 5 h of sustained gentamicin release from aquasomes and this can be attributed to the higher bacterial inoculum concentration.

Figure 4.7 shows the bactericidal activity of gentamicin loaded aquasomes against *S. aureus* (0.5 McFarland standard turbidity concentrations) over the duration of an 8h release study in comparison to the negative controls evidenced by a bar graph plotting the colony forming unit (CFUs) count over the duration of 8 h. This is pictorially represented in Figure 4.5 [images 1 (a) to 3(a) and 4(b) to 6(b)] show test plates and (1 (b) to 3(b) and 4(a) to 6(a)) negative controls (S. aureus in sterile PBS)]. The graph illustrates the progressive bactericidal activity of gentamicin which had a sustained release profile from the aquasomes over the duration of 8 h. Bactericidal activity (no CFU detected) was observed after 2 h of exposure to the gentamicin loaded aquasomes hand this was sustained over the 8h study. According to the *in vitro* release profile of gentamicin from gentamicin loaded aquasomes (Figure 4.4A), the amount of gentamicin that exerts bactericidal activity against S. aureus corresponds to 1.01mg of gentamicin released into PBS, when sampled after 5 h of gentamicin release from aquasomes. The two-tailed paired t-test showed a significant difference between the test group (gentamicin aquasomes) and the negative control group ($p= 0.0273$; $R^2= 0.6555$), indicating that the gentamicin released from the loaded aquasomes had a bactericidal effect on the inoculum of *S. aureus*, evidenced by the absence of CFUs after 2 h of gentamicin release.

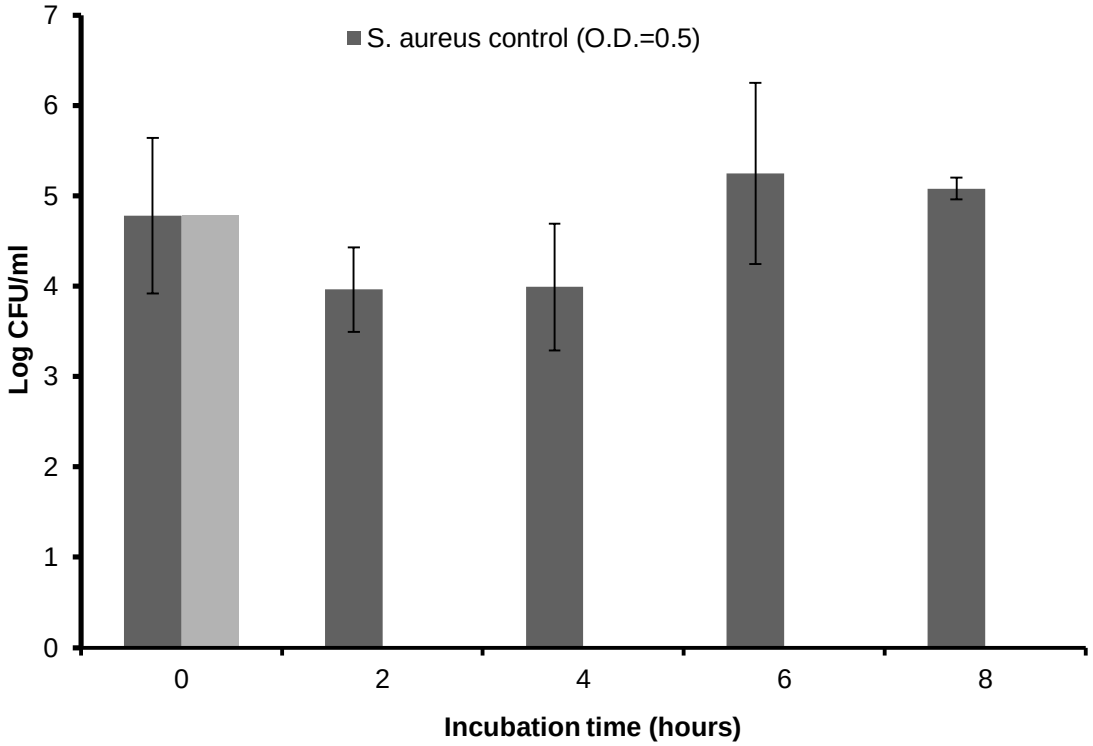

.

Figure 4.7 Antimicrobial activities of gentamicin-loaded aquasomes against S. aureus (stock solution, comparable to 0.5 McFarland standard). The graph illustrates the progressive bactericidal activity of gentamicin-loaded aquasomes at different time points (every 2 h for 8 h). Serially diluted sample aliquots were plated on agar plates in triplicates from test and control groups and incubated for 24 h. Gentamicin released from aquasomes exerted a bactericidal effect within 2 h and bacteria did not reproduce within the study period. Test results show that gentamicin loaded aquasomes demonstrated bactericidal activity up to 8 h (n=3).

The bactericidal activity of gentamicin loaded aquasomes against *S. aureus* (O.D=1) over the duration of 24 h release study is represented graphically in Figure 4.8. In comparison to the negative controls, the bactericidal activity of gentamicin from loaded aquasomes is evidenced by a bar graph plotting the colony forming units (CFUs) count over the duration of 24 h. This is pictorially represented in Figure 4.6 [images 1 (a) to 3(a) and 4(b) to 6(b)] show test plates and (1 (b) to 3(b) and 4(a) to 6(a)) negative controls (S. aureus in sterile PBS)]. The graph illustrates the progressive bactericidal activity of gentamicin which had a sustained release profile from the aquasomes over the duration of 24 h. Bactericidal activity was observed after 5 h of sustained gentamicin release from aquasomes. No CFU were observed after 5 h and this bactericidal activity sustained over the 24 h study. According to the *in vitro* release profile of gentamicin from gentamicin loaded aquasomes (Figure 4.4A), it

corresponds to 1.1mg of gentamicin released into PBS, when sampled after 5 h of gentamicin release from aquasomes. The two-tailed paired t-test showed a significant difference between the test group (gentamicin aquasomes) and the negative control group ($p= 0.0010$; $R^2= 0.7202$) indicating that the gentamicin released from the loaded aquasomes had a bactericidal effect on the inoculum of *S. aureus* when compared with the negative control group, evidenced by the absence of CFUs after 5 h of gentamicin release.

To examine the efficacy of the bactericidal activity of the gentamicin-loaded aquasomes, a higher inoculum of bacteria was used. The bacterial inoculum concentration used had an optical density (O.D) of 1, at 625nm in comparison to the O.D. of 0.5 McFarland turbidity standards, which has an O.D. range of 0.08 to 0.1, and thus a higher amount of gentamicin released from the gentamicin-loaded aquasomes was needed to exert a bactericidal effect. The gentamicin-loaded aquasomes also maintained bactericidal activity as no bacterial growth was observed in the test groups even after 24 h in comparison to the negative controls, which showed an almost constant log CFU/ml, count between the 5^{th} and 24^{th} h time points.

A similar study performed by Popat et al (2007) investigated the release of gentamicin from nanotubes as well as the bactericidal activity of gentamicin nanotubes (NT-G) against *Staphylococcus epidermis* and its osteoconductive ability. These drug-loaded nano-tubular surfaces were developed for direct application onto existing implants (at the interface of implant and tissue). Nanotubes (80nm width, 400nm length) were filled with 200μg, 400 μg and 600 μg gentamicin. There was a slower and more sustained release of gentamicin from nanotubes loaded with high amounts of gentamicin (600 μg) in comparison to those loaded with smaller amounts (200μg and 400 μg). A 70% decrease in bacterial colonies was observed on NT-G (600μg) in comparison to titanium (Ti) and unloaded nanotubes (NT) as well as enhancing osteoblastic differentiation in newborn mouse calvaria-derived MC3T3-E1 subclone 14 pre-osteoblastic cells. In the present study, 2mg/ml gentamicin solution per 100mg was used to fabricate gentamicin loaded aquasomes. In comparison to naked HA cores (in PBS, release medium, negative control), gentamicin loaded aquasomes showed efficacy in its bactericidal effect against *S. aureus* (up to O.D. of 1 at 625nm). HA nanocores used in this study have also exhibited increased osteoblast proliferation and differentiation, measured by increased ALP production (discussed in chapter 5).

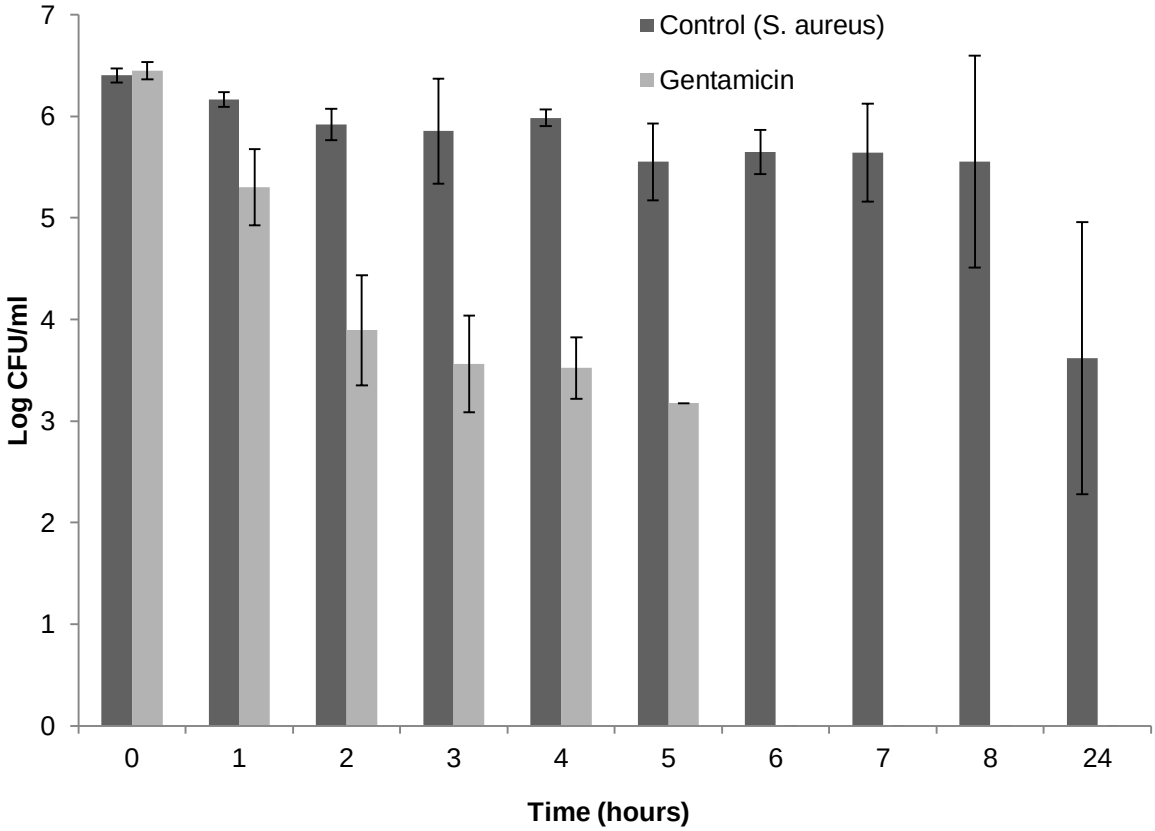

Figure 4.8 Antimicrobial activity of gentamicin-loaded aquasomes against S. aureus (stock solution, (B), optical density O.D. =1). This graph illustrates the progressive bactericidal activity of gentamicin loaded aquasomes at different time points (hourly for 8 h and at 24 h). Serially diluted sample aliquots were plated on agar plates in triplicates from test and control groups and incubated for 24 h. Gentamicin released from aquasomes exerted a bactericidal effect within 5 h and bacteria did not reproduce within the study period. Test results show that gentamicin loaded aquasomes demonstrated bactericidal activity up to 24 h (n=3).

4.3.4 In vitro cell toxicology assay (Thiazolyl Blue Tetrazolium Bromide (MTT) assay)

A thiazolyl blue tetrazolium bromide (MTT) assay was performed to measure cell death after exposure of cells to gentamicin to ensure that concentrations released from aquasome formulations are not toxic to cells used in this thesis. SAOS-2 cells, MG63 cells and HUVECs were exposed to different concentrations of gentamicin for 24 h, representing short term exposure to aquasomes (acute toxicity). Figure 4.8 illustrates the cell viabilities of SAOS-2 cells, MG63 cells and HUVECs after exposure to 0.5, 1.0, 1.5, 2.0 and 2.5 mg/ml of gentamicin in culture media.

Figure 4.9 demonstrates that the exposure of SAOS-2 cells and HUVECs to the high concentrations of gentamicin sulphate for 24 h showed that they have no acute toxic effects on the cell lines. For SAOS-2 cells and HUVECs, all concentrations of gentamicin showed an increment in percentage cell viability after gentamicin exposure indicating cell proliferation in both instances in comparison to control. However, MG63 cells exhibited a reduction in percentage cell viability after cells were exposed to gentamicin. However, an increase in gentamicin concentration did not have a significant effect on MG63 percentage cell viability ($p=0.9378$). This same trend was observed for SAOS-2 cells and HUVECs as the increasing concentration of gentamicin had no significant effect on percentage cell viability ($p=0.9378$). However, the differences in percentage cell viability between the different cell lines were found to be significant ($p<0.0001$). These results show that different concentrations of gentamicin may affect cell lines differently by enhancing cell proliferation. However, all gentamicin concentrations are safe to use for use in culture of cells used in this study.

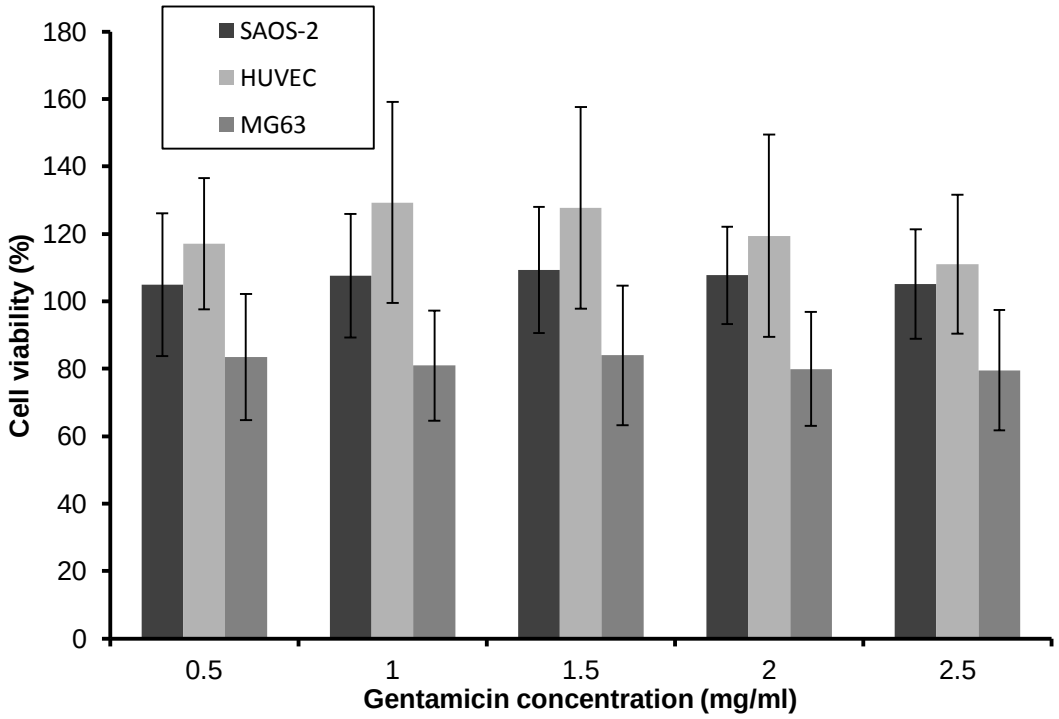

Figure 4.9 Percentage cell viability of SAOS-2 cells, MG63 cells and HUVECs after exposure to varying concentrations of gentamicin. MTT assay results of the cell viability of HUVECs, SAOS-2 and MG63 cells, after exposure to varying concentrations of gentamicin; (0.5, 1.0, 1.5, 2.0 and 2.5 mg/ml) in culture media for 24 h. Results show that gentamicin had no toxic effect on the cells with the exception of MG63 cells but rather increased the viability of the cells SAOS-2 and HUVECs) over the period of 24 h (n=24).

HA cement was used as a carrier system in the treatment of chronic, posttraumatic osteomyelitis investigated by *in vitro* and *in vivo* studies (Joosten et al, 2004). In the *in vitro* study, release of gentamicin from standard cylinders of HAC was measured by agar diffusion test. As a representative of mechanical properties, compression strength was measured in order to detect changes when mixing HAC with gentamicin. In the *in vivo* study, bone infection was induced and obtained after three weeks using S. aureus as pathogenic organism and white “New Zealand” rabbits. Animals were treated by debridement and filling the marrow either with HA alone or HA mixed with gentamicin (32 mg/g). Best evidence of the efficiency of treatment was observed in histopathological and microbiological findings. In all swabs of the control groups, taken 6 weeks following infection S. aureus were detected which were clonal to the strain used for induction of osteomyelitis\s. In HAC/gentamicin-treated animals, no growth was detectable after 7 days of culturing in BHI bouillon. In the HAC/ gentamicin-treated group, there was no histopathological evidence of infection. In all other groups, different stages of chronic osteomyelitis were found. No side effect was observed, neither locally or systemically by HAC or gentamicin (Joosten et al, 2004).

The nano-HA powder used in the gentamicin loaded aquasome formulation also contributes to the release profile of gentamicin from the aquasome formulation, by offering a larger surface area of gentamicin loading in the fabrication of the formulation. This ensures that the amount of gentamicin in the aquasome formulation is more than sufficient to demonstrate a controlled release profile over a longer duration and thus exert a prolonged bactericidal effect.

Rauschmann et al (2007) investigated the antibiotic release properties and biocompatibility of PerOssal®, a biodegradable composite of calcium sulphate and nanoparticulate HA. PerOssal® was used in comparison to calcium sulphate alone, to demonstrate improved surface area for drug loading and eliminate short term cytotoxicity, a commonly known characteristic of calcium sulphate. Specific surface area was 106m^2/g for PerOssal and 2.2m^2/g for pure calcium sulphate. Almost complete elution of gentamicin was found for both carrier materials (94.7% for PerOssal® vs. 95.8% for calclium sulphate) within 10 days. PerOssal® showed higher initial and lower release after approximately 5 days compared to calcium sulphate. No significant in vitro cytotoxic differences were found between PerOssal® and nontoxic cell culture medium. However, calcium sulphate showed cytotoxic effects in two out of four tests. The authors concluded that PerOssal® exhibited excellent properties regarding resorption, biocompatibility, and antibiotic release based on the results obtained. Based on this study, the favourable results can be largely attributed to the use of nano-HA.

4.4 CONCLUSIONS

Gentamicin has been established as an effective local treatment in bone infections. It has been extensively researched upon as an additive in orthopaedic biomaterials to prevent infections commonly implicated in surgeries. From the results, gentamicin loaded aquasomes have proven to be an effective antibiotic nano-carrier delivery system which have great potential in the treatment of bone infections for low and high inoculums of bacteria. For low inoculum and higher inoculum of *S. aureus (O.D=0.5; O.D=1)*, gentamicin released from loaded aquasomes exerted bactericidal activity against *S. aureus* within 2 h and 5 h respectively. Statistical analysis showed that the differences between the CFUs samples from test groups (gentamicin loaded-aquasomes) and control groups (*S. aureus), were stistically significant (p<0.0001). S. aureus* is implicated in most cases of osteomyelitis and thus the demonstration of the bactericidal effect of gentamicin-loaded aquasomes show promise in the treatment of bone infections *in vivo*. These results prove that gentamicin loaded aquasomes can provide a protective bactericidal cover for 24 h at the interface of local application of prophylaxis. However, further investigations on the duration of complete release of gentamicin from aquasomes need to be investigated to determine the duration of antibiotic protection gentamicin loaded-aquasomes can offer in *in vivo* and *in vitro* applications.

CHAPTER 5
THE DIFFERENTIATION EFFECT OF BMP-2- AND VEGF 121- LOADED AQUASOMES

5.1 INTRODUCTION

Osteogenesis involves the migration of mesenchymal stem cells (MSCs), their differentiation into osteoprogenitor cells, and their differentiation and maturation into osteocytes (Carriera et al, 2014). This process is tightly regulated by both local and systemic factors. Local factors such as growth factors play a major role in the modulation of osteogenesis and the most important growth factors implicated in this process are bone morphogenetic proteins (BMPs) (Mundy et al, 2001).

BMPs were first isolated by Urist and co-workers (1965) and proposed the name Bone Morphogenetic Protein in 1971. They constitute the largest sub-unit of the transforming growth factor βeta (TGF-β) family. BMPs are synthesized by osteoprogenitor cells, osteoblasts, chondrocytes and platelets (Sipe et al, 2004), but their production is not restricted to bone, since they also perform non-osteogenic functions. They play an important part in the development of osteoblasts and platelets including cell proliferation and differentiation, tooth morphogenesis, organogenesis, embryonic development, apoptosis, chemotaxis and repair of a wide variety of tissues (Ducy and Karsenty, 2000). Most importantly, in maintaining bone integrity and fracture healing, BMPs stimulate intramembranous/ endochondral ossifications by inducing mesenchymal stem cell differentiation into the osteoblastic lineage (Dragoo et al, 2003).

5.1.1 Structure of BMPs

Around 20 BMPs have been found and sub-grouped according to their sequence similarity and known functions. The BMP family is sub-grouped into four according to their amino acid sequence: (a) BMP2 and 4 (80% homology); (b) BMP3, BMP3B (GDF10); (c) BMP5, 6, 7, 8a and 8b (78% homology); (d) GDF5, 6, 7 (Carriera et al, 2014).

All BMPs are dimers and are synthesized as inactive precursor proteins constituting of about 120 amino acids (Figure 5.1). These include seven cysteine residues, six of which are built into a cystin knot linked with three intramolecular disulphide bonds (Xiao, Xiang and Xhao, 2007; Carriera et al, 2014). The seventh is involved in dimerization with another BMP monomer. Prior to secretion, BMPs consist of an N-terminal hydrophobic signal peptide, pro domain and mature peptide. The signal peptide is cleaved and consecutively undergoes glycosylation and dimerization. Such glycosylation increases their stability and half-life in the body. After dimerization, a prerequisite for bone induction, the pro-domain is proteolytically cleaved at a consensus Arg-X-X-Arg region to generate mature and active homodimers or heterodimers (Xiao, Xiang and Xhao et al, 2007; Carriera et al, 2014).

Being synthesized by a variety of cells, BMPs exerts an array of regulatory effects. The regulatory effects of BMPs depend upon the target cell type, differentiation stage, local BMPs concentration, as well as interactions with other secreted proteins (Figure 5.2) (Dimitriou, Tsiridis and Giannoudis, 2005; Carreira et al, 2014b)

Figure 5.1 Structure of BMP showing its receptor BRIAA
(Xiao et al, 2007)

Figure 5.2 Osteoblastic differentiation (Adapted from: Carreira et al, 2014)

5.1.2 BMP-2 in tissue engineering

BMPs are the most effective growth factors in improving healing of non-unions, fractures, spinal fusions and dental implants (Bessa, Cassa and Reiss, 2008, Carreira et al, 2014b). They have been extensively investigated and are most recently being used in advanced tissue engineering technologies to improve the regeneration of bone for fracture healing and in treatment of bone defects (Kisiel et al, 2012; Patel et al, 2008; Li et al, 2006 Bessa, Cassa and Reiss, 2008). Its osteogenic effects are highlighted in Table 5.1.

Based on its unique function of stimulating ectopic bone formation, BMPs have been complexed and adsorbed on various materials mentioned in numerous literatures. Its ability to stimulate bone formation by inducing the proliferation of osteoblasts as well as indirectly stimulate angiogenesis (formation of blood vessels) has been exploited in the research areas of orthopaedics (bone tissue engineering, bone fracture healing, bone implantation) (Sigurdsson et al, 1997; Liu, Engest and Kuffer, 2007; Fei et al, 2008) and dentistry (osteointegration of dental implants) (Sasche and Wagner, 2005).

the use of recombinant human BMPs (rhBMPs) are widely applied in tissue engineering products with rhBMPs loaded in delivery systems made of synthetic or natural polymers co-cultured with stem cells or osteoprogenitor cells (Kang et al, 2012; Kyriakdou et al, 2008; Unger et al, 2007). Such polymers include synthetic polymers like PLA, PGA, PLGA, PLA-Collagen, PLA-Collagen-HA and natural polymers like collagen, gelatin, hyaluronic acid, chitosan, dextran, fibrin and alginate (Bessa, Cassa and Reiss, 2006).

the main role of a delivery system for growths factors, in this case BMPs, is to retain the growth factor at the site of injury for a prolonged time frame, providing an initial support to which cells attach and form regenerated tissue. An appropriate bone tissue engineering material will exhibit osteoinductive and/or osteoconductive properties, while offering mechanical stability to the regenerating bone (Xu et al, 2005; Bessa et al, 2008; Schliepaeke, 2010).

Table 5.1 Osteogenic BMPs and their functions
(Xiao et al, 2007)

BMP	Functions
BMP-2	• Induces bone and cartilage formation. • Plays a key role in osteoblast differentiation • Induces the expression of other BMPs
BMP-3	• Induces bone formation
BMP-4	• *In vivo* and *in vitro* osteochondrogenic factor • Regulates the formation of teeth, limbs and bone from mesoderm. • It also plays a role in fracture repair
BMP-5	• Performs functions in cartilage development
BMP-7	• *In vivo* and *in vitro* osteochondrogenic factor • Plays a key role in osteoblast differentiation. • Also induces the production of SMADI. Also, key in renal development and repair
BMP-9	• Promoting chondrogenic differentiation of human multipotential mesenchymal cells

5.1.3 Vascular endothelial growth factor (VEGF)

As evidenced in a plethora of literature, VEGF is the major angiogenic factor involved in normal angiogenesis, appropriate callus architecture and mineralisation in fracture repair (Carano and Filvaroff, 2003). VEGF production is the major coupling mechanism between angiogenesis and osteogenesis during fracture repair (Geris et al, 2008).

VEGF expressed is detected on chondroblasts, chondrocytes, osteoprogenitor cells and osteoblasts (Kanczler and Oreffo, 2008; Geris et al, 2008). VEGF expression is induced by most osteoinductive growth factors as well as prostaglandins.

Additionally, VEGF has been observed to play a vital role in cartilage maturation and resorption. VEGF produced by hypertrophic chondrocytes instigates the endochondral ossification cascade by recruiting and differentiating osteoclastic cells that resorb cartilage and attracts osteoblasts (Geris et al, 2008).. Exogenously administered VEGF, in the absence of osteoprogenitors or a scaffold, boosted bone formation in an *in vivo* model of mouse femur fractures (Carano and Filvaroff, 2003).

5.1.4 Dual delivery of osteogenic and angiogenic growth factors

The dual delivery of angiogenic and osteogenic factors has been reported in the literature illustrating the importance of angiogenesis in the successful bone regeneration for the treatment of bone defects (Table 5.2). Angiogenesis precedes osteogenesis in bone regeneration for the re-establishment of vascularity. The principal angiogenic factor, VEGF and BMP have been synergistically administered for bone regeneration (Kanczler and Oreffo, 2008, Kempen et al, 2009). VEGF has been investigated to be implicated in osteogenesis and bone repair. Also, BMP-2 has been revealed to upregulate VEGF (an increase in cellular production) (Deckers et al, 2002). On the contrary, as earlier mentioned, inhibition of VEGF decreases angiogenesis, callus mineralisation and thus bone healing (Kanczler et al, 2010).

Table 5.2 Dual delivery of BMP-2 and VEGF growth factor in bone regeneration

Application and biomaterial used	*References*
Delivery to osteoprogenitor cells via Alginate-PDLLA composite scaffolds	*Kanczler et al, 2010*
BMSC driven bone regeneration using PLGA scaffolds	*Huang et al, 2005*
Induction of bone formation using CaP coated titanium implants	*Ramazanoglu et al, 2013*
In vivo osteogenic response using PLGA microspheres and/or PLGA scaffolds	*Hernandez et al, 2012*
Osteogenic differentiation of bone marrow derived stem cells (BMSCs)	*Bai et al, 2013*
In vivo model of bone regeneration using gelatin microparticles in scaffolds	*Patel et al, 2008*
Ectopic and Orthotopic bone regeneration using PLGA microspheres in polypropylene scaffolds	*Kempen et al, 2009*

5.1.5 Hydroxyapatite as an osteoconductive and osteoinductive nano-carrier for rhBMP-2

Hydroxyapatite is the naturally occurring inorganic form of calcium apatite and it constitutes 50% of the total mass of bone. Synthetic hydroxyapatite (HA) is chemically similar to the inorganic component of bone matrix (general formula: $Ca_{10}(OH)_2(PO_4)_6$) (Zhou and Lee, 2011). The close chemical similarity of HA to natural bone has led to extensive research efforts to use synthetic HA as a bone substitute and/or replacement in biomedical applications (Nayak, 2010). The major advantages of synthetic hydroxyapatite over bone substitutes are its biocompatibility, slow biodegradability rate *in situ*, osteoconductive and osteoinductive capacities (Zhou and Lee, 2011).

Porous hydroxyapatite offers a high binding affinity for a variety of pharmacological substances including antibiotics, hormones and enzymes (Nayak, 2010). Nanoscale hydroxyapatite incorporated with BMP-2 has been used in coating bone implants (Sasche and Wagner, 2005, Liu et al, 2007), as composites (Saito et al, 2005), fabricating osteoconductive porous scaffolds (Unger et al, 2007; Autefege et al, 2009) and formulating microparticles (Mizushuma et al, 2006).

5.1.6 Recent approaches to skeletal tissue engineering: delivery of angiogenic and osteogenic factors

Bone tissue engineering has evolved in the past two decades and has provided a lasting solution to the reconstruction of orthopaedic defects in comparison to the traditional clinical treatments which are associated with severe side effects such as disunions, infections and consequent pain. These traditional clinical treatments include autografting and allografting of cancellous bone, applying vascularised grafts and other bone transport techniques (Burg et al, 2000). Successful bone regeneration requires the production of a morphogenetic signal, the recruitment of responsive host cells that will respond to the signal, a suitable carrier of this signal that can deliver it to specific sites then serve as a scaffolding for the growth of the responsive host cells, that is, an osteoconductive carrier, and a viable, well vascularized host bed (Burg et al, 2000; Xu et al, 2005; Bessa et al, 2008).

According to Schliepaeke (2010), an appropriate scaffold or carrier system would also provide mechanical strength for bridging of the bone defect and resisting pressure from surrounding soft tissue as well as being porous enough to allow bone ingrowth and final replacement by regenerated bone. Osteoinductivity refers to the ability to cause pluripotent cells (such as undifferentiated mesenchymal cells) from a non-osseous environment to committedly differentiate into chondrocytes or osteoblasts. Osteoconductivity refers to the ability to support the ingrowth of capillaries and cells from the host into a three-dimensional structure to form bone. An osteoinductive material promotes the proliferation of host cells that stimulate the formation of bone which include endothelial cells, osteoprogenitor cells, chondroblasts and osteoblasts (Burg et al, 2000; Xu et al, 2005; Unger et al, 2007).

Biodegradable materials are also more suitable and desirable for the growth factors to be incorporated into the polymer matrix for gradual release over time with regard to degradation (Schliepaeke, 2010). Furthermore, the carrier should protect the BMPs from degradation and maintain its bioactivity whilst offering a controlled release of BMP over time to promote the formation of new bone at the treatment site. Such delivery systems suitable for the delivery of bone growth factors would provide sufficient mechanical strength to withstand soft tissue pressure in addition to connecting penetrability and degradability for unhindered bone ingrowth and eventual replacement by regenerated bone on the other.

Bone tissue engineering refers to the use of materials that can induce formation of bone tissue or act as a carrier or template for implanted bone cells or growth factors. According to Burg and colleagues (2000), these materials can be acellular or cellular. Acellular materials promote bone formation by having osteoconductive properties and can also allow bone ingrowth into the construct, but do not consist of a cellular component while cellular materials

have a cellular component added before implantation or treatment of bone defect. Acellular systems include naturally derived polymers (such as demineralised bone matrix and collagen), synthetic polymers (such as poly lactic-co-glycolic acid, PLGA, poly D-glycolic acid, PGA, poly lactic acid , PLA), composites (such as hydroxyapatite, tricalcium phosphate) and ceramics (such as hydroxyapatite, $Ca_{10}(PO_4)_6(OH)_2$, aragonite, $CaCO_3$).

5.1.7 Aims and Objectives

Combining the osteoconductive property of hydroxyapatite and osteoinductive properties of BMP-2 and VEGF-121, we report the formulation of BMP-2 and VEGF 121-loaded aquasomes as a potential aid in fracture healing. The aim of this research is to establish the potential of BMP-loaded aquasomes as osteoinductive nanoparticulate systems that promotes bone cell proliferation as well as induce angiogenesis via the proliferation of endothelial cells. VEGF-loaded aquasomes were also investigated to compare its proliferation and differentiation effect to BMP-loaded aquasomes. To establish these claims, BMP-2 and VEGF 121 released from aquasomes was quantified and BMP-loaded aquasomes were co-cultured with osteoprogenitor cells and assayed for ALP production to demonstrate the ability of aquasomes to be employed in bone regeneration.

To achieve this over-arching aim, the following set objectives were investigated:

1. *In vitro* release of BMP-2 and VEGF 121 from loaded aquasomes fabricated from 50ng/ml and 100ng/ml BMP-2 and VEGF 121 solutions.
2. *In vitro* administration of BMP-2 loaded aquasomes onto osteoprogenitor cells (MG63, osteoblast cell line) to analyse the differentiation effect of released BMP-2 from aquasomes.
3. *In vitro* administration of VEGF loaded aquasomes onto osteoprogenitor cells and osteoblasts to analyse the effect of released VEGF from aquasomes.
4. Co-culturing of endothelial cells (HUVECs, human umbilical vascular endothelial cells) and osteoblasts (SAOS-2) and/or osteoprogenitor cells (MG63) to demonstrate the effect of endothelial cells on osteoprogenitor cells and establish the link between osteogenesis and angiogenesis
5. *In vitro* administration of BMP-2 and VEGF 121-loaded aquasomes onto mesenchymal stem cells (AT-MSCs, adipose tissue mesenchymal stem cells) to analyse and compare the differentiation effects of released BMP-2 and VEGF 121 from aquasomes.

5. 2 MATERIALS AND METHODS

5.2.1 Materials

Lyophilised rhBMP-2 was purchased from eBioscience Ltd. (Hatfield, UK). Lyophilised VEGF 121 was purchased from Creative BioMart (Shirley, NY, USA). BMP-2 and VEGF121 development ELISA kits were purchased from Peprotech Ltd. (UK). Nano-hydroxyapatite powder (60nm) was purchased from MKNano Ltd. (Ontario, Canada). Trehalose dihydrtate was purchased from Fluka (Buchs, Switzerland). 1-step PNPP assay reagent was purchased from Thermo Fisher Ltd. (USA). Sirius Red/Fast Green Collagen Staining kit was purchased from Chondrex (Redmond, Washington, USA). 4-Nitrophenol (98%, NP) was purchased from Acros Organics (NJ, USA). DMEM/F12 with 15mM Hepes was purchased from Lonza (Belgium). Alizarin Red, Dimethyl Sulfoxide (DMSO), Fetal Bovine Serum (FBS) and 0.25% Trypsin EDTA was purchased from Sigma Aldrich (Poole, UK). Transwell inserts (pore sizes 0.4µm and 1.0µm) were purchased from Millipore (UK). The following cell culture reagents: Glutamax (Glutamine), Non-essential amino acids (NEAAs), penicillin/streptomycin and Hank's balanced salt solution (HBSS). All chemicals were of analytical grade.

5.2.2 Manufacture of aquasomes

Synthetic hydroxyapatite (HA), which is chemically and structurally similar to naturally occurring calcium apatite, the ceramic constituent of bone, was the inorganic core of choice for the manufacture of the aquasomes used in this study. BMP-2 and VEGF 121-loaded-aquasomes were manufactured using the same protocol as explained in Chapter 2 (Section 2.2), using 50ng/ml and 100ng/ml BMP-2 and VEGF 121 solutions.

To analyse the entrapment efficiency of aquasomes for BMP-2 and VEGF 121, the supernatant left after centrifugation to remove unadsorbed BMP in solution was aliquoted and analysed for BMP-2/VEGF 121.

5.2.3 Cell culture

The osteosarcoma fibroblast cell line MG63 was gifted by Dr Eustace Johnson (Figure 5.3) and was used as a pre-osteoblast/osteoprogenitor cell culture model to assess the osteogenic differentiation and proliferation effect of BMP-2 and VEGF 121- loaded aquasomes; BMP-2 and VEGF 121 spiked media of different concentration. The bone osteosarcoma epithelial cell line SAOS-2 (CLS, Germany) was used as an osteoblastic cell model and used as a positive control for osteoblastic cell behaviour. Adipose tissue mesenchymal stem cells (AT-MSCs) was gifted by Dr Eustace Johnson and was used to analyse the differentiation and proliferation effect of BMP-2 and VEGF 121-loaded

aquasomes and BMP-2 and VEGF 121 spiked media of different concentration, on mesenchymal stem cells. AT-MSCs, MG63 and SAOS-2 cells were grown in DMEM/F-12 supplemented with 10 % FBS, 1 % L-glutamine, 1 % NEAA, 1% penicillin/streptomycin in a humidified 37 °C incubator with 5% CO_2. The media was changed every 3-4 days. Thereafter the cells were passaged 6-7 days post seeding (at 70-80% confluency) by discarding old media, adding 5ml of HBSS Balanced solution (per T25cm^2 flask; 10ml per T75cm^2), and incubating for 5-10mins in an orbital shaking incubator to wash the cells. Trypsinising solution (made with 15-20% of 0.25% Trypsin EDTA solution) was added to flasks and returned to the orbital shaking incubator to incubate for 10mins. Flasks were then viewed under the microscope (Primovert, Carl Zeiss, and Germany) to ensure cells were lifted off the flask's surface. Cell solutions were transferred into centrifuge tubes and were centrifuged (1000rpm, 10mins). Supernatant was discarded and the pellet was re-suspended in pre-warmed media and mixed (pipetted up and down). The resulting cell solution was split into two flasks containing 5ml of media (per T25 flask, 15ml for T75 flasks).

Human Umbilical Vein Endothelial Cells (HUVECs, Gibco, UK) were used in this study to investigate the angiogenic effects of BMP-2 loaded aquasomes when exogenously administered to the cells as well as establish the osteogenic proliferation effect of endothelial cells when co-cultured with AT-MSCs or MG63. Cells were cultured in Medium 200 (M200, Gibco, UK) supplemented with the LSGS kit (Gibco, UK) which is constituted of the following concentrations per 500ml M200: fetal bovine serum, 2% v/v; hydrocortisone, 1 μg/ml; human epidermal growth factor, 10 ng/ml; basic fibroblast growth factor, 3 ng/ml; and heparin, 10 μg/ml. Cells are cultured at 37°C in humidified air with 5% CO_2. Media was changed every 2-3 days. Thereafter the cells were passaged 6-7 days post seeding (80-90% confluency) using the same protocol as stated above for AT-MSCs, MG63 and SAOS-2 cells.

Cells were cryopreserved for further use by centrifugation at 1000 rpm for 10 min to obtain
A cell pellet followed by resuspension of the pellet in 1ml Biofreeze cryopreservation solution (Biochrom, Germany). 1 ml of the cell suspension was aliquoted into cryovials and stored for 30mins at -80˚C and immediately transferred to liquid nitrogen for long-term storage.

5.2.4 Experimental design

5.2.4.1 BMP-2 bioactivity via ALP expression

100mg of BMP-loaded aquasomes were administered to MG63 cells (osteoprogenitor cells) and HUVECs (endothelial cells) *in vitro.* The amount of bioactive BMP released onto the cells was quantified and the differentiation effect of BMP on MG63 cells was measured via alkaline phosphatase (ALP) activity. HUVECs were also co-cultured with SAOS-2 cells and MG63 cells to link the synergistic nature of the osteogenic and angiogenic processes. Cell

lines were co-cultured using 12-well plates at different seeding densities. SAOS-2 and MG63 cell lines were seeded at $2x10^5$cells/ml in the well chambers with DMEM/F-12 and HUVECs at $1x10^5$cells/ml on transwell inserts. For each well chamber, 1ml of cell suspension was added and an extra 500µl was added to the well. For transwell inserts, 500µL of cell suspension was added to the 1.0µm pore size transwell inserts (Millipore, UK). When BMP-loaded aquasomes were exogenously administered, they were dispersed in corresponding cell culture medium and placed in transwell inserts when co-cultured with MG63 cells and in the well chambers when cultured with HUVECs. All control cell lines were mono-cultured. HUVECs and MG63 monocultures were used as negative controls, SAOS-2 cells as positive controls. The experimental design is illustrated in Table 5.3.

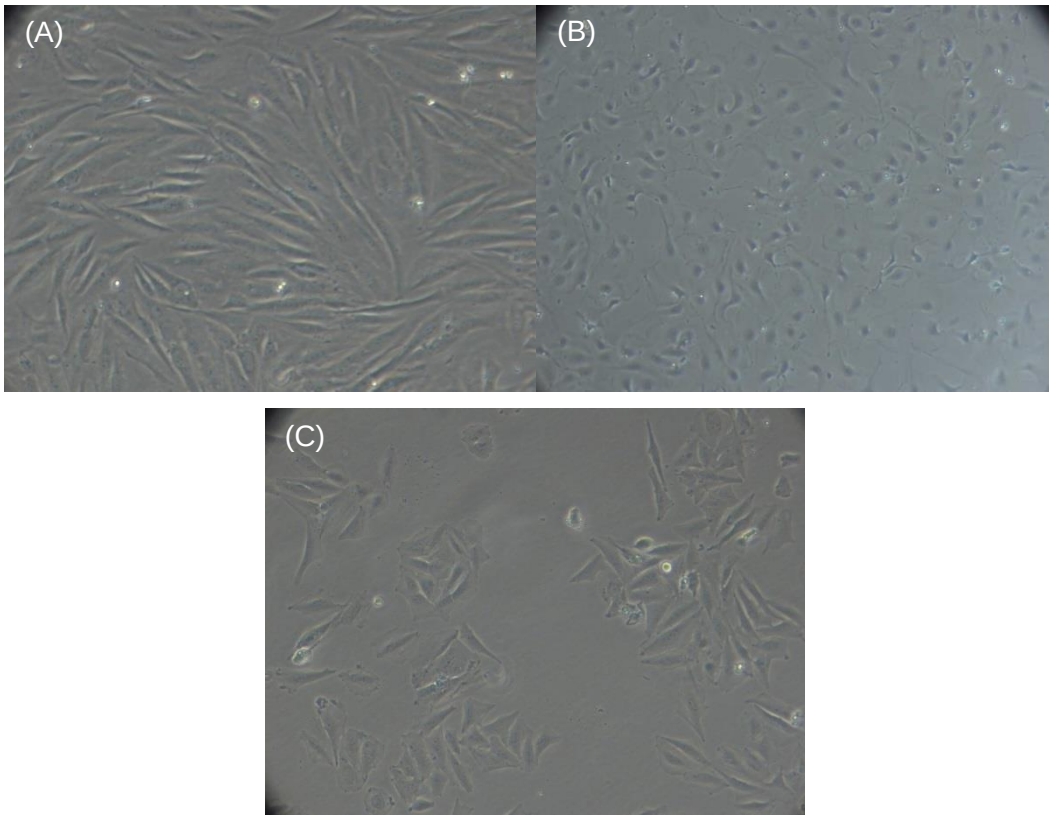

Figure 5.3 Microscopy images showing the morphology of the cells used in this study. (A) MG63 cells, (B) HUVECs, and (C) sub-confluent SAOS-2 cells (Magnification: 40X)

Table 5.3 Experimental design codes: Groups explained

Group names	*Interpretation*
BMP50/ VEGF50	Cells cultured with 50ng/ml BMP-2 or VEGF spiked media
HUVEC/MG63 or HUVEC/SAOS-2	Cells co-cultured with HUVECs grown on transwell inserts
BMP AQUA	Cells co-cultured with BMP-loaded aquasomes placed in well chambers and cells in transwell inserts
MG63/SAOS-2	Cells co-cultured with MG63 cells grown on transwell inserts
HUVECs (control); MG63 cells (control) SAOS-2 cells (control)	Cells cultured with basal media

Cell co-culture study legend		
	HUVEC	**MG63**
50ng/ml BMP-2	✓	✓
BMP-loaded aquasomes	✓	✓
MG63	✓	-
SAOS-2	✓	✓
50ng/ml VEGF 121	-	✓

5.2.4.2 AT-MSC differentiation study

AT-MSCs were seeded at 3.5 x 10^3 cells per cm^2 into 12 well plates (1ml cell suspension per and an additional 500µl culture medium) added to each well. Positive control cultures were then maintained with osteoblastic differentiation medium. This consisted of standard culture medium additionally supplemented with 50µM ascorbate 2-phosphate, 10nM dexamethasone (DEX) and 10mM β-glycerophosphate. AT-MSCs in osteogenic medium and SAOS2 served as a positive control. AT-MSCs were cultured with 50ng/ml and 25ng/ml BMP-2 (AT-MSCs BMP50, AT-MSCs BMP25), 50ng/ml and 25ng/ml VEGF 121 (AT-MSCs VEGF50, AT-MSCs VEGF25), BMP-2 and VEGF 121-loaded aquasomes (fabricated with 100ng/ml solutions; AT-MSCs BMP AQUA, AT-MSCs VEGF AQUA) and BMP-2 and VEGF 121 loaded aquasomes physically combined (AT-MSCs BMP/VEGF AQUA). All cultures were then maintained at 37°C, 5% (v/v) CO_2. Control and test media were replaced every 2-3 days and after 21 days in culture, samples were analysed for ALP activity. Experimental design for the study is illustrated in Table 5.4.

Table 5.4 Experimental design: AT-MSC differentiation study

Group names	*Interpretation*
AT-MSCs BMP50/ AT-MSCs VEGF50	Cells cultured with 50ng/ml BMP-2 or VEGF spiked media
AT-MSCs BMP25/ AT-MSCs VEGF25	Cells cultured with 25ng/ml BMP-2 or VEGF spiked media
AT-MSCs BMP AQUA/ AT-MSCs VEGF AQUA	Cells cultured with BMP-loaded OR VEGF-loaded aquasomes placed in transwell inserts and cells in well chambers
AT-MSCs BMP AQUA/VEGF AQUA	Cells cultured with BMP and VEGF-loaded aquasomes (exogenous dual delivery) aquasomes placed in transwell inserts and cells in well chambers
AT-MSCs Blank	Cells mono-cultured in osteogenic media

5.2.5 In vitro cell toxicology assay (Thiazolyl Blue Tetrazolium Bromide (MTT) assay)

to investigate whether the certain concentrations of BMP-2 and VEGF 121 adsorbed onto the aquasomes were toxic to cell lines used in this study (SAOS-2, MG63, HUVECs), a thiazolyl blue tetrazolium bromide (MTT) assay was performed to measure cell death after exposure of cells to the individual aquasome components (Hydroxyapatite, trehalose, BMP-2, VEGF) at different concentrations for 24h.

Each cell line was cultured in basal medium (Medium 200, HUVECs; DMEM/F12 Gibco®) supplemented with antibiotic supplement (Amphotericin B/Gentamycin) at 37°C in humidified air with 5% CO_2. Cells were trypsinised using 0.25% Trypsin/EDTA solution, centrifuged and passed into 96-well culture plates for the study. Cells were trypsinised, centrifuged and re-suspended in fresh media. Cells were counted and recorded for concentration per ml. Cell suspension was diluted with complete media to 75,000 to 100,000 cells per ml. 100µl of cells (7,500- 10,000 cells per ml) was added into each well and incubated overnight (37°C, 5% CO_2).

On day 2, after allowing cells to attach to the bottom of the wells, serum-free media was carefully removed. Cells were treated with 10, 20, 30, 40 and 50ng/ml BMP-2/VEGF121-spiked serum-free media (n=3), leaving a final volume of 100µl per well. After 24h, 20µl of 5 mg/ml MTT was aseptically added to each well. MTT reagent was also added to a set of wells without cells, acting as blank.

Plates were incubated for 3.5 h at 37°C, 5% CO_2 in an incubator. Wells were aspirated and 150µl of dimethyl sulphoxide (DMSO) was added per well. Well plates were covered with tinfoil and cells were agitated using an orbital shaker (300rpm) for 20mins. The absorbance readings of wells were then measured 590nm with a photometric scan between 540nm to 590nm to assay absorbance values at different wavelengths (Multiskan Spectrum- UV/Vis Microplate Spectrophotometer).

Cell viability was calculated using the formula below:

$$\text{Cell viability (\%)} = \frac{[\text{O.D OF TREATED WELL- OD OF BLANK}]}{[\text{OD OF UNTREATED WELL -OD OF BLANK}]} \times 100\%$$

5.2.6 In vitro BMP-2 release and bioactivity (ALP activity)

To establish the effect of BMP on MG63 differentiation, an ALP quantification assay was performed on MG63 cells exposed to BMP-containing media. ALP activity was analysed using the 1-step PNPP assay (ThermoFisher, UK). BMP-2 protein was quantified using a BMP development ELISA (Peprotech, USA).

For the co-culture experiments, media aliquots (1ml) were taken from the well chamber at the time points (days 2, 5, 7, 9, 12, 14, 16, 19 and 21) for MG63 cells and from the transwell inserts for HUVECs. Aquasomes were placed (in transwell inserts for MG63 cells and in the well chamber for HUVECs) and media aliquots were also taken from the well chamber for MG63 cells and from the transwell inserts for HUVECs to analyse the amount of ALP secreted. BMP released from aquasomes into media was analysed in a separate study. Media aliquots were taken at predetermined time intervals of 1, 3, 9, 13 and 21 days to analyse the amount of BMP-2 released. Aliquots were quantified for BMP-2.

To measure ALP activity (quantified by the production of PNPP product, 4-Nitrophenol), 100µl of the 1-Step PNPP was added to each well containing 100µl of sample (96 well plate). The solution in each well was mixed thoroughly by gently agitating the plate. Each plate was incubated at room temperature for 30 minutes or until sufficient colour developed. 50µL of 2N NaOH was then added to each well to stop the reaction. This solution was mixed thoroughly by agitating the plate. The absorbance of each well was measured at 405nm (Multiskan Spectrum- UV/Vis Microplate Spectrophotometer).

Absorbance values of blank wells and blank media were used to correct sample absorbance (ʎ) values. The principle of the reaction is illustrated in figure 5.4. The BMP ELISA protocol was followed as provided in the kit. 100µl of capture antibody was added to each ELISA plate

well (n=3), sealed and left to incubate overnight. Capture antibody was aspirated from wells and each plate was washed 4 times using 300 µl of wash buffer per well. Plates were blotted on paper towel to remove all liquid and 300 µl of block buffer was added to each well. Plates were incubated for at least 2h. Plates were further aspirated, washed 4 times and blotted on paper towel.

100 µl of the samples of each time point from the *in vitro* release study were added to wells (n=3). The plates were sealed and incubated for 2h. Plates were aspirated washed 4 times and blotted on paper towel. 100 µl of Avidin peroxidase was subsequently added to each well. Plates were incubated for 30mins at room temperature (25°C).

SigmaFast™ OPD was used as substrate. One OPD tablet (*o*-Phenylenediamine dihydrochloride) and one urea hydrogen peroxide tablet were dissolved in 20ml of distilled water. Care was taken to wrap solution in foil as solution is light-sensitive. 100µl of SigmaFast OPD solution was added to each well and monitored for colour development. Absorbance readings were monitored at 5min intervals for 50mins and OD was read at 405nm (Multiskan Spectrum- UV/Vis Microplate Spectrophotometer).

Figure 5.4 Principle of the PNPP assay

5.2.7 Statistical analysis

Statistical analysis was performed using GraphPad Prism software package. Data was analysed using a two-tailed paired t-test (significance level, $p<0.05$).

5.3 RESULTS AND DISCUSSION

The main objective of this study was to investigate the ability of BMP-2 and VEGF 121 loaded aquasomes to stimulate osteogenic activity when exposed to osteoprogenitor cells (MG63, osteoblast-like cell line) and mesenchymal stem cells (AT-MSCs). This was analysed primarily by ALP expression which is measured by 4-nitrophenol production.

5.3.1 In vitro release of BMP-2 and VEGF-121 from aquasomes

A release study of BMP-2- loaded aquasomes, fabricated with 50ng/ml and 100ng/ml BMP-2 solutions, was performed for the duration of 8h with samples taken at hourly time points. The *in vitro* cumulative release plots (figure 5.5A) show that release of BMP-2 from the aquasomes was dependent on BMP-2 loading. The amount of BMP-2 released ranged from 6-8.5 ng for the 50ng/ml BMP-2 loaded aquasomes and 15-51ng for the 100ng/ml BMP-2 loaded aquasomes. Percentage release (figure 5.5B) shows less than 5% release of BMP-2 after 8h in both cases demonstrating sustained release of BMP-2 from the aquasomes. The entrapment efficiency results of the BMP-2 showed 98.9% of BMP-2 adsorbed onto the aquasome formulation. That is, for every loading with 100ng/ml (in 10ml), 989.9ng is adsorbed and for every 50ng/ml (in 5ml), 245ng is adsorbed onto the aquasome formulation. Figure 5.5 C illustrates that the release of BMP-2 from aquasomes in media is similar to its release in PBS. This was investigated to compare the release of BMP-2 from aquasomes in PBS and in culture medium and identify if there was a reduction in BMP-2 quantified in culture media indicating degradation of BMP-2 by serum proteins. Figure 5.5C shows it can

be deduced that the serum proteins in cell culture may be degrading viable BMP-2 released from aquasomes as the amount of BMP-2 released in media is lower than BMP-2 released in PBS.

The role of VEGF in osteogenic differentiation and proliferation has been investigated and researched in the literature. Recently, the combined or sequential delivery of BMP-2 and VEGF to mesenchymal cells has resulted in enhanced osteoblast differentiation (Table 5.2). VEGF 121 was employed in this study to analyse the differentiation and proliferation effect of VEGF when exogenously administered to MG63 cells and AT-MSCs in culture medium or in aquasome formulation and compare the differentiation effect via the two modes of delivery.

Figure 5.6 illustrates the release of VEGF from aquasome formulations fabricated with 100ng/ml VEGF solutions with a similar entrapment efficiency of 98%. The profile shows a steady decline in VEGF release over the 8 h study. However, percentage release is similar to BMP-2 from the aquasomes which shows that less than 6% of VEGF has been released during the 8 h study, thus implying that VEGF-loaded aquasomes offer a prolonged release of the angiogenic factor.

These results demonstrate that the BMP-2 and VEGF 121 aquasome formulations can act as a delivery system for prolonged release of the growth factor which can elicit its osteogenic effect for a prolonged duration.

(A)

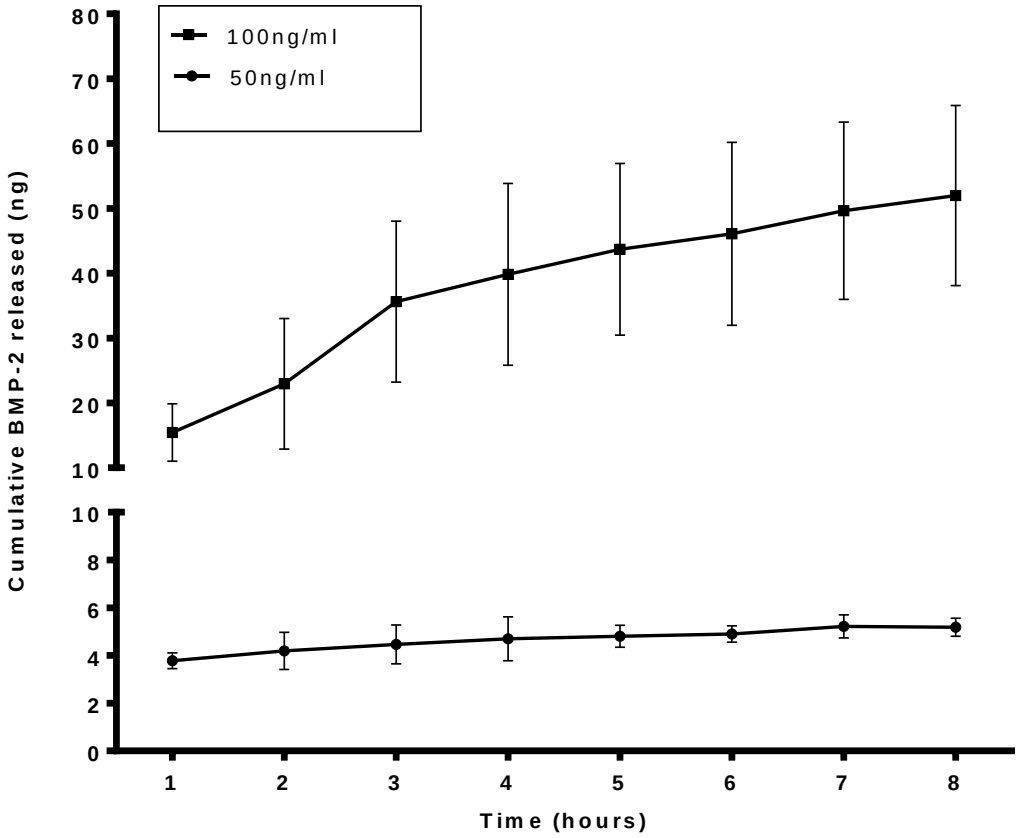
100ng/ml
50ng/ml
Cumulative BMP-2 released (ng)
80
70
60
50
40
30
20
10
10
8
6
4
2
0
1
2
3
4
5
6
7
8
Time (hours)

(B)

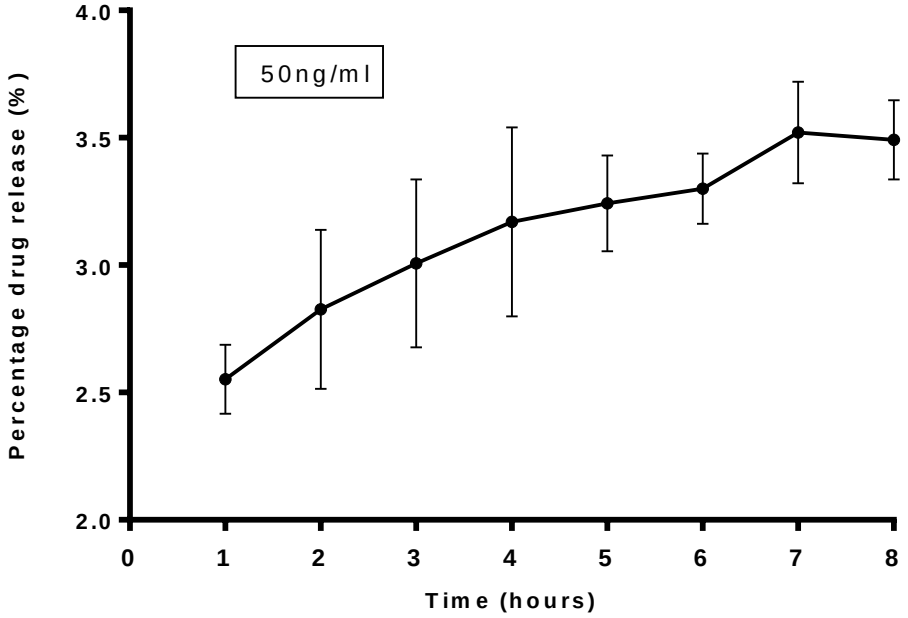
50ng/ml
Percentage drug release (%)
4.0
3.5
3.0
2.5
2.0
0
1
2
3
4
5
6
7
8
Time (hours)

(C)

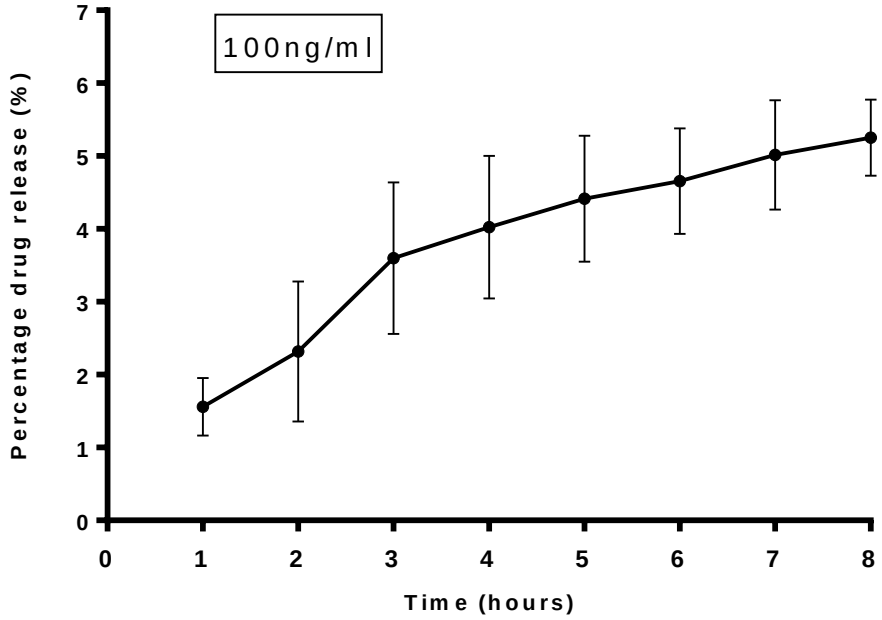

Figure 5.5 In vitro release of BMP-2 from BMP-2-loaded aquasomes.
(A) shows the cumulative release of BMP-2 from aquasomes (fabricated with 50ng/ml and 100ng/ml BMP-2 solutions) for the duration of 8h; (B) and (C) illustrate the percentage release of BMP-2 from the 50ng and 100ng aquasome formulations. Percentage release results show less than 5% release after 8h.

Table 5.5 BMP-2 release in media for the duration of 21 days

Time (days)	BMP released from aquasomes to media (ng)*
1	1.4933 ± 0.9451
3	1.6933 ± 0.9452
8	1.51 ± 1.3796
13	1.8933 ± 0.8083
21	1.26 ± 1.0392

** (n=3)*

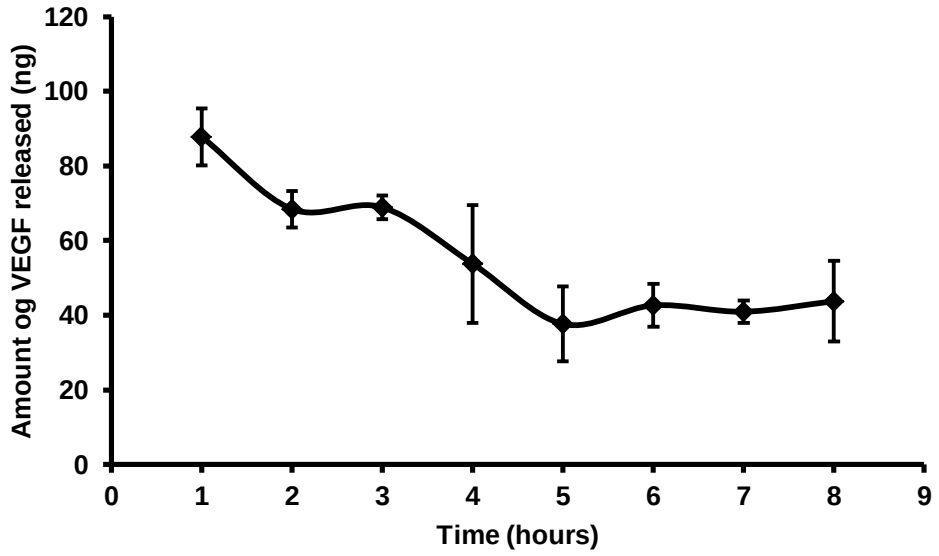

Figure 5.6 In vitro cumulative release of VEGF 121 from VEGF 121-loaded aquasomes. This graph shows the cumulative release of VEGF from aquasomes (fabricated with 100ng/ml VEGF solution) for the duration of 8h (n=3).

5.3.2 In vitro cell toxicology assay (Thiazolyl Blue Tetrazolium Bromide (MTT) assay)

A thiazolyl blue tetrazolium bromide (MTT) assay was performed to measure cell death after exposure of cells to the individual aquasome components (Hydroxyapatite, trehalose, BMP-2 and VEGF 121) at different concentrations for 24 h, representing short term exposure to aquasomes (acute toxicity). Figures 5.7, 5.8 and 5.9 illustrates the cell viabilities of SAOS-2 cells, MG63 cells and HUVECs after exposure to 0.2, 0.4, 0.6, 0.8, 1.0 and 2.0mg/ml of hydroxyapatite dispersed in culture medium; 0.00625, 0.0125, 0.025, 0.05, 0.1 and 0.2M of trehalose in culture media and 10, 20, 30, 40 and 50ng/ml of BMP-2 and VEGF 121 in culture media.

5.3.2.1 Effect of increasing hydroxyapatite concentration on proliferation of MG63, SAOS-2 and HUVECs

Figure 5.7 shows the percentage cell viabilities of SAOS-2 cells, MG63 cells and HUVECs after exposure to varying concentrations of hydroxyapatite dispersed in media (0.2, 0.4, 0.6, 0.8, 1.0 and 2.0mg/ml). The results represented in the graph demonstrates that the exposure of SAOS-2 cells and HUVECs increasing concentrations of hydroxyapatite after a short duration showed that they have no acute toxic effects on the cell lines. Rather, exposure of the cells to the varying concentrations of hydroxyapatite show a marked percentage increase in cell viability with demonstrates cell proliferation within the duration of 24 h. This same trend was observed with the MG63 cells although with slightly lower percentage cell viabilities. Hydroxyapatite is an osteoconductive material which supports the growth of

osteoblast like cells, owing to its similarities with natural apatite which is the inorganic component of bone. Its ionic dissociation in media can release Ca^{2+} and PO_4^{2-} which can promote osteoblast proliferation (Ramires et al, 2001).

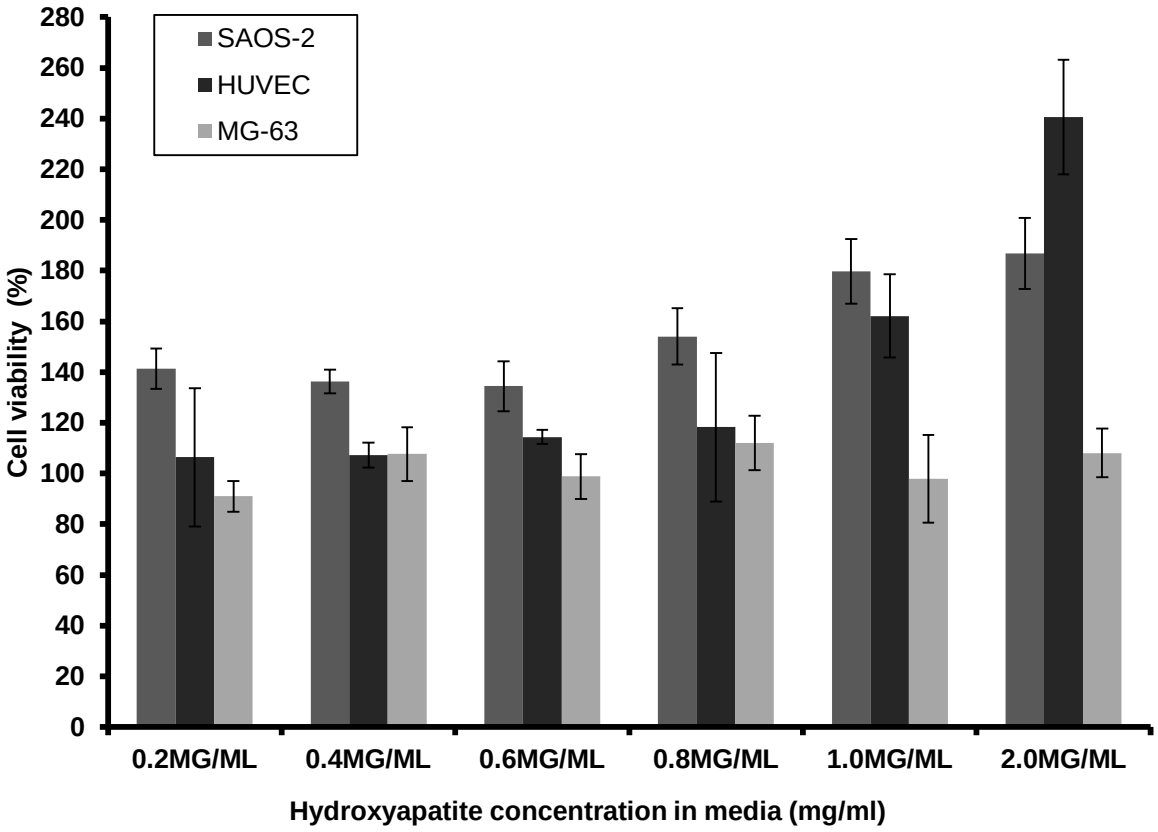

Figure 5.7 Cell viability of SAOS-2 cells, MG63 cells and HUVECs after exposure to varying concentrations of hydroxyapatite in media. MTT assay of SAOS-2 cells, MG63 cells and HUVECs after exposed to varying concentrations of hydroxyapatite (0.2, 0.4, 0.6, 0.8, 1.0 and 2.0mg/ml) after 24h. Results show that hydroxyapatite had no toxic effect on the cells but rather increased the viability of the cells over the period of 24h (n=24).

1.3.2.2 Effect of increasing trehalose concentration on proliferation of MG63, SAOS-2 and HUVECs

Figure 5.8 shows the percentage cell viabilities of SAOS-2 cells, MG63 cells and HUVECs after exposure to varying concentrations of trehalose (0.00625, 0.0125, 0.025, 0.05, 0.1 and 0.2M). The results represented in the Figure 5.8 demonstrates that the exposure of SAOS-2 cells and HUVECs to the increasing concentrations of trehalose after a short duration showed that they have no acute toxic effects on the cell lines. Rather, exposure of the cells to the varying concentrations of trehalose shows a marked percentage increase in cell viability which demonstrates cell proliferation within the duration of 24 h. However, there was an exception with the cells treated with 0.2M trehalose which showed a decline in percentage

cell viability of SAOS-2 and MG63 cells which illustrates an acute toxic effect on the cells. This decline was found to be statistically significant (p=0.0005). 0.2M trehalose is two times higher than the concentration of trehalose used in the fabrication of aquasomes in this study, which shows that the trehalose in the aquasome formulations have no toxic effect. In contrast, MG63 cells exhibited a different response to exposure to trehalose. Percentage cell viabilities ranged from 70-79% of the control group, with an exception of the cells exposed to 0.2M trehalose spiked media. Exposure of MG63 cells to 0.2M trehalose increased cell viabilities to 85.6% in comparison to the preceding trehalose concentration (0.1M, 70.4%), the reason behind the increase in percentage cell viability is inconclusive as research shows that trehalose at high concentrations is found to be non-toxic even at high concentrations (Benaroud, Lee and Goldberg, 2001; Jain and Roy, 2009).

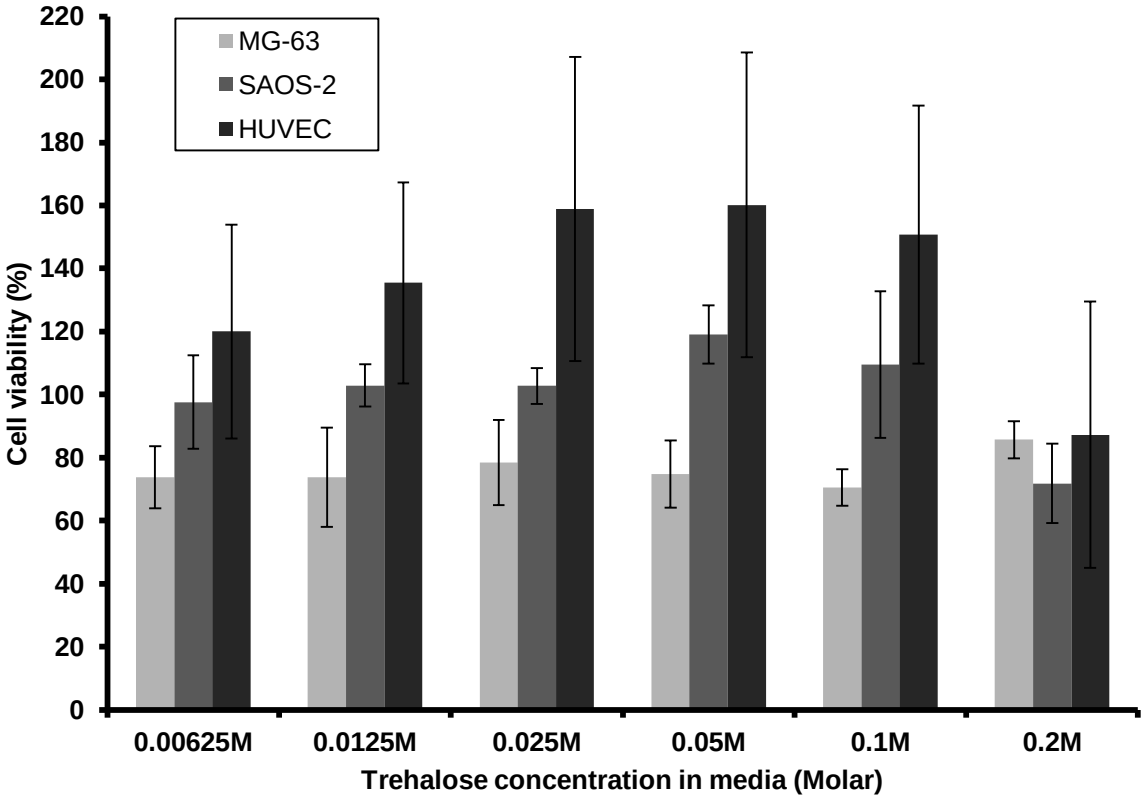

Figure 5.8 Cell viability of SAOS-2 cells, MG63 cells and HUVECs after exposure to varying concentrations of trehalose in media. MTT assay of SAOS-2 cells, MG63 cells and HUVECs after exposed to varying concentrations of trehalose (0.00625, 0.0125, 0.025, 0.05, 0.1 and 0.2M) after 24h. Results show that trehalose had no toxic effect on SAOS-2 and MG63 cells but rather cells proliferated over the period of 24h. MG63 cells experienced a decrease in percentage cell viability during the study (n=24).

5.3.2.3 Effect of increasing BMP-2 or VEGF 121 concentration on proliferation of MG63, SAOS-2 and HUVECs

Figure 5.9 A and B demonstrates that the exposure of SAOS-2 cells and HUVECs to high concentrations of BMP-2 and VEGF 121 for 24 h showed that they have no acute toxic effects on the cell lines. For SAOS-2 cells, MG63 cells and HUVECs, all concentrations of BMP-2 and VEGF 121 showed an increment in percentage cell viability after exposure to the varying concentrations of BMP-2 and VEGF-121 indicating cell proliferation in all instances.

Figures 5.9 A, B and C also illustrate a trend of increased cell viability which is directly proportional to increasing BMP-2 or VEGF 121 concentration. However, a noticeable decrease in percentage cell viability is observed with cells that are exposed to 50ng/ml BMP-2 or VEGF 121. This may suggest that prolonged exposure to high BMP-2 and VEGF 121 concentrations above 50ng/ml (in spiked media) may cause a decline in cell viability. This was observed in co-culture studies (see section 5.3.3) when SAOS-2 cells, MG63 cells and HUVECs were exposed to 100ng/ml BMP-2/VEGF 121 spiked media. After about 10 days of a 21-day study, all cells exposed to 100ng/ml BMP-2/VEGF 121 spiked media died off while cells exposed to 50ng/ml BMP-2/VEGF 121 spiked media were still thriving and proliferating (results not shown).

Figure 5.9 C shows that exposure of MG63 cells to 10ng/ml BMP-2 or VEGF 121 shows a decrease in cell viability (76.4%). The same trend observed with SAOS-2 cells and HUVECs (Figure 5.9 A and B) was also seen with MG63 cells where there was an increase in cell viability which was directly proportional to increasing BMP-2 or VEGF 121 concentration in spiked media. However, a noticeable decrease in percentage cell viability is observed when the cells are exposed to 50ng/ml BMP-2 or VEGF 121 spiked media which indicates that further exposure to concentrations of BMP-2 or VEGF 121 higher than 50ng/ml would result in a decline in percentage cell viability as highlighted above. Despite the observations made, the differences in percentage cell viabilities for all cell lines exposed to varying concentrations of BMP-2 were found to be insignificant ($p=0.3605$). In contrast, the differences in percentage cell viabilities for all cell lines as a result of exposure to various VEGF 121 concentrations were found to be significant ($p<0.0001$). Also, the differences in percentage cell viabilities between the different cell lines for both cases of exposure to BMP-2 and VEGF 121 were found to be significant ($p<0.0001$).

Figure 5.9 B and C also highlight an obvious difference in the percentage cell viabilities of MG63 cells and HUVECs when exposed to BMP-2 in comparison to the cell viabilities when exposed to VEGF 121. Exposure to the varying concentrations of VEGF 121 showed higher percentage cell viabilities in HUVECs and MG63 cells. VEGF-121 is a major angiogenic factor which induces the proliferation of HUVECs and subsequently the formation of

vasculature. It also induces the proliferation of osteoblasts and pre-osteoblasts. In comparison, BMP-2 exerts a stronger differentiation effect (tube formation) on HUVECs and exhibits a lesser proliferation effect on HUVECs (Finkenzeller, Hager, and Stark, 2012). BMP-2 induces the proliferation and differentiation of MG63 cells *in vivo*, which is not immediate but usually occurs after day 4 (see Figure 5.2). Although, a more rapid response can be observed in osteoprogenitor cells when exposed to higher doses as seen in Figure 5.9 C.).

The increase in proliferation of SAOS-2 cells and HUVECs in response to exposure to BMP-2 or VEGF 121 can be linked to the fact that SAOS-2 cells and HUVECs both secrete BMP and VEGF, which proliferate cells as well as other cell types when in co-culture (Deckers et al, 2002). Therefore, exposure to increased concentrations of exogenous added BMP-2 or VEGF 121 causes an increase in cell proliferation (Unger et al, 2007; Devescovi et al, 2008).

(A)

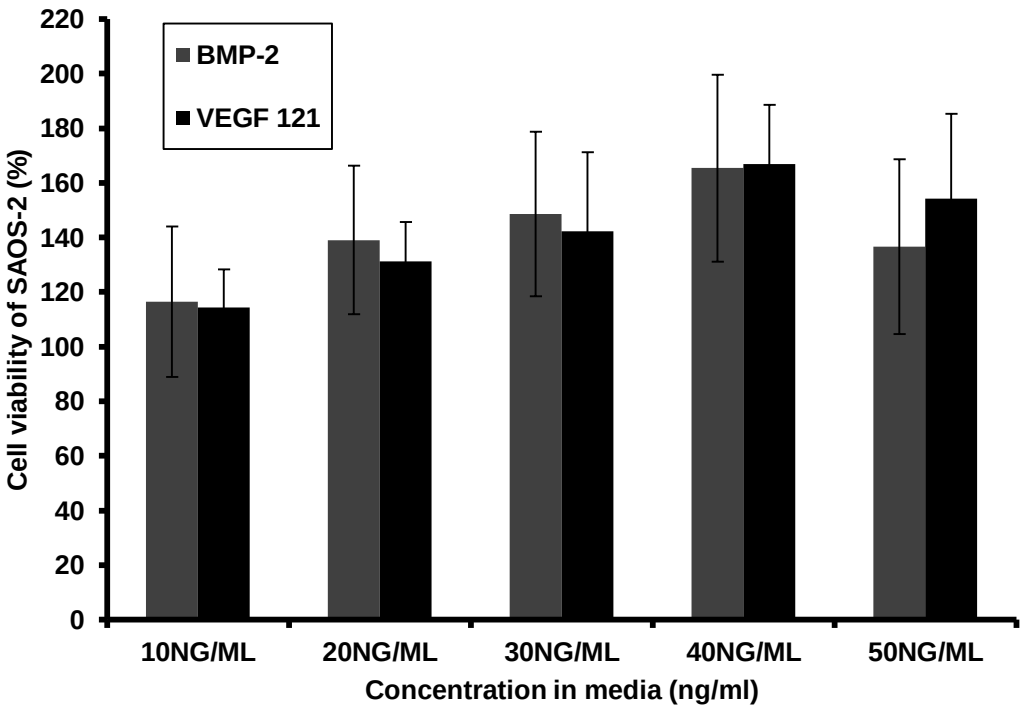

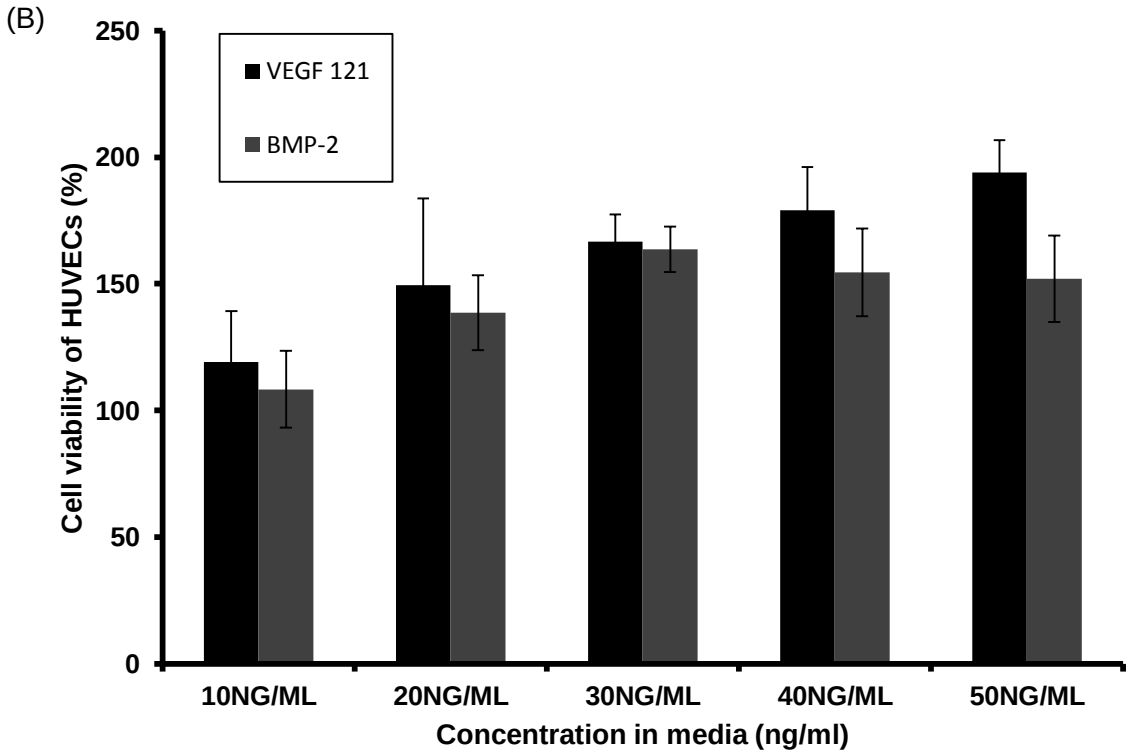

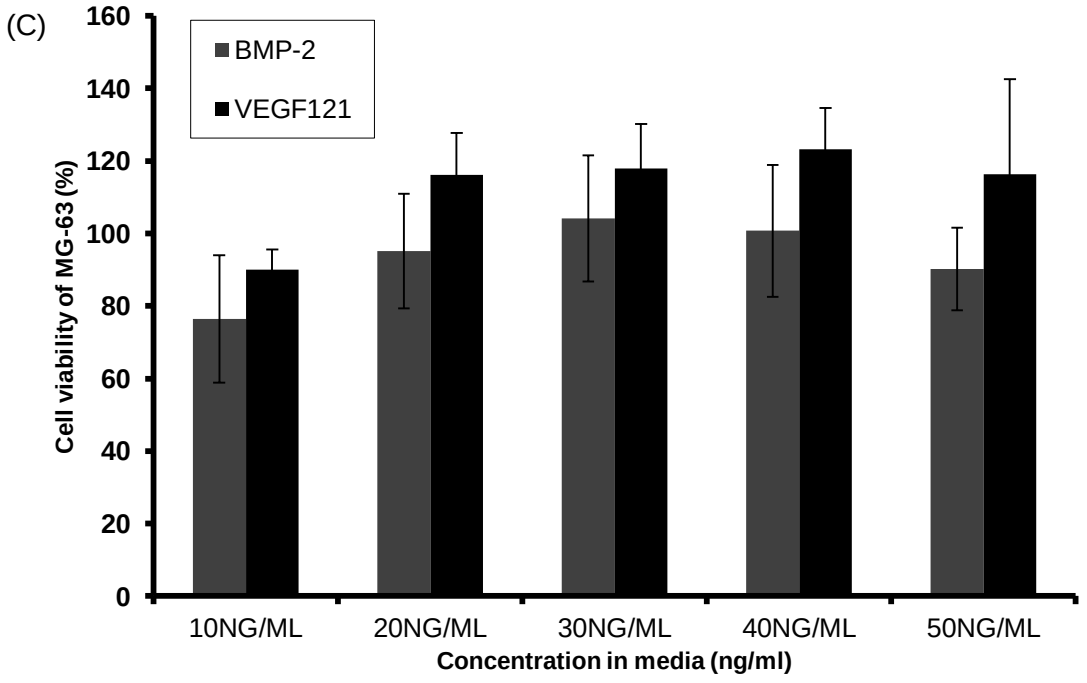

Figure 5.9 Cell viability of SAOS-2 cells, MG63 cells and HUVECs after exposure to varying concentrations of BMP-2 and VEGF 121 in media. MTT assay of (A) SAOS-2 cells, (B) HUVECs and (C) MG63 cells after exposure to varying concentrations of BMP-2 and VEGF 121 (10, 20, 30, 40 and 50ng/ml) after 24h. Results show that BSA had no toxic effect on the cells but rather increased the viability of the cells over the period of 24h (n=24).

5.3.3 Osteogenic potential of BMP-2 loaded aquasomes and its comparable effect with 50ng/ml BMP-2 spiked media on osteoblast cells

Figure 5.10 illustrates the amount of *p*-nitrophenol produced by the activity of secreted alkaline phosphatase (ALP) for a 21-day study. Alkaline is an ectozyme which is produced by bone cells and is an established biochemical marker of bone cell metabolism. ALP is an early to late osteogenic differentiation marker which indicates the progression and success of osteogenesis in tissue engineering. It is expressed in mesenchymal stem cells which committedly differentiate into osteoblasts as well as in osteoblastic cells as part of their normal metabolism. ALP as plays a major role in the mineralisation of bone (Golub et al, 2007; Birmingham et al, 2012). Bone-specific ALP is produced in extremely high amounts during the bone cycle's formation phase and is therefore an excellent universal indicator of bone formation activity (Christenson, 1997).

MG63 cells were cultured with BMP-2 aquasomes (MG63/BMP AQUA) and 50ng/ml spiked media respectively (MG63/BMP 50). The results in Figure 5.9 show that the amount of ALP expression from MG63 cells cultured with BMP-2 loaded aquasomes was higher than those cultured with 50ng/ml BMP spiked media with exceptions on days 9 and 14. The differences in 4-nitrophenol production between MG63/BMP AQUA and MG63/BMP 50 was found to be statistically insignificant ($p= 0.1886$). The sustained release of BMP-2 from the aquasomes and the Ca^{2+} and PO_4^{2-} ions from the gradual dissolution of hydroxyapatite may have created an osteoinductive and osteoconductive environment for the cells, which have promoted the production of ALP, especially in the later stages of the study. 50ng/ml BMP spiked media induced higher ALP expression (measured by 4-nitrophenol production) on days 9 and 14 which can be attributed to the higher availability of BMP-2 in the 50ng/ml spiked media in comparison to the lower amounts of BMP-2 constantly released from aquasomes.

In comparison to the MG63 blank group, both MG63/BMP AQUA (MG63 exposed to BMP-loaded aquasomes) and MG63/BMP 50 groups (MG63 exposed to 50ng/ml BMP-spiked media) produced more 4-nitrophenol than the MG63 blank with the exception of day 12 in which the reasons are inconclusive. The difference in 4-nitrophenol production between the MG63/BMP AQUA group and MG63 blank were found to be statistically significant ($p< 0.10$). However, the difference in 4-nitrophenol production between the MG63/BMP 50 group and MG63 blank were found to be statistically insignificant ($p=0.2813$). From the results graphically represented in Figure 5.10, it was deduced that the loading of the BMP-2 loaded aquasomes needed to be increased to enhance osteogenic differentiation. With a sustained delivery of BMP-2 from these aquasomes, higher ALP expression which infers successful osteogenic differentiation is expected.

Numerous studies have been published demonstrating the use of scaffolds, bone cements or carriers made of biodegradable material designed with BMP adsorbed onto or incorporated into them to allow local controlled release of BMP over a period of time (Kenley et al, 1994; Kempen et al, 2008; Patel et al, 2008; Fei et al, 2008).

A study by Sasche and co-workers (2005) reported the successful osseointegration of metal implants using non-glycosylated BMP-2 in female sheep. BMP-2-coated implants initiated significant new bone formation, initially in trabecular arrangements and were replaced by cortical-like bone after 20 weeks. The new bone was oriented towards the cylindrical implant. This animal model provided first evidence that application of non-glycosylated BMP-2 coated on solid implants may foster bone healing and regeneration even in aged-compromised individuals. The present study shows that BMP-2 loaded aquasomes induce osteoblast like cell differentiation, which shows successful osteogenesis. Results from Sasche et al (2005) illustrate the success of BMP-2 coated implants in the osseointegration of metal implants which imply the proliferation of osteoblasts aid in the integration of the metal implants into the bone structure.

Patel and co-workers (2008) conducted both *in vitro* and i*n vivo* studies to analyse the release of BMP-2 (radiolabelled) from gelatin microparticles embedded in a collagen scaffold. The effect of gelatin cross-linking, BMP-2 dose, and release medium on BMP-2 release kinetics was investigated. Results showed that release of BMP-2 could be systematically controlled from gelatin microparticles by altering the extent of gelatin crosslinking. It was also observed that higher doses of BMP-2 loaded in the gelatin microparticles resulted in decreased release from the gelatin microparticles. It was hypothesised that presumably, the ratio of free vs. bound growth factor is similar for both amounts, and therefore the effect on BMP-2 release was minimal for the investigated doses (Patel et al, 2008). These results show correlation with the present study as the aquasome formulation controls the release of BMP-2 available for the cells. The doses of BMP-2 released from aquasomes show minimal effect, however the effect is statistically significant in comparison to controls. An increase in BMP-loading of aquasomes may increase effect and will need to be explored.

Kempen and co-workers (2008) also conducted both *in vitro* and *in vivo* studies to analyse the bioactivity of BMP released from sustained delivery vehicles over a period of time. BMP-2 was incorporated into a gelatin hydrogel, PLGA microspheres embedded in a gelatin hydrogel, microspheres embedded in a poly (propylene fumarate) (PPF) scaffold and microspheres embedded in a PPF scaffold surrounded by a gelatin hydrogel. The release and bioactivity of BMP-2 were tested weekly over a period of 12 weeks in pre-osteoblast

W20-17 cell line culture and in a rat subcutaneous implantation model. Parameters measured were alkaline phosphatase induction and bone formation respectively.

The bioactivity of BMP-2 released from composites was much higher than similar concentrations of BMP-2 added directly to control cultures (Kempen et al, 2008). This illustrated that BMP-2 can be subject to degradation/ inactivation by molecules such as serum proteins in culture medium. The rate of BMP-2 release *in vivo* was found to be profoundly higher than *in vitro*. This is hypothesised to be attributed to the cellular enzymatic degradation of the composite or implant polymer made possible by the more protein-rich environment *in vivo*. The results show that the bioactivity of BMP-2 is retained when incorporated into composites prolonged sustained delivery (Kempen et al, 2008). This outcome is in agreement with the present study in which the BMP-2 released from aquasomes elicited higher ALP expression in comparison to 50ng/ml BMP-2 spiked media, which may have been degraded or inactivated by serum proteins in culture medium.

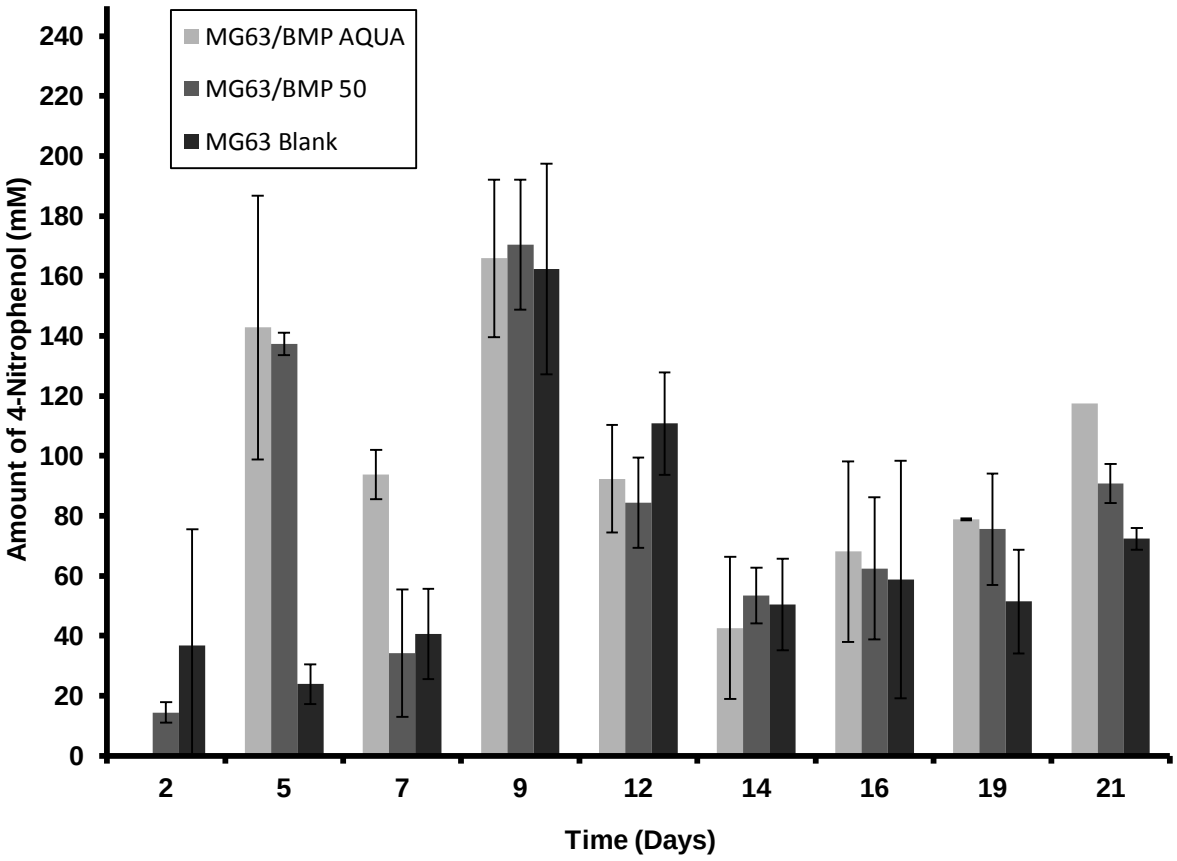

Figure 5.10 Comparison of the groups MG63/BMP AQUA, MG63/BMP50 and MG63 Blank to analyse the amount of ALP produced measured by 4-Nitrophenol production. The graph illustrates that the MG63/BMP AQUA had a higher rate of 4-Nitrophenol production for the 21-day study than the MG63/BMP50 group with the exception of days 9 and 14, illustrating the differentiation effect of BMP-2 released from BMP-2 loaded aquasomes when co-cultured with osteoblast-like cells, MG63. These results were compared to 4-Nitrophenol production of MG63 monocultures (MG63 Blank) (n=3).

5.3.4 Osteogenic potential of VEGF on MG63 cells and its comparable effect with MG63 co-cultured with HUVECs

VEGF, an angiogenic factor, is also involved in osteogenesis and bone repair by stimulating survival, recruitment and migration of major bone forming cells (Bai et al, 2013). Exogenous administration of VEGF is known to enhance osteoblastic differentiation and proliferation in tissue engineering (Kanczler et al, 2010; Ramazanoglu et al, 2013).

Figure 5.11 illustrates the amount of *p*-nitrophenol produced by the activity of secreted alkaline phosphatase (ALP) when MG63 was co-cultured with HUVECs (MG63/HUVECs) and MG63 in mono-culture with 50ng/ml VEGF 121 (MG63/BMP50) for a 21-day study. MG63/HUVECs exhibited higher ALP expression by having the higher 4-Nitrophenol production when compared with MG62/VEGF 50 monoculture. The difference in 4-nitrophenol production between the two groups were found to be statistically significant ($p<0.05$). It is well established in the literature that endothelial cells enhance osteoprogenitor/osteoblast cell growth when in co-culture. It has also been reported that the expression of early differentiation markers such as ALP is enhanced from osteoblast-like cells (MG63 cells) and mesenchymal cells of bone origin when in the presence of ECs (HUVECs) (Xue et al, 2005; Kaigler et al, 2005). In a similar co-culture study by Zhang and colleagues (2010[a]), MG63 cells proliferated in the presence of HUVECs, which showed higher cell numbers on titanium surfaces after 72h, in comparison to single cultures.

MG63 cells were co-cultured with SAOS-2 cells to examine if there will be an increase in ALP production in comparison to MG63 monocultures (MG63 Blank) and MG63 co-cultured with 50ng/ml BMP-2 spiked medium (MG63/BMP 50). SAOS-2 cells are well- characterised osteosarcoma cells, which are commonly used as an osteoblastic cell model. When MG63 cells were co-cultured with SAOS-2 cells (MG63/SAOS-2), the results were comparable to MG63/BMP 50 but were higher than the control (MG63 Blank). However, the differences in 4-nitrophenol between the two groups were found to be statistically insignificant at $p<0.05$ ($p=0.4168$, results not shown). In comparison, ALP production by MG63 co-cultured with 50ng/ml of VEGF-121 (MG63/VEGF 50) was higher than in the MG63/BMP50 group (Figure 5.10 and 5.11). VEGF is an angiogenic marker, which has been noted in literature to stimulate osteogenesis evidenced by increased ALP production (Deckers et al, 2002).

In a study by Zhang et al (2010[a]), expression levels of ALP in MG63 cells were stimulated in the presence of HUVECs and were found to be 2 times higher ($P < 0.01$) than in MG63 monocultures. This observation agrees with the previous assumption that osteoblasts stimulate the proliferation of endothelial cells (HUVECs) by producing VEGF, and that the stimulated ECs reciprocally enhance the proliferation of osteoblasts in co-culture (Zhang et

al, 2010[a], Zhang et al, 2010[b]). This was also observed in a study by Hoffmann et al (2008) where HUVECs in monoculture did not survive long term co-culture studies but thrived and proliferated when co-cultured with human osteoblasts which demonstrated that human osteoblasts support the survival and proliferation of endothelial cells (HUVECs). VEGF acts directly on osteoblasts increasing chemotaxis, proliferation and differentiation (Carano and Filvaroff, 2003). Several *in vitro* studies have already established that there is a reciprocal regulation between osteoblast-like cells and endothelial cells and VEGF acts as the main signalling between these cells (Kyriakidou et al, 2008).

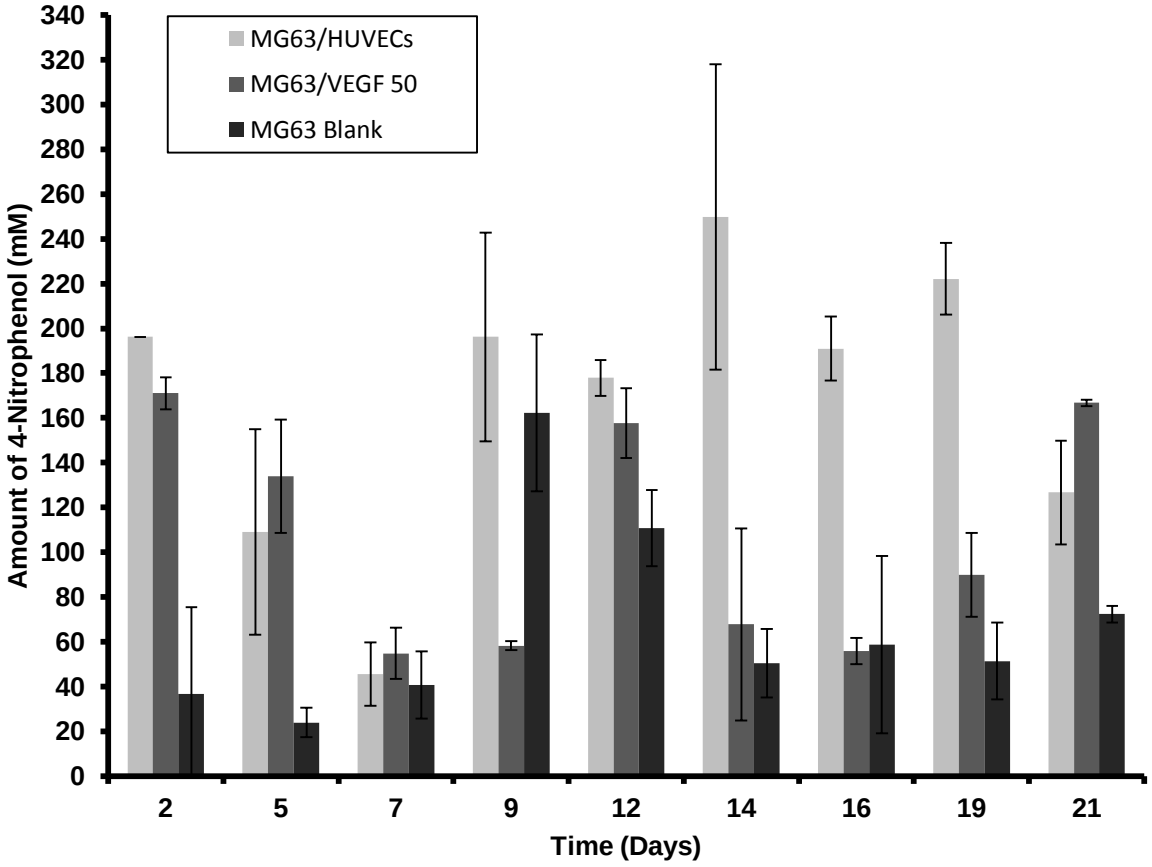

Figure 5.11 Comparison of the groups MG63/HUVECs, MG63/VEGF 50 and MG63 blank to analyse the amount of ALP produced measured by 4-Nitrophenol production. The graph illustrates that the MG63/HUVECs has a higher rate of 4-Nitrophenol production for 19 days in the 21-day study illustrating the proliferation effect of HUVECs when co-cultured with osteoblast-like cells, MG63 (n=3).

In figure 5.12, the graph illustrates the proliferation count of MG63 co-cultured with HUVECs or cultured in the presence of BMP-2/VEGF 121/BMP-loaded aquasomes to illustrate differentiation and/or proliferation effect in comparison with the control group (MG63 Blank). These results correlate with 4-nitrophenol produced by ALP secreted from the cell types MG63. A significant number of HUVECs did not survive the long-term culture period in a

monoculture and thus results are not shown. Such results were observed in similar studies (Unger et al, 2007; Hoffmann et al, 2008). The co-culture of endothelial cells with osteoblast-like cells MG63 and SAOS-2 increased the cell numbers of these cell types. These results correspond with the results in the literature which validate the proliferation effect of endothelial cells on osteoblastic cells (Kyriakidou et al, 2008, Zhang et al, 2010[b]).

The cell count of MG63 cells from the experimental groups MG63/BMP 50, MG63/VEGF 50 and MG63/BMP AQUA yielded higher results in comparison to MG63 blank (control). However, this graph illustrates an increase in the cell count of MG63 cells when exposed to BMP-2 aquasomes (MG63/BMP AQUA) in comparison to exposure to 50ng/ml VEGF spiked medium. This can be attributed to the presence of exogenous calcium from the hydroxyapatite nanocores in the aquasome formulation. Calcium present in the aquasome formulation offers osteoconductivity to the cells and aids in an increment in proliferation. Although BMP-2 released from the aquasomes was controlled yielding approximately less than 5% at each time point (Figure 5.5B), the concerted effect of BMP-2 and calcium in the aquasome formulation increased proliferation of MG63 cells and was comparable to the proliferation effect of exogenously added 50ng/ml BMP (Doostmohammadi et al, 2012; Rouahi et al 2006; Ramazanoglu et al, 2013). The differences in the cell numbers between MG63/BMP AQUA and MG63 Blank or MG63/VEGF 50 and MG63/BMP AQUA were however where found to be statistically insignificant ($p<0.10$). In contrast, the differences in cell number between MG63/HUVECs and MG63/BMPAQUA were statistically significant ($p<0.10$).

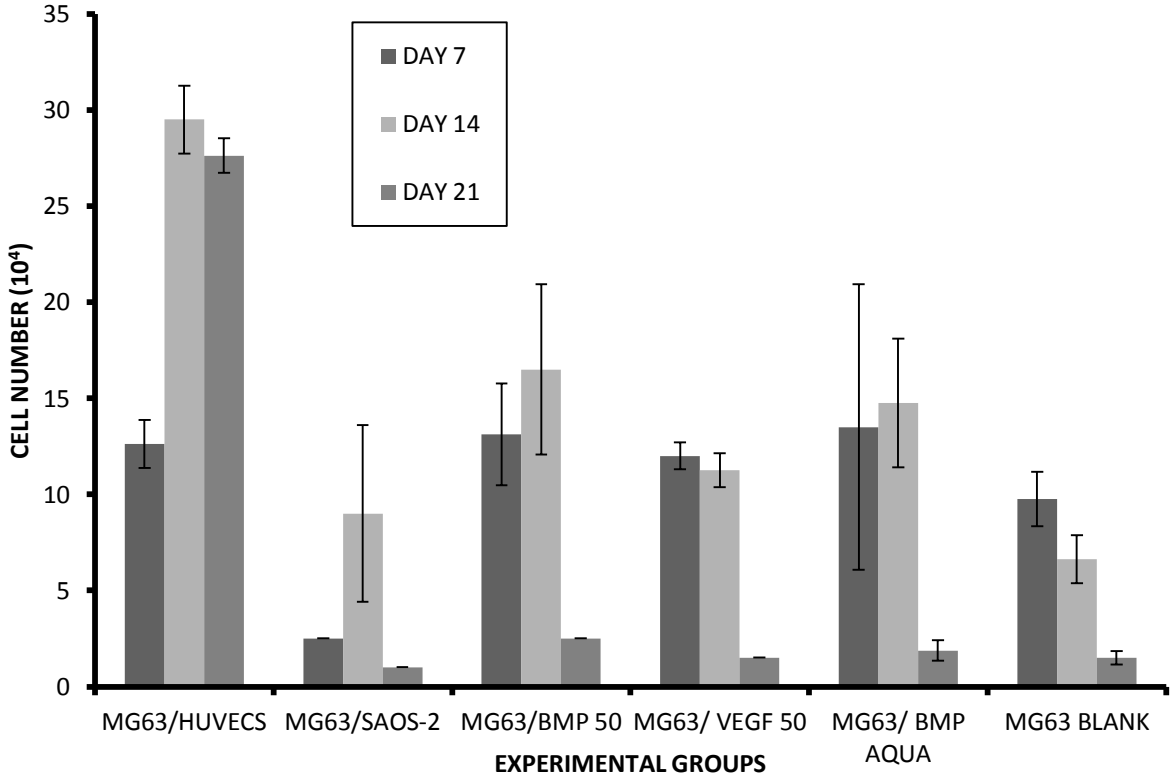

Figure 5.12 Proliferation counts of MG63 and SAOS-2 cells co-cultured with HUVECs or cultured in the presence of BMP-2/VEGF 121/BMP-loaded aquasomes. This graph illustrates the differentiation and/or proliferation effect of BMP-2 /VEGF on MG63 cells in comparison with the control group (MG63 BLANK) (n=3).

5.3.5 Adipose Tissue-Derived Mesenchymal Stem Cells (AT-MSC) differentiation study

AT-MSCs are isolated from the human adipose tissue and purified through several processes for selecting multi-potent MSCs-like cells. Adipose-derived MSCs (AT-MSCs) have attracted much interest as an alternative to BM-MSCs (bone marrow-derived mesenchymal stem cells). It has been reported that AT-MSCs are comparable to BM-MSCs with respect to the multi-lineage potential, growth kinetics, and cells senescence (Yoon et al, 2011). Adipose tissue-derived mesenchymal stem cells (ATMSCs) obtained from lipo-aspirates have been shown to have the multi-lineage potential to differentiate into adipogenic, chondrogenic, myogenic and osteogenic cells (Gun-Il Im et al, 2005; Keibl et al 2011).

AT-MSCs were used in this study to investigate the osteogenic differentiation and proliferation effect of BMP-2 and VEGF-121 released from aquasomes in mesenchymal stem cells in comparison to exogenously administered spiked media. AT-MSCs were exposed to

different concentrations of BMP-2 and VEGF 121; BMP-2 aquasomes, VEGF aquasomes and a physical combination of both aquasome formulations to investigate the differentiation effect of each exogenous administration. Figure 5.12 illustrates the differentiation of AT-MSCs after these treatments, measured by ALP expression (4-nitrophenol production). AT-MSCs exposed to osteogenic differentiation medium (Blank with O.M) were used as a positive control to compare the differentiation of AT-MSCs exposed to exogenous treatments. The differentiation of ATMSCs using osteogenic medium is well established and successfully differentiates mesenchymal stem cells into the osteoblastic lineage (Gun-Il Im et al, 2005, Bai et al, 2013).

Also, the treatment of AT-MSCs with 50ng/ml BMP yielded higher ALP activity in comparison to 25ng/ml BMP. However, the difference in ALP activity between AT-MSCs treated with 25ng/ml BMP and 50ng/ml BMP did not translate to a direct proportionality of 2 times more 4-nitrophenol production and this difference in 4-nitrophenol production between the groups were found to be statistically insignificant ($p=0.4411$). This may also demonstrate that an increase in exogenously administered BMP-2 may not necessarily translate in higher ALP activity but rather a controlled release of the growth factor over a prolonged period of time. For BMP (BMP-2) to elicit a therapeutic effect, it must be retained at the site of injury for a sufficient period, to allow the migration of pluripotent and osteoprogenitor cells, their proliferation and differentiation to promote the formation of bone. Appropriate carrier systems are required to promote local delivery of BMP to the site of injury and provide a sustained release profile over a long period of time (Jeon et al, 2008; Kempen et al, 2008; Luca et al, 2009). This is in agreement with a study by Patel et al (2008) which concluded that the dose effects of BMP-2 released from gelatin microparticles were minimal but rather a systematic release of BMP-2 from the gelatin microparticles yielded better results (Patel et al, 2008).

Also, the treatment of AT-MSCs with 25ng/ml VEGF yielded higher ALP activity in comparison to 50ng/ml VEGF. However, the difference in ALP activity between AT-MSCs treated with 25ng/ml BMP and 50ng/ml BMP did not translate to a direct proportionality of 2 times more 4-nitrophenol production. In constrast to difference observed between the two groups were found to be statistically significant ($p=0.0032$). This may also demonstrate that an increase in exogenously administered VEGF-121 may not necessarily translate in higher ALP activity but rather a controlled release of the growth factor over a prolonged period of time. Comparing the 4-nitrophenol production of ATMSCs exposed to 50BMP and 50VEGF, the differences were found to be statistically insignificant ($p=0.4302$) while the differences in 4-nitrophenol production of ATMSCs exposed to 25BMP and 25VEGF were found to be statistically significant ($p=0.116$).

The results show that the BMP-2 loaded aquasomes had the lowest amount of 4-nitrophenol produced in comparison to the other treatment groups. In comparison, VEGF 121 loaded – aquasomes exhibited higher 4-nitrophenol production. The differences between the 4-nitrophenol production of AT-MSCs exposed to BMP AQUA and VEGF AQUA were statistically significant ($p<0.0001$). Interestingly, the dual delivery of combined VEGF-121 and BMP-2 loaded aquasomes did not yield a higher ALP expression as expected. The differences in 4-nitrophenol production between the groups exposed to BMP/VEGF AQUA and BMP AQUA; and BMP/VEGF AQUA and VEGF AQUA were statistically significant ($p=0.0030$ and $p<0.0001$ respectively). This agrees with Patel et al (2008), Kempen et al (2009) and Kanzcler et al (2010) which investigated the sequential/dual delivery of VEGF and BMP-2 which yielded enhanced bone regeneration as opposed to a combined dual delivery of the growth factors. From literature, it has been observed that the step–wise exogenous treatment of mesenchymal stem cells with VEGF and BMP-2 yield higher success rate of osteogenic differentiation. This can be attributed to the sequential way angiogenesis and osteogenesis take place *in vivo.* Angiogenesis usually precedes osteogenesis for the establishment of vascularisation via the expression of angiogenic growth factors while osteogenic growth factors are constantly expressed during bone formation and remodelling. In Kempen et al (2009), although the VEGF/BMP- 2 combinations resulted in an additive effect on bone formation, this was less pronounced compared to the application of combinations of growth factor expressing cells. This difference could be the result of dose-related effects which can occur when using BMP-expressing cells.

In addition, VEGF 121 is a potent angiogenic factor which plays an important role in protecting cells. The release of VEGF from aquasomes as well as VEGF exogenously added to culture medium may have acted to keep the AT-MSCs viable sufficiently to enable differentiation and proliferation. This can subsequently lead to even higher local endogenous dosages of the osteoinductive growth factors. These results correspond to the results of the present study which showed that the co-culture of HUVECs with MG63 cells yielded higher ALP expression (Kanczler et al, 2010; Bai et al, 2013).

Comparing the 4-nitrophenol production of AT-MSCs exposed to BMP AQUA and 50BMP; and BMP AQUA and 25BMP, the differences were found to be statistically significant ($p<0.0001$; $p=0.0002$ respectively), demonstrating that BMP-2 induced ALP expression from exogenously administered 50ng/ml BMP-2 spiked media had a more pronounced effect than BMP-2 released from aquasomes. This can also be attributed to the minute amounts of BMP-2 released from aquasomes (less than 5%) available for BMP-2 induced osteogenic differentiation of AT-MSCs in comparison to the higher amounts of BMP-2 available in the BMP-2 spiked media.

Using the AT-MSCs cultured in osteogenic medium (Blank with O.M group) as a positive control, Figure 5.12 reveals a marked difference in 4-nitrophenol production in comparison to BMP AQUA, VEGF AQUA or BMP/VEGF AQUA groups. These differences in the 4-nitrophenol production were statistically significant in all comparisons ($p<0.0001$) which indicate that the ATMSCs successfully differentiated into the osteoblastic lineage cells when cultured in osteogenic medium (O.M). According to Christenson (1997), ALP is produced in extremely high amounts during the bone cycle's formation phase and is therefore an excellent universal indicator of bone formation activity. These results re-iterate that release of BMP-2 from aquasomes were in small amounts to have a pronounced differentiation effect. However, further investigations are required to increase optimal amounts of BMP-2 released from aquasomes to completely induce AT-MSC osteogenic differentiation.

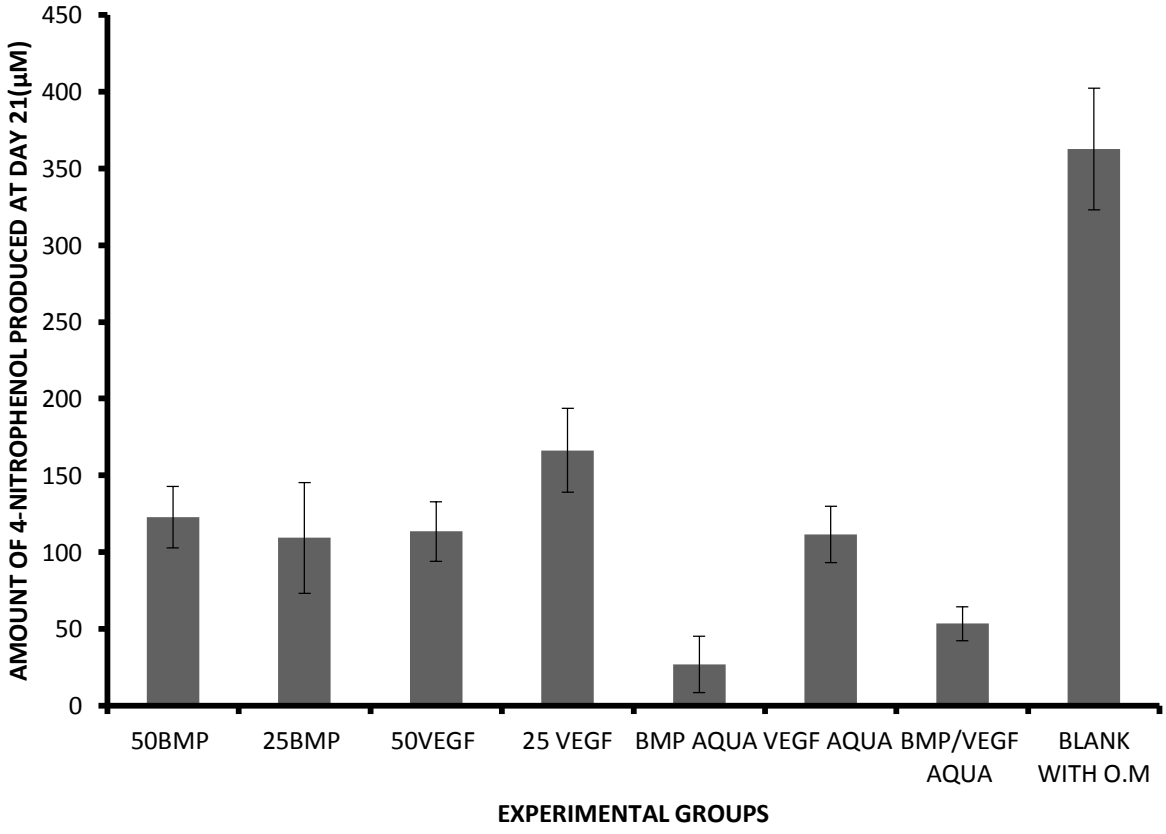

Figure 5.13 Study of AT-MSCs differentiation when exposed to different exogenous treatments. AT-MSCs were cultured with 50ng/ml and 25ng/ml BMP-2 (AT-MSCs BMP50, AT-MSCs BMP25), 50ng/ml and 25ng/ml VEGF 121 (AT-MSCs VEGF50, AT-MSCs VEGF25), BMP-2 and VEGF 121-loaded aquasomes (fabricated with 100ng/ml solutions; AT-MSCs BMP AQUA, AT-MSCs VEGF AQUA) and BMP-2 and VEGF 121 loaded aquasomes physically combined (AT-MSCs BMP/VEGF AQUA) (n=3).

5.4 CONCLUSION

These various studies show the potential use of BMP-2 -loaded aquasomes and VEGF 121-loaded aquasomes in bone regeneration. Combining the osteoconductive and osteoinductive properties of the components, synthetic hydroxyapatite and BMP/VEGF with a polyhydroxyl oligomer (trehalose), the delivery system proves to be a controlled release system for growth factors. The different loading doses of BMP-2 on aquasomes show that the release of BMP-2 or VEGF 121 from aquasome formulations is dose dependent. However, low percentages of release for the study period were observed which infer that BMP-2 and VEGF- 121 loaded aquasomes act as sustained and prolonged nanocarrier delivery systems. BMP-2 and VEGF-121 released from aquasomes induced ALP expression in MG63 cells which demonstrates its ability to stimulate osteoblast proliferation and differentiation. Its differentiation effects on AT-MSCs were not pronounced in comparison to positive control (AT-MSCs in osteogenic medium). In comparison, co-culture studies of HUVECs with MG63 cells demonstrated higher ALP expression compared to exogenous treatments with BMP-2/VEGF 121. VEGF exogenously administered in culture media was proven to have a protective effect on MG63 cells and AT-MSCs resulting in higher ALP production in most instances. However, further studies are required to optimise the amount and ratio of the release of BMP-2 and VEGF 121 and also compare the bioactivity of BMP-2 and VEGF 121 released from aquasomes in comparison to free rhBMP-2 and rhVEGF121 in media.

CHAPTER 6
GENERAL DISCUSSION

Aquasomes are nanoparticulate carrier systems with three-layered self-assembled structures. They consist of a central solid nano-crystalline (ceramic) core coated with polyhydroxy oligomers onto which biochemically active molecules are adsorbed. The solid ceramic core provides the structural stability, while the polyhydroxy oligomer coating protects against dehydration and stabilizes the biochemically active molecules. This major characteristic of maintaining the conformational integrity of bioactive molecules has made aquasomes to be generally described as a carrier system for delivery of peptide/protein-based pharmaceuticals.

To optimise the aquasome formulation and increase the drug/protein-loading capacity of aquasomes, a decrease in nanocore size for an optimal aquasome formulation was investigated in this thesis. The aquasome formulation used in preliminary studies in the present research, fabricated with hydroxyapatite nanopowders (<200nm particle size, BET), was optimised using hydroxyapatite nanopowders with smaller particle sizes (20nm, 40nm and 60nm) and a more uniform size distribution.

The effect of hydroxyapatite nanoparticle size and coating of hydroxyapatite (HA) nanoparticles on the surface area available for drug/protein adsorption during the fabrication of aquasomes was investigated using BET analysis. The decrease in nano-hydroxyapatite core sizes (60nm, 40nm and 20nm) showed a marked increase in surface area available for drug/protein adsorption with calculated BET surface areas as 54.42 m^2g^{-1}, 58.18 m^2g^{-1} and 65.37m^2g^{-1} respectively in comparison to the un-optimised HA nanocores which had a calculated surface area of 22.74 m^2g^{-1}.

Hydroxyapatite nanocores (20nm, 40nm and 60nm) were then coated with trehalose for 1.5h, 2.5h and 3h to investigate the increase in surface area available for drug/protein adsorption. Significant differences were observed for calculated surface area between the nano-core sizes (20nm, 40nm, 60nm) for each coating time (*$p<0.01$). No significant differences ($P>0.05$) were found for calculated surface areas when investigating coating time for specific nano-core sizes (i.e., 20nm 1.5h, 2.5h and 3h). These results evidently show that an increase in the duration of trehalose coating does not give a significantly different calculated BET surface area but the decrease in particle size and a uniform size distribution gives a definitely significant difference in the calculated surface areas

The zeta potential of the coated and uncoated hydroxyapatite nanocores were also analysed to measure the surface charge. The change in surface charge after coating established the adsorption of trehalose onto the nanocores. SEM and confocal imaging were also employed to understand the morphology of aquasomes and validate the adsorption of drug in aquasome formulations. Pictorial results using these imaging techniques evidently elucidated the morphology of and validated the adsorption of drug/protein in loaded aquasomes. Using

the fluorescence emitting drug, metronidazole, loaded onto aquasome formulations, the behaviour of aquasome nanoparticles was elucidated. The confocal images illustrated the adsorption of metronidazole onto the coated nanocores and the SEM and confocal images revealed the clustering of individual nanocores in the aquasome formulation. Generally, agglomeration of nanoparticles may affect the bioactivity of adsorbed bio-actives. However, trehalose, the oligomeric coating used in this study, is popular known to retain the conformational integrity of bioactive molecules and thus aggregation of nanocores may not pose a problem.

Optimisation of protein quantification using HPLC with an ELSD exhibited robustness and ease of performance in comparison to the conventional ELISA technique for quantifying proteins. The HPLC-ELSD analysed BMP-2, VEGF-121 and trehalose, the components of aquasomes individually. The results from this study demonstrated that the ELSD was more sensitive than the standard BMP ELISA.

Following the optimisation of the aquasome formulation used in this study, gels were investigated as a drug dosage form for the delivery of proteins for topical/transdermal delivery. BSA was used as a model protein to investigate the suitability of gels for the delivery of protein-loaded aquasomes. Non-aqueous silicone elastomer gels (NASEGS) have been used as delivery system, personal lubricants and for rectal application (Forbes et al, 2014). More recently, they have been employed in the vaginal delivery of HIV-1 microbicides (Forbes et al, 2013).

Various ratios of the gels components (ST-elastomer and cyclomethicone) were investigated to manufacture different gels with different textural and rheological characteristics. These gels also exhibited similar release trends which varied with changing the ratio of cyclomethicone in the gels and protein loading. 80/20 (ST-elastomer/cyclomethicone) and 70/30 (ST-elastomer/cyclomethicone) had similar release profiles, however, rheological and textural characterisation results proved the 80/20 gel to be the most suitable gel formulation with a more desirable hardness characteristic of pharmaceutical gels (18.33±2.86, Table 3.5) and well-defined viscous and elastic moduli without any cross-over between the two moduli indicating the gel's ability to maintain its gel structure without any destruction of the microstructure of the gel when exposed to strain of 0.15Pa.

Release from NASEGS exhibited sustained release of BSA of which the amount of BSA released was dependent on BSA loading into the gels. The release mechanism of BSA from NASEGS is elucidated in Figure 3.15A, illustrating the diffusion of a water-soluble drug, like BSA, through the hydrophobic silicone matrix. The minimal hydration of the pores of hydrophobic matrix causes the slow diffusion of BSA through the pores, culminating in the sustained release of BSA from the gels. The structures of the aqueous gels are rapidly

hydrated and eroded, enhancing the release of BSA through the water-soluble matrix thereby resulting in higher rates of BSA release from the aqueous gels. In comparison with BSA release from the aqueous gels, minute amounts of BSA (6-7 μg, highest amount released) were released from the 80/20 NASEGS. Release of BSA from BSA loaded aquasomes incorporated into the 80/20 NASEG formulation yielded 0.25μg BSA as the highest release (0.0035% per time point). The incorporation of BSA-loaded aquasomes in NASEGS can offer a delayed and sustained release of hydrophilic drugs/proteins in comparison to aquasomes loaded with hydrophobic drugs. Hydrophobic drugs dispersed in the NASEGS, have higher amounts of drug released (Forbes et al, 2014). Aquasomes in the NASEGS can be exploited for use in the delivery of antigens, antibodies, growth factors or hormones which require small amounts of drug/protein to be released for a prolonged periods of time.

In vitro permeation of BSA in the NASEGS was investigated to examine the performance of the gels on membranes *in vitro* to examine and its ability to effectively deliver proteins/drug through the stratum corneum *in vivo*. Franz cell studies using polycarbonate membranes (0.4μm pore size) were used to mimic the stratum corneum and analyse the permeation rate of BSA through the membranes. Permeation of BSA through the membrane showed consistent release of 1.5- 2.0μg every hour for 8 hours, from loaded aquasomes fabricated with 7mg/ml BSA solutions and incorporated into 80/20 NASEG formulation. The low cumulative permeation profile of BSA through the polycarbonate membrane may be applied for the sustained and prolonged delivery of potent proteins such as cytokines and growth factors, required at low concentrations to exert a biological effect. It was hypothesized that the rate of permeation through the membrane may be less than optimal based on the results from Figure 3.21.

Gentamicin-loaded aquasomes were also fabricated to investigate its potential as an antibiotic delivery system for treating bone infections. Bone infections have been a major concern in orthopaedics due to the common incidences of infections experienced in bone transplantations, orthopaedic surgeries as well as fractures. *Staphylococcus aureus* is the major causative organism implicated in bone infections and was used to challenge the efficacy of the bactericidal activity of gentamicin loaded aquasomes. The individual components (hydroxyapatite, trehalose) were tested for bactericidal activity which yielded negative results. Gentamicin-loaded aquasomes were tested against a low inoculum and higher inoculum of *S. aureus.* The results revealed that the gentamicin released from aquasomes had an effective bactericidal effect against a low inoculum of *S. aureus* (Stock solution A, O.D. compared with 0.5 McFarland standards) after 2 hours for an 8 hour study. It also had an effective bactericidal effect against a higher inoculum of *S. aureus* (Stock solution B, O.D =1 at 625nm) after 5 hours of incubation and retained its effect even after 24

hours, in comparison to controls. The results proved the efficacy of gentamicin loaded aquasomes as antibiotic carriers for the treatment of bone infections.

BMP-2 and VEGF 121 loaded aquasomes were fabricated as osteoinductive and angiogenic delivery systems that promote bone cell proliferation as well as induce angiogenesis via the proliferation of endothelial cells. To establish these claims, BMP released from aquasomes was quantified and BMP-loaded aquasomes were co-cultured with osteoprogenitor cells and assayed for ALP production, to demonstrate the ability of aquasomes to be employed in bone regeneration for fracture healing. Percentage release of BMP-2 and VEGF 121 from all aquasome formulations was less than 5% of the amount of protein adsorbed during the 8 hour release period. SAOS-2 cells, MG63 cells and HUVECs were exposed to the individual components of aquasomes for 24 hours (BMP-2, VEGF 121, Hydroxyapatite, and trehalose) and tested for acute cell toxicity using the MTT assay. The concentrations being used for aquasome manufacture were found to be safe and increased percentage cell viability for all three cell lines. When exposed to BMP-2 loaded aquasomes, MG63 had a higher ALP activity when compared to the control group (MG63 Blank). The differentiation effect of BMP-2-loaded aquasomes was comparable to that of 50ng/ml BMP-2 exogenously added to culture medium. However, co-culture with HUVECs yielded higher ALP activity. This was probably because the secretion of VEGF from the HUVECs induced an increment in the proliferation of MG63 cells as well as offered a protective activity on the cells causing MG63 cells to be more viable in long term cell culture. VEGF as a potent angiogenic factor plays an important role in protecting cells causing cells to thrive in long term culture (Ferrari et al, 2006). These results were also mirrored in the cell proliferation count assay where co-culture with cells yielded higher ALP activity across the groups in comparison to groups exposed to exogenous treatments.

A separate study investigating the differentiation effect of BMP-2 and VEGF- 121 loaded aquasomes on mesenchymal cells (ATMSCs) was performed to determine the differentiation effect of BMP-2 and VEGF 121 released from aquasomes in mesenchymal cells in comparison to cells cultured in osteogenic media. ATMSCs in osteogenic medium were used as a positive control. Results revealed that BMP-2 aquasomes (ATMSCs BMP AQUA) had a low differentiation effect in comparison to osteogenic media. However, VEGF aquasomes induced higher ALP activity in comparison to BMP aquasomes. A comparison between the group exposed to 50ng/ml VEGF and 25ng/ml VEGF showed that a higher dose of growth factor may not necessarily translate to higher ALP activity. Results also showed that dual delivery of BMP-2 aquasomes and VEGF aquasomes did not yield higher ALP activity in comparison to singular delivery of each growth factor-loaded aquasome formulation. This is in agreement of a study by Kempen et al (2009) which suggested sequential delivery of

angiogenic and osteogenic growth factor in a time dependent manner for enhanced osteogenic differentiation.

This thesis has focused on the potential of aquasomes as nanocarrier delivery systems for proteins, antibiotics and growth factors.

CHAPTER 7
FURTHER INVESTIGATIONS AND CONCLUDING REMARKS

1. Further research could investigate the permeation of BSA or another model protein from aquasomes incorporated into NASEGS with the addition of hydrophilic polymers to enhance protein drug release. Permeation studies using PDMS membranes, a closer substitute to the stratum corneum should also be examined to investigate the permeation of proteins from loaded aquasomes through such membranes.

2. It would be beneficial to conduct a longer term cell culture study to determine if the less pronounced differentiation effect of BMP-2 on MG63 and AT-MSCs was due to the release from aquasomes in smaller amounts in comparison to exogenous treatments. This means that the release of the growth factors in long term cult ure couldbe examined for sustained bioactivity, a concurrent study of different concentrations of BMP-2 released onto MG63 cells and ATMSCs could be examined for osteogenic differentiation after 4-6 weeks and an intensive immunohistochemical study could be performed to investigate the qualitative differentiation of MG63 and ATMSCs.

3. Further studies are required to optimise the amount and ratio of the release of BMP-2 and VEGF 121 and also compare the bioactivity of BMP-2 and VEGF 121 released from aquasomes in comparison to free rhBMP-2 and rhVEGF121 in media.

4. Further investigations on gentamicin loaded aquasomes could center on the delivery of gentamicin loaded aquasomes onto infected osteogenic cells to examine the efficacy of gentamicin loaded aquasomes to alleviate bone infections *in situ*. The duration of complete release of gentamicin from aquasomes could be investigated to determine the duration of antibiotic protection gentamicin loaded-aquasomes can offer in *in vivo* and *in vitro* applications.

5. Advancement in the ELSD-HPLC method technique could focus on the development of the assay to examine the complete aquasome formulation (coating and drug) in single analysis as opposed to two separate analyses. The developed method would achieve separate peaks for different components in the same analysis.

CHAPTER 8
REFERENCES

8.1 REFERENCES

Al-Achi, A., et al. (2013). Integrated Pharmaceutics: Applied Preformulation, Product Design, and Regulatory Science, John Wiley and Sons.

Allababidi, S., and Shah, J. C. (1998). Kinetics and mechanism of release from glyceryl monostearate-based implants: Evaluation of release in a gel simulating in vivo implantation. *Journal of Pharmaceutical Sciences*, *87*(6), 738–744. http://doi.org/10.1021/js9703986

Allen, L. V, Popovich, N. G., and Ansel, H. C. eds. (2011).Ansel's Pharmaceutical dosage forms and drug delivery systems; 9th ed. .

Alves, M. P., Scarrone, A. L., Santos, M., Pohlmann, A. R., and Guterres, S. S. (2007) Human skin penetration and distribution of nimesulide from hydrophilic gels containing nanocarriers. International Journal of Pharmaceutics, **341**(1-2):215–20. doi:10.1016/j.ijpharm.2007.03.031

Amin, S., Rajabnezhad, S., and Kohli, K. (2009). Hydrogels as potential drug delivery systems. Scientific Research and …, 3(11), 1175–1183. Retrieved from http://www.academicjournals.org/sre/PDF/pdf2009/Nov/Amin et al.pdf

Anderson, H. C., Gurley, D. J., Hsu, H. H. T., Aguilera, X. M., Davis, L. S. and Moylan, P. E. (1999) Secretion of a bone-inducing agent (BIA) by cultured sasos-2 human osteosarcoma cells. Journal of Musculoskeletal Research, **03**(01):39-48.

Arcos, D. and Vallet-Regi, M., (2013). Bioceramics for drug delivery. Acta Materialia, 61(3), 890–911. http://doi.org/10.1016/j.actamat.2012.10.039

Azi, M., Junior, M. K., Martinez, R., and Paccola, C. (2010). Bone cement and gentamicin in the treatment of bone infection: background and in vitro study. Acta Ortopédica Brasileira, 18(1), 31–34. http://doi.org/10.1590/S1413-78522010000100006

Baro, M., Sánchez, E., Delgado, a, Perera, a, and Evora, C. (2002). In vitro-in vivo characterization of gentamicin bone implants. Journal of Controlled Release : Official Journal of the Controlled Release Society, 83(3), 353–64. Retrieved from http://www.ncbi.nlm.nih.gov/pubmed/12387944

Barry, B. W. (2002). Drug delivery routes in skin: a novel approach. *Advanced Drug Delivery Reviews*, *54 Suppl 1*, S31-40. Retrieved from http://www.ncbi.nlm.nih.gov/pubmed/12460714

Benaroudj, N., Lee, D. H., and Goldberg, A. L. (2001) Trehalose accumulation during cellular stress protects cells and cellular proteins from damage by oxygen radicals. Journal of Biological Chemistry, **276**(26):24261–24267. http://doi.org/10.1074/jbc.M101487200

Bianco, A., Kostarelos, K., and Prato, M. (2005) Applications of carbon nanotubes in drug delivery. *Current Opinion in Chemical Biology* ***9***(6):674–679. http://doi.org/10.1016/j.cbpa.2005.10.005

Biondi, M., Ungaro, F., Quaglia, F., and Netti, P. A. (2008). Controlled drug delivery in tissue engineering. Advanced Drug Delivery Reviews, 60(2), 229–242. http://doi.org/10.1016/j.addr.2007.08.038

Birmingham, E., Niebur, G. L., Mchugh, P. E., Shaw, G., Barry, F. P. and McNamara, L. M. (2012) Osteogenic differentiation of mesenchymal stem cells is regulated by osteocyte and osteoblast cells in a simplified bone niche. European Cells and Materials **23**(353): 13–27. http://doi.org/vol023a02 [pii]

Bose, S., and Tarafder, S. (2012). Calcium phosphate ceramic systems in growth factor and drug delivery for bone tissue engineering: A review. Acta Biomaterialia, 8(4), 1401–1421. http://doi.org/10.1016/j.actbio.2011.11.017

Buckwalter, J., and Glimcher, M. (1995) Bone biology. The Journal of Bone and Joint Surgery **77:**1276-1289.

Campoccia, D., Montanaro, L., Speziale, P., and Arciola, C. R. (2010). Antibiotic-loaded biomaterials and the risks for the spread of antibiotic resistance following their prophylactic and therapeutic clinical use. *Biomaterials*, *31*(25), 6363–6377. http://doi.org/10.1016/j.biomaterials.2010.05.005

Campoccia, D., Montanaro, L., Speziale, P., and Arciola, C. R. (2010). Antibiotic-loaded biomaterials and the risks for the spread of antibiotic resistance following their prophylactic and therapeutic clinical use. Biomaterials, 31(25), 6363–6377. http://doi.org/10.1016/j.biomaterials.2010.05.005

Chai, F., Hornez, J. C., Blanchemain, N., Neut, C., Descamps, M., and Hildebrand, H. F. (2007). Antibacterial activation of hydroxyapatite (HA) with controlled porosity by

different antibiotics. Biomolecular Engineering, 24(5), 510–514. http://doi.org/10.1016/j.bioeng.2007.08.001

Chen, L., Mccrate, J. M., Lee, J. C.-M., and Li, H. (2011). The role of surface charge on the uptake and biocompatibility of hydroxyapatite nanoparticles with osteoblast cells. Nanotechnology, 22(10), 105708. http://doi.org/10.1088/0957-4484/22/10/105708

Cherian, A. K., Rana, A. C., and Jain, S. K. (2000). Self-Assembled Carbohydrate-Stabilized Ceramic Nanoparticles for the Parenteral Delivery of Insulin. Drug Development and Industrial Pharmacy, 26(4), 459–463. JOUR. http://doi.org/10.1081/DDC-100101255

Christenson, R. H. (1997) Biochemical markers of bone metabolism: an overview. Clinical Biochemistry **30**(8):573–593. http://doi.org/10.1016/S0009-9120(97)00113-6

Colas A., J. Siang, K. Ulman, Silicones in pharmaceutical applications, Chimie Nouvelle, Dow Corning, 1997, pp. 1–8, URL:http://www3.dowcorning.com/ content/publishedlit/52-1090-01.pdf, [21 June 2011].

Colas, A., and Curtis, J. (n.d.). Silicone Biomaterials : History and Chemistry Medical Applications of Silicones Dow Corning Corporation Biomaterials Science , 2 nd Edition About the Authors.

Cummings, S. R., San Martin, J., McClung, M. R., Siris, E. S., Eastell, R., Reid, I. R., Christiansen, C. (2009) Denosumab for prevention of fractures in postmenopausal women with osteoporosis. The New England Journal of Medicine **361**(8):756–65. doi:10.1056/NEJMoa0809493.

das Neves, J., and Bahia, M. F. (2006). Gels as vaginal drug delivery systems. *International Journal of Pharmaceutics*, *318*(1–2), 1–14. http://doi.org/10.1016/j.ijpharm.2006.03.012

Das Neves, J., da Silva, M. V., Gonçalves, M. P., Amaral, M. H., and Bahia, M. F. (2009) Rheological properties of vaginal hydrophilic polymer gels. Current Drug Delivery **6**(1):83–92. Retrieved from http://www.ncbi.nlm.nih.gov/pubmed/19418960 [accessed on 15.04.2014]

Dasgupta, S., Bandyopadhyay, A., and Bose, S. (2009). Reverse micelle-mediated synthesis of calcium phosphate nanocarriers for controlled release of bovine serum albumin. Acta Biomaterialia, 5(8), 3112–3121. http://doi.org/10.1016/j.actbio.2009.04.031

Deckers, M. L., Van Bezooijen R. L., Van Der Horst G., Hoogendam J., Van Der Bent C., Socrates E. Papapoulos, and Lowik, C. W. (2012) Bone morphogenetic proteins stimulate angiogenesis through osteoblast-derived vascular endothelial growth factor A, Endocrinology **143**(4):1545–1553.

Delgado-Charro, M. B. and Guy, R. H.,(2001). Transdermal iontophoresis for controlled drug delivery and non-invasive monitoring. *STP Pharma Sciences*, 11 (6), pp. 404-414.

des Rieux, A., Fievez, V., Garinot, M., Schneider, Y.-J. and Préat, V. (2006) Nanoparticles as potential oral delivery systems of proteins and vaccines: a mechanistic approach. Journal of Controlled Release **116**(1):1–27. http://doi.org/10.1016/j.jconrel.2006.08.013

Devescovi, V., Leonardi, E., Ciapetti, G. and Cenni, E. (2008) Growth factors in bone repair. La Chirurgia Degli Organi Di Movimento, **92**(3):161–8. http://doi.org/10.1007/s12306-008-0064-1

Doostmohammadi, A., Monshi, A., Salehi, R., Fathi, M. H., Karbasi, S., Pieles, U. and Daniels, A. U. (2012) Preparation, chemistry and physical properties of bone-derived hydroxyapatite particles having a negative zeta potential. *Materials Chemistry and Physics* **132**(2–3):446–452. http://doi.org/10.1016/j.matchemphys.2011.11.051

Downey, P. A. and Siegel, M. I. (2006) Bone biology and the clinical implications for osteoporosis. Physical Therapy **86:**77-91

Dunn, A. S., Campbell, P. G., and Marra, K. G. (2001). The influence of polymer blend composition on the degradation of polymer / hydroxyapatite biomaterials, 2, 673–677.

Ekdawi-Sever, N. C., Conrad, P. B. and de Pablo, J. J. (2001). Molecular sucrose solutions near the glass transition temperature. The *Journal of Physical Chemistry A, 105* (4), 734-742. http://doi.org/10.1021/jp002722i

Efstathopoulos, N., Giamarellos-Bourboulis, E., Kanellakopoulou, K., Lazarettos, I., Giannoudis, P., Frangia, K., … Nikolaou, V. S. (2008). Treatment of experimental osteomyelitis by Methicillin Resistant Staphylococcus Aureus with bone cement system releasing grepafloxacin. Injury, 39(12), 1384–1390. http://doi.org/10.1016/j.injury.2008.04.006

Eid, A. J., and Berbari, E. F. (2012). Osteomyelitis : review of pathophysiology , diagnostic modalities miseaupoint / in-depthreview, 60(1).

El-Husseiny, M., Patel, S., MacFarlane, R. J. and Haddad, F. S. (2011) Biodegradable antibiotic delivery systems. The Journal of Bone and Joint Surgery. **93**(2):151–157. http://doi.org/10.1302/0301-620X.93B2.24933

Faraji, A. H., and Wipf, P. (2009) Nanoparticles in cellular drug delivery. Bioorganic and Medicinal Chemistry **17**(8):2950–2962. doi:10.1016/j.bmc.2009.02.043

Fei, Z., Hu, Y., Wu, D., Wu, H., Lu, R., Bai, J., and Song, H. (2008). Preparation and property of a novel bone graft composite consisting of rhBMP-2 loaded PLGA microspheres and calcium phosphate cement. Journal of Materials Science. Materials in Medicine, 19(3), 1109–16. http://doi.org/10.1007/s10856-007-3050-5

Ferrari, G., Pintucci, G., Seghezzi, G., Hyman, K., Galloway, A. C. and Mignatti, P. (2006) VEGF, a prosurvival factor, acts in concert with TGF-beta1 to induce endothelial cell apoptosis. Proceedings of the National Academy of Sciences of the United States of America **103**(46):17260–17265. http://doi.org/10.1073/pnas.0605556103

Finkenzeller, G., Hager, S. and Stark, G. B. (2012) Effects of bone morphogenetic protein 2 on human umbilical vein endothelial cells. Microvascular Research **84**(1):81–85. http://doi.org/10.1016/j.mvr.2012.03.010

Friess, W. (1998). Collagen – biomaterial for drug delivery1Dedicated to Professor Dr. Eberhard Nürnberg, Friedrich-Alexander-Universität Erlangen-Nürnberg, on the occasion of his 70th birthday.1. European Journal of Pharmaceutics and Biopharmaceutics, 45(2), 113–136. http://doi.org/10.1016/S0939-6411(98)00017-4

Gallagher, J. C. (2008) Advances in bone biology and new treatments for bone loss. *Maturitas* **60**(1):65–69. doi:10.1016/j.maturitas.2008.04.005

Gelse, K., Pöschl, E., and Aigner, T. (2003). Collagens - Structure, function, and biosynthesis. Advanced Drug Delivery Reviews, 55(12), 1531–1546. http://doi.org/10.1016/j.addr.2003.08.002

Gibaldi, M., M. Lee, and A. Desai. 2007. Gibaldi's drug delivery systems in pharmaceutical care. American Society of Health-System Pharmacists, Bethesda, MD

Gillies, E. R. and Fréchet, J. M. J. (2005) Dendrimers and dendritic polymers in drug delivery. Drug Discovery Today **10**(1):35–43. http://doi.org/10.1016/S1359-6446(04)03276-3

Ginebra, M. P., Traykova, T., and Planell, J. A. (2006). Calcium phosphate cements as bone drug delivery systems: A review. Journal of Controlled Release, 113(2), 102–110. http://doi.org/10.1016/j.jconrel.2006.04.007

Ginebra, M.-P. P., Canal, C., Espanol, M., Pastorino, D., and Montufar, E. B. (2012). Calcium phosphate cements as drug delivery materials. *Advanced Drug Delivery Reviews*, *64*(12), 1090–1110. http://doi.org/10.1016/j.addr.2012.01.008

Giustina, A., Mazziotti, G. and Canalis, E. (2008) Growth hormone, insulin-like growth factors, and the skeleton. Endocrine Reviews **29**(5):535–59. doi:10.1210/er.2007-0036

Gogia, J. S., Meehan, J. P., Di Cesare, P. E., and Jamali, A. A. (2009). Local antibiotic therapy in osteomyelitis. Seminars in Plastic Surgery, 23(2), 100–7. http://doi.org/10.1055/s-0029-1214162

Golub, E. E., and Boesze-Battaglia, K. (2007) the role of alkaline phosphatase in mineralization. Current Opinion in Orthopaedics **18**(5):444–448. http://doi.org/10.1097/BCO.0b013e3282630851

Goth, A. (1964). *Medical Pharmacology* (Vol. 25). http://doi.org/10.1097/00000542-196407000-00040

Gough, J. E., Jones, J. R., and Hench, L. L. (2004). Nodule formation and mineralisation of human primary osteoblasts cultured on a porous bioactive glass scaffold. Biomaterials, 25(11), 2039–2046. http://doi.org/10.1016/j.biomaterials.2003.07.001

Goyal, A. K., Khatri, K., Mishra, N., Mehta, A., Vaidya, B., Tiwari, S. and Vyas, S. P. (2008) Aquasomes--a nanoparticulate approach for the delivery of antigen. Drug Development and Industrial Pharmacy **34**(12):1297–305. DOI:10.1080/03639040802071661

Gunatillake, P. a, and Adhikari, R. (2003). Biodegradable synthetic polymers for tissue engineering. European Cells and Materials, 5, 1–16; discussion 16. Retrieved from http://www.ncbi.nlm.nih.gov/pubmed/14562275

Gupta, K. M., Pearce, S. M., Poursaid, A. E., Aliyar, H. A., Tresco, P. A., Mitchnik, M. A., and Kiser, P. F. (2008). *Drug Delivery* Polyurethane Intravaginal Ring for Controlled Delivery of Dapivirine, a Nonnucleoside Reverse Transcriptase Inhibitor of HIV-1, *97*(10), 4228–4239. http://doi.org/10.1002/jps

Gupta, P., Vermani, K., and Garg, S. (2002). Hydrogels: from controlled release to pH-responsive drug delivery. *Drug Discovery Today*, *7*(10), 569–79. Retrieved from http://www.ncbi.nlm.nih.gov/pubmed/12047857

Habraken, W. J. E. M., Wolke, J. G. C., and Jansen, J. A. (2007). Ceramic composites as matrices and scaffolds for drug delivery in tissue engineering. Advanced Drug Delivery Reviews, 59(4–5), 234–248. http://doi.org/10.1016/j.addr.2007.03.011

Hadjidakis, D. J., and Androulakis, I. I. (2006). Bone remodeling. Annals of the New York Academy of Sciences, 1092, 385–396. http://doi.org/10.1196/annals.1365.035

Hägerström, H. (2003). Polymer gels as pharmaceutical dosage forms. *Acta Universitatis Upsaliensis*. Retrieved from http://uu.diva-portal.org/smash/get/diva2:163176/FULLTEXT01.pdf

Han, T., and Das, D. B. (2013). Permeability enhancement for transdermal delivery of large molecule using low-frequency sonophoresis combined with microneedles. *Journal of Pharmaceutical Sciences*, *102*(10), 3614–3622. http://doi.org/10.1002/jps.23662

Han, Y., Jin, B.-S., Lee, S.-B., Sohn, Y., Joung, J.-W., and Lee, J.-H. (2007). Effects of Sugar Additives on Protein Stability of Recombinant Human Serum Albumin during Lyophilization and Storage. Arch Pharm Res, 30(9), 1124–1131. http://doi.org/10.1007/BF02980247

Hanley, D, Adachi, J. D., Bell and Brown, V. (2012). Denosumab: mechanism of action and clinical outcomes. International journal of clinical practice, 66(12), pp. 1139–46. DOI:10.1111/ijcp.12022

Haugen, H. J., Monjo, M., Rubert, M., Verket, A., Lyngstadaas, S. P., Ellingsen, J. E., and Wohlfahrt, J. C. (2013). Porous ceramic titanium dioxide scaffolds promote bone formation in rabbit peri-implant cortical defect model. Acta biomaterialia, 9(2), pp. 5390–5399. DOI:10.1016/j.actbio.2012.09.009

Hench, L. L., and Paschall, H. (1973). Direct chemical bond of bioactive glass-ceramic materials to bone and muscle. Journal of Biomedical Materials Research, 7(3), 25–42. http://doi.org/10.1002/jbm.820070304

Hernández, A., Reyes, R., Sánchez, E., Rodríguez-Évora, M., Delgado, A., and Évora, C. (2012). In vivo osteogenic response to different ratios of BMP-2 and VEGF released

from a biodegradable porous system. Journal of Biomedical Materials Research - Part A, 100 A(9), 2382–2391. http://doi.org/10.1002/jbm.a.34183

Herrera, L. C., Tesoriero, M. V. D., and Hermida, L. G. (2012). *In Vitro* Release Testing of PLGA Microspheres with Franz Diffusion Cells, *5445*(May), 6–11.

Higashiyama, T. (2002). Novel functions and applications of trehalose. Pure and Applied Chemistry, 74(7), 1263–1269. DOI:10.1351/pac200274071263.

Hofmann, A., Ritz, U., Verrier, S., Eglin, D., Alini, M., Fuchs, S., and Rommens, P. M. (2008). The effect of human osteoblasts on proliferation and neo-vessel formation of human umbilical vein endothelial cells in a long-term 3D co-culture on polyurethane scaffolds. Biomaterials, 29(31), pp. 4217–4226. DOI:10.1016/j.biomaterials.2008.07.024

Hosseinkhani, H., Hosseinkhani, M., Khademhosseini, A., and Kobayashi, H. (2007). Bone regeneration through controlled release of bone morphogenetic protein-2 from 3-D tissue engineered nano-scaffold. *Journal of Controlled Release: Official Journal of the Controlled Release Society*, *117*(3), 380–86. http://doi:10.1016/j.jconrel.2006.11.018

Huang, Y.-C., Kaigler, D., Rice, K. G., Krebsbach, P. H. and Mooney, D. J. (2005). Combined angiogenic and osteogenic factor delivery enhances bone marrow stromal cell-driven bone regeneration. Journal of Bone and Mineral Research: the Official Journal of the American Society for Bone and Mineral Research, 20(5), 848–57. DOI:10.1359/JBMR.041226

Huang, H.-C., Barua, S., Sharma, G., Dey, S. K. and Rege, K. (2011). Inorganic nanoparticles for cancer imaging and therapy. *Journal of Controlled release: Official Journal of the Controlled Release Society, 155*(3), 344-57. http://doi.org/10.1016/j.jconrel.2011.06.004

Im, G. Il, Shin, Y. W., and Lee, K. B. (2005). Do adipose tissue-derived mesenchymal stem cells have the same osteogenic and chondrogenic potential as bone marrow-derived cells? *Osteoarthritis and Cartilage*, *13*(10), 845–853. http://doi.org/10.1016/j.joca.2005.05.005

Itokazu, M., Ohno, T., Tanemori, T., Wada, E., Kato, N., and Watanabe, K. (1997). Antibiotic-loaded hydroxyapatite blocks in the treatment of experimental osteomyelitis in rats. Journal of Medical Microbiology, 46(9), 779–783. http://doi.org/10.1099/00222615-46-9-779

Itokazu, M., Yang, W., Aoki, T., Ohara, A., and Kato, N. (1998). Synthesis of antibiotic-loaded interporous hydroxyapatite blocks by vacuum method and in vitro drug release testing. Biomaterials, 19(7–9), 817–819. http://doi.org/10.1016/S0142-9612(97)00237-8

Jain, N. K., and Roy, I. (2008). Effect of trehalose on protein structure. Protein Science : A Publication of the Protein Society, 18(1), 24–36. http://doi.org/10.1002/pro.3

Jain, S. S., Jagtap, P. S., Dand, N. M., Jadhav, K. R., and Kadam, V. J. (2012). AQUASOMES : A NOVEL DRUG CARRIER, 2(1), 184–192.

Jones, D. S., Woolfson, A. D., and Brown, A. F. (1997). Textural, viscoelastic and mucoadhesive properties of pharmaceutical gels composed of cellulose polymers. International Journal of Pharmaceutics, 151(2), pp. 223–233. DOI:10.1016/S0378-5173(97)04904-1

Jones, J. R., Tsigkou, O., Coates, E. E., Stevens, M. M., Polak, J. M., and Hench, L. L. (2007). Extracellular matrix formation and mineralization on a phosphate-free porous bioactive glass scaffold using primary human osteoblast (HOB) cells. Biomaterials, 28(9), 1653–1663. http://doi.org/10.1016/j.biomaterials.2006.11.022

Joosten, U., Joist, a., Frebel, T., Brandt, B., Diederichs, S., and Von Eiff, C. (2004). Evaluation of an in situ setting injectable calcium phosphate as a new carrier material for gentamicin in the treatment of chronic osteomyelitis: Studies in vitro and in vivo. Biomaterials, 25, 4287–4295. http://doi.org/10.1016/j.biomaterials.2003.10.083

Joosten, U., Joist, A., Gosheger, G., and Liljenqvist, U. (2005). Effectiveness of hydroxyapatite-vancomycin bone cement in the treatment of Staphylococcus aureus induced chronic osteomyelitis, 26, 5251–5258. http://doi.org/10.1016/j.biomaterials.2005.01.001

Jorge, L. S., Chueire, A. G., and Rossit, A. R. (2010). Osteomyelitis: a current challenge. Braz.J.Infect.Dis., 14(1678–4391 (Electronic)), 310–315. http://doi.org/10.1016/S1413-8670(10)70063-5

Kaigler, D., Krebsbach, P. H., West, E. R., Horger, K., Huang, Y. and Mooney, D. J. (2005). Endothelial cell modulation of bone marrow stromal cell osteogenic potential, *27*.

Kajihara, M., Sugie, T., Mizuno, M., Tamura, N., Sano, a, Fujioka, K., Kashiwazaki, Y., et al. (2000). Development of new drug delivery system for protein drugs using silicone (I).

Journal of controlled release, 66(1), 49–61. Retrieved from http://www.ncbi.nlm.nih.gov/pubmed/10708878

Kalita, S. J., Bhardwaj, A., and Bhatt, H. A. (2007). Nanocrystalline calcium phosphate ceramics in biomedical engineering. Materials Science and Engineering C, 27(3), 441–449. http://doi.org/10.1016/j.msec.2006.05.018

Kanczler, J. M. (2008). *Osteogenesis and Angiogenesis : the Potential for Engineering*, 100–114.

Kanczler, J. M. and Oreffo, R. O. C. (2008). Osteogenesis and angiogenesis : the potential for engineering, *European Cells and Materials*, **15**, pp. 100–114.

Kanczler, J. M., Ginty, P. J., White, L., Clarke, N. M. P., Howdle, S. M., Shakesheff, K. M., and Oreffo, R. O. C. (2010). The effect of the delivery of vascular endothelial growth factor and bone morphogenic protein-2 to osteoprogenitor cell populations on bone formation. Biomaterials, 31(6), 1242–50. DOI:10.1016/j.biomaterials.2009.10.059

Kang, Y., Kim, S., Fahrenholtz, M., Khademhosseini, A., and Yang, Y. (2013). Osteogenic and angiogenic potentials of monocultured and co-cultured human-bone-marrow-derived mesenchymal stem cells and human-umbilical-vein endothelial cells on three-dimensional porous beta-tricalcium phosphate scaffold. Acta Biomaterialia, 9(1), 4906–4915. http://doi.org/10.1016/j.actbio.2012.08.008

Keibl, C., Fügl, A., Zanoni, G., Tangl, S., Wolbank, S., Redl, H., and Van Griensven, M. (2011). Human adipose derived stem cells reduce callus volume upon BMP-2 administration in bone regeneration. Injury, 42(8), 814–820. http://doi.org/10.1016/j.injury.2011.03.007

Kempen, D. H. R., Lu, L., Heijink, A., Hefferan, T. E., Creemers, L. B., Maran, A., … Dhert, W. J. a. (2009). Effect of local sequential VEGF and BMP-2 delivery on ectopic and orthotopic bone regeneration. Biomaterials, 30(14), 2816–25. http://doi.org/10.1016/j.biomaterials.2009.01.031

Khopade, a J., Khopade, S., and Jain, N. K. (2002). Development of hemoglobin aquasomes from spherical hydroxyapatite cores precipitated in the presence of half-generation poly(amidoamine) dendrimer. *International Journal of Pharmaceutics*, *241*(1), 145–54. Retrieved from http://www.ncbi.nlm.nih.gov/pubmed/12086730

Kim, I. S., and Kim, S. H. (2002). Development of a polymeric nanoparticulate drug delivery system: In vitro characterization of nanoparticles based on sugar-containing conjugates. International Journal of Pharmaceutics, 245(1–2), 67–73. http://doi.org/10.1016/S0378-5173(02)00336-8

Kossovsky, N., Bunshah, R. F., Gelman, A., Sponsler, E., Umarjee, D. M., Suh, T. G, Deshpandey, C. V. (1990). A nondenaturing solid phase pharmaceutical carrier comprised of surface-modified nanocrystalline materials. Journal of Applied Biomaterials : An Official Journal of the Society for Biomaterials, 1(4), 289–294. http://doi.org/10.1002/jab.770010404

Kossovsky, N., Gelman, A., Hnatyszyn, H. J., Rajguru, S., Garrell, R. L., Torbati, S, Chows, G.-M. (1995). Surface Modified Nanodiamonds as Antigen Delivery Vehicles. *Bioconjugate Chemistry Communications*, *6*(5), 507–511. http://doi.org/10.1021/bc00035a001

Kossovsky, N., Gelman, A., Rajguru, S., Nguyen, R., Sponler, E., Hnatyszyn, H.J., Chow, K., Chung, A., Torres, M., Zemanovich, J., Crowder, J., Barnajian, P., Ly, K., Philose, J., Ammons, D., Anderson, X., Goodwin, C., Soliemanzadeh, P., Yao, G., Wei, K., (1996). Control of molecular polymorphism by a structured carbohydrate/ceramic delivery vehicle-aquasomes. Journal of Controlled Release, **39**, pp. 383–388.

Kriwet, K., and Miiller-goymann, C. C. (1995). journal of pharmaceutics Diclofenac release from phospholipid drug systems and permeation through excised human stratum corneum, *125*, 231–242.

Kurtoglu, Y. E., Navath, R. S., Wang, B., Kannan, S., Romero, R., and Kannan, R. M. (2009). Poly(amidoamine) dendrimer-drug conjugates with disulfide linkages for intracellular drug delivery. Biomaterials, 30(11), 2112–2121. http://doi.org/10.1016/j.biomaterials.2008.12.054

Kyriakidou, K., Lucarini, G., Zizzi, a., Salvolini, E., Mattioli Belmonte, M., Mollica, F. and Ambrosio, L. (2008). Dynamic Co-Seeding of Osteoblast and Endothelial Cells on 3D Polycaprolactone Scaffolds for Enhanced Bone Tissue Engineering. Journal of Bioactive and Compatible Polymers, 23(3), pp. 227–243. DOI:10.1177/0883911508091905

Lee, C. H., Singla, A., and Lee, Y. (2001). Biomedical applications of collagen. *International Journal of Pharmaceutics*, *221*(1–2), 1–22. http://doi.org/10.1016/S0378-5173(01)00691-3

Lee, D.-W., Yun, Y.-P., Park, K., and Kim, S. E. (2012). Gentamicin and bone morphogenic protein-2 (BMP-2)-delivering heparinized-titanium implant with enhanced antibacterial activity and osteointegration. Bone, 50(4), pp. 974–982. DOI:10.1016/j.bone.2012.01.007

Lee, D.-W., Yun, Y.-P., Park, K., and Kim, S. E. (2012). Gentamicin and bone morphogenic protein-2 (BMP-2)-delivering heparinized-titanium implant with enhanced antibacterial activity and osteointegration. Bone, 50(4), 974–82. doi:10.1016/j.bone.2012.01.007

Lee, S. H., and Shin, H. (2007). Matrices and scaffolds for delivery of bioactive molecules in bone and cartilage tissue engineering. Advanced Drug Delivery Reviews, 59(4–5), 339–359. http://doi.org/10.1016/j.addr.2007.03.016

Leja, K., and Lewandowicz, G. (2010). Polymer Biodegradation and Biodegradable Polymers – a Review, *19*(2), 255–266.

Lieberman, J. R., Daluiski, A. and Einhorn, T. A. (2002). The Role of Growth factors in the repair of bone: Biology and Clinical Applications, *the Journal of Bone and Joint Surgery*, **84** (6), ***pp.*** 1032- 1044

Liu, X., Xie, Z., Zhang, C., Pan, H., Rahaman, M. N., Zhang, X., … Huang, W. (2010). Bioactive borate glass scaffolds: In vitro and in vivo evaluation for use as a drug delivery system in the treatment of bone infection. Journal of Materials Science: Materials in Medicine, 21(2), 575–582. http://doi.org/10.1007/s10856-009-3897-8

Liu, Y., Enggist, L., Kuffer, A. F., Buser, D., and Hunziker, E. B. (2007). The influence of BMP-2 and its mode of delivery on the osteoconductivity of implant surfaces during the early phase of osseointegration. Biomaterials, 28(16), 2677–86. http://doi.org/10.1016/j.biomaterials.2007.02.003

Lopez, R. F. V, Bentley, M. V. L. B., Delgado-Charro, M. B., and Guy, R. H. (2001). Iontophoretic Delivery of 5-Aminolevulinic Acid (ALA): Effect of pH. *Pharmaceutical Research*, *18*(3), 311–315. article. http://doi.org/10.1023/A:1011050829531

Lozano, D., Trejo, C. G., Gómez-Barrena, E., Manzano, M., Doadrio, J. C., Salinas, A. J., and Buján, J. (2012). Osteostatin-loaded onto mesoporous ceramics improves the early phase of bone regeneration in a rabbit osteopenia model. Acta biomaterialia, 8(6), pp. 2317–2323. DOI:10.1016/j.actbio.2012.03.014

Lowry, D. and Abdulrazzaq, F. (2012). Effect of Temperature and Time on the Coating and Loading Processes of Aquasome Manufacture. *CRS Newsletter*: *A publication of the Controlled Release Society,* 29(4).

Lu, J., Liong, M., Zink, J. I., and Tamanoi, F. (2007). Mesoporous silica nanoparticles as a delivery system for hydrophobic anticancer drugs. Small, 3(8), 1341–1346. http://doi.org/10.1002/smll.200700005

Luca, L., Rougemont, A., Walpoth, B., Gurny, R. and Jordan, O. (2010). The effects of carrier nature and pH on rhBMP-2-induced ectopic bone formation. *Journal of controlled release, 147, pp. 38-44*. D.O.I: 10.1016/j.jconrel.2010.06.011

Luthra, K. (2008). Clinical Biochemistry - Basic Concept of Clinical Biochemistry, 01–31. http://doi.org/110 029

M. Teller, U. Gopp, H.-G. Neumann, K.-D. K. (2007). Release of Gentamicin From Bone Regenerative Materials: An *In Vitro* Study. Journal of Biomedical Materials Research. Part B, Applied Biomaterials, 83(2), 340–344. http://doi.org/10.1002/jbmb

Maeda, H., Brandon, M., and Sano, a. (2003). Design of controlled-release formulation for ivermectin using silicone. *International Journal of Pharmaceutics*, *261*(1–2), 9–19. http://doi.org/10.1016/S0378-5173(03)00293-X

Maeda, H., Ohashi, E., Sano, A., Kawasaki, H., and Kurosaki, Y. (2003). Investigation of the release behavior of a covered-rod-type formulation using silicone. *Journal of Controlled Release : Official Journal of the Controlled Release Society*, *90*(1), 59–70. Retrieved from http://www.ncbi.nlm.nih.gov/pubmed/12767707

Makadia, H. K., and Siegel, S. J. (2011). Poly Lactic-co-Glycolic Acid (PLGA) as Biodegradable Controlled Drug Delivery Carrier. Polymers, 3(3), 1377–1397. http://doi.org/10.3390/polym3031377

Malam, Y., Loizidou, M., and Seifalian, A. M. (2009). Liposomes and nanoparticles: nanosized vehicles for drug delivery in cancer. Trends in Pharmacological Sciences, 30(11), 592–599. http://doi.org/10.1016/j.tips.2009.08.004

Malcolm, R. K., Edwards, K.-L., Kiser, P., Romano, J., and Smith, T. J. (2010). Advances in microbicide vaginal rings. *Antiviral Research*, *88 Suppl 1*, S30-9. http://doi.org/10.1016/j.antiviral.2010.09.003

Malcolm, R. K., Woolfson, a D., Toner, C. F., Morrow, R. J., and McCullagh, S. D. (2005). Long-term, controlled release of the HIV microbicide TMC120 from silicone elastomer vaginal rings. The *Journal of Antimicrobial Chemotherapy*, *56*(5), 954–6. http://doi.org/10.1093/jac/dki326

Malik, N., Wiwattanapatapee, R., Klopsch, R., Lorenz, K., Frey, H., Weener, J. W., Duncan, R. (2000). Dendrimers: Relationship between structure and biocompatibility in vitro, and preliminary studies on the biodistribution of 125I-labelled polyamidoamine dendrimers in vivo. *Journal of Controlled Release*, *65*(1–2), 133–148. http://doi.org/10.1016/S0168-3659(99)00246-1

Manzano, M., and Vallet-Regi, M. (2012). Revisiting bioceramics: Bone regenerative and local drug delivery systems. Progress in Solid State Chemistry, 40(3), 17–30. http://doi.org/10.1016/j.progsolidstchem.2012.05.001

Martins, P., Rosa, D., Fernandes, A., and Baptista, P. V. (2014). Nanoparticle Drug Delivery Systems: Recent Patents and Applications in Nanomedicine. Recent Patents on Nanomedicine, 3(2), 105–118. http://doi.org/10.2174/1877912304666140304000133

Mashak, A., and Rahimi, A. (2009). Silicone Polymers in Controlled Drug Delivery Systems: A Review. *Polymer Journal*, *18*(4), 279–295.

Mcgillis, S. T., and Fein, H. (2005). Topical Treatment Strategies for Non-Melanoma Skin Cancer and Precursor Lesions, 174–183. http://doi.org/10.1016/j.sder.2004.06.005

Mendel, V., Simanowski, H. J., Scholz, H. C., and Heymann, H. (2005). Therapy with gentamicin-PMMA beads, gentamicin-collagen sponge, and cefazolin for experimental osteomyelitis due to Staphylococcus aureus in rats. Archives of Orthopaedic and Trauma Surgery, 125(6), 363–368. http://doi.org/10.1007/s00402-004-0774-2

Mesariya, S., Joshi, K., Jain, H., and Upadhyay, U. M. (2011). Aquasomes - A self-assembled nanotechnology system, 2(3), 492–496.

Middleton, J. C., and Tipton, a J. (2000). Synthetic biodegradable polymers as orthopedic devices. Biomaterials, 21(23), 2335–46. Retrieved from http://www.ncbi.nlm.nih.gov/pubmed/11055281

Mizushima, Y., Ikoma, T., Tanaka, J., Hoshi, K., Ishihara, T., Ogawa, Y., and Ueno, A. (2006). Injectable porous hydroxyapatite microparticles as a new carrier for protein and

lipophilic drugs. Journal of Controlled Release : Official Journal of the Controlled Release Society, 110(2), 260–5. http://doi.org/10.1016/j.jconrel.2005.09.051

Morrow, R. J., Woolfson, a D., Donnelly, L., Curran, R., Andrews, G., Katinger, D., and Malcolm, R. K. (2011). Sustained release of proteins from a modified vaginal ring device. *European Journal of Pharmaceutics and Biopharmaceutics : Official Journal of Arbeitsgemeinschaft Für Pharmazeutische Verfahrenstechnik e.V*, *77*(1), 3–10. http://doi.org/10.1016/j.ejpb.2010.10.010

Moses, M., Brem, H., and Langer, R. (2003). Advancing the field of drug delivery: taking aim at cancer. *Cancer Cell*, *4*(5), 337–41. Retrieved from http://www.ncbi.nlm.nih.gov/pubmed/14667500

Mundy, G. R., Chen, D., Ph, D., Zhao, M., Dallas, S., Xu, C., and Harris, S. (2001). Growth Regulatory Factors and Bone, pp. 105–115.

Mundy, G. R., Chen, D., Ph, D., Zhao, M., Dallas, S., Xu, C., and Harris, S. (2001). Growth Regulatory Factors and Bone, *pp.* 105–115. *In vitro–in vivo* characterization of gentamicin bone implants.pdf. (n.d.).

N. Kossovsky, A. Gelman, S. Rajguru, R. Nguyen, E. Sponsler, H. J. H., K. Chow, A. Chung, M. Torres, J. Zemanovich, J. Crowder, P. B., K. Ly, J. Philipose, D. Ammons, S. Anderson, C. Goodwin, P. S., and G. Yao, K. W. (1996). Control of molecular polymorphisms by a structured carbohydrate/ceramic delivery vehicle - aquasomes. Journal of Controlled Release, 39, 383–388.

Nandi, S. K., Mukherjee, P., Roy, S., Kundu, B., De, D. K., and Basu, D. (2009). Local antibiotic delivery systems for the treatment of osteomyelitis - A review. Materials Science and Engineering C, 29(8), 2478–2485. http://doi.org/10.1016/j.msec.2009.07.014

Nanjwade, B. K., Hiremath, G. M., Manvi, F. V., and Srichana, T. (2013). Formulation and Evaluation of Etoposide Loaded Aquasomes. *Journal of Nanopharmaceutics and Drug Delivery*, *1*(1), 92–101. http://doi.org/10.1166/jnd.2013.1016

Nayak, A. K. (2010). Hydroxyapatite Synthesis Methodologies : An Overview, *2*(2), *pp*. 903–907.

Nayak, K., A., and Dhara, A. K. (2010). Nanotechnology in drug delivery applications: A review. Archives of Applied Science Research, 2(2), 284–293. Retrieved from http://scholarsresearchlibrary.com/archive.html

Nelson, C. L., Hickmon, S. G., and Skinner, R. A. (1997). Treatment of experimental osteomyelitis by surgical debridement and the implantation of bioerodable, polyanhydride-gentamicin beads. Journal of Orthopaedic Research. http://doi.org/10.1002/jor.1100150214

Neun, D., and Ulman, K. (n.d.). Silicones as Excipients for Topical Pharmaceutical Applications Dow Corning.

Ng, S.-F., Rouse, J., Sanderson, D., and Eccleston, G. (2010). A Comparative Study of Transmembrane Diffusion and Permeation of Ibuprofen across Synthetic Membranes Using Franz Diffusion Cells. *Pharmaceutics*, *2*(2), 209–223. http://doi.org/10.3390/pharmaceutics2020209

Pandey, R. S., Sahu, S., Sudheesh, M. S., Madan, J., Kumar, M., and Dixit, V. K. (2011). Carbohydrate modified ultrafine ceramic nanoparticles for allergen immunotherapy. International Immunopharmacology, 11(8), 925–31. doi:10.1016/j.intimp.2011.02.004

Panyam, J., and Labhasetwar, V. (2003). Biodegradable nanoparticles for drug and gene delivery to cells and tissue. Advanced Drug Delivery Reviews, 55(3), 329–347. http://doi.org/10.1016/S0169-409X(02)00228-4

Park, J., Lutz, R., Felszeghy, E., Wiltfang, J., Nkenke, E., Neukam, F. W., and Schlegel, K. (2007). The effect on bone regeneration of a liposomal vector to deliver BMP-2 gene to bone grafts in peri-implant bone defects. *Biomaterials*, *28*(17), *pp.* 2772–2782. doi:10.1016/j.biomaterials.2007.02.009

Patel, Z. S., Yamamoto, M., Ueda, H., Tabata, Y. and Mikos, A. G. (2008). Biodegradable gelatin microparticles as delivery systems for the controlled release of bone morphogenetic protein-2. Acta Biomaterialia, 4(5), 1126–38. doi:10.1016/j.actbio.2008.04.002

Patel, Z. S., Young, S., Tabata, Y., Jansen, J. a, Wong, M. E. K., and Mikos, A. G. (2008). Dual delivery of an angiogenic and an osteogenic growth factor for bone regeneration in a critical size defect model. Bone, 43(5), 931–40. http://doi.org/10.1016/j.bone.2008.06.019

Patil, S., Sandberg, A., Heckert, E., Self, W., and Seal, S. (2007). Protein adsorption and cellular uptake of cerium oxide nanoparticles as a function of zeta potential. Biomaterials, 28(31), pp.4600–7. DOI:10.1016/j.biomaterials.2007.07.029

Patri, A. K., Majoros, I. J., and Baker, J. R. (2002). Dendritic polymer macromolecular carriers for drug delivery. *Current Opinion in Chemical Biology*, *6*(4), 466–471. http://doi.org/10.1016/S1367-5931(02)00347-2

Paul, W., and Sharma, C. P. (2003). Ceramic Drug Delivery :, 17(April 2003). http://doi.org/10.1177/088532803030571

Peppas, N. a, Bures, P., Leobandung, W., and Ichikawa, H. (2000). Hydrogels in pharmaceutical formulations. *European Journal of Pharmaceutics and Biopharmaceutics : Official Journal of Arbeitsgemeinschaft Für Pharmazeutische Verfahrenstechnik e.V*, *50*(1), 27–46. Retrieved from http://www.ncbi.nlm.nih.gov/pubmed/10840191

Petchsangsai, M., Wonglertnirant, N., Rojanarata, T., Opanasopit, P., and Ngawhirunpat, T. (2012). Microneedles-Mediated Transdermal Delivery, *6*(9), 439–442.

Petchsangsai, M., Wonglertnirant, N., Rojanarata, T., Opanasopit, P., and Ngawhirunpat, T. (2012). Microneedles-Mediated Transdermal Delivery, *6*(9), 439–442.

Popat, K. C., Eltgroth, M., LaTempa, T. J., Grimes, C. A., and Desai, T. A. (2007). Decreased Staphylococcus epidermis adhesion and increased osteoblast functionality on antibiotic-loaded titania nanotubes. Biomaterials, 28(32), 4880–4888. http://doi.org/10.1016/j.biomaterials.2007.07.037

Prausnitz, M. R., and Langer, R. (2009). Transdermal drug delivery, *26*(11), 1261–1268. http://doi.org/10.1038/nbt.1504.Transdermal

Price, J. S., Tencer, A. F., Arm, D. M., and Bohach, G. A. (1996). Controlled release of antibiotics from coated orthopedic implants. Journal of Biomedical Materials Research, 30(3), 281–286. http://doi.org/10.1002/(SICI)1097-4636(199603)30:3<281::AID-JBM2>3.0.CO;2-M

Puppi, D., Chiellini, F., Piras, A. M., and Chiellini, E. (2010). Polymeric materials for bone and cartilage repair. Topical Issue on Biomaterials, 35(4), 403–440. http://doi.org/DOI: 10.1016/j.progpolymsci.2010.01.006

Ramazanoglu, M., Lutz, R., Rusche, P., Trabzon, L., Kose, G. T., Prechtl, C., and Schlegel, K. A. (2013). Bone response to biomimetic implants delivering BMP-2 and VEGF: An immunohistochemical study. Journal of Cranio-Maxillofacial Surgery, 41(8), 826–835. http://doi.org/10.1016/j.jcms.2013.01.037

Ranade, V.V. and Hollinger, M.A. (2003). Drug Delivery Systems, CRC, New York, 230-231.

Rawat, M., Singh, D., Saraf, S., and Saraf, S. (2008). Development and *In Vitro* Evaluation of Alginate Gel–Encapsulated, Chitosan-Coated Ceramic Nanocores for Oral Delivery of Enzyme. Drug Development and Industrial Pharmacy, 34(2), 181–188. JOUR. http://doi.org/10.1080/03639040701539479

Razak, S., Sharif, N., and Rahman, W. (2012). Biodegradable Polymers and their Bone Applications: A Review. *ijens.org*, (February). Retrieved from http://www.ijens.org/Vol_12_I_01/123101-8585-IJBAS-IJENS.pdf

Rezwan, K., Chen, Q. Z., Blaker, J. J., and Boccaccini, A. R. (2006). Biodegradable and bioactive porous polymer/inorganic composite scaffolds for bone tissue engineering. Biomaterials, 27(18), 3413–3431. http://doi.org/10.1016/j.biomaterials.2006.01.039

Roether, J. a, Gough, J. E., Boccaccini, a R., Hench, L. L., Maquet, V., and Jerome, R. (2002). Novel bioresorbable and bioactive composites based on bioactive glass and pollactide foams for bone tissue engineering. Journal of Materials Science: Materials in Medicine, 13(12), 1207–1214. http://doi.org/10.1023/A:1021166726914

Rohan, L. C., and Sassi, A. B. (2009). Vaginal Drug Delivery Systems for HIV Prevention, *11*(1), 78–87. http://doi.org/10.1208/s12248-009-9082-7

Rojas-Oviedo, I., Salazar-López, R., Reyes-Gasga, J., and Quirino-Barreda, C. T. (2007). Elaboration and structural analysis of aquasomes loaded with indomethacin. *European Journal of Pharmaceutical Sciences : Official Journal of the European Federation for Pharmaceutical Sciences*, *32*(3), 223–30. http://doi.org/10.1016/j.ejps.2007.07.008

Rouahi, M., Champion, E., Gallet, O., Jada, A., and Anselme, K. (2006). Physico-chemical characteristics and protein adsorption potential of hydroxyapatite particles: Influence on *in vitro* biocompatibility of ceramics after sintering. *Colloids and Surfaces B: Biointerfaces*, *47*(1), 10–19. http://doi.org/10.1016/j.colsurfb.2005.11.015

Rubin, J., Rubin, C., and Jacobs, C. R. (2006). Molecular pathways mediating mechanical signaling in bone. *Gene*, *367*, *pp.* 1–16. DOI:10.1016/j.gene.2005.10.028

Russell, R. G. (1997). The assessment of bone metabolism in vivo using biochemical approaches. *Hormone and metabolic research*, *29*(3), 138–144. DOI:10.1055/s-2007-979007

Ruszczak, Z., and Friess, W. (2003). Collagen as a carrier for on-site delivery of antibacterial drugs. Advanced Drug Delivery Reviews, 55(12), 1679–1698. http://doi.org/10.1016/j.addr.2003.08.007

Salerno, C., Carlucci, A. M., & Bregni, C. (2010). Study of in vitro drug release and percutaneous absorption of fluconazole from topical dosage forms. *AAPS PharmSciTech*, *11*(2), 986–993. http://doi.org/10.1208/s12249-010-9457-1

Salgado, A. C. G. B., Da Silva, A. M. N. N., Machado, M. C. J. C., Duarte, M. A. D. S. C., and Ribeiro, H. M. D. O. M. (2010). Development, stability and in vitro permeation studies of gels containing mometasone furoate for the treatment of dermatitis of the scalp. *Brazilian Journal of Pharmaceutical Sciences*, *46*(1), 109–114. http://doi.org/10.1590/S1984-82502010000100012.

Sachse, A., Wagner, A., Keller, M., Wagner, O., Wetzel, W.-D., Layher, F. and Mollenhauer, J. (2005). Osteointegration of hydroxyapatite-titanium implants coated with nonglycosylated recombinant human bone morphogenetic protein-2 (BMP-2) in aged sheep. Bone, 37(5), pp. 699–710. doi:10.1016/j.bone.2005.06.011

Sanchez, C. J., Ward, C. L., Romano, D. R., Hurtgen, B. J., Hardy, S. K., Woodbury, R. L., … Wenke, J. C. (2013). Staphylococcus aureus biofilms decrease osteoblast viability, inhibits osteogenic differentiation, and increases bone resorption in vitro. BMC Musculoskeletal Disorders, 14(1), 187. http://doi.org/10.1186/1471-2474-14-187

Schliephake, H. (2010). Application of bone growth factors--the potential of different carrier systems. Oral and Maxillofacial Surgery, 14(1), 17–22. http://doi.org/10.1007/s10006-009-0185-1

Schnaper, H. W., Kopp, J. B., Poncelet, A. C., Hubchak, S. C., Stetler-Stevenson, W. G., Klotman, P. E., and Kleinman, H. K. (1996). Increased expression of extracellular matrix proteins and decreased expression of matrix proteases after serial passage of glomerular mesangial cells, 2528, 2521–2528.

Schnieders, J., Gbureck, U., Thull, R., and Kissel, T. (2006). Controlled release of gentamicin from calcium phosphate-poly(lactic acid-co-glycolic acid) composite bone cement. Biomaterials, 27(23), 4239–4249. http://doi.org/10.1016/j.biomaterials.2006.03.032

Séné C., Neun D., Tan-Sien-Hee L. and Ulman K., (2002). Silicones as excipients for topical pharmaceutical applications: the Silky Touch product family from Dow Corning, Dow Corning, pp. 1–12, URL:http://www4.dowcorning.com/content/ publishedlit/52-1034-01.pdf.

Shi, Z., Huang, X., Cai, Y., Tang, R., and Yang, D. (2009). Size effect of hydroxyapatite nanoparticles on proliferation and apoptosis of osteoblast-like cells. Acta Biomaterialia, 5(1), 338–345. http://doi.org/10.1016/j.actbio.2008.07.023

Sigurdsson. T.J., Fu. E., Tatakis, N. D., Rohrer, M. D. and Wikesjo, U. M. (1997). Bone morphogenetic protein-2 for peri-implant bone regeneration and osseointegration, *Clinical Oral Implants Research*, 8, *pp*. 367-374.

Singh, R., and Lillard, J. W. (2009). Nanoparticle-based targeted drug delivery. Experimental and Molecular Pathology, 86(3), 215–23. http://doi.org/10.1016/j.yexmp.2008.12.004

Solheim, E. (1998). Current concepts Growth factors in bone, pp. 410–416.

Soriano, I., and Evora, C. (2000). Formulation of calcium phosphates / poly (d , l -lactide) blends containing gentamicin for bone implantation, 68, 121–134.

Stetler-stevenson, W. G., and Cheresh, D. A. (1999). Matrix metalloproteinases in angiogenesis : a moving target for therapeutic intervention, 103(9), 1237–1241.

Stigter, M., Bezemer, J., De Groot, K., and Layrolle, P. (2004). Incorporation of different antibiotics into carbonated hydroxyapatite coatings on titanium implants, release and antibiotic efficacy. Journal of Controlled Release, 99(1), 127–137. http://doi.org/10.1016/j.jconrel.2004.06.011

Summersgill, J. T. Schupp, L. G. and Raff, M. J. (1982). Comparative penetration of metronidazole, clindamycin, chloramphenicol, cefoxitin, ticarcillin, and moxalactam into bone *Antimicrobial Agents and Chemotherapy*, 21(4), *pp*. 601-603.

Talukdar, M. M., Vinckier, I., Moldenaers, P., and Kinget, R. (1996). Rheological characterization of xanthan gum and hydroxypropylmethyl cellulose with respect to controlled-release drug delivery. *Journal of pharmaceutical sciences*, *85*(5), *pp.* 537–40. DOI:10.1021/js950476u

Torres, M. P., Determan, A. S., Anderson, G. L., Mallapragada, S. K., and Narasimhan, B. (2007). Amphiphilic polyanhydrides for protein stabilization and release. Biomaterials, 28(1), 108–116. http://doi.org/10.1016/j.biomaterials.2006.08.047

Tu, J., Bolla, S., Barr, J., Miedema, J., Li, X., and Jasti, B. (2005). Alginate microparticles prepared by spray-coagulation method: preparation, drug loading and release characterization. International Journal of Pharmaceutics, 303(1–2), 171–81. http://doi.org/10.1016/j.ijpharm.2005.07.008

Ulery, B. D., Nair, L. S., and Laurencin, C. T. (2011). Biomedical Applications of Biodegradable Polymers. Journal of Polymer Science. Part B, Polymer Physics, 49(12), 832–864. http://doi.org/10.1002/polb.22259

Uludag, H., Friess, W., Williams, D., Porter, T., Timony, G., D'augusta, D., Blake, C., Palmer, R., Biron, B. and Wozney, J. (1999), rhBMP-Collagen Sponges as Osteoinductive Devices: Effects of in Vitro Sponge Characteristics and Protein pI on in Vivo rhBMP Pharmacokinetics. Annals of the New York Academy of Sciences, 875: 369–378. doi:10.1111/j.1749-6632.1999.tb08519.x

Umashankar, M. S., Sachdeva, R. K., and Gulati, M. (2010). Aquasomes: a promising carrier for peptides and protein delivery. *Nanomedicine : nanotechnology, biology, and medicine*, *6*(3), *pp.* 419–26. DOI:10.1016/j.nano.2009.11.002

Unger, R. E., Sartoris, A., Peters, K., Motta, A., Migliaresi, C., Kunkel, M., and Kirkpatrick, C. J. (2007). Tissue-like self-assembly in cocultures of endothelial cells and osteoblasts and the formation of microcapillary-like structures on three-dimensional porous biomaterials. *Biomaterials*, *28*(27), *pp.* 3965–3976. DOI:10.1016/j.biomaterials.2007.05.032

Urist, M. R., and Strates, B. S. (1971). Bone Morphogenetic Protein. Journal of Dental Research, 50(6), 1392–1406. http://doi.org/10.1177/00220345710500060601

Utreja S, Jain NK. Solid lipid nanoparticles. In: Jain NK, editor. Advances in Controlled and Novel Drug Delivery. New Delhi, India: CBS Publishers; 2001. pp. 408–425

Valenta, C. (2005). The use of mucoadhesive polymers in vaginal delivery. *Advanced Drug Delivery Reviews*, *57*(11), 1692–712. http://doi.org/10.1016/j.addr.2005.07.004

Valerio, P., Pereira, M. M., Goes, A. M., and Leite, M. F. (2004). The effect of ionic products from bioactive glass dissolution on osteoblast proliferation and collagen production. Biomaterials, 25(15), 2941–2948. http://doi.org/10.1016/j.biomaterials.2003.09.086

Vengala, P., Dintakurthi, S., and Subrahmanyam, C. V. S. (2013). Lactose coated ceramic nanoparticles for oral drug delivery. *Journal of Pharmacy Research*, *7*(6), 540–545. http://doi.org/10.1016/j.jopr.2013.06.015

Verma, N. a, Lee, A. C., Herold, B. C., and Keller, M. J. (2011). Topical prophylaxis for HIV prevention in women: becoming a reality. *Current HIV/AIDS Reports*, *8*(2), 104–13. http://doi.org/10.1007/s11904-011-0075-7

Verron, E., Khairoun, I., Guicheux, J., and Bouler, J.-M. (2010). Calcium phosphate biomaterials as bone drug delivery systems: a review. Drug Discovery Today, 15(13–14), 547–552. http://doi.org/10.1016/j.drudis.2010.05.003

Wachol-Drewek, Z., Pfeiffer, M. and Scholl, E. B. S. (1996). Comparative investigation of drug delivery of collagen implants saturated in antibiotic solutions and a sponge containing gentamicin, 17(17), 1733–1738.

Wang, H.-L., Miyauchi, M., and Takata, T. (2002). Initial attachment of osteoblasts to various guided bone regeneration membranes: an in vitro study. Journal of Periodontal Research, 37(5), 340–4. Retrieved from http://www.ncbi.nlm.nih.gov/pubmed/12366856

Wein, F., and Bruinink, A. (2013). Human triple cell co-culture for evaluation of bone implant materials. *Integrative biology : quantitative biosciences from nano to macro*, *5*(4), 703–11. doi:10.1039/c3ib20250j

Woolfson, D., Malcolm, R. K., Morrow, R. J., Toner, C. F., and McCullagh, S. D. (2006). Intravaginal ring delivery of the reverse transcriptase inhibitor TMC 120 as an HIV microbicide. *International Journal of Pharmaceutics*, *325*(1–2), 82–9. http://doi.org/10.1016/j.ijpharm.2006.06.026

Wright, H. L., McCarthy, H. S., Middleton, J., and Marshall, M. J. (2009). RANK, RANKL and osteoprotegerin in bone biology and disease. *Current reviews in musculoskeletal medicine*, *2*(1), *pp.* 56–64. DOI:10.1007/s12178-009-9046-7

Wu, P., and Grainger, D. W. (2006). Drug/device combinations for local drug therapies and infection prophylaxis. Biomaterials, 27(11), 2450–2467. http://doi.org/10.1016/j.biomaterials.2005.11.031

Wu, T., Zhang, Q., Ren, W., Yi, X., Zhou, Z., Peng, X., … Lang, M. (2013). Controlled release of gentamicin from gelatin/genipin reinforced beta-tricalcium phosphate scaffold for the treatment of osteomyelitis. Journal of Materials Chemistry B, 1, 3304. http://doi.org/10.1039/c3tb20261e

Xiao, Y.-T., Xiang, L.-X., and Shao, J.-Z. (2007). Bone morphogenetic protein. *Biochemical and biophysical research communications*, *362*(3), *pp.* 550–553. DOI:10.1016/j.bbrc.2007.08.045

Xie, Z., Liu, X., Jia, W., Zhang, C., Huang, W., and Wang, J. (2009). Treatment of osteomyelitis and repair of bone defect by degradable bioactive borate glass releasing vancomycin. Journal of Controlled Release, 139(2), 118–126. http://doi.org/10.1016/j.jconrel.2009.06.012

Xu, Z. P., Zeng, Q. H., Lu, G. Q., and Yu, A. B. (2006). Inorganic nanoparticles as carriers for efficient cellular delivery. Chemical Engineering Science, 61(3), 1027–1040. http://doi.org/10.1016/j.ces.2005.06.019

Xynos, I. D., Edgar, a J., Buttery, L. D., Hench, L. L., and Polak, J. M. (2000). Ionic products of bioactive glass dissolution increase proliferation of human osteoblasts and induce insulin-like growth factor II mRNA expression and protein synthesis. Biochemical and Biophysical Research Communications, 276, 461–465. http://doi.org/10.1006/bbrc.2000.3503

Yamamura, K., Iwata, H., and Yotsuyanagi, T. (1992). Synthesis of antibiotic-loaded hydroxyapatite beads and in vitro drug release testing. Journal of Biomedical Materials Research, 26(8), 1053–1064. http://doi.org/10.1002/jbm.820260807

Yang, L., and Webster, T. J. (2009). Nanotechnology controlled drug delivery for treating bone diseases. *Expert Opinion on Drug Delivery*, *6*(8), 851–64. http://doi.org/10.1517/17425240903044935

Yoon, I.-S., Chung, C. W., Sung, J.-H., Cho, H.-J., Kim, J. S., Shim, W.-S., … Kim, D.-D. (2011). Proliferation and chondrogenic differentiation of human adipose-derived mesenchymal stem cells in porous hyaluronic acid scaffold. Journal of Bioscience and Bioengineering, 112(4), 402–408. http://doi.org/10.1016/j.jbiosc.2011.06.018

Young, C. S., and Dolan, J. W. (2003). Success with Evaporative Light-Scattering Detection. LCGC Europe. www.lcgceurope.com.

Yu, X., Wang, L., Jiang, X., Rowe, D., and Wei, M. (2012, September). Biomimetic CaP coating incorporated with parathyroid hormone improves the osseointegration of titanium implant. *Journal of materials science. Materials in medicine, pp.* 4682-4687. DOI:10.1007/s10856-012-

Zhang, L., and Webster, T. J. (2009). Nanotechnology and nanomaterials: Promises for improved tissue regeneration. Nano Today, 4(1), 66–80. http://doi.org/10.1016/j.nantod.2008.10.014

Zhou, H., and Lee, J. (2011). Nanoscale hydroxyapatite particles for bone tissue engineering. *Acta biomaterialia*, *7*(7), *pp*. 2769–2781. DOI:10.1016/j.actbio.2011.03.019

Zilberman, M., and Elsner, J. J. (2008). Antibiotic-eluting medical devices for various applications. Journal of Controlled Release, 130(3), 202–215. http://doi.org/10.1016/j.jconrel.2008.05.020

8.2 WORLDWIDE WEB SOURCES

Transparency Market Research, (2016). Nanotechnology Drug Delivery Market: Global Industry Analysis, Size, Share, Growth, Trends, and Forecast 2015 – 2023. Available at: http://www.transparencymarketresearch.com/nanotechnology-drug-delivery.html. [Accessed 23rd November 2016].

BCC Research, (2014). Nanoparticles in Biotechnology, Drug Development and Drug Delivery **(**BIO113B). Available at: https://www.bccresearch.com/market-research/biotechnology/nanoparticles-biotechnology-drug-development-drug-delivery-report-bio113b.html. [Accessed 23rd November 2016].

Shimadzu Corporation (2016). Principles and practical applications of Shimadzu's ELSD-LT II Evaporating Light Scattering Detector. Available at: www.ssi.shimadzu.com/products/literature/lc/c190e108.pdf [Accessed 10th September 2016]

Waters Corporation (2009). 2424 Evaporative Light Scattering Detector: Operator's guide. Available at: www.waters.com/webassets/cms/support/docs/71500121802rb.pdf [Accessed 10th September 2016]

Amgen, (2012). Introduction to Bone Biology. Available at: www.youtube.com/watch?v=ingWoakkiTc. [Accessed 11th November 2015].

RESEARCH PARTICIPATIONS

Udo-Chijioke, O., Marshall, L., Perrie, Y. and Lowry, D. 2014. Nanoparticulate drug delivery systems for the local delivery of growth factors to enhance fracture-healing, proceedings at UK and Ireland Controlled Release Society Symposium (UKICRS 2014), Cork, Scotland

Udo-Chijioke, O., Marshall, L., Perrie, Y. and Lowry, D. 2014. Nanoparticulate drug delivery systems for the local delivery of growth factors for fracture healing, proceedings at UK Pharmaceutical Science Symposium (UKPharmSci 2014), Hertfordshire, UK

Udo-Chijioke, O., Marshall, L., Perrie, Y. and Lowry, D. 2014. Nanoparticulate drug delivery systems for the local delivery of growth factors for fracture healing, proceedings at UK Pharmaceutical Science Symposium (MIBio Conferefnce 2014), Cambridge, UK

Udo-Chijioke, O., Marshall, L., Perrie, Y. and Lowry, D. 2015. Local delivery of growth factors via ceramic nanoparticles for fracture healing, proceedings at UK and Ireland Controlled Release Society Symposium (UKICRS 2015), Nottingham, UK.

Udo-Chijioke, O., Marshall, L., Perrie, Y. and Lowry, D. 2015. Nanoparticulate delivery of growth factors for fracture healing, proceedings at Controlled Release Society Annual Conference (CRS 2015), Edinburgh, Scotland

Udo-Chijioke, O., Perrie, Y., Marshall, L. and Lowry, D. 2015. Ceramic nanoparticulate systems for the local delivery of growth factors and antibiotics for fracture healing, proceedings at the 2015 UKPharmSci Symposium (podium presentation), Nottingham, UK.

CHAPTER 9
APPENDIX

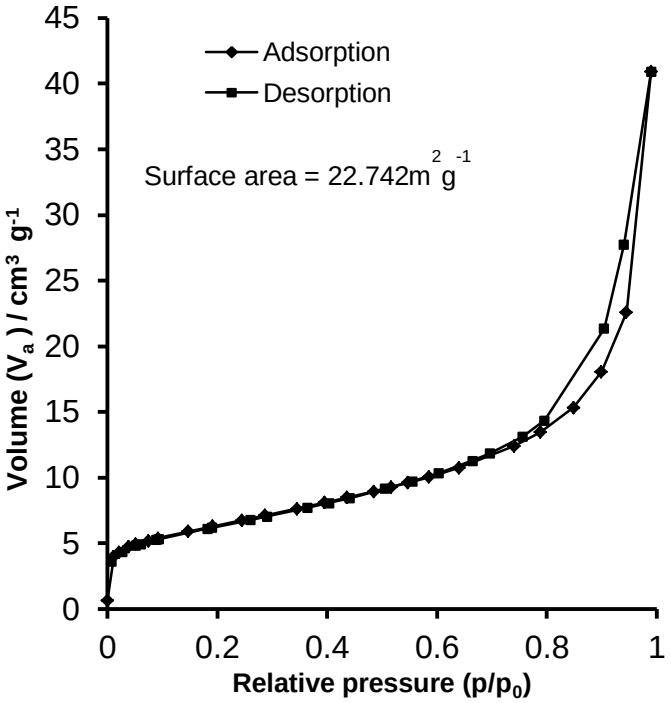

Appendix I. Adsorption/Desorption Isotherm plot for hydroxyapatite nanocores showing calculated surface area as 22.742m^{2}g^{-1}. Using N_2 as an adsorbate, the surface area was calculated by the volume of gas adsorbed and desorbed on the surface of the hydroxyapatite nanocores, with multilayer formation evidenced by two inflection points.

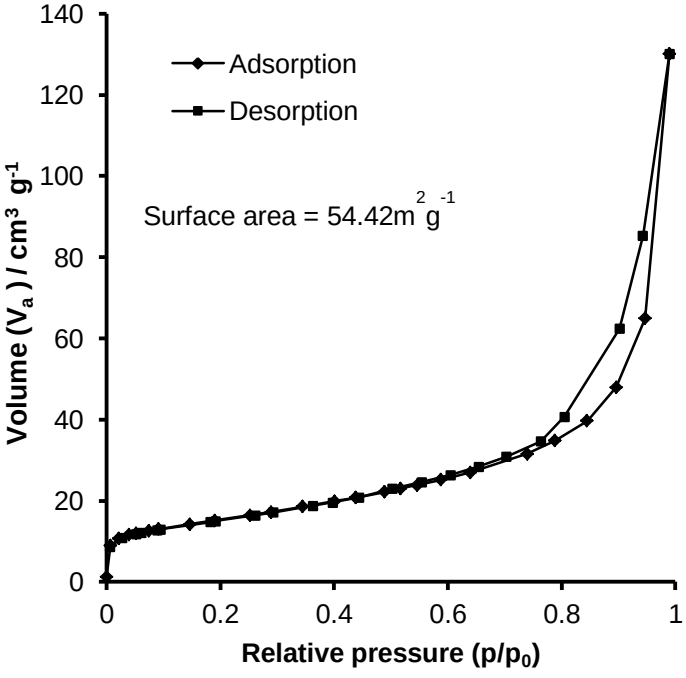

Appendix II. Adsorption/Desorption Isotherm plot for 60nm nano-hydroxyapatite powder showing calculated surface area as 54.423m^{2}g^{-1}. The surface area was calculated by the volume of N_2 gas adsorbed and desorbed on the surface of the hydroxyapatite nanocores, with multilayer formation evidenced by two inflection points.

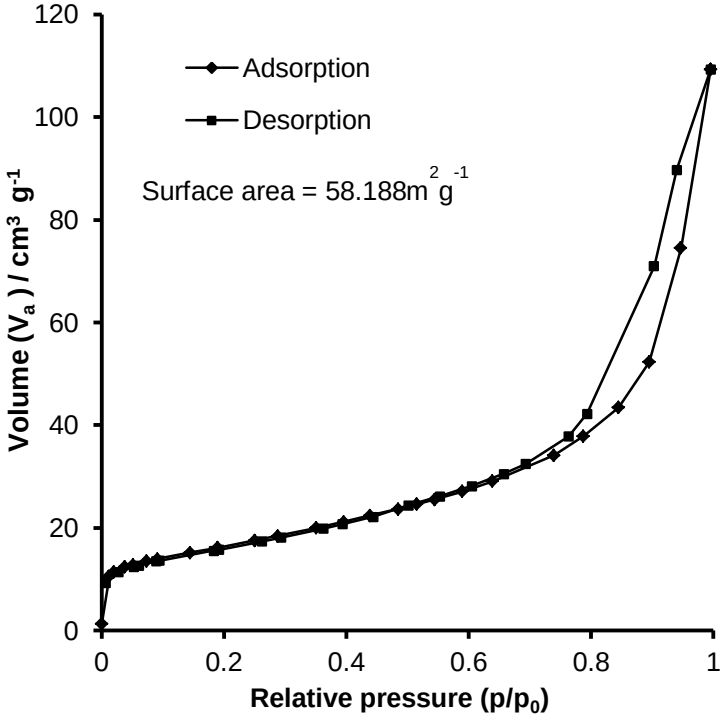

Appendix III. Adsorption/Desorption Isotherm plot for 40nm nano-hydroxyapatite powder showing calculated surface area as 58.188m^{2}g^{-1}. The surface area was calculated by the volume of N_2 gas adsorbed and desorbed on the surface of the hydroxyapatite nanocores, with multilayer formation evidenced by two inflection points.

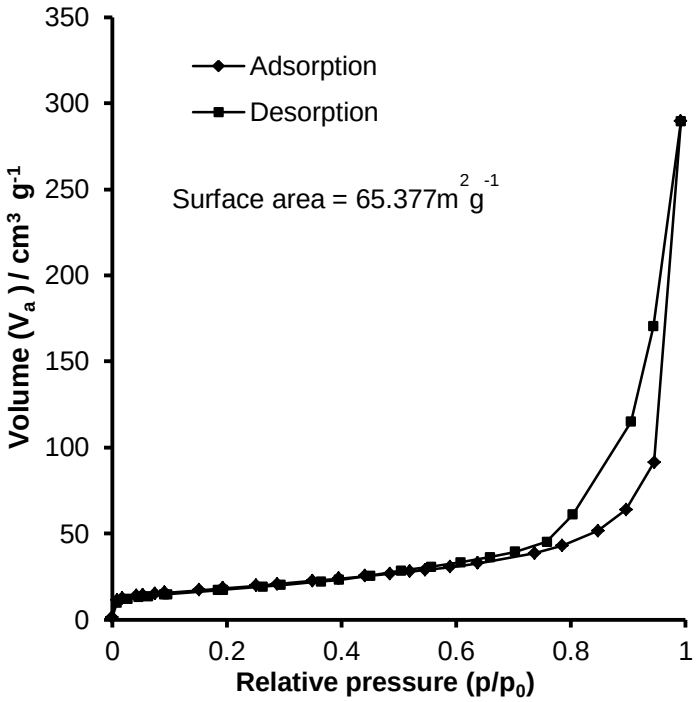

Appendix IV. Adsorption/Desorption Isotherm plot for 20nm nano-hydroxyapatite powder showing calculated surface area as 65.377m^{2}g^{-1}. The surface area was calculated by the volume of N_2 gas adsorbed and desorbed on the surface of the hydroxyapatite nanocores, with multilayer formation evidenced by two inflection points.

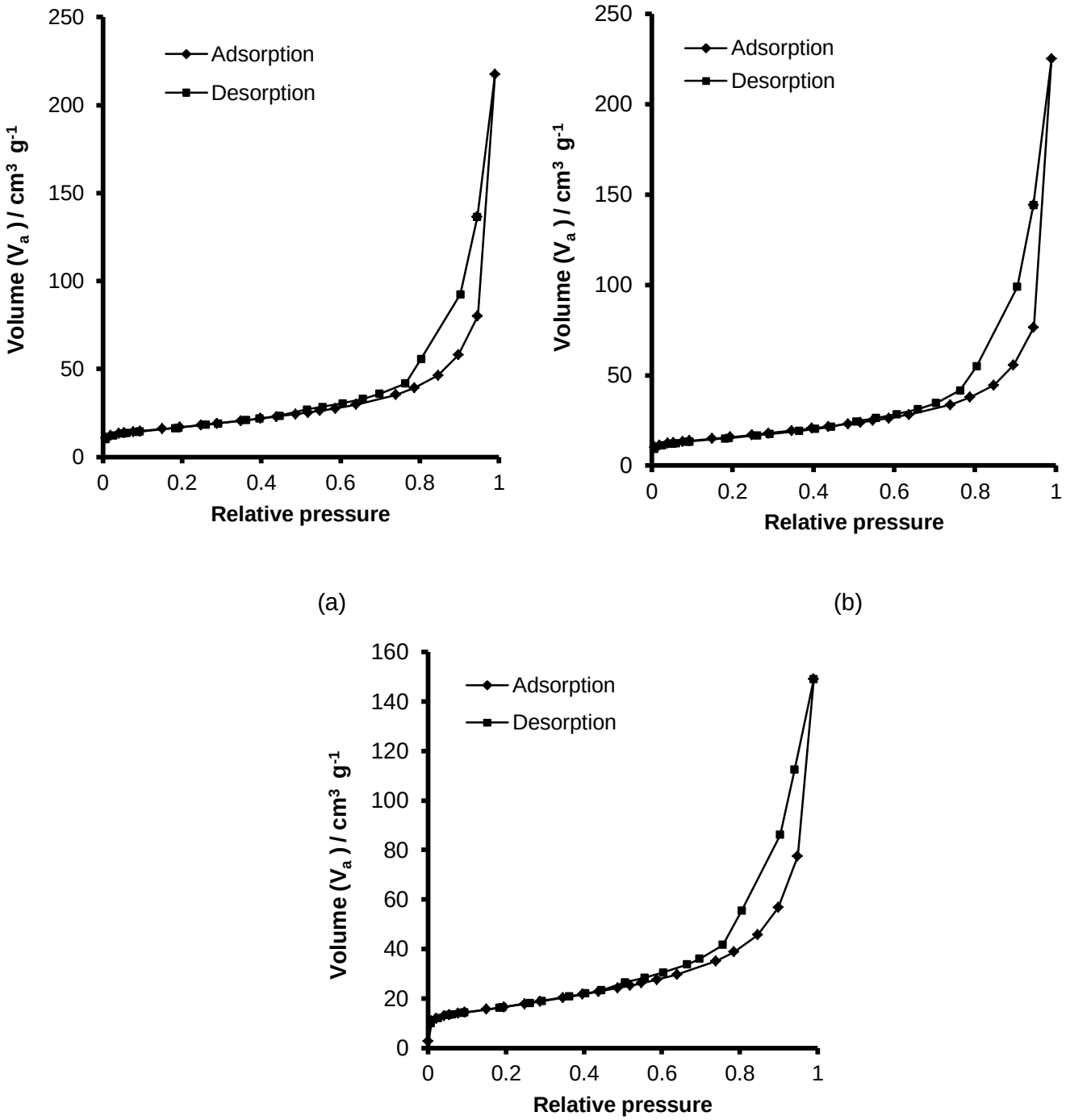

Appendix V. Adsorption/Desorption Isotherm plot for 20nm nano-hydroxyapatite powder coated with trehalose. (a) 1.5hrs, (b) 2.5hrs and (c) 3hrs, showing calculated surface areas as 60.176, 56.242 and 58.689m^2g^{-1} respectively. These plots illustrate type III isotherms indicated low gas-solid affinity between the N_2 and the nano-HA particles.

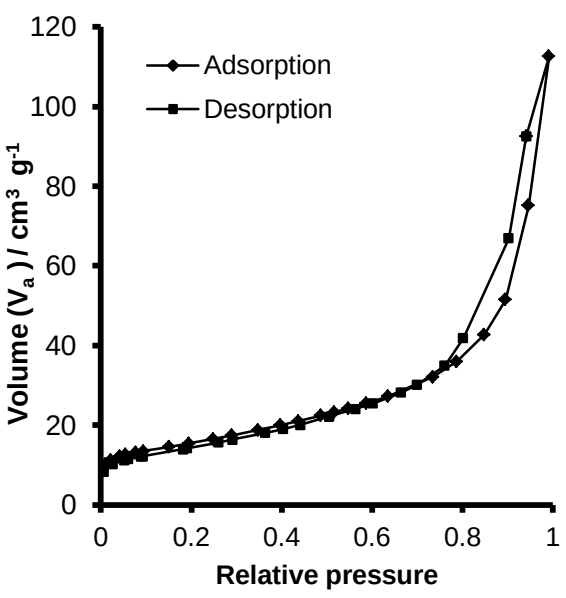

(a)

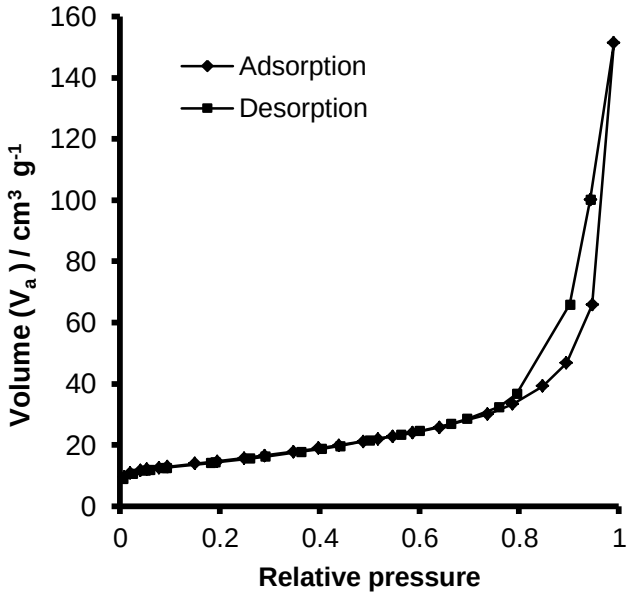

(b)

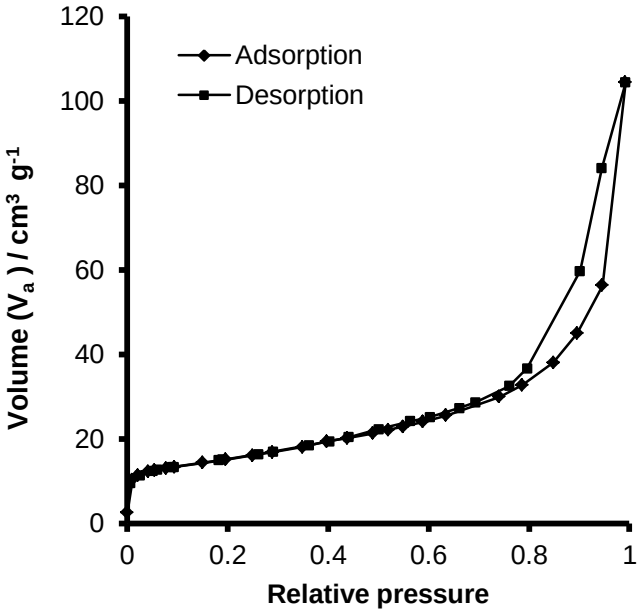

(c)

Appendix VI. Adsorption/Desorption Isotherm plot for 40nm nano-hydroxyapatite powder coated with trehalose. (a) 1.5hrs, (b) 2.5hrs and (c) 3hrs, showing calculated surface areas as 54.889, 52.184 and 53.558m^2g^{-1} respectively. These plots illustrate type III isotherms indicated low gas-solid affinity between the N_2 and the nano-HA particles.

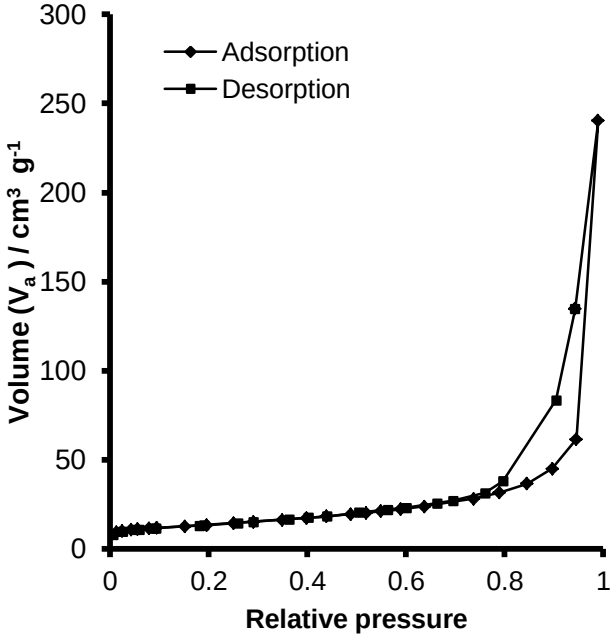

(a)

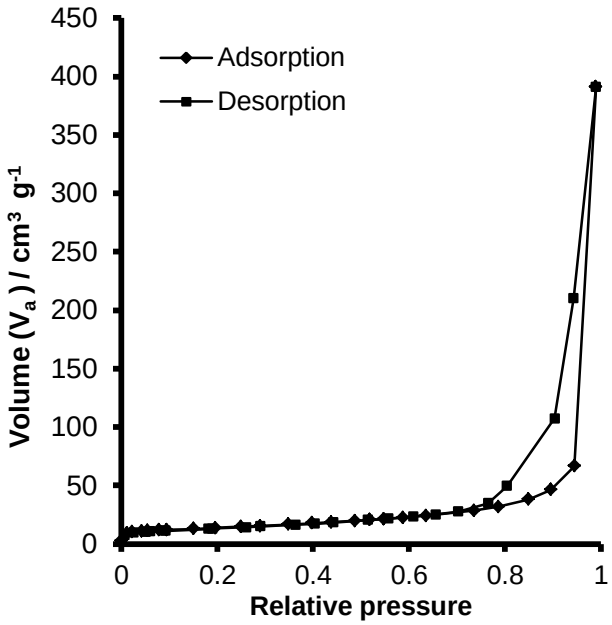

(b)

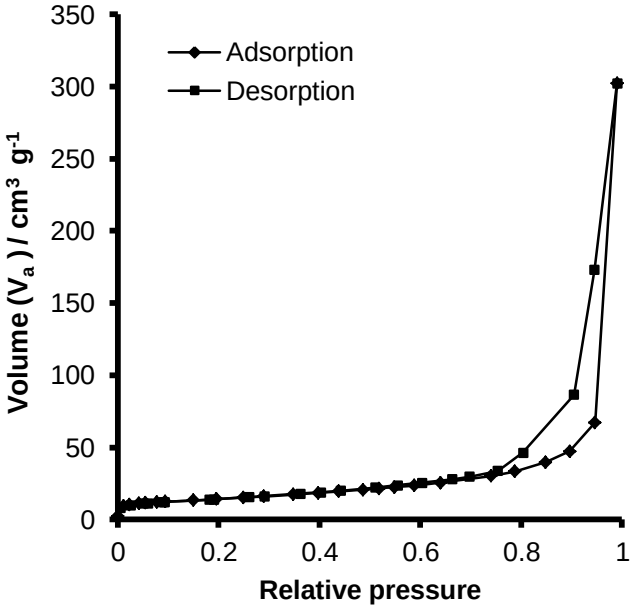

(c)

Appendix VII. Adsorption/Desorption Isotherm plot for 60nm nano-hydroxyapatite powder coated with trehalose. (a) 1.5hrs, (b) 2.5hrs and (c) 3hrs, showing calculated surface areas as 47.767, 48.145 and 50.439m^2g^{-1} respectively. These plots illustrate type III isotherms indicated low gas-solid affinity between the N_2 and the nano-HA particles.

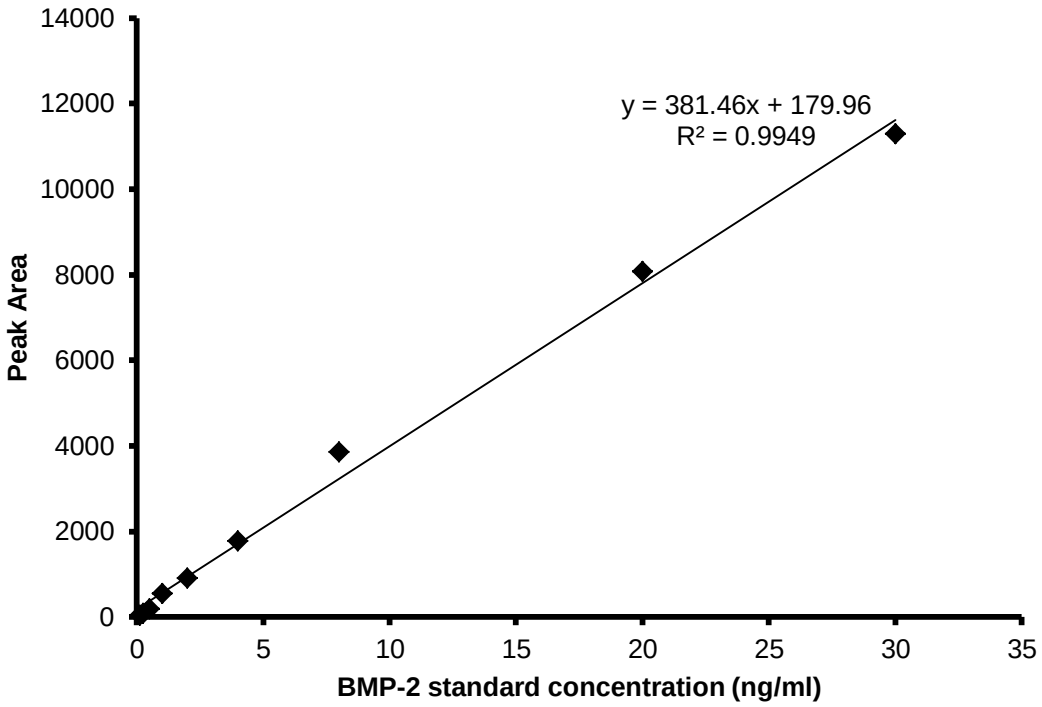

Appendix VIII. BMP-2 calibration using ELSD-LC showing R^2 as 0.9949. BMP-2 standards ranging from 0.125 to 30ng/ml were analysed in isocratic mode and detected with an optical gain of 2.

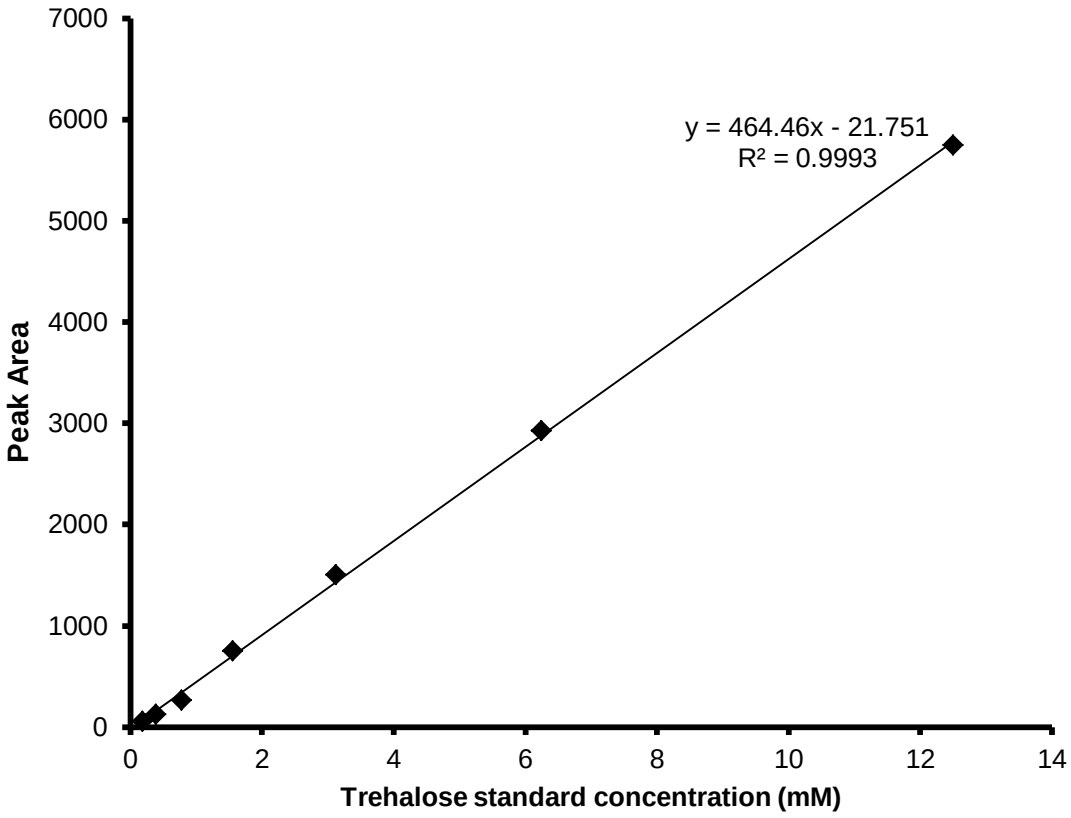

Appendix IX. Trehalose calibration using ELSD-LC showing R^2 as 0.9993. Trehalose standards ranging from 0.19 10 12mM were analysed in isocratic mode and detected with an optical gain of 2.

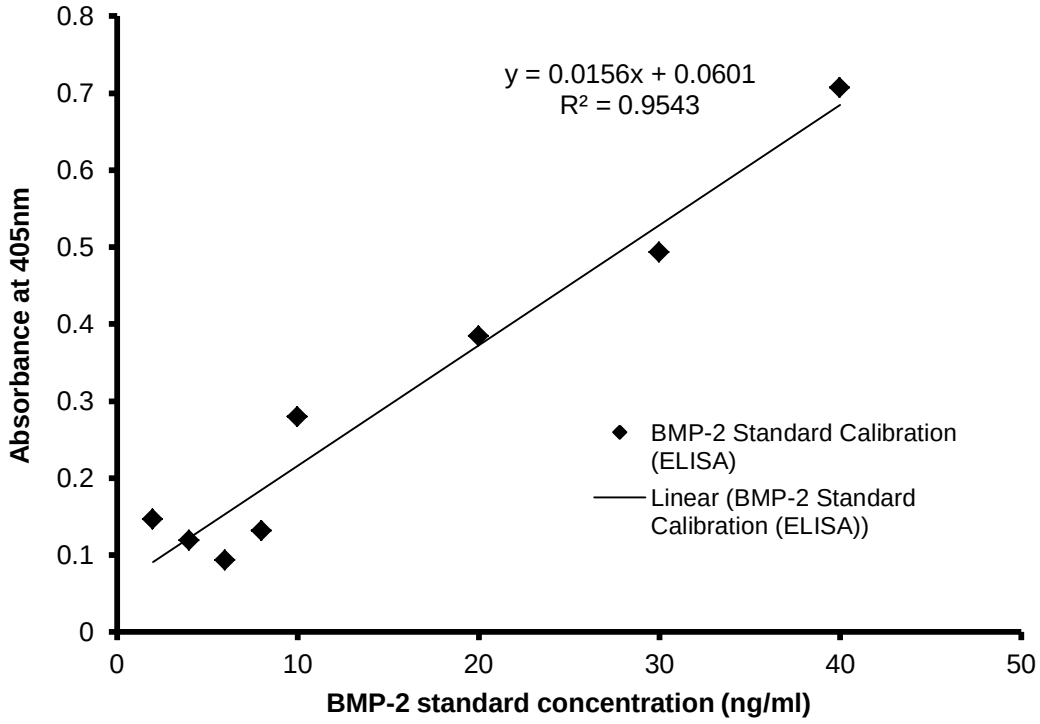

Appendix X. BMP-2 calibration using ELISA showing R^2 as 0.9543. BMP-2 standards ranging from 0.125 to 30ng/ml were analysed using the ELISA technique and UV absorbance was read at 405nm.